# Characterizing the biochemical and toxicological effects of nanosilver *in vivo* using zebrafish (*Danio rerio*) and *in vitro* using rainbow trout (*Oncorhynchus mykiss*)

by

Andrey Massarsky

Thesis submitted to the

Faculty of Graduate and Postdoctoral Studies

University of Ottawa

In partial fulfillment of the requirements for the

PhD degree in the

Ottawa-Carleton Institute of Biology

Thèse soumise à la

Faculté des Études Supérieurs et Postdoctorales

Université d'Ottawa

En vue de la réalisation partielle du doctorat à

L'Institut de Biologie Ottawa-Carleton

***This dissertation is dedicated in loving memory of my grandmother Valentina Tulina. I am eternally grateful for her efforts to ensure my academic success from the first day I started school. I have no doubt that she is smiling from up above as I acquire my PhD.***

## Acknowledgments

It is hard to believe that five years of graduate studies have passed by so quickly. There are many people, whom I would like to thank from the bottom of my heart for everything they have done for me throughout my journey as a graduate student. First and foremost I would like to thank my supervisor Dr. Thomas W. Moon for ever so patiently instilling in me the love for scientific research. His outstanding guidance and mentoring throughout the years have not only opened my eyes to the vast research tools, but also dramatically improved my abilities to think critically and write and present scientific knowledge. My accomplishments would have been impossible without Dr. Moon, and for this I will forever be indebted to him. Secondly, I would like to express my sincere gratitude to my co-supervisor Dr. Vance L. Trudeau, who despite having multiple students in his own lab, always found the time to inquire about my progress and make valuable suggestions pertaining to my experiments. Dr. Trudeau also played a pivotal role in reviewing all of my manuscripts, often pointing out things that were missed by other editors, thus ensuring the high quality of the final product.

Furthermore, I would like to extend my thanks to my committee members: Drs. Jules Blais, William Willmore, and Paul White, for stimulating discussions that helped to shape this thesis into an interesting narrative. I would also like to recognize the input of many collaborators and colleagues, including Dr. Chris Metcalfe, Dr. Greg Goss, Dr. Azam Tayabali, Kathy Nguyen, and Dr. Antoine Morin. Special thanks also go to Bill Fletcher and Vishal Saxena for taking excellent care of the fish facility and ensuring that my experiments ran as smoothly as possible.

I would like to express my gratitude to the Department of Biology personnel. Dr. John Basso always had a great advice when I was in doubt, including his recommendation to pursue an Honors project with Dr. Moon. Moreover, my numerous teaching assistantships with Dr. Basso have not only taught me a great deal of microbiology and molecular biology techniques, but also improved my skills to instruct undergraduate students. Lise Belanger and Yves Genest helped tremendously with the organization of my mini-courses, which were my summer highlights for the past three years. Finally, Doreen Smith, Isabelle Morissette, and Gita Kangas booked my numerous committee meetings and processed a myriad of documents and contracts.

I would also like to acknowledge my labmates over the past five years, who shaped my PhD studies into an unforgettable adventure. These include Dr. Shahram Eisa-Beygi, Aziz Al-Habsi, Dr. Paul M. Craig, Kim Mitchell, Marilyn Vera Chang, Rand Pasha, Pamela Stroud, and Rance Nault. I was also fortunate to supervise very talented undergraduate students: Lisa Dupuis, Jessica Taylor, Ren Abraham, Laura Strek, and Justine Labarre, who contributed to the progress of my research.

Finally, I would like to thank my family: my parents Elena and Michael, for their spiritual and generous financial support during my studies; my brother Alexey, for all the encouragement and great stress-relieving squash matches; my grandparents Lyudmila and Rudolf, who showed a lot of support from Germany; my in laws Pier and Letty, for their support and great company on Friday-gym evenings. Lastly, I would like thank my beautiful wife Cintia for putting up with my workaholic tendencies for the past five years and comforting me on the days when everything seemed hopeless.

## Abstract

Many consumer and medical products contain engineered nanomaterials (ENMs) due to their unique properties arising from their small size of <100 nm in at least one dimension. Although ENMs could greatly improve the quality of daily life, concerns for their health and environmental safety emerged in recent years because the same properties that make ENMs beneficial may also render them toxic. The small size allows ENMs' entrance into the cell where they may attach to biological molecules and membranes, disrupting their function and/or leading to oxidative stress and/or damage.

This thesis focused on silver nanoparticles (AgNPs). Several articles demonstrated that during washing AgNPs are released from the AgNP-impregnated fabrics and could pose a risk to aquatic species. Given that the toxicity mechanisms of AgNPs are yet to be clearly understood this thesis investigated the effects of AgNPs from 'oxidative stress' and 'endocrine disruption' points of view, using both *in vivo* and *in vitro* model fish systems.

A 4 d exposure of zebrafish (*Danio rerio*) embryos to AgNPs increased mortality, delayed hatching, and increased oxidative stress. The silver ion ($Ag^+$) was more effective in eliciting these effects at equivalent silver concentrations. Moreover, the Ag-chelator cysteine reduced the toxicity of both Ag-types. Despite these effects AgNPs or $Ag^+$ did not affect the ability of zebrafish larvae or adults (raised to adulthood in Ag-free water) to increase cortisol levels, but there were differential effects on the expression of corticotropin-releasing factor (CRF)-related genes, suggesting that other physiological processes regulated by CRF may be impacted.

Furthermore, a 48 h exposure of rainbow trout (*Oncorhynchus mykiss*) erythrocytes and hepatocytes to AgNPs or $Ag^+$ increased oxidative stress, but $Ag^+$ was more potent. Moreover, AgNPs elevated lipid peroxidation, while $Ag^+$ increased DNA damage, suggesting different modes of action for the two Ag-types. Cysteine treatment reduced the toxicity of $Ag^+$ and AgNPs, while buthionine sulfoximine, which inhibits glutathione synthesis, increased it, suggesting the importance of glutathione in silver toxicity. Finally, AgNPs increased glycogenolysis in trout hepatocytes independently of the β-adrenoreceptor or the glucocorticoid receptor.

## Résumé

Plusieurs produits de consommation et produits médicaux contiennent les nanomatériaux fabriqués (ENMs) à cause de leur propriétés spéciales attribuées à leur petite taille de <100 nm dans au moins une dimension. Les ENMs peuvent améliorer la qualité de la vie courante; cependant, des craintes concernant leur sécurité sont récemment apparues, car les propriétés rendant les ENMs bénéfiques peuvent aussi les rendre toxiques. Leur petite taille leur permet d'accéder les cellules où ils peuvent s'adhérer aux molécules et membranes biologiques, dérangeant leur fonction et/ou menant au stress oxydant.

Cette dissertation centre sur les nanoparticules d'argent (AgNPs). C'était démontré que certains produits relâchent les AgNPs pouvant poser des risques aux espèces aquatiques. Les mécanismes de la toxicité des AgNPs ne sont pas encore bien connus, donc cette dissertation illustre les effets oxydatifs et endocriniens des AgNPs chez les poissons en utilisant les modelés *in vivo* et *in vitro*.

L'exposition des embryons de poisson zèbre (*Danio rerio*) aux AgNPs pendant 4 jours a mené à la mortalité, à l'éclosion retardée et au stress oxydant. L'ion d'argent ($Ag^+$) était plus efficace à provoquer ces effets. En plus, le chélateur d'Ag cystéine a réduit la toxicité des deux types d'argent. Malgré ces effets, les AgNPs et l'$Ag^+$ n'ont pas influencé la capacité des larves de poisson zèbre ou les poissons adultes (élevés sans argent) à augmenter le niveau du cortisol. Cependant, l'expression des gènes associés à la corticolibérine était affectée, suggérant que d'autres processus physiologiques régulés par la corticolibérine pourraient être affectés.

De plus, l'exposition des érythrocytes et des hépatocytes de truite arc-en-ciel (*Oncorhynchus mykiss*) aux AgNPs ou au $Ag^+$ pendant 48 heures a augmenté le niveau de stress oxydant, où l'$Ag^+$ était plus efficace. Aussi, les AgNPs ont augmenté la peroxydation des lipides, tandis que l'$Ag^+$ a augmenté les dommages à l'ADN, suggèrent que les deux types d'argent ont des mécanismes différents. La cystéine a réduit et le buthionine sulfoximine (inhibe la synthèse du glutathion) a augmenté la toxicité des AgNPs et $Ag^+$, suggérant l'importance du glutathion à la toxicité d'argent. Les AgNPs ont aussi augmenté la glycogénolyse chez les hépatocytes indépendamment du récepteur adrénergique β ou du récepteur des glucocorticoïdes.

## Table of Contents

## List of Figures

## List of Tables

## List of Abbreviations

| | |
|---|---|
| ACTH | Adrenocorticotropic hormone |
| $Ag^+$ | Silver ion |
| $AgNO_3$ | Silver nitrate |
| AgNPs | Silver nanoparticles |
| α-KG | α-ketoglutarate |
| ALT | Alanine aminotransferase |
| ANOVA | Analysis of variance |
| AST | Aspartate aminotransferase |
| β-AR | β-adrenoreceptor |
| BCA | Bicinchoninic acid |
| BSA | Bovine serum albumin |
| BSO | Buthionine sulfoximine |
| C | Cerebellum |
| cAMP | Adenosine 3',5'-cyclic monophosphate |
| CAT | Catalase |
| CORT | Cortisol |
| CRF | Corticotropin-releasing factor |
| CRF-BP | Corticotropin-releasing factor binding protein |
| CRF-R1 and R2 | Corticotropin-releasing factor receptors 1 and 2 |
| Cys | Cysteine |
| DAG | Diacylglycerol |
| DCHF-DA | 2'7'-dichlorodihydrofluorescin diacetate |
| DLS | Dynamic Light Scattering |
| DNPH | 2,4-dinitrophenylhydrazine |
| dpf | Days post fertilization |
| DTNB | 5,5'-dithiobis(2-nitrobenzoic acid) |
| Eh | Redox state |
| ENMs | Engineered nanomaterials |
| ETC | Electron-transport chain |
| FA | Fulvic acid |
| FBPase | Fructose-1,6-bisphosphatase |
| GCR | Glucocorticoid receptor |
| GFP | Green fluorescent protein |
| GPase | Glycogen phosphorylase |
| GPx | Glutathione peroxidase |
| GR | Glutathione reductase |
| GSH | Reduced glutathione |
| GSSG | Oxidized glutathione |

| | |
|---|---|
| GST | Glutathione-S-transferase |
| $H_2O_2$ | Hydrogen peroxide |
| HA | Humic acid |
| HEK | Human epidermal keratinocyte |
| hpf | Hours post fertilization |
| HPI | Hypothalamic-pituitary-interrenal |
| HPT | Hypothalamic-pituitary-thyroid |
| $IP_3$ | Inositol-1,4,5-triphosphate |
| ISO | Isoproterenol |
| LDH | Lactate dehydrogenase |
| M | Medulla |
| MIFE | Mifepristone |
| NMs | Nanomaterials |
| NOM | Natural organic matter |
| NP | Nanoparticle |
| NS | Not significant |
| $O_2^{\cdot -}$ | Superoxide anion |
| $OH^{\cdot}$ | Hydroxyl radical |
| OL | Optic lobe |
| PBDE | Polybrominated diphenyl ether |
| PCA | Perchloric acid |
| PDI | Polydispersity index |
| PECs | Predicted environmental concentrations |
| PEPCK | Phosphoenolpyruvate carboxykinase |
| $PIP_2$ | Phosphatidylinositol-4,5-bisphosphate |
| PKA | Protein kinase A |
| PLCγ | Phospholipase-Cγ |
| PLP | Pyridoxal phosphate |
| POMC | Pro-opiomelanocortin |
| PROP | Propranolol |
| PVP | Polyvinylpyrrolidone |
| RFU | Relative fluorescence unit |
| RIA | Radioimmunoassay |
| ROS | Reactive oxygen species |
| SD | Standard deviation |
| SEM | Standard error of the mean |
| SOD | Superoxide dismutase |
| STEM | Scanning Transmission Electron Microscope |
| STP | Sewage treatment plant |
| t/a | Tons per annum |

| | |
|---|---|
| TBARS | Thiobarbituric acid reactive substance |
| TCA | Trichloroacetic acid |
| TED | Transmission electron diffraction |
| tel | Telencephalon |
| TEM | Transmission Electron Microscope |
| TGSH | Total glutathione |
| $TiO_2$NPs | Titanium dioxide nanoparticles |
| TYT | Tyrosine aminotransferase |
| WIP | Waste incineration plant |
| WWTP | Wastewater treatment plant |
| ζ-potential | Zeta-potential |

# CHAPTER 1
# General Introduction

*1.1. Rationale for the study*

Silver nanoparticles (AgNPs) are incorporated into many consumer and medical products due to their antimicrobial properties. The potential environmental risk of AgNPs is yet to be fully understood. The aquatic organisms are of particular concern since water bodies often serve as sinks for anthropogenic activities. Oxidative stress has been proposed by the scientific literature as one of the toxicity mechanisms for engineered nanomaterials (ENMs) including AgNPs. On the other hand, ENM-mediated endocrine disruption as a potential toxicity mechanism received much less attention despite the demonstrated ability of ENMs to attach to cell membranes and other cellular components, thus disrupting their physiological function. Therefore, this thesis aimed to investigate the toxicity mechanisms of AgNPs in fish using both *in vivo* (zebrafish) and *in vitro* (rainbow trout erythrocytes and hepatocytes) models with the ultimate goal of improving the understanding of the toxic potential of AgNPs. To set up the stage for the studies described in this thesis the literature on ENMs is summarized in the following sections and the final section specifies the hypotheses and objectives.

*1.2. What are nanomaterials?*

'Nanomaterials' (NMs) are small particles with at least one dimension of less than 100 nm (Oberdörster et al., 2005; Seetharam and Sridhar, 2007) or nanostructures embedded within larger materials (CCA, 2008). Anthropogenic NMs include (1) incidental NMs, such as diesel/gasoline by-products (carbon black, soot) of power-generating plants and petroleum-powered engines, and (2) ENMs, which are designed for a specific function (Oberdörster et al., 2007) and are the focus of this thesis. There are

also natural NMs, such as viruses and materials generated in forest fires and volcanic eruptions (Oberdörster et al., 2005).

Engineered nanomaterials possess unique properties attributed to their size, shape, chemical composition, surface structure and charge, solubility, and coating (Nel et al., 2006; Oberdörster et al., 2007). The two main characteristics that make ENMs unique, are their small size and high surface area to volume ratio; their small size allows for increased uptake and interaction with biological systems (Oberdörster et al., 2005, 2007; Nel et al., 2006, 2009; Fischer and Chan, 2007), whereas the high surface area to volume ratio permits unique catalytic and oxidative reactions on the ENM surface (Nel et al., 2006, 2009; Fischer and Chan, 2007; Auffan et al., 2009). Other properties of ENMs, especially coating, are important determinants of their behavior and toxicity potential (Scown et al., 2010a).

The unique properties of ENMs are applicable in many domains, including optics, engineering, electronics, alternative energy, soil and water remediation, and consumer products (Oberdörster et al., 2007; Handy et al., 2008). In fact, as of October 2013 there were 1628 reported consumer products that contained ENMs, including cosmetics, tooth-pastes, antimicrobial and anti-stain coatings, clothing, children toys, and sporting goods (Nanotechproject, 2013). Nanotechnology can also be applied in medicine (i.e. nanomedicine), where ENMs could be used for drug-delivery and diagnostic purposes, as well as investigation and understanding of molecular processes and structures (Oberdörster et al., 2005; Nel et al., 2006). For example, a sensitive nanosensor chip for the detection of early cancer biomarkers was recently developed (Nanotech News, 2009), and hybrids of biomaterials (e.g. enzymes, antigens, antibodies, receptors) and ENMs

could be designed to regulate biochemical pathways by DNA binding and inhibition/activation of transcription/translation, and even detect single-mismatches in DNA sequences (Schmid, 2004).

Nanotechnology is rapidly gaining popularity and its global market was valued at $20.1 billion in 2011 and is expected to double by 2017 (BCC, 2012). Recent studies reporting adverse effects of ENMs in various organisms (as discussed in this thesis), have raised safety concerns for the general public and governments around the world. The investigation of biochemical and toxicological effects of AgNPs described in this thesis arises from the decision in 2006 by the Organization for Economic Co-operation and Development to coordinate research on the toxicity of ENMs. As part of this international initiative Canada agreed to research the toxicity of titanium dioxide and silver nanoparticles. More specifically, Dr. Chris Metcalfe from Trent University, Peterborough, ON, Canada, received a grant and collaborated with my supervisors (and other researchers) to carry out research on nanotoxicity (see section 6.5 for more details).

### *1.3. Silver nanoparticles (AgNPs) as antimicrobial agent*

Silver nanoparticles are the most commonly used ENM and as of October 2013 were incorporated into 383 reported consumer and medical products, including clothing, appliances, wound dressings, and utensils (Nanotechproject, 2013). Their prevalent use is due to the antimicrobial properties of silver that have been known since the ancient times when silver vessels were used to disinfect water and wine (Yu et al., 2013). Similarly, early Americans (European immigrants) used silver coins to disinfect stored water. Prior to the 1800s silver was used to treat several infections, wounds, and ulcers (Chernousova

and Epple, 2013). The use of silver nitrate ($AgNO_3$) emerged in the late 19$^{th}$ century to treat eye infections, and in the mid-20$^{th}$ century $AgNO_3$ was discovered as an effective treatment for burn wounds (Fong and Wood, 2006). More recently, nanotechnology has improved the efficacy of silver as an antimicrobial agent through the synthesis and the subsequent incorporation of the AgNPs into various products (Kim et al., 2007; Chernousova and Epple, 2013).

The bactericidal activity of AgNPs is attributed to the release of silver ion ($Ag^+$) and nano-specific effects of AgNPs. It is known that AgNPs in wound dressings allow a controlled release of $Ag^+$ into the wound (Fong and Wood, 2006). $Ag^+$ interacts strongly with thiol groups, thus inactivating important enzymes, including the ones involved with electron-transport chain and DNA replication (Morones, et al., 2005; Gordon et al., 2010). In addition, $Ag^+$ denatures DNA and RNA (Fong and Wood, 2006) and leads to DNA condensation (Feng et al., 2000), ultimately affecting DNA replication and RNA translation. $Ag^+$ can also bind to electron donor groups, especially phosphorus and sulphur, in DNA and proteins, making them unavailable for various cellular processes (Clement and Jarrett, 1994). Furthermore, the $Ag^+$-mediated generation of reactive oxygen species (ROS) has also been reported (Foldbjerg et al., 2009; Gordon et al., 2010). In addition to the release of $Ag^+$, AgNPs damage the bacterial cell by attaching to the cell membrane, disrupting its proper function (Sharma et al., 2009), and generating ROS, which further damage the cell membrane and intracellular components (Hwang et al., 2008; Foldbjerg et al., 2009). The broad-spectrum bactericidal action of AgNPs is effective against Gram negative and Gram positive strains, as well as drug-resistant bacteria (Lara et al., 2010). The antiviral capacity of AgNPs against human

immunodeficiency virus type 1 (Elechiguerra et al., 2005) and hepatitis B virus (Lu et al., 2008) has also been reported.

*1.4. AgNP production*

To date only a few articles have estimated the production of AgNPs (and other ENMs). Such information is essential to predict the environmental concentrations and thus the risk associated with AgNPs (and other ENMs). Mueller and Nowack (2008) estimated the global production of AgNPs at 500 tons per annum (t/a). This estimate is based on the global production of silver (25,620 t/a), of which 95% is used for jewellery, photography, and industrial applications, suggesting that a maximum of 5% (1230 t/a) could be directed towards the production of AgNPs.

Schmid and Riediker (2008) estimated the production of AgNPs (and six other ENMs), but only in industries of Switzerland. The study surveyed 197 Swiss companies. Forty three companies were identified as ENM producers (or users), of which 15 companies produced (or used) AgNPs. The AgNPs production (or use) was estimated at 3.1 t/a among these surveyed Swiss companies. In comparison, the production (or use) for titanium dioxide nanoparticles ($TiO_2$NPs) was estimated at 435 t/a based on this survey.

Hendren et al. (2011) estimated the production of AgNPs (and four other ENMs) in the US. Ten companies that produced AgNPs were identified within the US, whose lower and upper limits for AgNP production were estimated at 2.8-20 t/a. In comparison, the production limits for $TiO_2$NPs in the US were estimated at 7800-38,000 t/a. Similarly, Piccinno et al. (2012) estimated the production of AgNPs (and nine other ENMs)

worldwide and specifically in Europe. Companies and institutions within the nanomaterial industrial sector were identified and surveyed. The results showed that AgNPs are produced in moderate quantities of 0.6-55 and 5.5-550 t/a in Europe and worldwide, respectively. In comparison, $TiO_2$NP production was estimated at 55-3000 and 550-5500 t/a in Europe and worldwide, respectively.

It is noteworthy that although AgNPs accounted for 24% of the total reported consumer products containing ENMs in 2013 (Nanotechproject, 2013), they are not the most produced ENMs. This may change, however, as there has been a 15-fold increase in the number of reported consumer products containing AgNPs between 2006 (~25 products) and 2013 (383 products) (Nanotechproject, 2013). Moreover, the linear increase in the number of reported consumer products containing AgNPs can be described by the equation y = 52.385x – 105,053, where y corresponds to the number of products and x is the year (Fig. 1.1). Assuming that the increase of AgNP-containing products is maintained at the same rate (~52 products/year), I predict that by 2020 there would be 765 consumer products with AgNPs (Table 1.1). It is likely that the increase in AgNP-containing products would lead to a proportional increase in AgNP production. Therefore, it is possible that 12.2-1216 tons of AgNPs would be produced in 2020 (Table 1.1), assuming the current worldwide production of 5.5-550 t/a estimated by Piccinno et al. (2012).

### *1.5. AgNP release into the environment*

Only a handful of studies have addressed the release of AgNPs from consumer products into the environment. A few key factors, including the method of incorporation

of ENM into the product and the product's lifetime and usage, will influence the release of ENMs from the various consumer products (Mueller and Nowack, 2008). Benn and Westerhoff (2008) examined several sock brands that contained AgNPs and demonstrated that some fabrics released as much as 68 μg Ag per g of fabric during a single washing cycle, whereas other fabrics released no detectable Ag during washing; the total amount of Ag present in the fabric did not predict how much Ag would be released. A much higher release of 377 μg/g was reported by Geranio et al. (2009), who simulated the washing of different AgNP-containing textiles; the authors also reported that at least 50% of Ag in the washing liquid was in the form of particles >450 nm in size. Similarly Lorenz et al. (2012) reported that 4.5-575 μg/g silver was released into the washing liquid in the form Ti/Si-AgCl nanocomposites, AgCl and $Ag_2S$ nanoparticles, AgCl particles, and agglomerated AgNPs. A recent study reported that physical activity resulting in sweating can also release Ag (von Goetz et al., 2013). At this time we remain unaware of all the factors affecting the release of Ag from AgNP-containing products or how much Ag is ultimately released and in what form.

The fate of AgNPs released from products containing these NPs has been modeled by several authors. Mueller and Nowack (2008) reported that the more prominent flows for AgNPs, at least in Switzerland, are between the products and the sewage treatment plant (STP), landfill, and waste incineration plant (WIP) (Fig. 1.2A). In a more recent study Mueller et al. (2013) estimated that 87% of AgNPs that enter WIP will make their way onto the landfill. Mueller and Nowack (2008) also estimated that 31% of AgNPs will dissociate into $Ag^+$, especially from textiles and plastics, and will be lost from the system; however, Blaser et al. (2008) predicted that $Ag^+$ will flow into the STP (Fig 1.2A), where

at least 94% will be removed and the remainder, a maximum of 6% $Ag^+$, will be present in the STP effluent mostly bound to particles, dissolved organic matter, sulfides, etc. (Wood et al., 1999). Gottschalk et al. (2009) also estimated the flow of AgNPs (and other ENMs) from commercial products to various compartments. The STP influent, sludge application to soil, and deposition onto landfill were the predominant flows for AgNPs (Fig. 1.2B). The efficacy of STP to remove AgNPs was assumed at 90.6-99.5%. It was predicted that approximately 16% of AgNPs would reach the surface water (Fig. 1.2B).

Furthermore, Gottschalk et al. (2009) estimated the environmental concentration of AgNPs in surface water at 0.088-2.63 ng/L and the predicted sedimentation rate was 0.153-10.18 µg/kg/a. In contrast, Blaser et al. (2008) predicted much higher concentrations of 40-320 ng/L and 2-14 mg/kg in surface water and sediment, respectively; these predicted environmental concentrations (PECs) were similar to the surface water PEC of 30-80 ng/L estimated by Mueller and Nowack (2008). On the other hand, the measured titanium concentrations in STP sludge reported by Kiser et al. (2009) resembled the PEC estimates for $TiO_2$NPs reported by Gottschalk et al. (2009). Furthermore, the water surface concentrations reported for colloidal and particulate Ag in various Texas rivers ranged <0.01-148 ng/L (Wen et al., 1997), which covers the range of both Blaser et al. (2008) and Gottschalk et al. (2009).

Assuming that the production and incorporation of AgNPs into commercial products increase at the same rate, one may predict that AgNP concentrations in surface water and sediment would increase proportionally. Therefore, using the information noted above, I predict that the AgNP concentrations in surface water, sediment, and sludge-treated soil would increase ~1.7-fold between 2014 and 2020 [see Table 1.1; these estimates are

based on the PECs reported by Blaser et al. (2008) and Gottschalk et al. (2009)]. This would imply that the risk of AgNPs to aquatic environments will increase, as will the need for ecotoxicological assessments.

*1.6. Environmental fate of AgNPs*

The fate of AgNPs (and other ENMs) in the aquatic environment remains largely unknown. Out of all the publications related to environmental health and safety of ENMs published by 2013 only 10% addressed environmental fate and transport, while 90% addressed the potential biological effects (Hendren et al., 2013). Furthermore, the properties of AgNPs, including the shape, size, and coating (also known as capping or stabilizing agent) will likely impact their fate (and ultimately toxicity) in the aquatic environment (Scown et al., 2010a; Levard et al., 2012; Yu et al., 2013).

However, before reaching the aquatic environment the AgNPs will have to pass through the wastewater treatment plant (WWTP). In a recent study, a pilot WWTP was fed with municipal wastewater containing a Ag background concentration of 1.5 μg/L (Kaegi et al., 2011). The influent was supplemented with AgNPs (stabilized with polyoxyethylene fatty acid ester) for 24 d and thereafter the WWTP operation continued for 17 d without AgNP addition. The mass balance indicated that AgNPs were present in the sludge (85%), wastewater (10%), and effluent (5%) (Kaegi et al., 2011). These flows correlated well with the predicted fluxes discussed in the previous section as well as in Hou et al. (2012), who reported complete removal of citrate-capped AgNPs from wastewater. As for speciation, the majority of AgNPs were present as $Ag_2S$ particles in both the sludge and effluent and only 8-15% remained as AgNPs (Kaegi et al., 2011).

Kaegi et al. (2012) also reported that the transformation of AgNPs into $Ag_2S$ occurred within 2 h; however, this transformation may be affected by the coating of AgNPs. Similarly Kim et al. (2010) reported that AgNPs in sewage sludge samples from various US WWTPs were present as 5-20 nm $Ag_2S$ particles.

Once the effluent is introduced into the surface water, the AgNPs are likely to undergo further transformations, including oxidation, dissolution, and/or sulfidation, depending on the environmental conditions (Levard et al., 2012). The transformation and fate of AgNPs have been investigated in a recent mesocosm study (Lowry et al., 2012), which included several plant species, mosquitofish (*Gambusia holbrooki*), and other species that colonized the mesocosm over the 18-month study period. The applied polyvinylpyrrolidone (PVP)-coated AgNPs (16.6 mg/L) rapidly precipitated from the water column during the first eight days and by the end of the study the Ag concentration was <0.05% of the initial dose. The AgNPs were found in the sediment (60%), soil (7%), and plants (0.2%). The mosquitofish and some of the invertebrate species did have Ag body burdens of 0.5-2.0 μg/g, suggesting that these species do remove at least some of the Ag from the water. As for speciation, the majority of AgNPs in the sediment were in the form of $Ag_2S$ (55%) and Ag-cysteine (27%), and only 18% remained unchanged. Despite the extensive sulfidation, the Ag remained bioavailable to the organisms present in the mesocosm.

The transformation of AgNPs into $Ag_2S$ (and AgCl) is thermodynamically favored, based on the solubility of the products ($K_{sp}$) and their stability constants ($K_f$) (Levard et al. 2012). The formation of $Ag_2S$, AgCl, and $Ag^0$ as major species was simulated in freshwater (and seawater) as a function of redox state (Eh) and pH (Levard et al., 2012).

AgCl was the favored form under aerobic conditions whereas $Ag_2S$ was predicted to form under anaerobic conditions. The authors also noted that the formation of $Ag_2S$ in WWTP is favorable due to pH and Eh conditions as was demonstrated by others (Kim et al., 2010; Kaegi et al., 2011).

In addition to sulfidation, AgNPs can also bind to natural organic matter (NOM), which is abundant in natural waters (Domingos et al., 2009; Liu et al., 2010a; Stankus et al., 2011; Thio et al., 2011; Kim et al., 2012). A recent study by Furman et al. (2013) showed that NOM, such as fulvic and humic acids (FA and HA, respectively), reduced the aggregation of citrate-capped AgNPs (20 mg/L), and that HA increased the mobility of AgNPs in the aquatic environment, while FA reduced it. Similarly, Gao et al. (2012) reported that AgNPs (unspecified coating) were stabilized with HA (<10 mg/L), whereas higher HA concentrations (>10 mg/L) induced aggregation. Other studies that addressed the behavior of AgNPs in natural waters in the presence and absence of humic materials and other organic solutes showed condition- and coating-dependent agglomeration or stabilization of AgNPs (Chappell et al. 2011; Li and Lenhart, 2012; Piccapietra et al., 2012). Moreover, two recent studies reported that AgNPs can be regenerated through sunlight-driven reduction of $Ag^+$ by organic matter (Hou et al., 2013; Yu et al., 2014), emphasizing the importance of environmental factors in determining the fate of AgNPs.

In light of these studies, it is apparent that AgNPs will transform and complex with other molecules within the aquatic environment, depending on environmental conditions and the NP capping agent. The transformations include the low solubility $Ag_2S$ or AgCl particles, and complexes with other molecules, such as NOM, which can either aggregate and precipitate the particles, or render them mobile. These dynamics are important

determinants of AgNP toxicity, since the precipitating Ag species would accumulate in the sediment and potentially affect the bacteria, algae, and bottom feeding organisms (including some fish species), whereas the soluble AgNP complexes would remain in the water column, potentially affecting pelagic species.

*1.7. Toxicity of AgNPs in fish*

A myriad of effects have been reported in fish exposed to AgNPs. Kashiwada et al. (2012) reported that Japanese medaka (*Oryzias latipes*) embryos exposed to 0.5-1 mg/L AgNPs (unspecified capping agent) up to 14 d demonstrated cardiovascular defects, ischemia, underdeveloped central nervous system, and differential expression of oxidative stress-, embryogenesis-, and morphogenesis-related genes. Fathead minnow (*Pimephales promelas*) embryos exposed to NanoAmor and Sigma AgNPs (0.625-25 mg/L) for 4 d showed increased mortality and developmental abnormalities; the uptake of AgNPs was also noted (Laban et al., 2010). Chae et al. (2009) reported that an acute exposure of juvenile medaka to Sigma AgNPs (1-25 μg/L) for up to 10 d influenced the expression of genes related to cellular and DNA damage/repair, metal detoxification, metabolic regulation, and oxidative stress. Pham et al. (2012) also reported that AgNP exposure (Sigma AgNPs at 1μg/L for 28 d) induced the expression of genes related to metal detoxification, oxidative and inflammatory stress, and immune response in the liver of medaka; there were also signs of estrogenic effects of AgNPs. Furthermore, Bilberg et al. (2010) showed an increased basal metabolic rate in the Eurasian perch (*Perca fluviatilis*) in response to a 3 d exposure to 63-300 μg/L PVP-coated AgNPs. Bilberg et al. (2011) also demonstrated that a 30 min exposure to PVP-coated AgNPs (0.45-45

μg/L) disrupted olfaction in the Eurasian perch and the Crucian carp (*Carassius carassius*).

In addition, zebrafish (*Danio rerio*) embryos were used as a model in a few studies. Asharani et al. (2008) reported physical deformities in zebrafish embryos, including bent and twisted notochord, pericardial edema, reduced heart rate, and degeneration of body parts, in response to a 72 h exposure to BSA- and starch-coated AgNPs at concentrations of 50-100 mg/L. Similar findings were documented by Bar-Ilan et al. (2009) in zebrafish embryos exposed to uncoated AgNPs at ~10 mg/L for 5 d and by Lee et al. (2007), who exposed embryos for 5 d to uncoated AgNPs (~4.3-76.6 ng/L). Griffitt et al. (2009) demonstrated that 1 mg/L AgNPs (metal oxide coating) exposure in adult zebrafish altered gill filament morphology and global gene expression. The delay in zebrafish embryo hatching in response to AgNPs (with various coatings) exposure was a common finding in a number of studies (Asharani et al., 2008; 2011; Yeo and Kang, 2008; Bar-Ilan et al., 2009; George et al., 2011; Powers et al., 2011).

AgNP bioaccumulation has also been reported. Gagné et al. (2012) showed that citrate-stabilized AgNPs (0.06-6 μg/L) accumulated in the liver of rainbow trout (*Oncorhynchus mykiss*) after a 4 d exposure, suggesting that some of these particles pass through the gills into the blood and accumulate in the liver. Farmen et al. (2012) reported that AgNPs (1-100 μg/L; unspecified coating) accumulated in the gills of Atlantic salmon (*Salmo salar*) after a 48 h exposure period; AgNPs also induced the expression of stress and metal detoxification genes and suppressed the expression of $Na^+$,$K^+$-ATPase. Similarly, Scown et al. (2010b) noted detectable levels of Ag in the gills and liver of rainbow trout exposed to AgNPs (10-100 μg/L; unspecified coating) for 10 d. Since the

Ag concentration in the liver was twice that in the gills, the authors suggested that AgNP uptake may also occur through the gut epithelium (Scown et al., 2010b). Intestinal absorption is indeed an important route of AgNP uptake as shown by Gaiser et al. (2012), who reported that significant amounts of Ag were found in various tissues, including gills, intestine, liver, and bile of the common carp (*Cyprinus carpio*) exposed to AgNPs (0.01 and 0.1 μg/L; unspecified coating) for 21 d; the Ag concentration in the intestine was 2-9-fold higher than in the gills. In contrast, Kwok et al. (2012) showed that the gills were the main site of AgNP (PVP-coated) uptake in medaka.

The effects of AgNPs reported by the majority of these studies occurred at concentrations higher than the PECs discussed in section 1.5, suggesting that AgNPs pose minimal risk to fish; however, the majority of these studies were acute. Prolonged exposures to more environmentally relevant concentrations of AgNPs did result in bioaccumulation in common carp (Gaiser et al., 2012) and did affect gene expression in medaka (Pham et al., 2012), suggesting that AgNPs may negatively impact fish. Moreover, as mentioned in section 1.5 most of the AgNPs that make their way into the aquatic environment will be found in the sediment, meaning that demersal fish species could be at a higher risk than pelagic fish species.

### *1.8. Proposed mechanisms of ENM toxicity*

#### *1.8.1. Overview*

As mentioned in the previous section multiple effects are reported in fish exposed to AgNPs. Nonetheless, the precise toxicity mechanisms of AgNPs (and other ENMs) remain unclear. It should be noted that the toxicity of ENMs will depend on

physicochemical characteristics, including composition, size, surface structure, solubility, shape, and aggregation (Nel et al., 2006), meaning that not all ENMs would be equally toxic. Several review papers over the past decade discussed 'nanotoxicity' and proposed a few mechanisms: 1) ROS generation and subsequent oxidative stress and damage to cellular components (cell membrane, proteins/enzymes, DNA); 2) dissolution and release of toxic species in the form of metal ions; 3) endocrine disruption [this is mostly based on Nel et al. (2009), who discussed the potential interactions of ENMs biological surfaces, including cellular receptors], and 4) inflammation and cell/tissue injury (fibrosis, granuloma formation, 'asbestos-like' effects), which are more pertinent to fibrous ENMs like carbon nanotubes (Buzea et al., 2007; Oberdörster et al., 2007; Chen and Schluesener, 2008; Gonzalez et al., 2008; Klaine et al., 2008; Auffan et al., 2009; Møller et al., 2010; Sharifi et al., 2012). Some of these mechanisms are discussed in the following sections.

*1.8.2. ROS generation and oxidative stress*

ROS are naturally generated by all aerobic organisms in what is termed 'the oxygen paradox' to reflect the toxicity of oxygen and the inability of aerobic organisms to survive in its absence. Oxygen is the final electron acceptor within the mitochondrial electron-transport chain (ETC) (Davies, 1995). It is estimated that 0.1-0.4% of oxygen is converted into the oxygen radical superoxide anion ($O_2^{\cdot -}$) due to 'leaky' ETC, making the mitochondria the main contributors of $O_2^{\cdot -}$ (Hermes-Lima, 2005). The reductive environment of the cellular milieu facilitates the conversion of $O_2^{\cdot -}$ into other ROS including hydrogen peroxide ($H_2O_2$) and highly reactive hydroxyl radical ($OH^{\cdot}$) (Figure

1.3), which could damage cellular components (Davies, 1995). Cell defense systems against oxidative stress and damage include 1) antioxidant compounds [e.g. reduced glutathione (GSH), vitamins C and E] and enzymes [superoxide dismutase (SOD), catalase (CAT), glutathione peroxidase (GPx)] (Figure 1.3); 2) direct repair systems, which could repair oxidized amino acids in damaged proteins and DNA hydroperoxides; and, 3) indirect repair systems, which remove and replace damaged components (Davies, 2000). Consequently, unbalanced generation of ROS (natural and ENM-derived) could overwhelm the defense systems and result in damage.

The ability of ENMs to generate ROS stems from the unique catalytic redox reactions that occur on the surface of these particles; this is especially relevant for particles that are <30 nm in size, which display a high surface area to volume ratio (Auffan et al., 2009). Previous studies demonstrated the ability of AgNPs to generate ROS and induce oxidative stress (e.g. Carlson et al., 2008; Choi and Hu, 2008; Neal, 2008; Piao et al., 2011). Therefore, I have studied the effects of AgNPs on the antioxidant system in order to better understand the involvement of oxidative stress in the toxicity of AgNPs (see section 1.10).

### *1.8.3. Dissolution*

The dissolution and release of metal ions have also received attention from the scientific community, especially in relation to metallic ENMs. More specifically, the debate on whether the toxicity of AgNP is due to its nanoscale properties, the dissolving $Ag^{+}$, or both is still ongoing (Lubick, 2008; Beer et al., 2012). Previous studies suggested that AgNP dissolution is dependent upon coating, size, concentration, and experimental

conditions (ionic strength, pH, temperature) (Fabrega et al., 2009; Kittler et al., 2010; Liu and Hurt, 2010; Zhang et al., 2011; Hadioui et al., 2013; Chambers et al., 2014). Assessment of AgNP dissolution is an important parameter since the toxicity of AgNPs has been shown to increase with increased dissolution (Kittler et al., 2010; Chambers et al., 2013). As mentioned in section 1.3 the antimicrobial properties of $Ag^+$ encouraged the incorporation of AgNPs into consumer products; however, the toxicity of $Ag^+$ is also well documented in fish, especially in relation to its ability to disrupt osmoregulation through the inhibition of gill $Na^+$,$K^+$-ATPase (Wood et al., 1999). Therefore, I have assessed the dissolution of AgNPs and compared the toxicity of AgNPs to $Ag^+$ in order to better understand the importance of Ag-type in Ag toxicity (see section 1.10).

*1.8.4. Endocrine disruption*

As defined by the World Health Organization's International Program on Chemical Safety an endocrine disruptor is "an exogenous substance or mixture that alters the function(s) of the endocrine system and consequently causes adverse health effects in an intact organism, or its progeny, or (sub) populations" (IPCS, 2002). Endocrine disruption is mediated by an interaction of a xenobiotic compound with hormone receptor or nonreceptor pathways, hormone secretion, and modulation of feedback mechanisms (Witorsch and Thomas, 2010). Although a significant progress has been made over the past decade in understanding the endocrine-disrupting potential of common pollutants (see references in Marty et al., 2011), the potential of ENMs to affect the endocrine system is still at its infancy even though it has been proposed that ENMs are likely to interact with cellular membranes, which could impact hormone- and non-hormone-

mediated signaling cell signaling (Nel et al., 2009). A recent review emphasized the importance of investigating endocrine disrupting potential of ENMs, which to date has only been addressed in a few studies focusing primarily on mammalian systems (Lu et al., 2013).

The hormone-regulated process that I have investigated is the stress response. Fish display a typical vertebrate stress response that includes 1) the immediate response mediated by the sympathetic nervous system ('fight-or-flight' response), and 2) the delayed hypothalamic–pituitary–interrenal (HPI) axis-mediated response. The former involves the adrenergic system mediated by the catecholamines (epinephrine and/or norepinephrine). Catecholamines increase cardiac contraction and liberation of fatty acids by adipose tissue (Van Heeswijk et al., 2006), as well as mobilization of energy reserves primarily through glycogenolysis and to a lesser extent through gluconeogenesis [both of these processes are mediated primarily by the hepatic β-adrenoreceptors (ARs)] (Nickerson et al., 2001). On the other hand, the HPI axis involves the synthesis and release of cortisol, which binds to the cytosolic glucocorticoid receptor (GCR) and ultimately increases hepatic gluconeogenesis (Mommsen et al., 1999; Vijayan et al., 2003; To et al., 2007).

### *1.9. Model systems*

#### *1.9.1. Zebrafish*

The zebrafish is one of the more effective aquatic models to study the effects of emerging pollutants including ENMs. It shares with mammals important anatomical features like the blood-brain barrier, endothelial cells, and immunogenic responses (Fako

and Furgeson, 2009), allowing numerous comparisons to be made (Schmale et al., 2007). Fecundity of zebrafish is high, producing potentially 200-300 embryos in a single day under laboratory conditions. The clarity of the zebrafish embryos allows for visualization of *in vivo* processes such as organogenesis, vasculogenesis, and abnormalities that may arise during development. Furthermore, the digestive, nervous and cardiovascular systems are similar to the human systems, making zebrafish potential models for human disease (Lieschke and Currie, 2007). Moreover, the entire genome has been sequenced, making zebrafish an attractive model for gene expression studies. Another important feature of the zebrafish embryo is the chorion that surrounds and protects the organism during development. Intercrossing layers contain pores between 500 and 700 nm (Fako and Furgeson, 2009), and this size is sufficient to potentially allow ENMs including AgNPs to pass through by passive diffusion and target the embryo.

Zebrafish have been mostly used in developmental biology and molecular genetics. However, more recently zebrafish have also been recognized as a valuable vertebrate model for toxicology and drug discovery, which is evident from the increased number of studies using zebrafish as a model, especially in high-throughput, large-scale toxicity screening studies (Hill et al., 2005; Fako and Furgeson, 2009). As noted in section 1.7, zebrafish was a common model to study AgNP toxicity and this will be further elucidated in Chapters 2 and 3 where I have used this species for the study of AgNP effects on oxidative stress and stress response.

*1.9.2. Rainbow trout erythrocytes and hepatocytes*

Erythrocytes are a sensitive model for oxidative stress resulting from their susceptibility to peroxidation. Although erythrocytes possess an extensive antioxidant defense system including antioxidant enzymes and substrates (Fig. 1.4), these cells are susceptible to peroxidation due to the high content of poly-unsaturated fatty acids in their cell membrane and high cytoplasmic oxygen and iron concentrations, which continuously produce ROS (Li et al., 2013). Unlike their mammalian counterparts, fish erythrocytes are nucleated and contain mitochondria (Thorgaard et al., 2002), providing additional sources of ROS. As discussed in Chapter 4 erythrocytes have antioxidant enzymes and relatively large glutathione reserves, which could be easily measured in order to assess oxidative stress. In addition, the hemolysis assay is a quick and accurate method to measure cell viability.

Hepatocytes are the other *in vitro* model used in this thesis. These cells are standard tools for studies involving the hormonal regulation of metabolism, including catecholamines and their downstream processes, including glycogen and glucose metabolism (Mommsen et al., 1988; Moon, 2004). Chapter 5 duscusses receptor-mediated glucose production as a marker of endocrine disruption. Hepatocytes are also extensively used in the field of toxicology. Liver is a major organ involved in xenobiotic metabolism; it possesses a wide range of detoxifying enzymes involved in a variety of reactions to render xenobiotic compounds more soluble to be eliminated from the organism (Guillouzo, 1998; Castano et al., 2003). Similarly to erythrocytes, hepatocytes possess an extensive antioxidant defense system, making them applicable in oxidative stress studies as discussed in Chapter 4.

*1.10. Thesis hypotheses and objectives*

The overall objective of this thesis was to investigate the toxicity mechanisms of AgNPs in fish. To this end the following hypotheses were tested:

1. AgNP exposure in zebrafish embryos and trout erythrocytes and hepatocytes results in oxidative stress; and,
2. Exposure to AgNPs disrupts the HPI axis-mediated stress response in zebrafish and interferes with the cell signaling associated with the β-AR and GCR systems in rainbow trout hepatocytes.

First, the role of oxidative stress in AgNP toxicity in zebrafish embryos was investigated (Chapter 2). The embryos were exposed for 4 d to AgNPs or $Ag^+$ at equivalent silver concentrations; the toxicity of $Ag^+$ in fish is well documented and AgNPs are known to undergo dissolution releasing $Ag^+$ to the medium. Generation of ROS and antioxidant levels were assessed after Ag-exposure. These experiments established a LC50 for AgNPs and $Ag^+$, and identified a single concentration of Ag for subsequent experiments on the zebrafish stress response (Chapter 3). The role of oxidative stress in AgNP toxicity was further elucidated in trout erythrocytes and hepatocytes (Chapter 4). In these experiments the cells were exposed for 48 h and the uptake of AgNPs, ROS generation, antioxidant levels, and damage to lipids, DNA, and proteins were assessed. These experiments established the cytotoxic AgNP concentration range, and identified a set of sub-cytotoxic concentrations that were used in subsequent experiments investigating the functions of the β-AR and GCR (Chapter 5).

**Table 1.1.** Predicted environmental concentrations (PECs) of AgNPs. The PECs in surface water, sediment, and sludge-treated soil are presented by year based on the increase in AgNP-containing consumer products and AgNP production. See footnotes as well as sections 1.4 and 1.5 for more details.

| Year | Number of products[a] | AgNP production worldwide (t/a)[b] | PEC surface water (ng/L)[c] | PEC sediment (µg/kg/a)[c] | PEC surface water (ng/L)[d] | PEC sediment (mg/kg/a)[d] | Sludge-treated soil (µg/kg/a)[c] |
|---|---|---|---|---|---|---|---|
| 2006 | **25** | 0.4-46 | 0.012-0.35 | 0.020-1.35 | 7-59 | 0.4-2.6 | 0.070-0.32 |
| 2007 | 84 | 1.3-133 | 0.039-1.17 | 0.068-4.53 | 25-197 | 1.2-8.6 | 0.234-1.06 |
| 2008 | 136 | 2.2-216 | 0.064-1.90 | 0.111-7.37 | **40-320** | **2.0-14.0** | 0.381-1.72 |
| 2009 | 188 | 3.0-300 | **0.088-2.63** | **0.153-10.18** | 55-443 | 2.8-19.4 | **0.526-2.38** |
| 2010 | 241 | 3.8-383 | 0.113-3.37 | 0.196-13.04 | 71-567 | 3.5-24.8 | 0.674-3.05 |
| 2011 | **313** | 5.0-498 | 0.147-4.38 | 0.255-16.95 | 92-736 | 4.6-32.2 | 0.876-3.96 |
| 2012 | 346 | **5.5-550** | 0.162-4.84 | 0.281-18.71 | 102-813 | 5.1-35.6 | 0.967-4.38 |
| 2013 | **383** | 6.1-609 | 0.179-5.36 | 0.312-20.74 | 113-901 | 5.6-39.4 | 1.072-4.85 |
| 2014 | 450 | 7.2-716 | 0.211-6.30 | 0.367-24.39 | 132-1060 | 6.6-46.4 | 1.260-5.70 |
| 2015 | 503 | 8.0-799 | 0.235-7.03 | 0.409-27.22 | 148-1183 | 7.4-51.8 | 1.407-6.36 |
| 2016 | 555 | 8.8-882 | 0.260-7.77 | 0.452-30.06 | 163-1306 | 8.2-57.1 | 1.553-7.03 |
| 2017 | 608 | 9.7-966 | 0.284-8.50 | 0.452-32.90 | 179-1430 | 8.9-62.5 | 1.700-7.69 |
| 2018 | 660 | 10.5-1049 | 0.309-9.23 | 0.537-35.73 | 194-1553 | 9.7-67.9 | 1.846-8.35 |
| 2019 | 712 | 11.3-1132 | 0.333-9.96 | 0.580-38.57 | 210-1676 | 10.5-73.3 | 1.993-9.02 |
| 2020 | 765 | 12.2-1216 | 0.358-10.70 | 0.622-41.41 | 225-1799 | 11.2-78.7 | 2.140-9.68 |
| *Sum*[e] | na | 94.9-9488 | na | 4.857-323.16 | na | 87.8-614.4 | 16.698-75.55 |

[a] *Number of reported products containing AgNPs. The bold numbers represent the number provided by Nanotechproject (2013). The rest of the numbers are calculated using the equation y = 52.385x – 105,053, where y is the number of products and x is the year, generated from the known number of products.*

[b] *Production of AgNPs worldwide in tons per annum. The bold numbers represent the estimated production reported by Piccinno et al. (2012). The production for other years is calculated proportionally to the estimated increase in AgNP-containing products.*

[c,d] *Predicted environmental concentrations for surface water and sediment. The bold numbers represent the estimated PEC as reported by Gottschalk et al. (2009)[c] and Blaser et al. (2008)[d]. The PEC for other years is calculated proportionally to the increase in AgNPs production.*

[e] *The Sum refers to the total amount of AgNPs produced and accumulated in sediment or the sludge-treated soil by 2020. The units are in t, µg/kg or mg/kg, depending on the units of the column's heading; 'na' denotes 'not applicable'.*

**Figure 1.1.** Number of reported consumer products that contain ENMs between 2005 and 2013. 'Total' refers to the number of consumer products that contain any ENMs (y = 200.13x – 401,093; $r^2$ = 0.97). 'AgNPs' refers to the number of consumer products that contain only AgNPs (y = 52.385x – 105,053; $r^2$ = 0.99). The data are derived from http://www.nanotechproject.org.

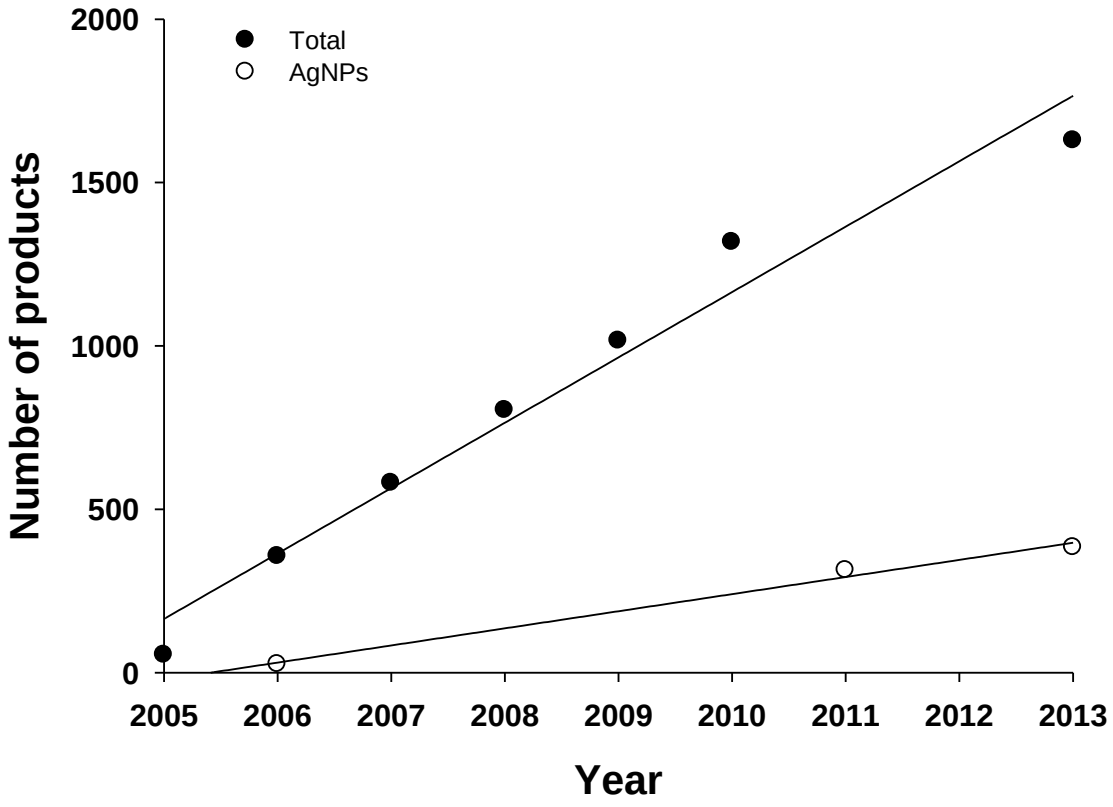

**Figure 1.2.** Flow of AgNPs from products into various compartments in Switzerland (A) and the US (B). The top number is based on the estimated usage of AgNPs in tons per annum (t/a) and the bottom number in brackets refers to the percentage that a given amount represents. 'WIP' signifies 'waste incineration plant'. 'STP' signifies 'sewage treatment plant'. 'Other' refers to reuse, export, and dissolution. Dashed arrows were used to clarify the flows if the arrows were crossing each other. Modified from Mueller et al. (2008) and Gottschalk et al. (2009).

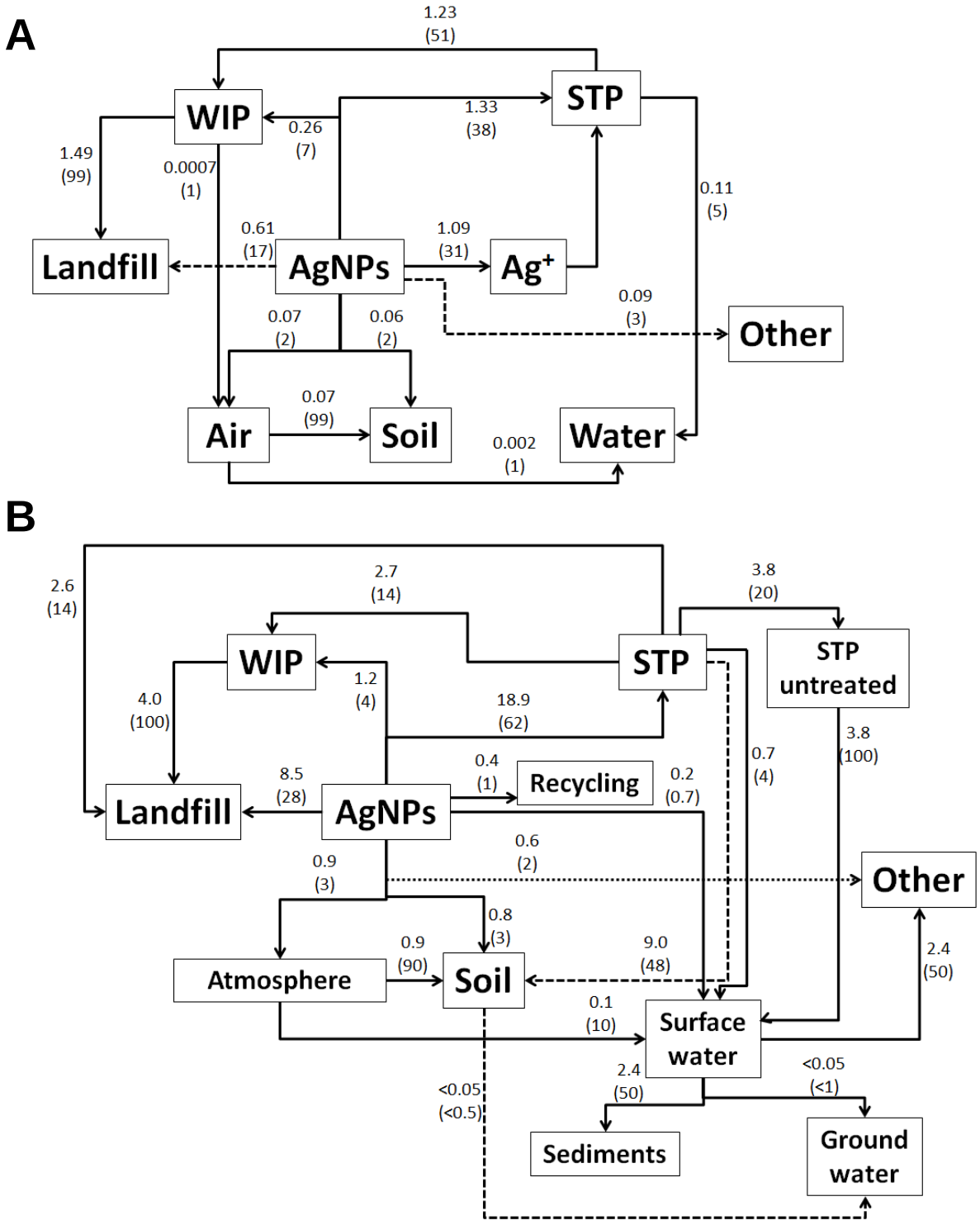
A
1.23
(51)
WIP
STP
1.33
(38)
0.26
(7)
1.49
(99)
0.0007
(1)
0.11
(5)
0.61
(17)
1.09
(31)
Landfill
AgNPs
Ag+
0.09
(3)
Other
0.07
(2)
0.06
(2)
0.07
(99)
Air
Soil
Water
0.002
(1)
B
2.6
(14)
2.7
(14)
3.8
(20)
WIP
STP
STP
untreated
1.2
(4)
4.0
(100)
18.9
(62)
3.8
(100)
0.7
(4)
0.4
(1)
Recycling
0.2
(0.7)
8.5
(28)
Landfill
AgNPs
0.6
(2)
0.9
(3)
Other
0.8
(3)
0.9
(90)
9.0
(48)
2.4
(50)
Atmosphere
Soil
0.1
(10)
Surface
water
2.4
(50)
<0.05
(<1)
<0.05
(<0.5)
Sediments
Ground
water

**Figure 1.3.** The antioxidant system considered in this thesis. Reactive oxygen species (ROS) include the superoxide anion ($O_2^{\cdot -}$), hydrogen peroxide ($H_2O_2$), and hydroxyl radical ($OH^{\cdot}$). The antioxidants include the enzymes superoxide dismutase (SOD), catalase (CAT), glutathione peroxidase (GPx), glutathione reductase (GR), glutathione-S-transferase (GST), and the tripeptide glutathione (GSH; reduced form), which is converted to its oxidized form (GSSG) upon reaction with ROS.

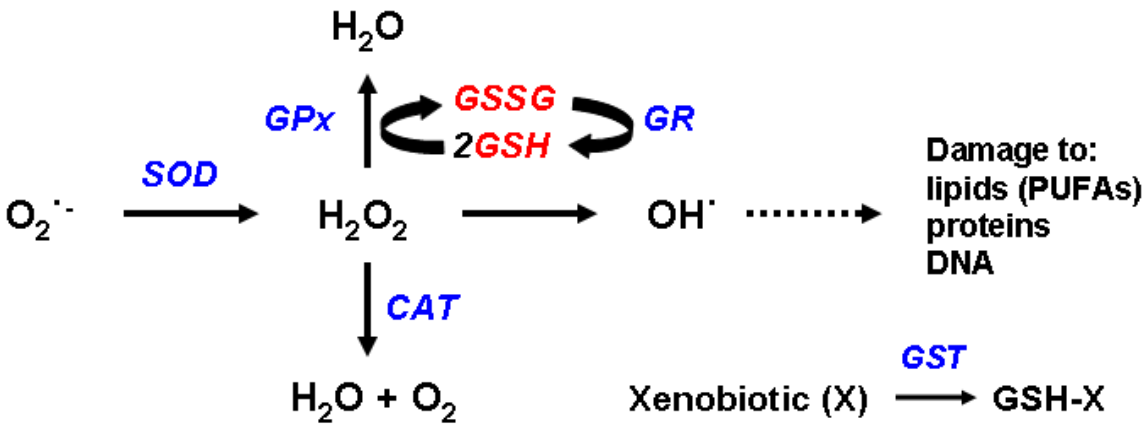

# CHAPTER 2
# Assessment of nanosilver toxicity during zebrafish (*Danio rerio*) development

This chapter is based upon the following article: Massarsky, A., Dupuis, L., Taylor, J., Eisa-Beygi, S., Strek, L., Trudeau, V.L., Moon, T.W., 2013. Assessment of nanosilver toxicity during zebrafish (*Danio rerio*) development. Chemosphere 92, 59-66.

Permission was obtained from the journal for incorporation of this article into this thesis. The article is based on the work that was conducted with the assistance of the undergraduate students Lisa Dupuis, Jessica Taylor, and Laura Strek, whom I directly supervised, as well as my colleague Dr. Shahram Eisa-Beygi, who shared his expertise on the ROS assay and microscopic imaging. I designed and conducted these experiments, and wrote the manuscript. Drs. Vance Trudeau and Thomas Moon provided input into the preparation of the manuscript and funding for the project.

*2.1. Introduction*

Nanotechnology is rapidly expanding with applications in engineering, electronics, medicine, and environmental remediation (Oberdörster et al., 2007). Engineered nanomaterials (ENMs) have at least one dimension of less than 100 nm and are more reactive than bulk materials of the same composition (Horie et al., 2012). As of October 2013 more than 1600 reported consumer products contained ENMs, with silver nanoparticles (AgNPs) representing the most prevalent ENM (Nanotechproject, 2013). Silver is known to have antiseptic properties, and nanotechnology enables the incorporation of AgNPs into various products, including wound dressings (Kim et al., 2007), clothing, kitchenware, children toys, and many more (Nanotechproject, 2013). Moistened AgNPs release Ag ions ($Ag^+$), which inactivate bacterial cell electron transport and DNA replication (Fong and Wood, 2006). Silver ions can also interact with thiol groups, which are found in antioxidants, thus contributing to oxidative stress (Morones et al., 2005; Chen and Schluesener, 2008). Moreover, AgNPs can attach to cell membranes, disturbing permeability and respiration (Morones et al., 2005), and generate reactive oxygen species (ROS) (Jones et al., 2011), which could damage lipids, proteins, and DNA.

Increased usage of AgNPs will lead to their emergence in the aquatic environment; e.g. AgNP-impregnated socks can release as much as 650 μg Ag after washing (Benn and Westerhoff, 2008). However, the fate and behavior of AgNPs in the aquatic environment are largely unknown. A recent study of a pilot wastewater treatment plant (WWTP) showed that AgNPs sorbed to wastewater biosolids and were mostly present as the less toxic $Ag_2S$ (Kaegi et al., 2011). A mesocosm study showed that despite significant

sulfidation, AgNPs remained bioavailable in the water column and accumulated in some of the organisms (Lowry et al., 2012). Furthermore, multiple effects are reported in fish exposed to silver. In Japanese medaka (*Oryzias latipes*) embryos exposure to AgNPs induced cardiovascular defects, ischemia, underdeveloped central nervous system, and expression of oxidative stress-, embryogenesis-, and morphogenesis-related genes (Kashiwada et al., 2012). In juvenile medaka AgNPs affected cellular and DNA damage/repair while $Ag^+$ altered the inflammatory response (Chae et al., 2009). AgNPs also altered the gill filament morphology and global gene expression in zebrafish (*Danio rerio*) (Griffitt et al., 2009), increased basal metabolic rate in the Eurasian perch (*Perca fluviatilis*), and disrupted olfaction in the Eurasian perch and the Crucian carp (*Carassius carassius*) (Bilberg et al., 2010; 2011). Silver ion also leads to osmoregulatory failure in fish, including a decrease in the $Na^+$,$K^+$-ATPase activity in rainbow trout gill at $Ag^+$ concentrations as low as 1.7 ng/mL (Wood et al., 1999).

There remains limited knowledge concerning mechanisms of uptake, biological fate and effects, and modes of action of ENMs including AgNPs in waterborne exposure scenarios (Stone et al., 2010). This study examined the effects of AgNPs on the developing zebrafish embryo and oxidative stress as a potential toxicity mechanism for Ag toxicity. It was hypothesized that exposure to AgNPs will generate ROS and elicit oxidative stress in the developing embryos. Thus, in addition to the heart rate and hatching success, the antioxidant levels were assessed. The toxicity of AgNPs was compared to $Ag^+$ (as $AgNO_3$) as $Ag^+$ is known to be toxic to fish (Wood et al., 1999). Finally, the effects of AgNPs and $Ag^+$ were assessed in the presence of the $Ag^+$ chelator

cysteine that may also bind to and induce aggregation of AgNPs (Hajizadeh et al., 2012). This was done to assess whether the observed effects are silver specific.

## *2.2. Materials and methods*

### *2.2.1. Silver nanoparticles (AgNPs) and silver nitrate ($AgNO_3$)*

The AgNPs used in this study were carboxy-functionalized, stabilized by sodium polyacrylate (31% total Ag), and dispersed in water (Vive Nano, 13010L). Aqueous stock solution of 1500 µg/mL was diluted to working concentrations in zebrafish egg water [containing an anti-fungal (3 mL/L 0.01% methylene blue) and salts (16 mL/L 60X E3 embryo media – in g/L: 17.2 NaCl, 0.76 KCl, 4.9 $MgSO_4 \bullet H_2O$, 2.9 $CaCl_2$)]. Silver nitrate ($AgNO_3$; source of $Ag^+$) was purchased from Sigma-Aldrich (204390) (63.5% total Ag) and a 100 µg/mL stock solution was prepared in ultrapure water. Total Ag concentrations noted on the Figures are based on the Ag contents of each Ag-type.

### *2.2.2. Characterization of AgNPs*

AgNP size and polydispersity index (PDI) were assessed using Dynamic Light Scattering (DLS; Zetasizer Nano, Malvern Instruments Ltd). Briefly, a 10 µg/mL AgNP solution was prepared in zebrafish egg water for DLS, and the measurements were repeated ten times to obtain the mean particle size and PDI. Scanning Transmission Electron Microscope (STEM; JEOL JSM-7500F Field Emission Scanning Electron Microscope) was used to visualize and confirm the DLS results. Briefly, a 10 µg/mL AgNP solution was prepared in MilliQ water, applied to a carbon-coated grid, and left to

dry overnight prior to visualization; photos were captured from transmission electron diffraction (TED) and back scattering of electrons.

The dissolution of AgNPs was assessed using the Amicon Ultra Centrifugal Filters (3 kDa; UFC800324) following the manufacturer's protocol. Briefly, 3.5 mL of the AgNP solution was applied to the device and centrifuged for 40 min at 8000 rpm (Sorvall RC centrifuge with SS-34 rotor) at room temperature. The flow through was then collected and analyzed using a Varian Atomic Absorption Spectrometer (AA240) fitted with a Ag 1.5" hollow cathode lamp (Perkin Elmer Atomax, N2025300). This method was used to assess the dissolution of the Vive Nano AgNPs used here; however, ICP-MS was used to analyze the flow through and a value of 0.04% $Ag^{+}$ was obtained (personal communication, Dr. Chris Metcalfe, Trent University).

*2.2.3. Zebrafish embryo collection*

Adult wild type zebrafish obtained from a local supplier (Big Al's Aquarium, Ottawa, ON) were maintained in holding tanks at 28°C on a 14:10 h light-dark cycle in a flow-through system (Aquatic Habitats, Apopka, FL) using aerated, dechloraminated City of Ottawa tap water. Plastic embryo collection traps were set between 4 and 6 PM and collected the following morning within 1 h of spawning between 9 and 10 AM. Collected embryos were placed in Petri dishes containing egg water and incubated at 28°C until separated into experimental groups. All experiments were performed on embryo batches generated from at least three ($n \geq 3$) separate 'mating events' with each treatment having two replicate Petri dishes. All procedures used were approved by the University of

Ottawa Animal Care Protocol Review Committee and conform to the guidelines of the Canadian Council for Animal Care for the use of animals in research and teaching.

*2.2.4. Experimental set-up*

At 3 h post fertilization (hpf), 10-20 embryos were randomly assigned to 5.3 cm plastic Petri dishes, containing a total volume of 14 mL egg water supplemented with 1 ml of AgNPs, $AgNO_3$ ($Ag^+$), or MilliQ water (for control embryos). Each treatment was performed in duplicate. Total Ag concentrations used were 0.03, 0.16, 0.31, 0.78, and 1.55 µg/mL, which are similar to concentrations of AgNPs used in previous studies with zebrafish embryos (Asharani et al., 2008; 2011; Bar-Ilan et al., 2009; George et al., 2011; Powers et al., 2011). These concentrations are higher than the predicted environmental concentrations of 0.088-2.63 ng/L AgNPs in surface water (Gottschalk et al., 2009). Our preliminary exposures to predicted environmental levels did not impact embryo survival or hatching success; hence, higher concentrations were chosen for the remainder of the study. For 'rescue' experiments, cysteine (Cys; 8.8 µM final concentration) was prepared in water and added to the egg water prior to the addition of the aforementioned Ag treatments. Although Cys complexes with Ag at 1:1 (Liu and Sun, 1981), its concentration in this study was ~1.6 times lower than the highest $Ag^+$ concentration in order to maintain neutral pH of the embryo medium.

All exposures were carried out in an incubator (Heraeus D-6450) at 28°C until 4 d post fertilization (dpf) without medium change. Embryos were not fed as the yolk sac provides sufficient nutrients until depleted at approximately 6 dpf (Westerfield, 2000). At 4 dpf the zebrafish larvae were euthanized with an overdose of tricaine methanesulfonate

(0.016%), rinsed with ice-cold distilled water to remove excess AgNPs, $Ag^{+}$, and Cys, and preserved in an appropriate medium: for enzyme assays, ice-cold 50 mM potassium phosphate buffer (KPB-50; pH 7.0), and for glutathione assays, ice-cold 5% sulfosalicylic acid (previously bubbled with nitrogen gas for 20 min). The samples were frozen in liquid nitrogen and stored at -80°C until analyzed.

*Note:* Embryos that were used for the detection of reactive oxygen species were pre-treated with 0.003% 1-phenyl-2-thiourea to supress pigmentation in developing embryos (Elsalini and Rohr, 2003). This was done to ensure that the pigmentation did not interfere with the fluorescent signal during microscopic observations of the larvae as described in section 2.2.6.

*2.2.5. Embryo toxicity analysis*

Zebrafish embryos were observed daily using a Nikon NBZ 1500 light dissecting microscope. Abnormalities, including non-depleted or malformed yolk sac, malformations of the spine and tail, formations around the pericardial or yolk sac regions, stunted growth, degraded and opaque tissues, and edema in the body cavity, pericardial or yolk sac regions, were noted. In addition, embryo heart rate was assessed at 48 hpf using direct microscopic observation for 15 s for a minimum of 5 embryos at each concentration. Embryonic heart beat in zebrafish is first detectable at 24 hpf and is an important indicator of health (Asharani et al., 2008). Hatching success was assessed at 48 hpf, which is the average time when zebrafish embryos hatch (Westerfield, 2000); thus, any impact of Ag on hatching should be maximized at this time.

*2.2.6. Reactive oxygen species (ROS) generation*

The relative levels of ROS were estimated as previously described (Wu et al., 2011). Briefly, 72 hpf embryos were incubated in 1 μg/mL of the cell-permeable chloromethyl-2'7'-dichlorodihydrofluorescin diacetate (CM-$H_2$DCFDA; Invitrogen, Carlsbad, CA) for 2 h in the dark at room temperature. Upon a series of washes in zebrafish egg medium, embryos were examined on a Nikon NBZ 1500 dissecting microscope with the green fluorescent protein (GFP) filter, equipped with a Nikon DXM 1200 C digital camera. The lowest and the middle Ag concentrations (0.03 and 0.31 μg/mL) were chosen for the assay to ensure sufficient embryo survival for the assay. The experiment was repeated three times with ten replicate larvae per treatment. The fluorescence data were quantified by using a scoring system, such that the embryos that resembled the majority of the controls received a score of 1, and those that displayed higher fluorescence received a score of 2. The average scores (ROS-score) from the three separate experiments were then subjected to statistical analysis.

We attempted to validate this technique using the method described in Deng et al. (2009), which involves the centrifugation of larval homogenate and the assessment of the resulting supernatant using 2'7'-dichlorodihydrofluorescin diacetate (DCHF-DA). However, it appears that silver (both AgNPs and $Ag^+$) interferes with this assay possibly by inhibiting the esterases that cleave the diacetate group, thus lowering the generation of fluorescent product. Lower fluorescence has been consistently observed with embryos exposed to AgNPs and $Ag^+$ despite a series of rinsing with phosphate buffered saline (PBS) prior to homogenization, suggesting silver uptake by the larvae. Similar

observations were made with silver (AgNPs or $Ag^{+}$) added to the supernatant from control embryos. The decrease in fluorescence was dependent on silver concentration.

*2.2.7. Glutathione levels*

Glutathione levels were estimated as previously described (Hermes-Lima and Storey, 1996). Whole frozen zebrafish larvae (in 5% sulfosalicylic acid) were thawed and homogenized using a Kontes Micro Ultrasonic Cell Disruptor for 10 s, followed by a 5 min centrifugation at 5000 g (4°C) in a Beckman Coulter Microfuge® R centrifuge. The supernatant was used to assess total glutathione (TGSH) and oxidized glutathione (GSSG). TGSH was estimated by the rate of reduction of 5,5'-dithiobis(2-nitrobenzoic acid) (DTNB) at 412 nm by TGSH compared to a standard GSH curve. The reaction media contained 1 U/mL GR, 100 mM KPB (KPB-100), 0.25 mM NADPH, and 0.6 mM DTNB (prepared in KPB-100) and 10 µL sample supernatant. To estimate GSSG, the supernatant was treated with 24 mM 2-vinylpyridine in 500 mM KPB (KPB-500) for 90 min at room temperature to derivatize any reduced glutathione (GSH). GSSG was then estimated as described above but with GSSG standards. The GSH was then calculated using the equation TGSH = GSH + 2GSSG.

*2.2.8. Antioxidant enzymes activities*

Whole frozen zebrafish larvae (in KPB-50) were thawed and homogenized as above, followed by a 15 min centrifugation at 15,000 g (4°C) as above. The activities of the enzymes were assessed using a SpectraMax Plus Spectrophotometer (Molecular Devices, Sunnyvale, CA) and SOFTmax Pro software. The following assays were adapted from

Lushchak et al. (2001): Glutathione reductase (GR; EC 1.8.1.7) was assessed by following the oxidation of NADPH at 340 nm in a reaction medium containing 0.25 mM NADPH and 1 mM GSSG in KPB-50; Glutathione peroxidase (GPx; EC 1.11.1.9) was assessed by a coupled assay measuring the oxidation of NADPH catalyzed by GR at 340 nm in a reaction medium containing 1 U/mL yeast GR, 15 mM GSH, 4 mM sodium azide, 0.25 mM NADPH, and 0.2 mM $H_2O_2$ in KPB-50; Catalase (CAT; EC 1.11.1.6) was assessed by following the decomposition rate of 10 mM $H_2O_2$ at 240 nm in KPB-50. Superoxide dismutase (SOD; EC 1.15.1.1) was assessed with the SOD Assay Kit (Sigma, 19160), which is an indirect assay method based on xanthine oxidase and a color reagent that absorbs at 450 nm. All enzyme activities are reported based on protein concentrations assessed using the bicinchoninic acid (BCA) assay method (Sigma) and bovine serum albumin (BSA) as a standard.

*2.2.9. Statistical analysis*

Statistical analyses were conducted using SigmaPlot (SPW 11; Systat Software, Inc., San Jose, CA). Three-way analysis of variance (ANOVA) with a post-hoc Holm-Sidak method was used to test for significance in all measured endpoints. The three independent variables were Ag-type (AgNP or $Ag^+$), Ag concentration, and presence/absence of Cys. The ANOVA results are summarized in Table 2.1. A one-way ANOVA was used twice to determine the differences in ROS-score between the control and $Ag^+$ and between the control and the AgNP groups (see Fig. 2.5K). In all cases $P \leq 0.050$ was considered significant. The data are presented as means and standard deviation (SD) or standard error of the mean (SEM).

*2.3. Results*

*2.3.1. Characterization of AgNPs*

The average size of AgNPs used in this study in zebrafish egg water was 8.39 ± 0.98 nm based upon DLS estimates (Fig. 2.1A), with an average PDI of 0.156 ± 0.025, suggesting that the particles were relatively monodisperse. STEM analysis using TED showed dispersed AgNP particles of ~10-20 nm with some small aggregates (Fig. 2.1B). Back scattering STEM confirmed that particles seen in TED were indeed AgNPs seen as white dots (Fig. 2.1C).

As for dissolution, the stock AgNP solution was found to contain 0.5% silver ions. Ultrafiltration of lower concentrations (0.31-100 μg/mL) yielded Ag concentrations that were below the detection limit of the instrument (0.02 μg/mL), suggesting that at these lower concentrations the dissolution is less than 0.5%.

*2.3.2. Zebrafish embryo mortality, hatching, heart rate, and abnormalities*

Both forms of Ag were toxic to zebrafish embryos in a dose-dependent manner (Fig. 2.2A). There was a significant effect of Ag-type and concentration on total mortalities at 96 hpf. The $Ag^+$ was more toxic than AgNPs as the calculated LC50s at 96 hpf were 0.07 and 1.18 μg/mL, respectively (Fig. 2.2B). Cys treatment significantly (Table 2.1) reduced mortality for both Ag-types (Fig. 2.2A); even at the highest $Ag^+$ concentration the mortality dropped from 77% to 37%. Hatching success declined at 48 hpf for both Ag-types in a dose-dependent manner (Fig. 2.3A). There was a significant effect of Ag-type and concentration; however, $Ag^+$ was more potent than AgNP in delaying hatching. Cys treatment significantly (Table 2.1) improved the hatching success; even at the highest

$Ag^+$ concentration, the hatching improved from 16% to 42%. Moreover, both Ag-types significantly reduced embryo heart rate at 48 hpf, but not in a dose-dependent manner (Fig. 2.3B). Cys treatment generally restored the normal heart rate of most groups but this Cys-effect was less clear than for mortality and hatching. Furthermore, AgNPs appeared to adsorb to the embryo chorion as evident from the orange coloration, which was absent in presence of 8.8 μM Cys (Fig. 2.4).

The incidence of abnormalities generally increased with both Ag-types especially at the higher concentrations and included non-depleted yolk, bent tail, malformed spine, and edema (data not shown). It is important to note that even though both Ag-types resulted in embryonic abnormalities, there were no consistent trends (i.e. embryos exposed to the higher concentrations of $Ag^+$/AgNP did not always develop abnormalities).

In a separate experiment embryos were exposed to UV light (intensity of 2500 $\mu W/cm^2$ UV-B, 85 $\mu W/cm^2$ UV-A for 4 h at 3 hpf) together with $Ag^+$ or AgNP to test the photocatalytic properties of AgNPs. UV-treatment had no additional effects on mortality, hatching, or abnormalities (data not shown). The UV, however, reduced the heart rate by 15% regardless of treatment (data not shown).

### *2.3.3. ROS generation and antioxidant levels*

Both Ag-types appeared to elevate ROS (Fig. 2.5). Overall, the exposed embryos were more likely to display a higher fluorescence and had a higher ROS-score. This was especially evident with the embryos exposed to 0.31 μg/mL $Ag^+$ (Fig. 2.5F) with 75% of the embryos displaying the higher fluorescence phenotype, these embryos also had a significantly (Table 2.1) higher ROS-score (Fig. 2.5K). Despite the increased ROS

generation, the exposed embryos appeared normal on the bright field images (Fig 2.5). The generation of ROS is supported by the glutathione results as both Ag-types significantly reduced TGSH levels and $Ag^+$ was more potent than AgNPs (Fig. 2.6A). This decrease in TGSH was a result of a dose-dependent depletion of GSH, which was most potent in the case of $Ag^+$ treatment. Cys treatment significantly improved the levels of TGSH and even at the highest $Ag^+$ concentration the TGSH doubled. Levels of GSSG generally increased with increasing concentrations of both Ag-types, but none of these changes were statistically significant (Fig. 2.6B). Embryos treated with Cys showed equivalent GSSG levels, which were lower than the GSSG levels in control embryos not treated with Cys; this effect was independent of Ag treatment. The ratio of GSSG to TGSH was calculated as a measure of oxidative stress (Fig. 2.6C), and increased with Ag concentration independent of Ag-type. This trend was absent with Cys treatment.

Antioxidant enzymes activities are summarized in Table 2.2. GR activities were not statistically different between any Ag treatments nor did the addition of Cys have any effect on activities. GPx activities also were not significantly different between Ag treatments, although a trend for lower GPx activities with increasing $Ag^+$ concentrations was apparent and most replicates at the highest $Ag^+$ concentration had below background activities. This tendency was eliminated by Cys treatment. Interestingly, Cys-treated control embryos had higher GPx activities than their Cys-free counterparts. CAT activities showed no significant differences between any Ag treatments; however, Cys significantly increased CAT activities. Finally, SOD activities did not show significant differences between any Ag treatments, while Cys significantly decreased SOD activity.

**Table 2.1.** Summary of statistical analysis (P-values). Three-way ANOVA with post-hoc Holm-Sidak method was used to assess statistical differences ($P \leq 0.050$) on data found in Figures 2.2, 2.3, 2.6 and Table 2.2. The three factors were Ag-type, Ag concentration, and cysteine (Cys). 'NS' denotes 'not significant'.

| Endpoint | Ag-type (A) | Cys +/- (B) | Ag conc (C) | Interactions | | | |
|---|---|---|---|---|---|---|---|
| | | | | AxB | AxC | BxC | AxBxC |
| Mortality | < 0.001 | < 0.001 | < 0.001 | < 0.001 | NS | < 0.001 | 0.028 |
| Hatching | < 0.001 | < 0.001 | < 0.001 | < 0.001 | NS | NS | < 0.001 |
| Heart rate | < 0.001 | < 0.001 | NS | NS | NS | NS | < 0.001 |
| TGSH | < 0.001 | < 0.001 | < 0.001 | 0.011 | NS | < 0.001 | < 0.001 |
| GSSG | NS | < 0.001 | NS | NS | NS | NS | NS |
| GSSG/TGSH | NS | < 0.001 | 0.050 | NS | NS | NS | NS |
| GR | NS | NS | NS | NS | NS | NS | NS |
| CAT | NS | 0.004 | NS | NS | NS | NS | NS |
| SOD | NS | < 0.001 | NS | NS | NS | NS | NS |
| GPx | NS | 0.011 | NS | NS | NS | NS | NS |

**Table 2.2.** Activities of antioxidant enzymes in zebrafish exposed to various $Ag^{+}$ or AgNP concentrations in the presence or absence of cysteine (Cys) until 4 dpf. The activities of catalase (CAT), glutathione reductase (GR), glutathione peroxidase (GPx), and superoxide dismutase (SOD) were assessed in 96 hpf larvae. Data are presented as Mean ± SEM (n = 8-13 for Cys non-treated embryos and 3-4 for Cys-treated embryos). Three-way ANOVA with post-hoc Holm-Sidak method was used to assess statistical differences (see Table 2.1).

| | | | CAT[1] | | GR[2] | | GPx[2] | | SOD[1] | |
|---|---|---|---|---|---|---|---|---|---|---|
| | Ag conc (μg/mL) | | No Cys | Cys | No Cys | Cys | No Cys | Cys | No Cys | Cys |
| C | | | 25.0±2.5 | 28.6±6.4 | 8.6±0.7 | 10.6±0.3 | 24.0±3.6 | 37.7±2.3 | 2.9±0.4 | 2.1±0.1 |
| | 0.03 | $Ag^+$ | 20.5±2.9 | 20.8±3.0 | 8.3±1.0 | 9.5±0.5 | 18.4±4.6 | 26.5±5.3 | 3.0±0.4 | 1.9±0.1 |
| | | AgNP | 21.3±3.6 | 32.6±6.5 | 8.5±1.2 | 9.2±1.7 | 20.1±4.5 | 19.9±7.0 | 3.9±0.8 | 2.0±0.3 |
| | 0.16 | $Ag^+$ | 24.5±2.9 | 22.6±0.8 | 8.1±1.5 | 10.0±0.2 | 19.3±6.7 | 25.5±10.0 | 3.5±0.5 | 1.8±0.1 |
| | | AgNP | 24.4±2.7 | 29.4±3.3 | 8.7±1.0 | 8.8±0.4 | 12.4±4.2 | 19.4±4.2 | 3.8±0.6 | 1.7±0.1 |
| | 0.31 | $Ag^+$ | 22.7±3.8 | 26.5±2.3 | 9.9±2.6 | 10.3±0.9 | 17.0±6.2 | 21.4±4.6 | 3.8±0.6 | 2.0±0.2 |
| | | AgNP | 25.2±2.5 | 32.2±3.2 | 8.4±1.1 | 9.9±0.4 | 13.6±4.8 | 24.2±3.7 | 7.3±1.8 | 1.9±0.1 |
| | 0.78 | $Ag^+$ | 22.4±2.7 | 26.7±6.3 | 8.2±1.7 | 9.8±0.6 | 10.4±3.8 | 23.6±4.2 | 3.1±0.6 | 1.9±0.1 |
| | | AgNP | 25.8±2.4 | 28.7±2.5 | 9.3±1.2 | 8.8±0.4 | 12.5±4.4 | 18.6±1.8 | 3.6±0.5 | 1.9±0.1 |
| | 1.55 | $Ag^+$ | 22.2±3.1 | 33.0±6.9 | 8.4±1.8 | 8.1±1.2 | 3.5±3.5* | 19.9±4.6 | 3.2±0.6 | 2.0±0.2 |
| | | AgNP | 18.3±1.7 | 26.6±2.4 | 8.0±1.4 | 8.7±0.2 | 14.6±5.2 | 19.2±2.6 | 3.5±0.4 | 1.7±0.1 |

[1] *μmol/min/mg*

[2] *nmol/min/mg*

** most of the replicates in this group were below the detection limit*

**Figure 2.1.** Characterization of Vive Nano AgNPs used in this study. A. Dynamic Light Scattering (DLS) results of a 10 µg/mL AgNP solution prepared in egg water. Data are presented as Mean + SD (n = 10). B,C. Scanning Transmission Electron Microscope (STEM) results of a 10 µg/mL AgNP solution prepared in MilliQ water. Photos were captured from transmission electron diffraction (TED) (B) and back scattering of electrons (C).

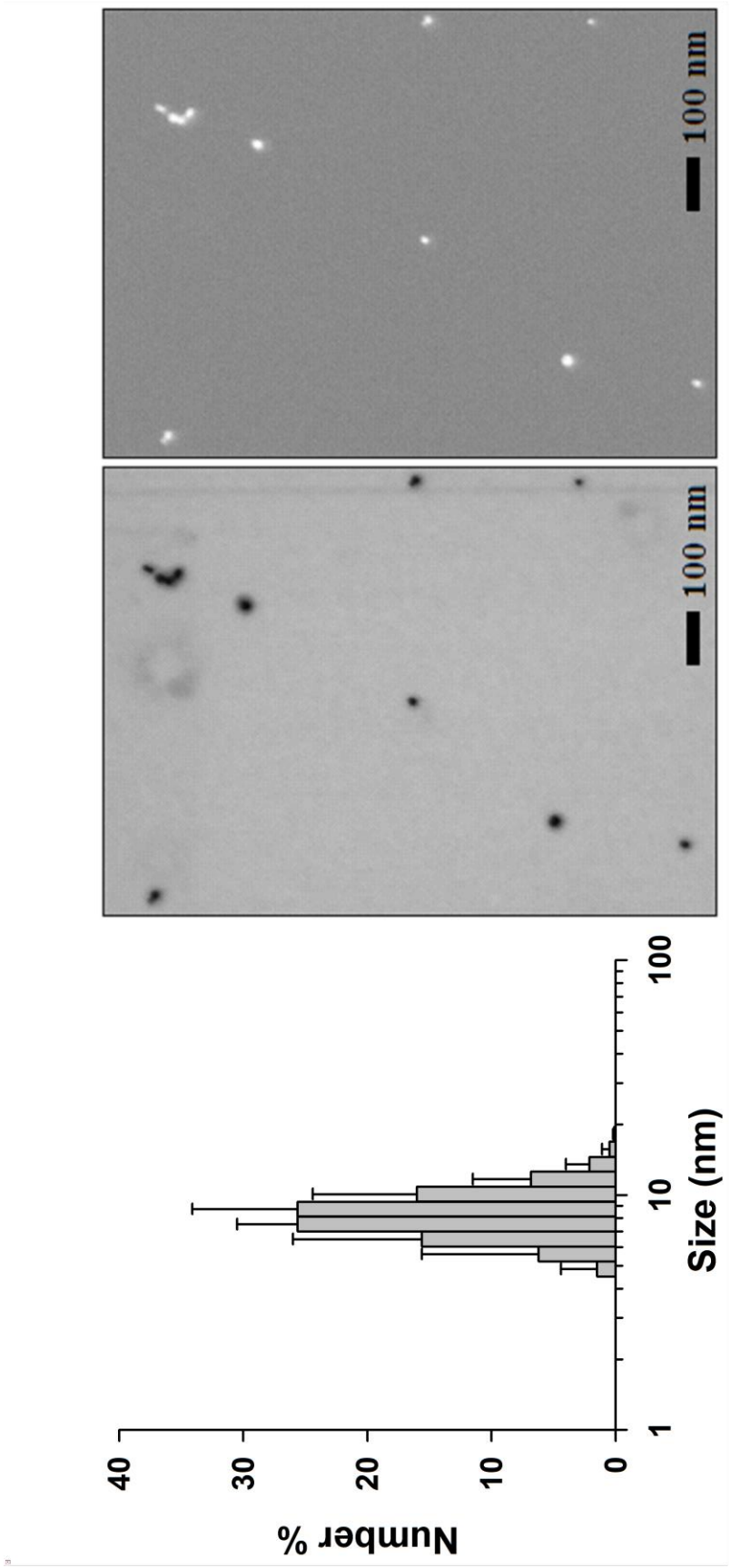
100 nm
100 nm
Number %
40
30
20
10
0
1
10
100
Size (nm)

**Figure 2.2.** Mortality of zebrafish exposed to various $Ag^+$ or AgNP concentrations in the presence or absence of cysteine (Cys) until 4 dpf. A. Mortality of zebrafish embryos after 96 hpf is presented as a percentage of those embryos that died. Data are presented as Mean + SEM (n = 7-15). Three-way ANOVA with post-hoc Holm-Sidak method was used to assess statistical differences (see Table 2.1). B. Probit analysis was used to determine the LC50 values for $Ag^+$ and AgNP based on the mortality data. The $r^2$ values are 0.96 and 0.75 for $Ag^+$ and AgNP, respectively.

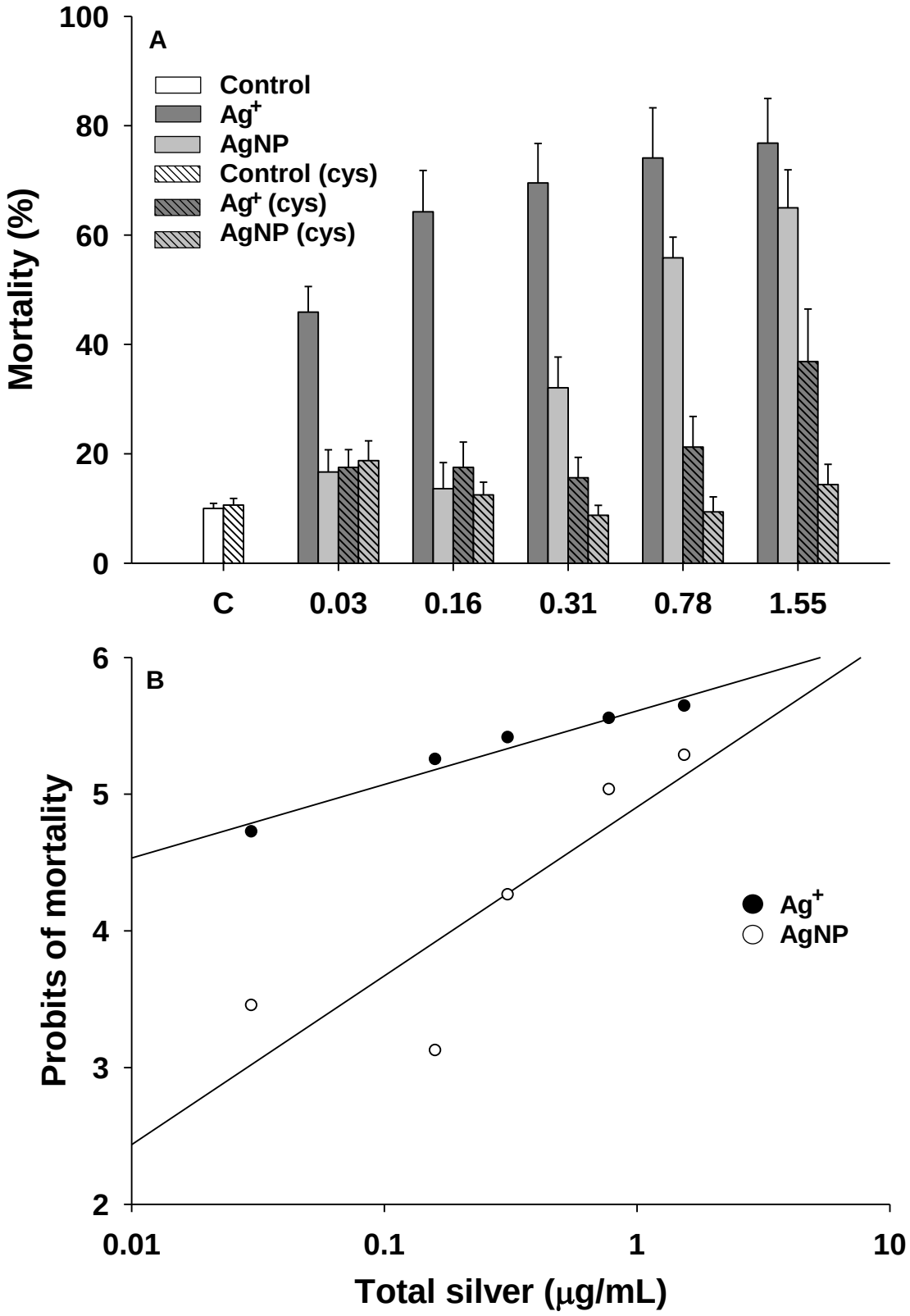
A
Control
Ag+
AgNP
Control (cys)
Ag+ (cys)
AgNP (cys)
Mortality (%)
100
80
60
40
20
0
C
0.03
0.16
0.31
0.78
1.55
B
Probits of mortality
6
5
4
3
2
Ag+
AgNP
0.01
0.1
1
10
Total silver (μg/mL)

**Figure 2.3.** Hatching success and heart rate of zebrafish exposed to various $Ag^{+}$ or AgNP concentrations in the presence or absence of cysteine (Cys) until 4 dpf. A. Hatching success of zebrafish embryos at 48 hpf is presented as a percentage of total live embryos (n = 7-15). B. Heart rate of zebrafish embryos at 48 hpf (n = 8-17). Data are presented as Mean + SEM in both graphs. Three-way ANOVA with post-hoc Holm-Sidak method was used to assess statistical differences (see Table 2.1).

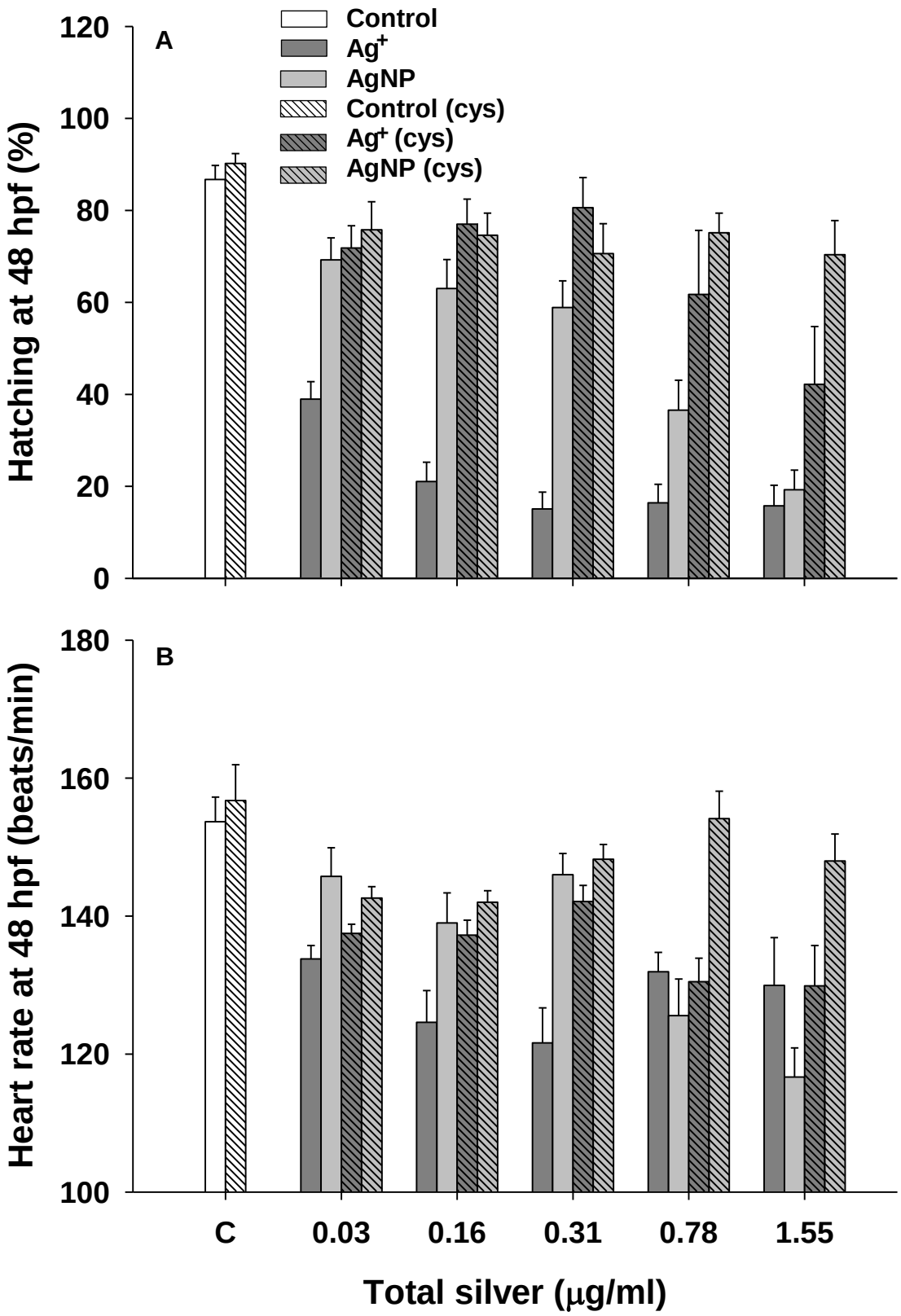
A
Control
Ag+
AgNP
Control (cys)
Ag+ (cys)
AgNP (cys)
Hatching at 48 hpf (%)
120
100
80
60
40
20
0
B
Heart rate at 48 hpf (beats/min)
180
160
140
120
100
C
0.03
0.16
0.31
0.78
1.55
Total silver (μg/ml)

**Figure 2.4.** Adsorption of AgNPs to the chorion of the zebrafish embryo at 24 hpf. The representative images are shown for A. Control embryos; B. Embryos exposed to AgNPs (1.55 μg/mL) in the presence of cysteine (Cys; 8.8 μM); C. Embryos exposed to AgNPs (1.55 μg/mL) in the presence of Cys (4.4 μM); D. Embryos exposed to AgNPs (1.55 μg/mL) in the absence of Cys.

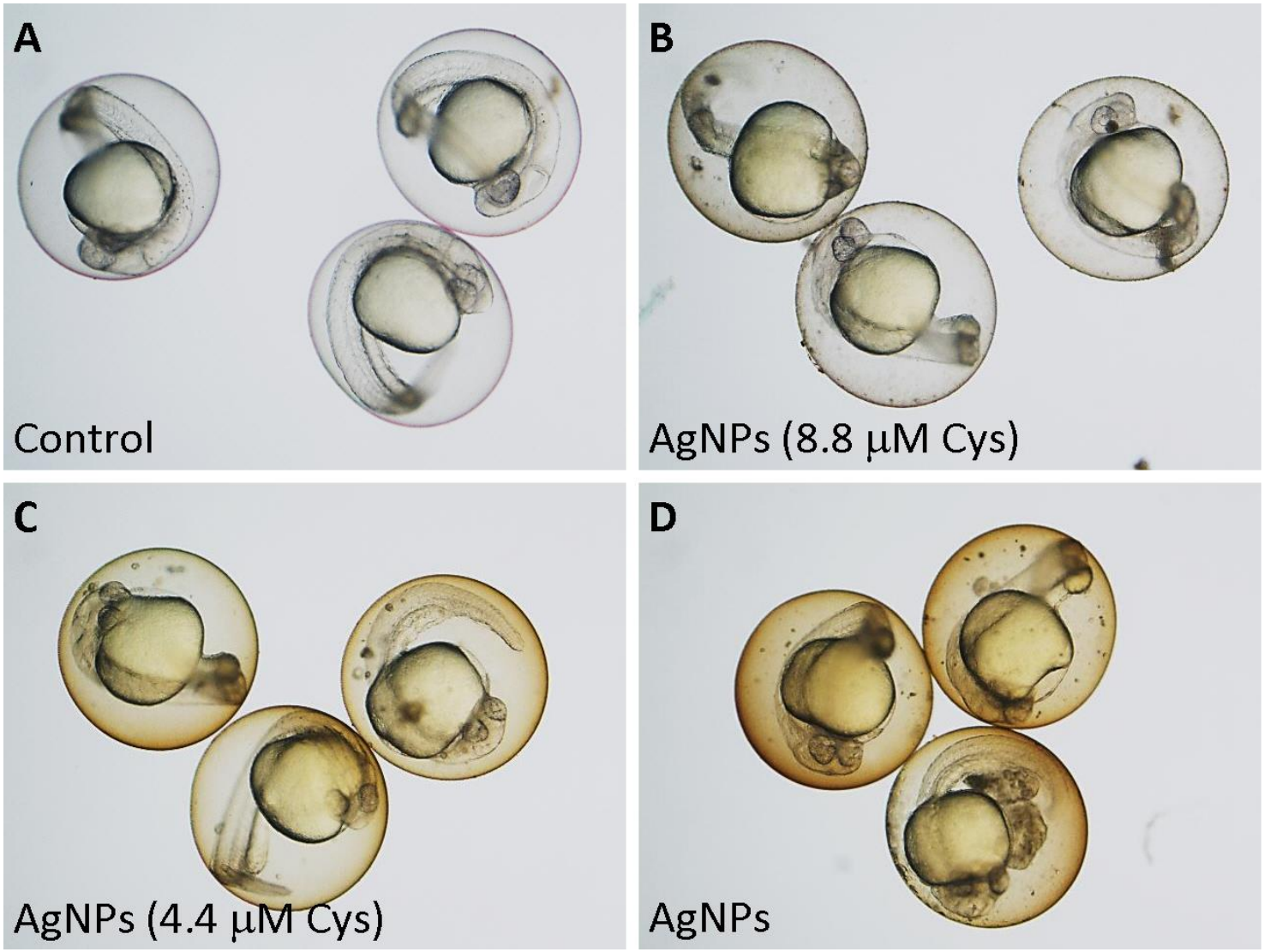
A
Control
B
AgNPs (8.8 μM Cys)
C
AgNPs (4.4 μM Cys)
D
AgNPs

**Figure 2.5.** Reactive oxygen species (ROS) generation in zebrafish exposed to various $Ag^+$ or AgNP concentrations until 3 dpf. Bright field images are displayed in panels A, C, E, G, and I, whereas panels B, D, F, H, and J display the same images using the GFP filter. The representative images from three different experiments are shown for (A and B) Control embryo; (C and D) Embryo exposed to 0.03 μg/mL $Ag^+$; (E and F) Embryo exposed to 0.31 μg/mL $Ag^+$; (G and H) Embryo exposed to 0.03 μg/mL AgNP; (I and J). The percentage on each of the fluorescent images refers to the percentage of embryos displaying the phenotype displayed on the image. K. The fluorescence data were quantified using a scoring system (ROS-score), such that a score of 1 was assigned if the image resembled the majority of the controls and 2 if it did not. Data are presented as Mean + SEM. The asterisk indicates statistical differences between the exposed and the control embryos. One-way ANOVA was used to assess statistical differences ($P \leq 0.050$).

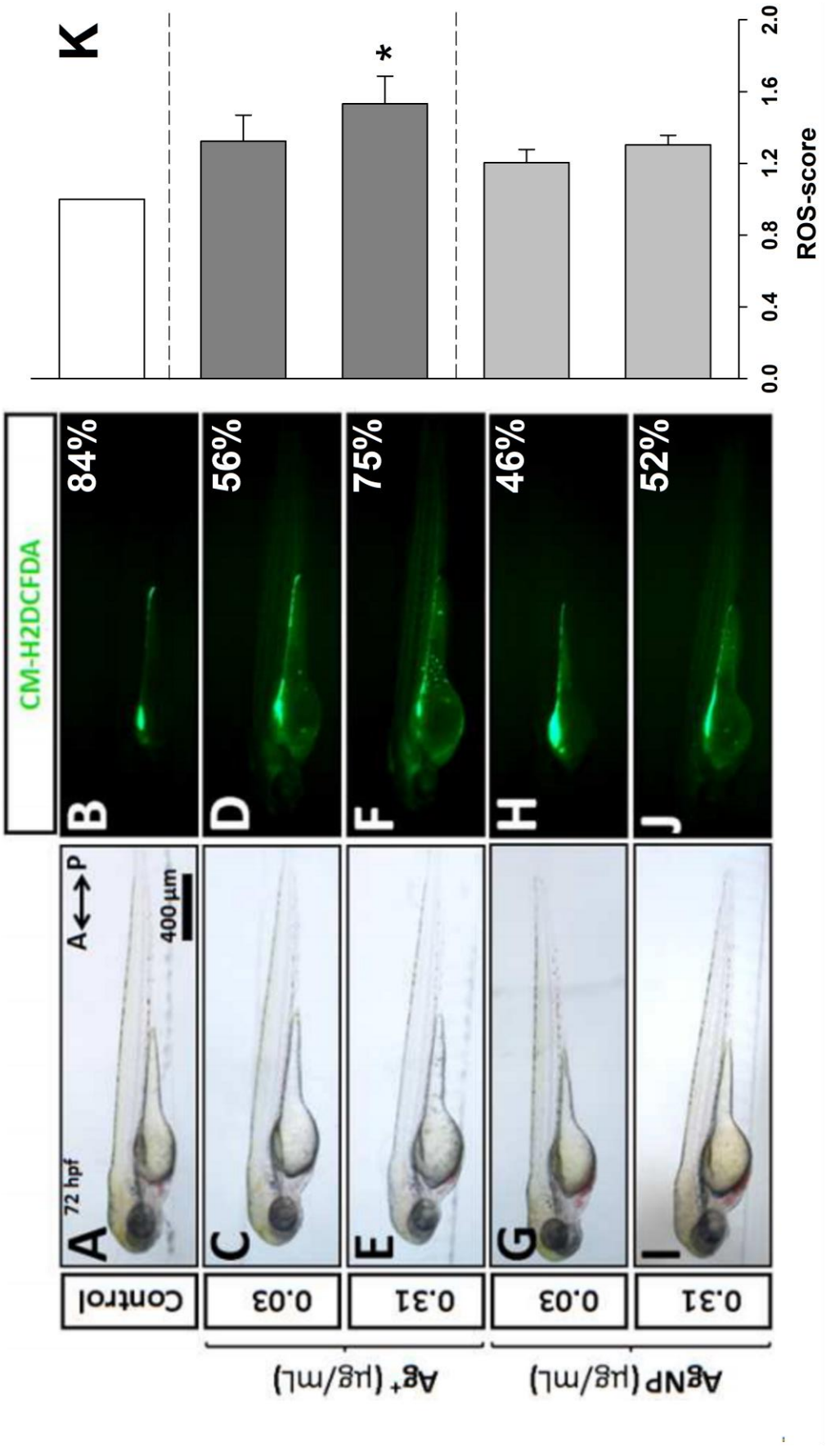
K
ROS-score
0.0
0.4
0.8
1.2
1.6
2.0
*
CM-H2DCFDA
A
72 hpf
A↔P
400 µm
B
84%
C
D
56%
E
F
75%
G
H
46%
I
J
52%
Control
0.03
0.31
0.03
0.31
Ag+ (µg/mL)
AgNP (µg/mL)

**Figure 2.6.** Glutathione levels in zebrafish exposed to various $Ag^{+}$ or AgNP concentrations in the presence or absence of cysteine (Cys) until 4 dpf. A. Total glutathione (TGSH = GSH + 2GSSG) levels. B. Oxidized glutathione (GSSG) levels. C. Ratio of GSSG to TGSH. Data are presented as Mean + SEM (n = 4-9). Three-way ANOVA with post-hoc Holm-Sidak method was used to assess statistical differences (see Table 2.1).

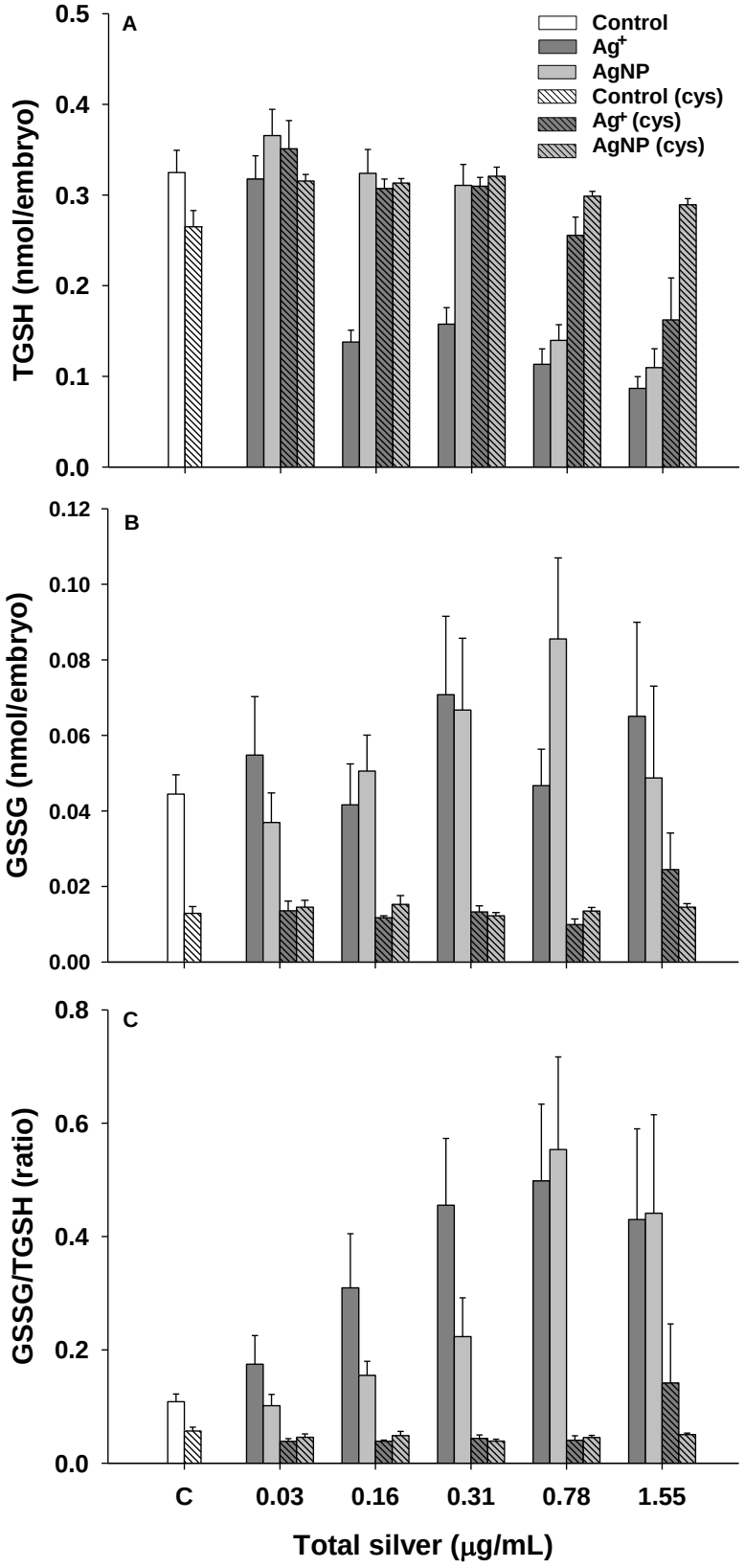
A
B
C
Control
Ag+
AgNP
Control (cys)
Ag+ (cys)
AgNP (cys)
TGSH (nmol/embryo)
GSSG (nmol/embryo)
GSSG/TGSH (ratio)
0.0
0.1
0.2
0.3
0.4
0.5
0.00
0.02
0.04
0.06
0.08
0.10
0.12
0.0
0.2
0.4
0.6
0.8
C
0.03
0.16
0.31
0.78
1.55
Total silver (μg/mL)

*2.4. Discussion*

We demonstrate that $Ag^+$ had greater effects than AgNP on zebrafish embryos. The amount of dissolved $Ag^+$ from AgNPs was low and estimated at less than 0.5%. Assuming 0.5% dissolution, the exposure concentrations of 0.03-1.55 μg/mL AgNPs would have contributed amounts of $Ag^+$ between 0.15 and 7.8 ng/mL, which were less than the lowest $Ag^+$ concentration used in this study. However, these low $Ag^+$ concentrations originating from the dissolution of AgNPs are in the same range as those that inhibit the trout gill $Na^+$,$K^+$-ATPase (Wood et al., 1999). Nonetheless, our study suggests that the effects seen for AgNPs are not simply due to $Ag^+$ dissolution. This may explain why $Ag^+$ was a more potent form of silver at the lower concentrations. However, at the higher concentrations the toxicity of AgNPs was similar to that of $Ag^+$, suggesting that AgNPs are also toxic.

The LC50 at 96 hpf for AgNPs was reported at 1.18 μg/mL. This LC50 is much lower than previously reported LC50s, which ranged 10-100 μg/mL (Asharani et al., 2008; 2011; Bar-Ilan et al., 2009). These discrepancies may be due to the differences in AgNPs size and capping agent. There was less difference for $Ag^+$ LC50 reported here (0.07 μg/mL) and elsewhere (0.03 μg/mL; Bar-Ilan et al., 2009). Moreover, several physical deformities were observed at all concentrations of both $Ag^+$ and AgNPs, but without a consistent trend. Physical deformities in zebrafish embryos, including bent and twisted notochord, pericardial edema, and degeneration of body parts, were noted previously using concentrations of 50-100 μg/mL of BSA- and starch-coated AgNPs (5-20 nm) (Asharani et al., 2008) and 100 μM (roughly 10 μg/mL) of synthesized colloidal nanosilver (3-100 nm) (Bar-Ilan et al., 2009). The mortality and higher incidence of

physical deformities could be at least partially attributed to the depressed heart rate observed in this study. AgNPs have been previously shown to interfere with normal activity of cardiac muscles. Improper blood flow to the brain and the spinal cord could starve the cells of essential nutrients and gases leading to decomposition (Asharani et al., 2008).

Furthermore, the hatching of embryos at 48 hpf was significantly delayed by both forms of silver. The $Ag^{+}$ was more effective and delayed the hatching even at the lowest concentration. However, at the higher concentrations the delay was similar for both types of silver, suggesting that AgNPs toxicity is not solely due to $Ag^{+}$ dissolution. Delay in hatching in response to AgNPs exposure was documented previously (Asharani et al., 2008; 2011; Yeo and Kang, 2008; Bar-Ilan et al., 2009; George et al., 2011; Powers et al., 2011) and could be attributed to the adsorption of AgNPs to the embryo chorion evident from the orange coloration. This was not expected because the pores of the chorion are 500-700 nm in diameter (Fako and Furgeson, 2009) and the AgNPs used here are 10-20 nm and non-aggregating. The adsorption of AgNPs to the chorion must be related to interactions between the AgNPs and components of the chorion, which could impact the transport of molecules between the internal and the external environments and delay hatching and/or decrease survival. In addition, AgNPs have been shown to inhibit the protease enzymes responsible for hatching (personal communication Drs. Kimberly Ong and Greg Goss, University of Alberta). Future studies should investigate whether the AgNPs are passing through the chorion.

The effects on hatching, heart rate, and survival were abolished by Cys, a non-essential amino acid, which contains a reactive thiol group. It has been previously shown

that silver ions have a high affinity for thiol-containing molecules including Cys (Liu and Sun, 1981; Liau et al., 1997; Kramer et al., 2009) and that Cys can protect from silver ions toxicity (Hussain et al., 1992; Liau et al., 1997; Yin et al., 2011). Cysteine also adsorbs to the surface of AgNPs, an effect that can be used to detect Cys since the Cys-AgNP complex results in a shift of surface absorption (Wu et al., 2009; Hajizadeh et al., 2012). Our study clearly demonstrates the ability of Cys to reduce the toxicity of both types of silver, possibly due to the formation of these Cys-Ag complexes. Furthermore, the adsorption of AgNPs noted above was prevented by Cys treatment as the embryos exposed concurrently to AgNPs and Cys had chorion similar in color to the control embryos. The effects of Cys on AgNP toxicity in this study contrast those of Navarro et al. (2008) and Yin et al. (2011), who both used Cys to differentiate the AgNP from $Ag^+$ dissolution from AgNPs effects. The former study suggested that the toxicity of AgNPs in algae (*Chlamydomonas reinhardtii*) was due to $Ag^+$ dissolution since Cys reduced AgNP toxicity; whereas the latter study reported that Cys did not affect the toxicity of AgNPs in common grass (*Lolium multiflorum*). These discrepancies suggest that the effect of Cys on AgNPs should be examined more closely in future studies.

Although the mechanisms for AgNP toxicity remain speculative, oxidative stress may be involved (Yeo and Kang, 2008; Chae et al., 2009; Wise et al., 2010). Our data supports this view as both types of silver generated ROS, reduced glutathione levels, and increased GSSG/TGSH ratios. The $Ag^+$ was more potent than the AgNPs in elevating ROS and reducing the GSH levels even at the lowest concentrations used. The depletion of GSH is indicative of oxidative stress since GSH acts as an electron donor to neutralize ROS (Park, et al., 2009; Tuncer, et al., 2010). This is consistent with Hussain et al. (2005)

and Piao et al. (2011), showing that in rat and human liver cells AgNP exposure resulted in GSH depletion, reduced mitochondrial potential, and increased ROS levels; $Ag^{+}$-mediated generation of ROS is also reported (Park et al., 2009). Alternatively, AgNPs were reported to interfere with the activity of GSH-synthesizing enzymes, reducing GSH levels (Piao et al., 2011). Activities of these enzymes were not measured in this study. Furthermore, $Ag^{+}$ has a strong affinity for redox-reactive and protective SH groups, like those found in GSH, that could be responsible for the observed GSH depletion (Carlson, et al. 2008; Kramer et al., 2009). It is unclear as to which mechanism is responsible for the observed depletion of GSH, perhaps all three are involved but it is certain that decreased GSH levels would increase the embryo susceptibility to oxidative damage. Moreover, it would be expected that as GSH reacts with ROS the levels of GSSG would increase; however, this study showed only a slight, insignificant trend for increased levels of GSSG upon exposure to both types of Ag.

The glutathione levels improved with Cys addition, such that only the highest $Ag^{+}$ concentration showed a reduction while the rest of the Ag-treated embryos displayed TGSH levels that were similar to the control group. It is possible, however, that in addition to the formation of Cys-Ag complexes Cys may also act as an antioxidant (Rayburn and Friedman, 2010; Tuncer et al., 2010). Importantly, it is the cysteine residue that confers antioxidant activity to GSH. Furthermore, Cys treatment reduced the GSSG levels in comparison with Cys-free embryos, which is also observed for the control groups. This could be explained by the ability of Cys to act as an antioxidant, thus reducing the usage of GSH and its conversion into GSSG. This would be also true of the control embryos since minimal oxidative stress naturally occurs in all aerobic organisms.

Despite the depletion of GSH with both $Ag^+$ and AgNPs the activities of antioxidant enzymes did not change with either form of silver. It was predicted that the activities would increase to compensate for falling GSH levels, especially with GR, which recycles GSSG in order to replenish GSH (Mannervik, 1987). There was a tendency for decreased GPx activity with increasing concentrations of total Ag. As GPx eliminates hydroperoxides by reduction of GSH, the decrease in its activity may relate to the observed decreased levels of GSH (Mannervik, 1987). The activities of CAT and SOD were also not affected by either type of silver. This could be due to the lack of formation of hydrogen peroxide and superoxide anions, suggesting that perhaps other ROS are formed. Alternatively, the GSH levels, although depleted, may be sufficient to neutralize ROS without elevating the activities of these enzymes.

In conclusion, AgNP and $Ag^+$ were both toxic to zebrafish embryos. Toxicity responses observed include mortality, delayed hatching, physical deformities, and depressed heart rate. Co-treatments with the chelator Cys overcame these effects. Both types of silver increased ROS production and decreased TGSH levels; in both cases $Ag^+$ was more potent than AgNPs. The addition of Cys improved TGSH levels. Overall our results show that oxidative stress plays a role in the toxicity of AgNPs and $Ag^+$.

# CHAPTER 3
# Acute embryonic exposure to nanosilver or silver ion does not disrupt the stress response in zebrafish (*Danio rerio*) larvae and adults

This chapter is based upon the following article: Massarsky, A., Strek, L., Craig, P.M., Eisa-Beygi, S., Trudeau, V.L., Moon, T.W., 2014. Acute embryonic exposure to nanosilver or silver ion does not disrupt the stress response in zebrafish (*Danio rerio*) larvae and adults. Sci. Total Environ. 478, 133-140.

Permission was obtained from the journal for incorporation of this article into this thesis. The article is based on the work that was conducted with the assistance of the undergraduate student Laura Strek (summer 2012; internship student from Université Nice Sophia Antipolis, France), whom I directly supervised, as well as my lab colleagues Drs. Paul Craig (RT-PCR work) and Shahram Eisa-Beygi (zebrafish spawning, husbandry, and dissections). I designed and conducted these experiments, and wrote the manuscript. Drs. Vance Trudeau and Thomas Moon provided input into the preparation of the manuscript and funding for the project.

*3.1. Introduction*

The advent of nanotechnology is considered the largest engineering innovation since the Industrial Revolution (Roco, 2005). Engineered nanomaterials (ENMs) are particles, tubes, rods, or fibers of less than 100 nm in at least one dimension (Niemeyer, 2001). ENMs are applicable in many fields, including healthcare, electronics, cosmetics, and clothing due to their unique physicochemical properties (Niemeyer, 2001). However, the same properties that make ENMs beneficial may also contribute to their toxicity, especially in relation to their ability to generate reactive oxygen species (ROS) and induce oxidative stress (Oberdörster et al., 2005; Lynch et al., 2007; Aillon et al., 2009; Prencipe et al., 2009).

The most common ENM in consumer products is silver nanoparticles (AgNPs) (Nanotechproject, 2013). The antimicrobial properties of silver (Ag) have been exploited since the 1800s (Chernousova and Epple, 2013), and in the mid-20$^{th}$ century Ag was introduced to treat burn wounds (Fong and Wood, 2006). Today Ag is commonly used in wound dressings and coatings of medical products. In recent years nanotechnology has improved the use of Ag for antimicrobial purposes through the synthesis and the subsequent incorporation of the AgNPs into various household and consumer products, including clothing, children toys, air and water purifiers (Nanotechproject, 2013).

ENMs have the potential to improve the quality of life, but they also raise health and safety concerns, especially in relation to the aquatic environment (Moore, 2006). Their application in clothing and personal care and household products may lead to their introduction into sewage treatment plants and ultimately into the aquatic environment. For example, studies demonstrated that various AgNP-textiles released 4.5-575 μg Ag/g

textile under various washing conditions (Benn and Westerhoff, 2008; Geranio et al., 2009; Lorenz et al., 2012), and a recent study reported that physical activity resulting in sweating can release even more Ag than normal washing (von Goetz et al., 2013). Although the environmental concentrations of AgNPs are unknown, Blaser et al. (2008) predicted concentrations of 40-320 ng/L, whereas Gottschalk et al. (2009) estimated 0.088-2.63 ng/L AgNPs in surface water.

A number of studies investigated the toxicity of AgNPs (concentrations ranged from 0.004 ng/mL to 0.1 mg/mL) in zebrafish (*Danio rerio*). These studies demonstrated that exposure to AgNPs altered gill filament morphology and global gene expression in adult zebrafish (Griffitt et al., 2009) and increased physical deformities in zebrafish embryos, including bent and twisted notochord, pericardial edema, reduced heart rate, and degeneration of body parts (Lee et al., 2007; Asharani et al., 2008; Bar-Ilan et al., 2009). Moreover, AgNPs delayed zebrafish embryo hatching (Yeo and Kang, 2008; George et al., 2011; Asharani et al., 2011; Powers et al., 2011) and led to oxidative stress (Chapter 2; Massarsky et al., 2013).

Although a variety of effects are reported, the potential of AgNPs to act as endocrine disruptors has not been sufficiently addressed. To the best of our knowledge this is the first study that attempted to examine the potential of AgNPs to disrupt zebrafish endocrine function, specifically the ability to elevate cortisol levels in response to stress. Cortisol is the principal corticosteroid in teleost fish secreted in response to stress and plays a key role in the regulation of the endocrine stress response (Mommsen et al., 1999), and pioneering studies by Hontela and colleagues demonstrated that

environmental contaminants including metals could disrupt the ability of fish to elevate cortisol levels when stressed (e.g. Hontela et al., 1995).

Fish display a typical vertebrate stress response, including an immediate response mediated by the sympathetic nervous system and specifically epinephrine/norepinephrine ('fight-or-flight' response), and a delayed hypothalamic–pituitary–interrenal (HPI) axis-mediated response. The HPI axis involves the corticotropin-releasing factor (CRF), which is produced in the preoptic area of the teleost brain located within the telencephalic stalk region (Folgueira et al., 2004) in response to hypothalamic stimulation (Alderman and Vijayan, 2012). In turn, CRF stimulates the release of the adrenocorticotropic hormone (ACTH) from the pituitary by specific G-protein coupled receptors (CRF-R1 and CRF-R2) and its further regulation by a shared binding protein (CRF-BP). Consequently, ACTH, which is synthesized from pre-pro-opiomelanocortin (pre-POMC), stimulates cortisol synthesis and release by interrenal cells of the fish head kidney (To et al., 2007). The HPI axis in zebrafish is fully developed by 4 d post fertilization (dpf) (Alsop and Vijayan, 2009); potentially, exposure to a toxicant during these early stages may impede its proper development. Therefore, this study aimed to investigate whether the early life exposure to AgNPs or $Ag^{+}$ can disrupt the formation of the HPI axis, thus affecting the ability of zebrafish larvae and/or adults to respond to a standardized stressor. To this end we examined whole-body (larvae) and plasma (adults) cortisol levels, as well as the abundance of CRF-related transcripts in larvae and in the adult brain. Cholesterol (cortisol precursor) and triglycerides (potential energy source) were also assessed in zebrafish larvae.

*3.2. Materials and methods*

*3.2.1. Silver nanoparticles (AgNPs) and silver nitrate ($AgNO_3$)*

The AgNPs used in this study were carboxy-functionalized, stabilized by sodium polyacrylate (31% total Ag) (Vive Nano, 13010L), and dispersed in water. These AgNPs were prepared in egg water and were characterized previously (Chapter 2; Massarsky et al., 2013) using Dynamic Light Scattering (8.39 ± 0.98 nm; average polydispersity index of 0.156 ± 0.025) and Scanning Transmission Electron Microscope (~10-20 nm). The amount of dissolved silver in the stock solution was estimated at 0.5% (Chapter 2; Massarsky et al., 2013). $AgNO_3$ (63.5% total Ag; source of $Ag^+$) was purchased from Sigma-Aldrich (204390) and a 100 μg/mL stock solution was prepared in MilliQ water. All Ag concentrations presented here are total Ag concentrations based upon the % Ag content of both AgNPs and $AgNO_3$.

*3.2.2. Experimental set-up*

See Chapter 2 (section 2.2.3) for details on zebrafish husbandry and embryo collection procedures. At 2 h post fertilization (hpf), 20 embryos were randomly assigned to 5.3 cm plastic Petri dishes, containing a total volume of 14 mL egg water supplemented with 1 mL of AgNPs, $AgNO_3$ ($Ag^+$), or MilliQ water (for control embryos). The nominal exposure concentrations were 0.5 and 0.05 μg/mL total Ag for AgNPs and $Ag^+$, respectively. These concentrations were used here as they led to similar mortality rates in our previous study (Chapter 2; Massarsky et al., 2013). The $Ag^+$ chelator cysteine (Cys) that also binds to and induces aggreagtion of AgNPs (Hajizadeh et al., 2012) was used in rescue experiments. Cysteine (8.8 μM final concentration) was

prepared in water and added to the egg water prior to the addition of each Ag treatment. Static exposures were conducted in an incubator at 28°C until 4 dpf, similarly to our previous study (Chapter 2; Massarsky et al., 2013). The embryos were not fed as the yolk sac provides sufficient nutrients until depleted at approximately 6 dpf (Westerfield, 2000). Throughout the exposure period heart rate (at 48 hpf), hatching success (at 56 hpf), and survival (every 24 h) were evaluated. At 4 dpf the surviving larvae from control and treatment groups were either 1) stressed using swirling as per Alsop and Vijayan (2008), left for 5 min, then euthanized on ice, rinsed with ice-cold distilled water, frozen on dry ice, and stored at -80°C until further analysis, or 2) raised to adulthood (10 months) in clean water without Ag to assess the adult stress response (the experimental set-up is summarized in Figure 3.1). These fish were housed at a maximum density of 5 fish/L in 3 L tanks and fed approximately 1% body weight twice a day; the food consisted of 2:1:1 mixture of Adult Zebrafish Complete Diet (Zeigler®), Spirulina Aquarium Flake Food (Ocean Star International), and Golden Pearls 300-500 μm (Artemia International LLC). All experiments were performed on embryo batches generated from at least four ($n \geq 4$) separate 'mating events' with each treatment having two replicate Petri dishes. Embryos from four batches ($n = 4$) were raised to adulthood.

### *3.2.3. Adult zebrafish tissue collection*

Ten months old adult zebrafish were stressed using the standard netting stress of Ramsay et al. (2009) and euthanized in ice-cold water. The fish were weighed and blood (5-15 μL) from the amputated-tail region was carefully collected into a 0.2 mL PCR tube using a heparinized capillary tube. The blood was centrifuged at 7000 g for 2 min and the

resulting plasma was collected into a fresh 0.2 mL PCR tube (plasma from two fish of same sex was pooled to ensure sufficient volume for cortisol analysis). The cranial cap was removed and the telencephalon (Fig. 3.2) was carefully excised, placed into a 1.5 mL tube, and frozen on dry ice; at least two telencephalons were combined to ensure sufficient RNA. Both CRF and CRF-BP genes are primarily expressed in the zebrafish telencephalon (Alderman and Bernier, 2007), and to minimize the sampling time only the telencephalon was collected. All samples were frozen as quickly as possible and stored at -80°C until analyzed. Fish were euthanized between 10 am and 1 pm.

### *3.2.4. Lipid extraction*

Total lipid extraction was performed using a modification of the Folch method (Folch et al., 1957). Briefly, frozen zebrafish larvae were transferred to 15 mL Falcon tubes to which 7.5 mL 2:1 chloroform-methanol (v/v) was added. The contents were homogenized for 10 s with a tissue homogenizer (Polytron, Kinematica GmbH Kriens, Luzern Brinkmann Instruments). The samples were incubated for 15 min at room temperature to ensure an optimal extraction, and extracts were washed with 2 M KCl containing 5 mM EDTA (1 part KCl to 5 parts extract). The tubes were shaken for 10 s and incubated at room temperature for 30 min to ensure layer separation. The bottom organic layer was collected into glass tubes and evaporated to dryness under a stream of nitrogen gas. Following drying, 0.2 mL 2-methoxy-ethanol was added to each tube to dissolve the lipid fraction. The tubes were vortexed for 10 s and contents were transferred to fresh 1.5 mL conical centrifuge tubes.

*3.2.5. Cortisol, cholesterol, and triglycerides assays*

Cortisol content in larval lipid extracts and adult plasma was assessed using a radioimmunoassay (RIA) $^{125}$I kit as per the manufacturer's protocol (MP Biomedicals, Orangeburg, NY). Cholesterol and triglycerides contents were assessed in larval lipid extracts using the cholesterol and triglycerides liquid reagent kits (TECO Diagnostic, Anaheim, CA) following manufacturer's protocols.

*3.2.6. Total RNA extraction and cDNA synthesis*

Total RNA from frozen zebrafish larvae was extracted using TRIzol Reagent (Invitrogen, Carlsbad, CA) according to the manufacturer's protocol. Total RNA from the zebrafish telencephalon was isolated using a commercially available RNeasy mini-prep kit (Qiagen) following manufacturer's protocol. Total RNA concentration and purity were determined using a NanoDrop 2000 Spectrophotometer (Thermo Scientific). The RNA quality was further confirmed using gel electrophoresis. Samples were stored at -80°C until cDNA synthesis using a QuantiTect Reverse Transcription kit (Qiagen) following manufacturer's protocol.

*3.2.7. Quantitative RT-PCR analysis*

*3.2.7.1. Zebrafish larvae*

Primers for CRF, CRF-BP, CRF-R2, POMCb, and β-actin (see Alderman and Bernier, 2009) were acquired from Invitrogen (Table 3.1). Amplicon sizes were confirmed using PCR and gel electrophoresis. Quantitative RT-PCR was performed using a CFX96 Real-Time PCR detection system (BIORAD) with Brilliant III SYBR Green

Master Mix (Agilent Technologies, Santa Clara, CA). Each reaction contained 10 μL SYBR Green Master Mix, 0.3 μL of diluted (1:500) reference dye, 1 μL of each the forward and reverse gene-specific primers (0.25 μM), 6.7 μL RNase/DNase-free purified water (Roche), and 1 μL diluted cDNA. The PCR cycling conditions were as follows: initial denaturation at 95°C for 3 min, 40 cycles of 95°C for 20 s, 60°C for 20 s, and 72°C for 30 s. A melt curve analysis was used at the end of each run to validate the amplification of only one product. Standard curves were constructed for each target gene using serial dilutions of a reference pool of representative cDNA from all experiments. Both RNase/DNase-free $H_2O$ and non-reverse transcribed RNA control samples were assayed to ensure no contamination was present in the reagents or in the primers used. To account for cDNA production and loading differences, all samples were normalized to the abundance of the housekeeping gene β-actin, which did not change significantly between experimental treatments. The abundance of each transcript was further normalized to the control group.

*3.2.7.2. Zebrafish adults*

The mRNA abundance in adult zebrafish telencephalon was quantified using a Rotor-Gene Q Real-Time PCR machine (Qiagen). An additional set of primers was designed using Integrated DNA Technology software (www.idtdna.com; Table 3.1) to generate smaller amplicon sizes to account for the shorter cycling durations. Each reaction contained 5 μL Rotor-Gene SYBR Green PCR Master Mix (Qiagen), 1 μL of each the forward and reverse gene-specific primers (1 μM), 2 μL RNase/DNase-free purified water (Roche), and 1 μL diluted cDNA. The PCR Cycling conditions were as

follows: initial denaturation at 95°C for 3 min, 40 cycles of 95°C for 10 s, and 60°C for 15 s. Relative quantification of target transcript abundance was determined using the Rotor-Gene Q software package (Qiagen). Standard curve analysis and contamination controls were performed as above, and transcript abundance was normalized to β-actin as above. The abundance of each transcript was further normalized to the control group.

### *3.2.8. Statistical analysis*

Statistical analyses were conducted using SigmaPlot (SPW 11; Systat Software, Inc., San Jose, CA). One-way analysis of variance (ANOVA) with a post-hoc Holm-Sidak method was used to assess the effect of treatment (i.e. control, AgNPs, or $Ag^{+}$) on gene expression in larval and adult zebrafish. Two-way ANOVA with a post-hoc Holm-Sidak method was used to assess the effects of treatment and Cys on mortality, hatching, cortisol, cholesterol, and triglycerides levels in zebrafish larvae. Three-way ANOVA with a post-hoc Holm-Sidak method was used to assess the effects of treatment, sex, and stress on plasma cortisol levels in adult zebrafish. Significant differences from one- and two-way ANOVA tests are indicated as letters and asterisks on the corresponding graphs, whereas the results from the three-way ANOVA are summarized in Table 3.2. Linear regression analysis was used to assess the relationship between fish mass and tank density. In all cases $P \leq 0.050$ was considered significant. The data are presented as means and standard error of the mean (SEM).

*3.3. Results*

*3.3.1. Embryo and adult zebrafish parameters*

Both AgNPs (0.5 µg/mL) and $Ag^+$ (0.05 µg/mL) significantly increased embryo mortality. The average mortalities at 96 hpf for AgNPs and $Ag^+$ were 40% and 30%, respectively (Fig. 3.3A); most mortalities occurred by 24 hpf. Hatching at 56 hpf was also significantly delayed by both Ag-types, with only 40-50% of the embryos hatching by 56 hpf (Fig. 3.4B). Cys treatment significantly reduced mortality and increased hatching success in Ag-treated embryos. There was no effect of treatment on heart rate at 48 hpf between the treated and control embryos, and with or without Cys; zebrafish larvae had heart rates of ~110 beats/min (data not shown).

Interestingly, adult zebrafish mass at 10 months was significantly increased in fish exposed to AgNPs as embryos (Fig. 3.4); however, this may reflect the number of fish in a tank as there was a significant relationship between fish mass and the average number of fish per tank (Fig. 3.4, inset), with the least populated tanks containing the bigger fish. Housing the same number of fish per tank was not possible due to space limitations.

*3.3.2. Cortisol, cholesterol, and triglycerides*

The cortisol levels in zebrafish larvae were not affected by Ag-type. Stressed larvae (4 dpf) had significantly higher cortisol levels by 2-3 times than the unstressed larvae (Fig. 3.5). Similarly adult zebrafish exposed to Ag as embryos/larvae and raised in Ag-free water for 10 months, responded to a netting stress by significantly increasing plasma cortisol levels (Fig. 3.6). In fact stressed fish had 20-40 times higher levels than their unstressed counterparts regardless of treatment (Table 3.2). Moreover, the unstressed

female fish had significantly higher cortisol levels than the males, but the males had higher cortisol levels than the females when stressed (Fig. 3.6); there were significant effects of sex and a significant interaction between sex and stress (Table 3.2). There was no effect of Cys on cortisol levels in any treatment (data not shown). The cholesterol and triglycerides levels were not significantly affected by Ag-type or Cys in zebrafish larvae (data not shown); adults were not assessed.

### *3.3.3. Transcript abundance*

As Cys did not impact cortisol levels, transcript abundance was assessed only in non-Cys treated larvae/adults. Moreover, we did not predict that stress would induce differences in transcript abundance given the short timeframe of the stressor (30 s for larvae and 6 min for adults), so only the non-stressed larvae/adults were assessed. All four transcripts (CRF, CRF-BP, CRF-R2, and POMCb) assessed were significantly down-regulated by $Ag^{+}$ in zebrafish larvae (Fig. 3.7). CRF-R1 transcripts were not detected in zebrafish larvae (data not shown). Abundance of these transcripts in the adult zebrafish telencephalon was differentially affected by $Ag^{+}$ and sex of the fish. The abundance of CRF-BP and CRF-R1 transcripts in males was down- and up-regulated, respectively (Fig. 3.8A), whereas the abundance of CRF and CRF-R1 in females was down-regulated (Fig. 3.8B). Transcripts for CRF-R2 and POMCb were not detected in the telencephalon region. Abundance of CRF and CRF-related transcripts was not significantly affected by AgNPs; however, there were trends for decreased abundance of CRF-BP and increased abundance of CRF-R1 in males, while in females the abundance of CRF and CRF-R1 was decreased.

**Table 3.1.** Primer sequences and amplicon sizes for the genes of interest used for larval and adult zebrafish gene expression analysis.

| Gene | Accession No. | Sequence 5'-3' | Size (bp) |
|---|---|---|---|
| CRF | BC085458 | F[1]: CGAGACATCCCAGTATCCAA<br>R[1]: GATGACAGTGTTGCGCTTCT | 465 |
| | | F[2]: GCCGATTTCCCTAGATCTGAC<br>R[2]: TCTTTGGCTGATGGGTTCG | 147 |
| CRF-BP | NM001003459 | F[1]: GCTGTGCTTCCTCCTGTTG<br>R[1]: CCTGATTGGTGGAGCCTGA | 483 |
| | | F[2]: CTAAAGCGAGAGTTACCAGAGG<br>R[2]: GATAACGTCAGTAGGTTCGCC | 150 |
| CRF-R1 | XM691254.2 | F[2]: CTGGGCTAAGAAAGGGAACTAC<br>R[2]: TGAAGAGGATGAATGCGACC | 152 |
| CRF-R2 | XM681362 | F[1]: GAATCGCTTACAGAGAGTGT<br>R[1]: ACCATCCAATGAAGAGGAAG | 465 |
| POMCb | NM001083051 | F[1]: GTTCTGTCCGTCTTGGCTTT<br>R[1]: GTGAACTGCTGTCCATTGCC | 639 |
| β-actin | AF057040 | F[1]: GGTATTGTGATGGACTCTGG<br>R[1]: AGCCACCGATCCAGACGGA | 583 |
| | | F[2]: TGAATCCCAAAGCCAACAGAG<br>R[2]: CCAGAGTCCATCACAATACCAG | 139 |

[1] *Sequences used for zebrafish larvae Quantitative RT-PCR analysis*
[2] *Sequences used for zebrafish adult Quantitative RT-PCR analysis*

**Table 3.2.** Summary of statistical analysis (P-values). Three-way ANOVA with post-hoc Holm-Sidak method was used to assess statistical differences ($P \leq 0.050$) on data found in Figure 3.6. The three factors were treatment (control, AgNP, $Ag^{+}$), sex, and stress. 'NS' denotes not significant.

| Factor/interaction | P-value |
|---|---|
| Treatment (A) | NS |
| Sex (B) | 0.047 |
| Stress (C) | < 0.001 |
| AxB | NS |
| AxC | NS |
| BxC | 0.037 |
| AxBxC | NS |

**Figure 3.1.** Zebrafish stress response experimental set-up. Embryos were exposed to $Ag^{+}$ or AgNPs until 4 dpf. The larvae were then 1) euthanized, or 2) stressed and euthanized, or 3) raised to adulthood in Ag-free water and then 1) euthanized, or 2) stressed and euthanized. Whole larvae and adult plasma and brain samples were used for cortisol and gene expression analyses.

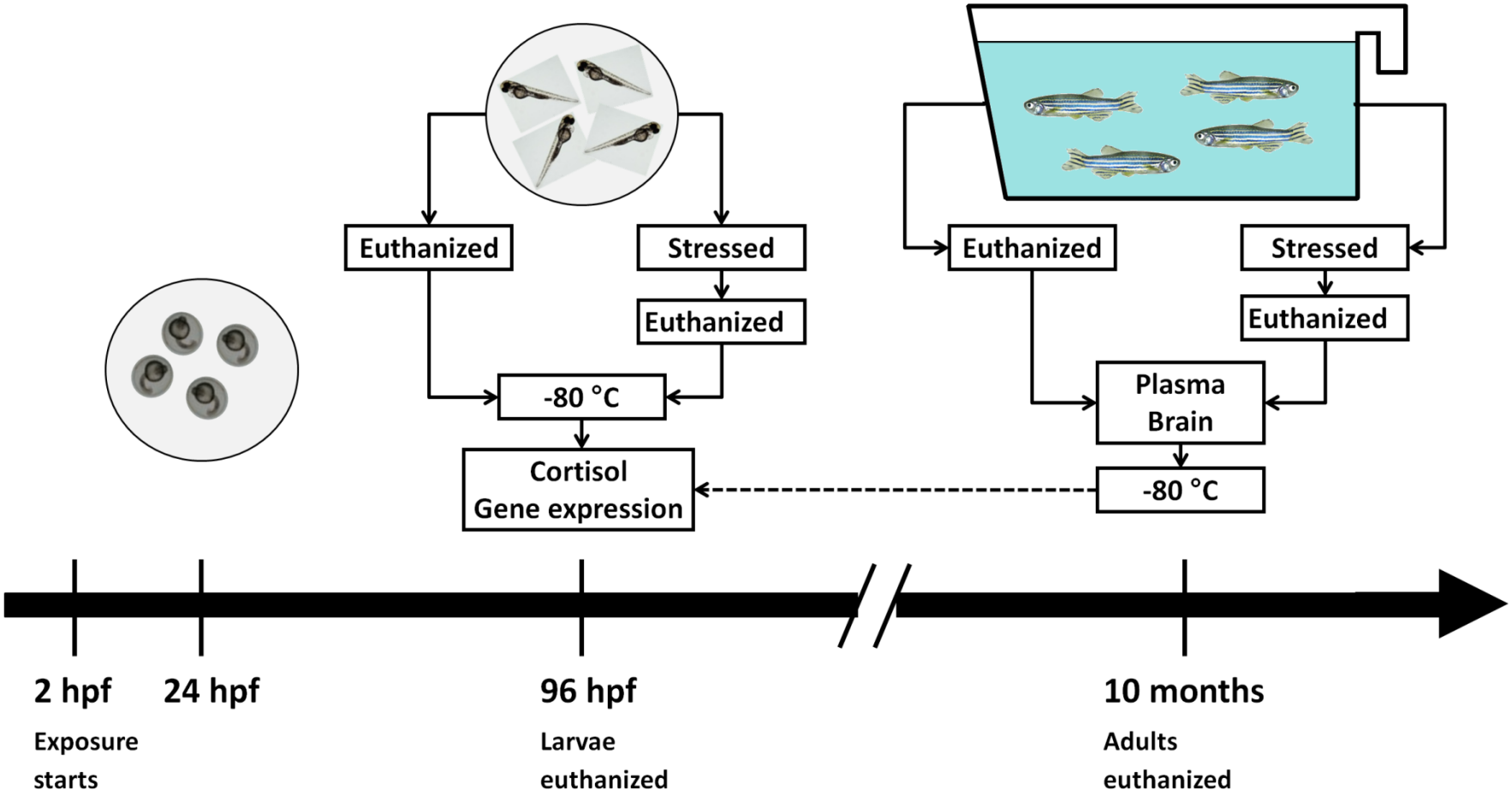
Euthanized
Stressed
Euthanized
-80 °C
Cortisol
Gene expression
Euthanized
Stressed
Euthanized
Plasma
Brain
-80 °C
2 hpf
24 hpf
96 hpf
10 months
Exposure
starts
Larvae
euthanized
Adults
euthanized

**Figure 3.2.** Photomicrograph of the zebrafish brain regions: telencephalon (tel), optic lobe (OL), cerebellum (C), and medulla (M). The excised area is shown by the red oval.

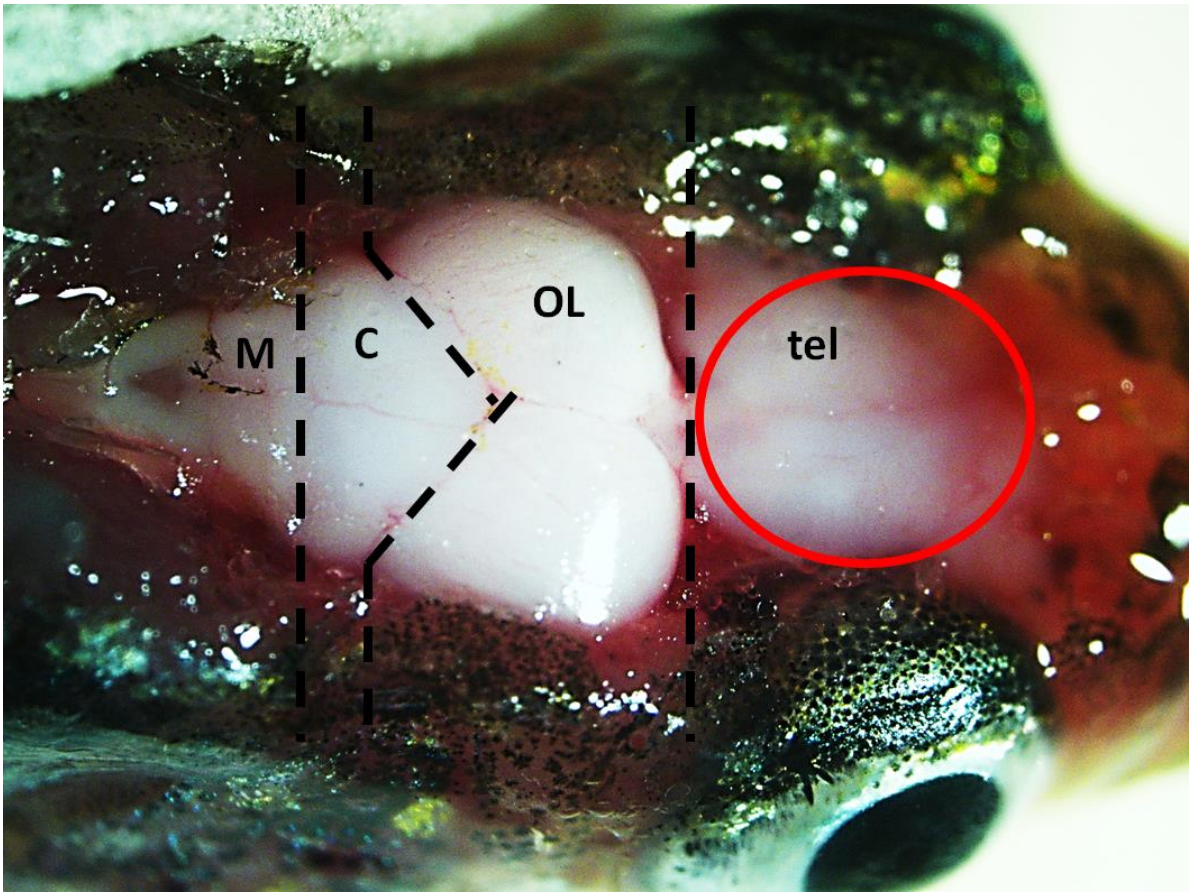

**Figure 3.3.** Mortality and hatching of zebrafish exposed to $Ag^{+}$ (0.05 µg/mL) or AgNP (0.5 µg/mL) in the presence or absence of cysteine (Cys) until 4 dpf. A. Mortality of zebrafish embryos after 96 hpf is presented as a percentage of those embryos that died. B. Hatching success of zebrafish embryos at 56 hpf is presented as a percentage of total live embryos. Data are presented as Mean + SEM (n = 5-17 and 4-16 for mortality and hatching, respectively). Capital and small letters indicate differences within treatments in the absence and presence of cysteine (Cys), respectively. The asterisks indicate differences between Cys-treated and non-treated embryos within the same treatment. Two-way ANOVA with post-hoc Holm-Sidak method was used to assess statistical differences ($P \leq 0.050$).

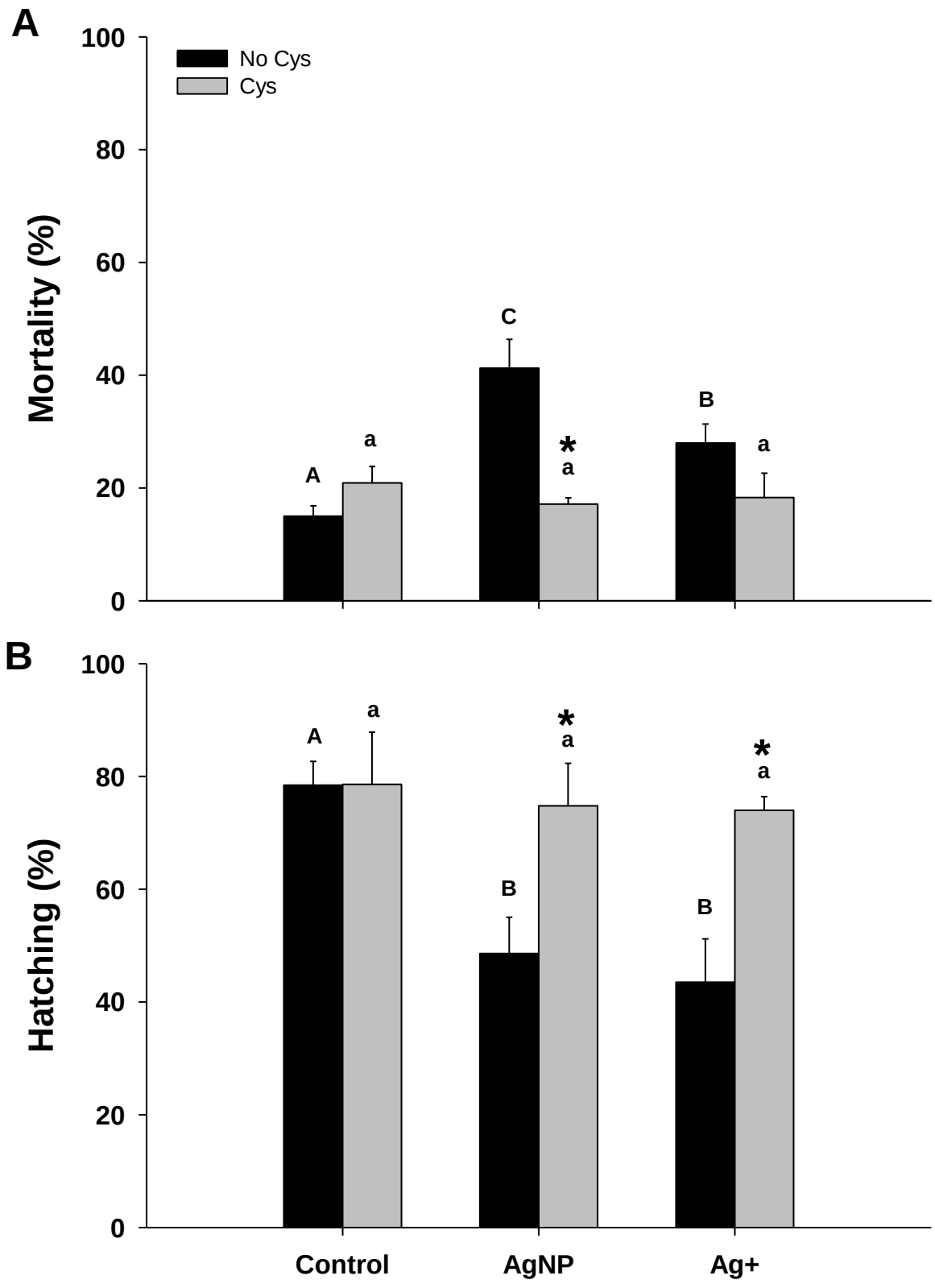
A
100
80
60
40
20
0
No Cys
Cys
Mortality (%)
A
a
C
*
a
B
a
B
Hatching (%)
A
a
*
a
B
*
a
B
Control
AgNP
Ag+

**Figure 3.4.** Adult zebrafish mass at the end of the experiment (10 months) that were treated with $Ag^{+}$ or AgNP as embryos until 4 dpf (see Fig. 3.3 for details). Data are presented as Mean + SEM (n = 4). Capital and small letters indicate differences within treatments in the absence and presence of cysteine (Cys), respectively. Two-way ANOVA with post-hoc Holm-Sidak method was used to assess statistical differences ($P \leq 0.050$). Inset: linear regression analysis of the fish mass as a function of the average number of fish per tank: (1) control, (2) control (+Cys), (3) AgNPs, (4) AgNPs (+Cys), (5) $Ag^{+}$, (6) $Ag^{+}$ (+Cys). Data are presented as Mean ± SEM (n = 4). The $r^2$ and P values are 0.81 and 0.015, respectively; the equation of the line is y = -0.0287x + 1.0382.

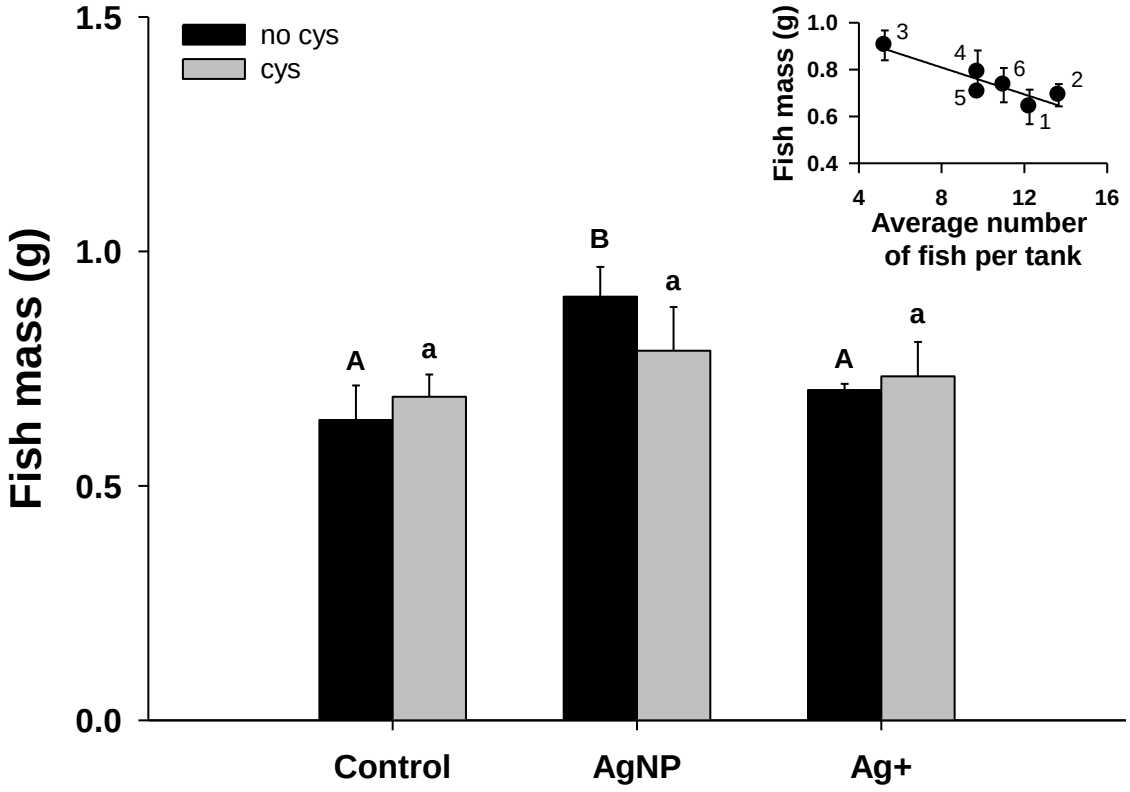

**Figure 3.5.** Whole-body cortisol levels in unstressed and stressed zebrafish larvae (4 dpf) following exposure to $Ag^{+}$ or AgNP until 4 dpf (see Fig. 3.3 for details). Data are presented as Mean + SEM (n = 3-9). Capital and small letters indicate differences within treatments in unstressed and stressed larvae, respectively. The asterisks indicate differences between stressed and unstressed larvae within the same treatment. Two-way ANOVA with post-hoc Holm-Sidak method was used to assess statistical differences ($P \leq 0.050$).

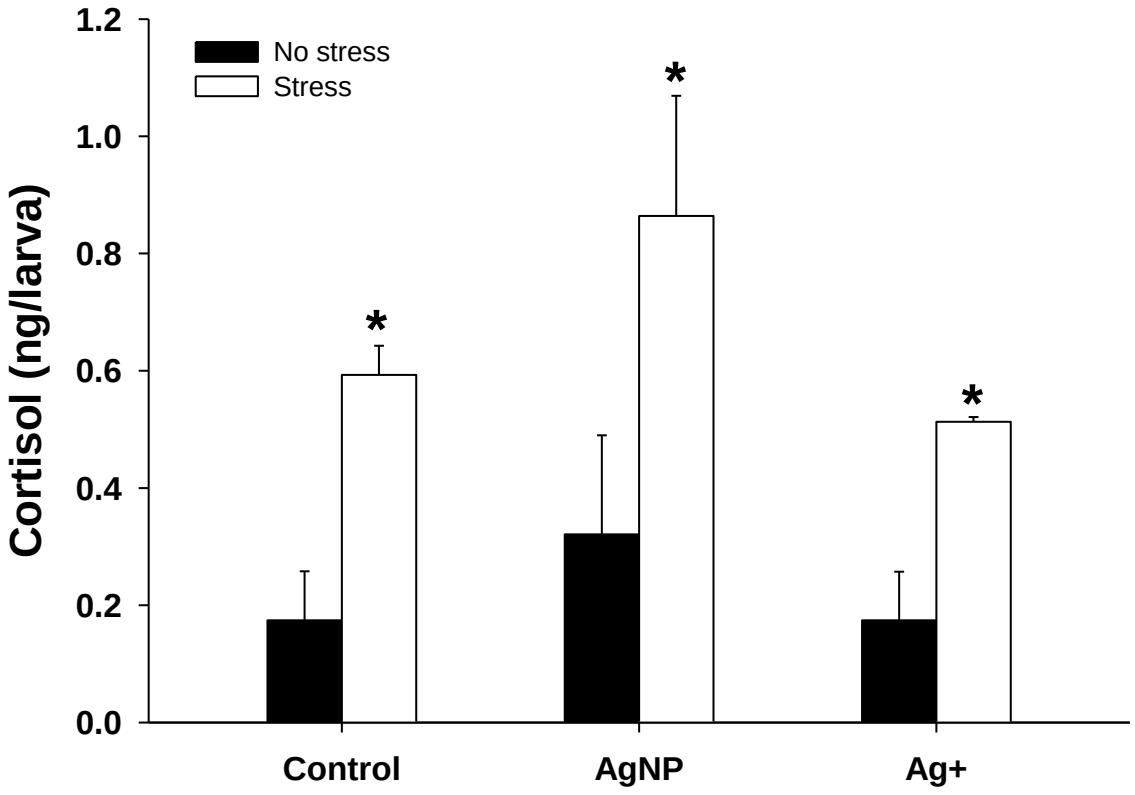

**Figure 3.6.** Plasma cortisol levels in unstressed and stressed male and female adult zebrafish (10 months) that were treated with $Ag^{+}$ or AgNP as embryos until 4 dpf (see Fig. 3.3 for details). Data are presented as Mean + SEM (n = 4). Three-way ANOVA with post-hoc Holm-Sidak method was used to assess statistical differences (see Table 3.2).

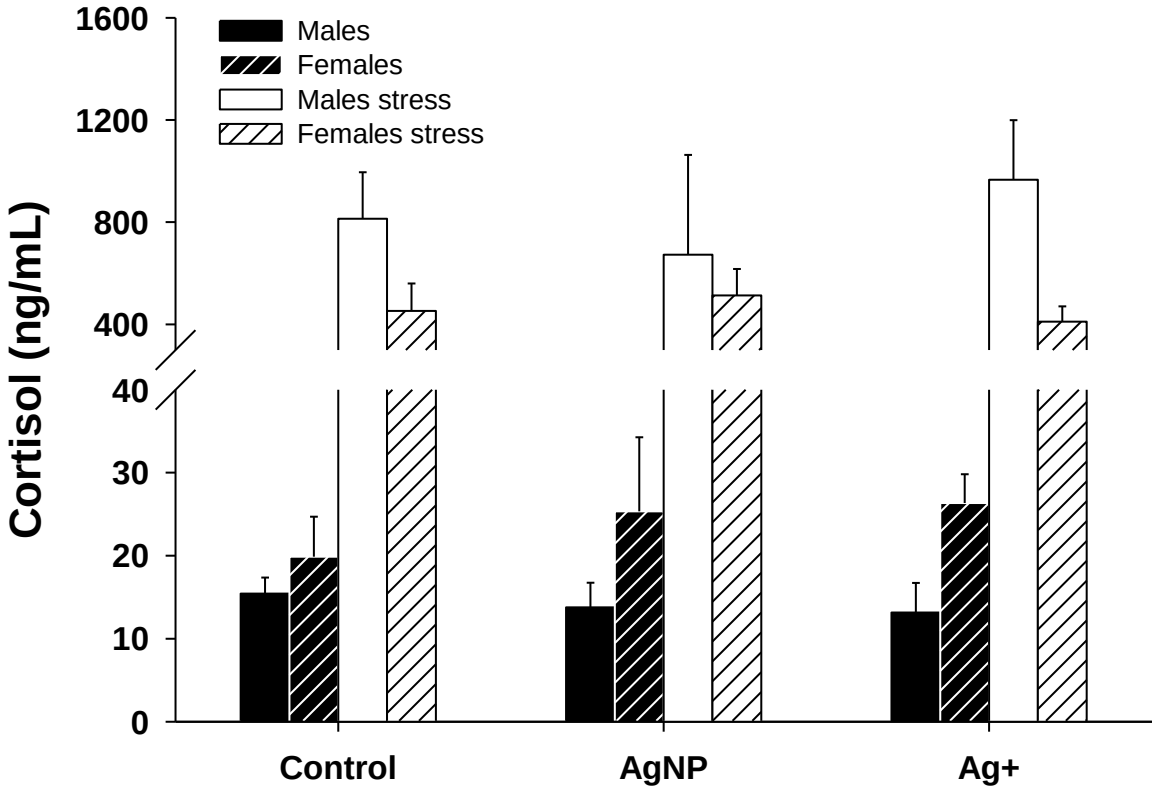

**Figure 3.7.** Transcript abundance within the HPI axis in 4 dpf zebrafish larvae following exposure to $Ag^{+}$ or AgNP until 4 dpf (see Fig. 3.3 for details): CRF, CRF-BP, CRF-R2, and POMCb. Transcript abundance was normalized to the control group (see section 3.2.7 for details). Data are presented as Mean + SEM (n = 7). The letters indicate differences in transcript abundance between treatments for a specific gene. One way-ANOVA with post-hoc Holm-Sidak method was used to assess statistical differences ($P \leq 0.050$).

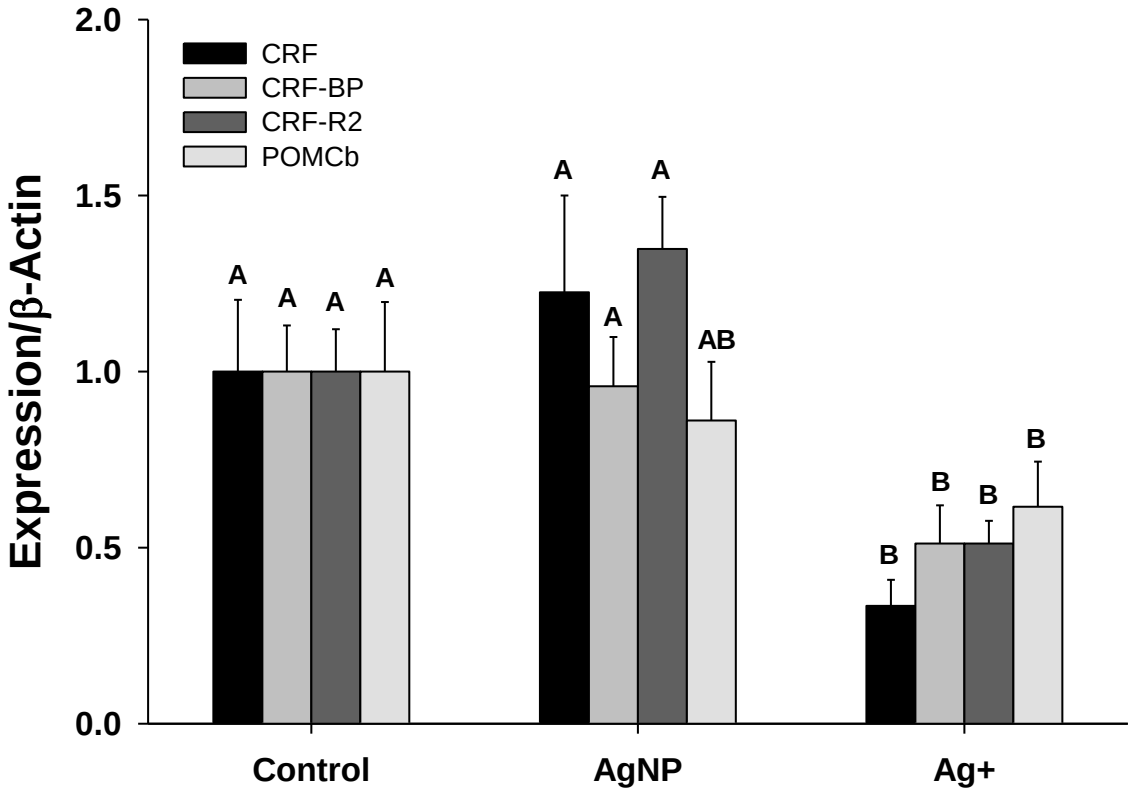

**Figure 3.8.** Transcript abundance within the HPI axis in 10 month old male (A) and female (B) zebrafish that were treated with $Ag^{+}$ or AgNP as embryos until 4 dpf (see Fig. 3.3 for details): CRF, CRF-BP, and CRF-R1. Transcript abundance was normalized to the control group (see section 3.2.7 for details). Data are presented as Mean + SEM (n = 4). The letters indicate differences in transcript abundance between treatments for a specific gene. One way-ANOVA with post-hoc Holm-Sidak method was used to assess statistical differences ($P \leq 0.050$).

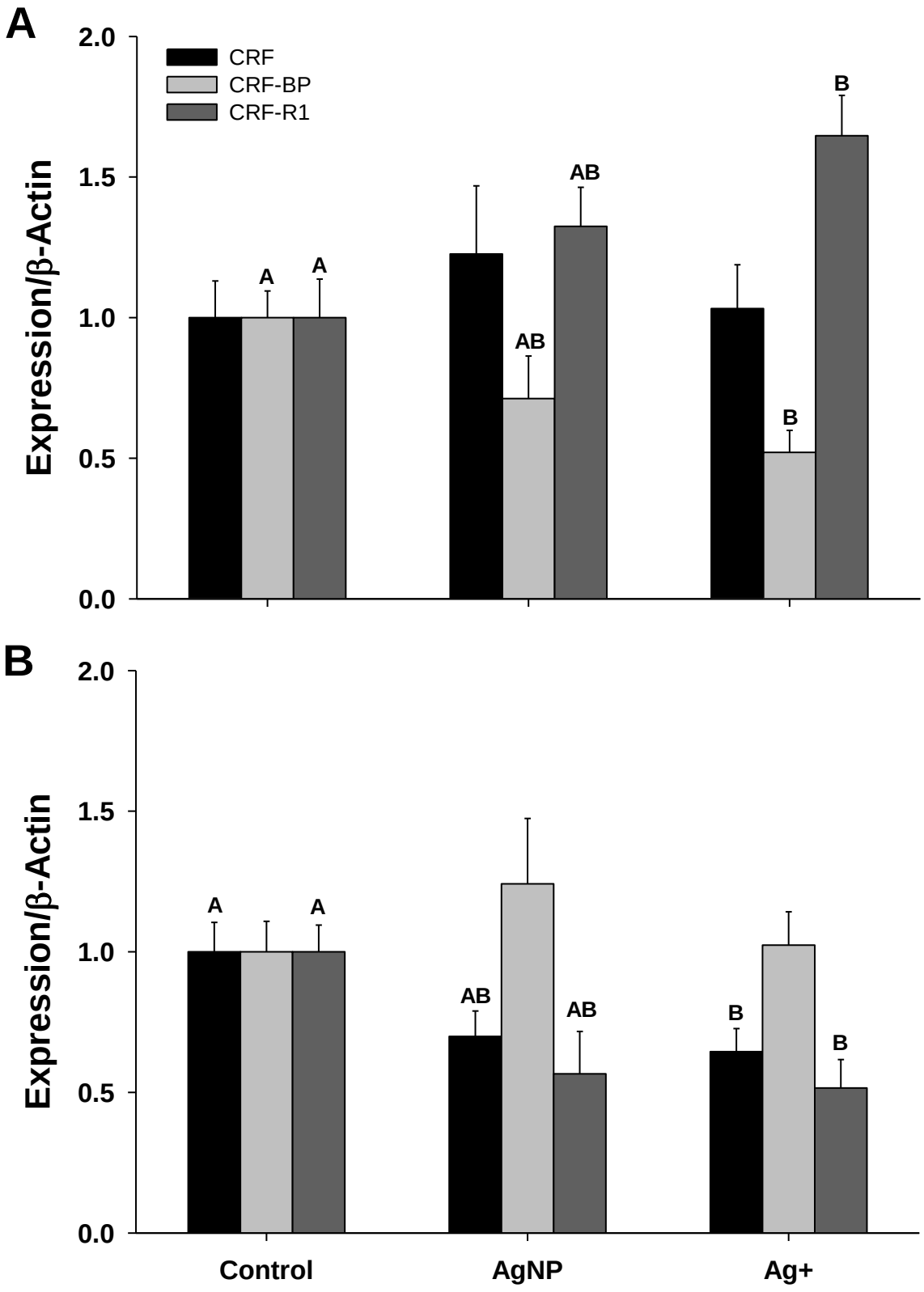
A
2.0
1.5
1.0
0.5
0.0
Expression/β-Actin
CRF
CRF-BP
CRF-R1
A
A
AB
AB
B
B
B
2.0
1.5
1.0
0.5
0.0
Expression/β-Actin
A
A
AB
AB
B
B
Control
AgNP
Ag+

*3.4. Discussion*

This study for the first time demonstrated that an acute exposure to AgNPs or $Ag^{+}$ during the early life stages did not impede the ability of larval and adult zebrafish to elevate cortisol levels in response to a stressor, at least under the conditions described in this study. The nominal concentrations used here were 0.5 and 0.05 μg/mL total Ag for AgNPs and $Ag^{+}$, respectively. These concentrations were chosen since the relatively low mortality ensured sufficient larval survival, and the viability and hatching values at these concentrations were similar to our previous study (Chapter 2; Massarsky et al., 2013). It is important to note that the AgNP concentration used in this study is similar to previous studies, although higher than the environmental concentrations of 0.088-2.63 and 40-320 ng/L in surface water predicted by Gottschalk et al. (2009) and Blaser et al. (2008), respectively. As reported previously (Chapter 2; Massarsky et al., 2013), environmentally relevant concentrations of AgNPs did not affect zebrafish embryos, at least with respect to mortality, hatching, or oxidative stress.

The ability of environmental pollutants, especially metals, to impact the HPI axis and/or cortisol levels in fish was addressed in several studies with variable results. Cadmium disrupted the biosynthesis of cortisol through the suppression of corticosteroidogenic gene transcripts in rainbow trout (*Oncorhynchus mykiss*) without affecting cortisol production (Sandhu and Vijayan, 2011). Basal cortisol levels were not affected in the sabalo (*Prochilus lineatus*) exposed to aluminum (Camargo et al., 2009) or in the round goby (*Neogobius melanostomus*) from contaminated areas (Marentette et al., 2013). In contrast, basal cortisol levels were increased in zebrafish exposed to copper (Craig et al., 2009) and selenomethionine (Thomas and Janz, 2011), Nile tilapia

(*Oreochromis niloticus*) exposed to mercury (Cogun et al., 2011) and heavy metals (Firat and Kargin, 2011), and carp (*Cyprinus carpio*) exposed to a variety of pollutants (Firat and Alici, 2012). Lastly, chromium exposure in snakehead (*Channa punctatus*) decreased basal cortisol levels (Mishra and Mohanty, 2009). Overall, these studies indicate the importance of pollutant-type and fish species in eliciting a cortisol-mediated stress response.

In contrast, in this study we hypothesized that an acute exposure to AgNPs or $Ag^{+}$ during the early stages of zebrafish development would alter the proper formation and functioning of the HPI axis in zebrafish embryos, and that these changes would persist in the adult fish. This hypothesis was not supported by the cortisol data, which clearly showed that both the larvae and the adult zebrafish were able to elevate cortisol levels in response to a stressor equal to that of the control fish. Two issues should be raised with respect to plasma cortisol levels in adult zebrafish. First, it is feasible to obtain enough plasma to assess cortisol levels when combining 2-3 fish and perhaps future studies should assess plasma cortisol instead of whole-body cortisol as generally done. Only a few studies report plasma cortisol levels for zebrafish. Filby et al. (2010) reported that subordinate (or 'naturally' stressed) zebrafish had higher cortisol levels than their dominant counterparts (50-100 vs 75-175 ng/mL); this difference was especially apparent in males. Félix et al. (2013) reported similar plasma cortisol levels in unstressed zebrafish, such that males had slightly higher concentrations than females (57 vs 46 ng/mL). In contrast, the plasma cortisol levels for unstressed zebrafish adults reported here ranged from 15 to 25 ng/mL and were similar to the 20 ng/mL levels reported by Ziv et al. (2013) for unstressed male zebrafish. The cortisol levels for stressed fish reported

here ranged from 400 to 800 ng/mL, which probably reflects the maximal cortisol levels elicited by the netting stress since the acute confinement method mentioned in Ziv et al. (2013) elevated cortisol levels by only 1.5-fold.

Second, female fish had higher cortisol levels when unstressed while males had higher levels when stressed. These differences could have been potentially missed if whole-body cortisol levels were assessed. For example, Fuzzen et al. (2011) found no sex differences in whole-body cortisol levels in unstressed or stressed (vortex stress) adult zebrafish. In contrast, Filby et al. (2010) reported higher plasma cortisol levels in subordinate (and supposedly stressed) males and to a lesser extent in females. Other studies reporting sex differences in plasma cortisol levels in zebrafish were not found. Sex differences in cortisol levels and their physiological importance should be investigated further (using more natural stressors) since it appears that the ability to cope with stress may be affected by sex.

Although Ag treatments did not affect larval cortisol levels, whole-body transcript levels of CRF, CRF-R2, CRF-BP, and POMCb were significantly down-regulated in $Ag^{+}$-exposed larvae, suggesting that the HPI axis-mediated stress response could be impaired. This was unexpected since no changes in cortisol levels were observed in $Ag^{+}$-exposed larvae. Also, $Ag^{+}$ (0.05 μg/mL) was less toxic than AgNPs (0.5 μg/mL) based on the mortality data and one would have predicted that changes should be observed in the AgNPs-exposed larvae; given this did not happen, the toxicity mechanisms of AgNPs and $Ag^{+}$ may be quite different. Although CRF and CRF-related genes are most commonly known to be involved with the regulation of the HPI axis-mediate stress response, these genes also influence most if not all physiological functions in vertebrates, including

nervous, cardiovascular, immune, muscular, and reproductive systems, as well as behavior and food intake (Yao and Denver, 2007; Alderman and Bernier, 2009). Additionally, the CRF system is thought to play an important role during early development of zebrafish embryos (Alderman and Bernier, 2009). Thus, it is possible that other systems, which were not considered here, could be affected in zebrafish larvae in response to $Ag^{+}$ exposure. This is especially important since the whole-body transcript levels were measured in the larvae, which may have masked even larger changes.

The transcript abundance for CRF, CRF-R1, and CRF-BP was also affected in the adult zebrafish telencephalon. Significant changes were only observed in fish that were exposed to $Ag^{+}$ as embryos. In males the abundance of CRF transcripts was unaffected, while that of CRF-BP and CRF-R1 was down- and up-regulated, respectively. In females the abundance of CRF-BP transcripts was unaffected, while that of CRF and CRF-R1 was down-regulated. Precisely what these changes indicate is not clear, but these changes did not affect the ability of fish to elevate cortisol levels in response to a stressor. Alternatively, CRF-related peptides such as urotensin I could also elevate cortisol levels during stress (Alderman and Bernier, 2009); therefore, if the function of HPI axis was impaired, the urotensin I system could potentially compensate and increase cortisol levels. This could explain why differences were observed for CRF-related transcript levels but not cortisol levels. Finally, transcript abundance differed between males and females, which could lead to the observed sex differences in cortisol levels in unstressed and stressed fish.

Previous studies investigating the effects on the transcript levels of CRF and CRF-related genes in larval and adult zebrafish emphasize the complexity of CRF regulation

and how it is impacted under various conditions. Embryos exposed to perfluorooctane sulfonate (Shi et al., 2009), polybrominated diphenyl ethers (PBDE; Yu et al., 2010; Chen et al., 2012), and microcystin (Yan et al., 2012) increased CRF transcript levels. These studies, however, focused on the hypothalamic-pituitary-thyroid (HPT) axis, which emphasizes the important role of CRF outside the HPI axis. In zebrafish adults, prochloraz exposure down-regulated the transcript levels of brain CRF, CRF-BP, and CRF-R2, and decreased plasma cortisol levels (Liu et al., 2011), while PBDE exposure down-regulated brain CRF transcript levels (Yu et al., 2011). Moreover, adult zebrafish subjected to a restraint stress decreased the transcript levels of brain CRF and CRF-related genes and increased whole-body cortisol levels (Ghisleni et al., 2012). In contrast, unpredictable chronic stress elevated brain CRF transcript levels (Piato et al., 2011; Chakravarty et al., 2013) and increased whole-body cortisol levels (Piato et al., 2011). Lastly, transport stress did not change the transcript levels of brain CRF, but increased whole-body cortisol levels (Dhanasiri et al., 2013). This further supports the complexity of the CRF and its involvement in physiological processes.

In conclusion, we demonstrate that even though the acute exposure to AgNPs and $Ag^{+}$ until 4 dpf influenced embryo viability and hatching, these Ag compounds did not impact the ability of zebrafish larvae or adults to elevate cortisol when stressed. Furthermore, we demonstrate that embryonic exposure to $Ag^{+}$ down-regulated CRF and CRF-related genes in larvae, and although these changes did not impair the cortisol-mediated stress response, other systems not considered in this study, could have been affected. The abundance of these transcripts was also differentially affected in the telencephalon of the male and female adults exposed to $Ag^{+}$ as embryos, suggesting

potential sex-differences in response to $Ag^{+}$. Currently there are no studies on the impact of either AgNPs or $Ag^{+}$ on the fish HPI axis; our transcript results suggest that $Ag^{+}$ may influence the CRF signaling, which should be pursued in future studies.

# CHAPTER 4
# Nanosilver cytotoxicity in rainbow trout (*Oncorhynchus mykiss*) erythrocytes and hepatocytes

This chapter is based upon the following article: Massarsky, A., Abraham, R., Nguyen, K.C., Rippstein, P., Tayabali, A.F., Trudeau, V.L., Moon, T.W., 2014. Nanosilver cytotoxicity in rainbow trout (*Oncorhynchus mykiss*) erythrocytes and hepatocytes. Comp. Biochem. Physiol. C 159, 10-21.

Permission was obtained from the journal for incorporation of this paper into this thesis. The article is based on the work that was conducted with the assistance of the undergraduate student Ren Abraham (2012), whom I directly supervised, as well as my colleagues Kathy Nguyen (PhD student, Carleton University) and Dr. Azam Tayabali (Health Canada, Ottawa), who financed the Transmission Electron Microscope work carried out by Peter Rippstein (The Heart Institute, uOttawa). I designed and conducted these experiments, and wrote the manuscript. Drs. Vance Trudeau and Thomas Moon provided input into the preparation of the manuscript and funding for the project.

*4.1. Introduction*

As of October 2013 more than 1600 reported consumer products contained engineered nanomaterials (ENMs) with silver nanoparticles (AgNPs) being the most common (Nanotechproject, 2013). The increased interest in nanotechnology over recent years has raised safety concerns. ENMs have at least one dimension of less than 100 nm (Oberdörster et al., 2007; Handy et al., 2008). Particles of such size have a high surface area to volume ratio and thus are more reactive, especially in relation to free radical chemistry and formation of reactive oxygen species (ROS) (Lynch et al., 2007; Auffan et al., 2009; Prencipe et al., 2009), which in turn could damage cellular components (Oberdörster et al., 2005; Aillon et al., 2009).

Silver ions ($Ag^+$) are well known to be toxic to fish through the inhibition of gill $Na^+$,$K^+$-ATPase and carbonic anhydrase and subsequent disruption of ionoregulation, which ultimately may lead to fish death (Morgan and Wood, 2004). Silver ions also accumulate in the blood, kidney, and liver of exposed fish (Wood et al., 1999). As an antimicrobial agent, $Ag^+$ has been applied extensively in medicine and advancements in nanotechnology enabled the incorporation of AgNPs into many products as mentioned in Chapter 1.

The widespread usage of AgNPs will lead to their appearance in the aquatic environment; e.g., clothing items impregnated with AgNPs were reported to release 68-377 μg/g Ag in simulated washing experiments (Benn and Westerhoff, 2008; Geranio et al., 2009). However, the fate and behavior of AgNPs in the aquatic environment remain unknown. Although Kaegi et al. (2011) reported that most AgNPs sorbed to wastewater biosolids and were transformed into $Ag_2S$, these findings could depend on the AgNP

coatings. A recent mesocosm study reported that AgNPs remained bioavailable in the water column and accumulated in some organisms despite significant sulfidation (Lowry et al., 2012). Also, AgNPs have been shown to disrupt ionoregulation in rainbow trout (*Oncorhynchus mykiss*) by inhibiting the gill $Na^+$,$K^+$-ATPase (Schultz et al., 2012) and to accumulate in the liver of rainbow trout (Gagné et al., 2012), suggesting that some of these particles pass through the gills into blood and accumulate in the liver. Moreover, we have demonstrated the ability of AgNPs to elicit oxidative stress in zebrafish (*Danio rerio*) embryos (Chapter 2; Massarsky et al., 2013) without affecting the cortisol-mediated stress response (Chapter 3; Massarsky et al., 2014a).

Although several studies have previously addressed the cytotoxicity of AgNPs (see section 4.4), this study emphasizes the relationship between AgNP toxicity and oxidative stress and cellular damage to lipids, DNA, and proteins by examining the various components of the antioxidant pathway in rainbow trout erythrocytes and hepatocytes, as both of these cell types may be affected by AgNPs. It needs to be noted that erythrocytes are a sensitive *in vitro* model for oxidative stress due to their susceptibility to peroxidation arising from the high content of poly-unsaturated fatty acid in their cell membranes and high cytoplasmic oxygen and iron concentrations, which continuously produce ROS (Li et al., 2013). On the other hand, hepatocytes are extensively used in the field of toxicology since liver is a major organ involved in xenobiotic metabolism (Guillouzo, 1998; Castano et al., 2003). The well-studied toxicant $Ag^+$ (as $AgNO_3$) serves as a 'reference point' for the toxicity of AgNPs. In addition to decreased cell viability, it was predicted that AgNPs and $Ag^+$ would generate ROS, which in turn would decrease glutathione levels, increase damage to lipids, DNA, and proteins, and increase the

activities of cellular antioxidant enzymes. The enzymes assessed in this study were: glutathione-S-transferase (GST), glutathione reductase (GR), glutathione peroxidase (GPx), catalase (CAT), and superoxide dismutase (SOD). Moreover, the effects of AgNPs and $Ag^{+}$ were assessed in the presence and absence of cysteine (Cys) (see Chapter 2 for details). Finally, buthionine sulfoximine (BSO) co-exposure was used to reveal the importance of reduced glutathione (GSH) in silver toxicity as BSO is known to inhibit γ-glutamylcysteine synthetase thereby reducing GSH levels.

## *4.2. Materials and methods*

### *4.2.1. Silver nanoparticles (AgNPs) and silver nitrate ($AgNO_3$)*

An aqueous solution of carboxy-functionalized AgNPs stabilized with sodium polyacrylate (31% Ag) (Vive Nano, 13010L) was used in this study. The stock solution of 1500 µg/mL was stored in dry and dark cabinet at room temperature as per manufacturer's recommendation, and was diluted to working concentrations in culture medium on the day of each experiment. Silver nitrate ($AgNO_3$; 63.5% Ag) was purchased from Sigma Chemical Co. (product 204390) and a 750 µg/mL stock solution was prepared in ultrapure water and diluted to working concentrations in culture medium. Total nominal Ag concentrations noted on the figures were based on the Ag content of each Ag-type used.

### *4.2.2. Characterization of AgNPs*

The size, polydispersity index (PDI), and zeta-potential (ζ-potential) of the AgNPs were obtained using Dynamic Light Scattering (DLS; Zetasizer Nano, Malvern

Instruments Ltd). The size measurements (n=10) were performed on a freshly prepared 31 μg/mL AgNP solution in either MilliQ water or culture medium (see section 4.2.4 for details). The Zetasizer automatically calculated the PDI for each measurement. The ζ-potential measurements (n=4) were performed on freshly prepared AgNP solutions of various concentrations in either MilliQ water or culture medium. Scanning Transmission Electron Microscope (STEM; JEOL JSM-7500F Field Emission Scanning Electron Microscope) was used to visualize and confirm the DLS results; a 10 μg/mL AgNP solution was prepared in MilliQ water and applied to a carbon-coated grid, air-dried overnight, and photos were captured from transmission electron diffraction (TED). The dissolution of AgNPs was reported at 0.5% (Chapter 2; Massarsky et al., 2013).

Furthermore, light microscopy and UV-visible spectroscopy were used to determine the effect of culture medium, BSO, and/or Cys on AgNPs. Briefly, culture medium or MilliQ water (0.2 mL) were distributed among the wells on a 96-well plate; some wells also received BSO $[1\ mM]_{final}$ and/or Cys $[0.35\ mM]_{final}$. The AgNPs $[31\ \mu g/mL]_{final}$ were then added to the wells. Digital pictures were taken using a Nikon NBZ 1500 dissecting microscope, equipped with a Nikon DXM 1200 C digital camera, to capture changes in color and precipitate formation. Spectrophotometric measurements were then taken at 350-500 nm to estimate the absorption maximum, which typically peaks at ~400 nm depending upon the nanoparticle size (Thomas et al., 2008; Ahamed et al., 2011; Song et al., 2012). The plate was incubated at 13°C with gentle rotation. The microscopic observations and spectrophotometric measurements were repeated at 24 and 48 h. Also, a 12-well plate was set up in a similar fashion (the volumes were adjusted accordingly) for DLS measurements that were performed at 24 and 48 h.

*4.2.3. Fish*

Hatchery-reared female rainbow trout (250 g) were obtained from Linwood Acres (Campellcroft, ON, Canada). The fish were housed at the University of Ottawa Aquatic Care Facility in 3 $m^3$ tanks supplied with 13°C dechloraminated City of Ottawa tap water and acclimated for at least one month. The fish were kept under 12:12 h light-dark cycle and were fed a commercial diet (3 PT classic floating grower feed; Martin Mills, Elmira, ON, Canada) at 1% body weight once per day. All experiments were conducted under a protocol approved by the University of Ottawa Animal Care Protocol Review Committee in accordance with institutional animal care guidelines as defined by the Canadian Council on Animal Care.

*4.2.4. Erythrocyte and hepatocyte isolation*

Rainbow trout were euthanized with an overdose of benzocaine and blood was collected from the caudal vein using a heparinized syringe into a 50 mL Falcon tube containing 15 mL culture medium [in mM: 136.9 NaCl, 5.4 KCl, 0.8 $MgSO_4$, 5 $NaHCO_3$, 0.33 $Na_2HPO_4$, 0.44 $KH_2PO_4$, 5 Hepes, 5 Na-Hepes, 1.5 $CaCl_2$, 1X essential and non-essential amino acids (Sigma M7145, M5550), 1X antibiotics (Invitrogen 15240), and 1% bovine serum albumin (BSA); pH 7.63] supplemented with 50 U/mL heparin. The tube with medium-diluted blood was centrifuged, the medium was discarded, and the cells were resuspended in fresh culture medium. The procedure was repeated once more and the cells were kept on ice during hepatocyte isolation. Hepatocytes were isolated according to Mommsen et al. (1994). Briefly, Hanks' medium was prepared (in mM: 136.9 NaCl, 5.4 KCl, 0.8 $MgSO_4$, 5 $NaHCO_3$, 0.33 $Na_2HPO_4$, 0.44 $KH_2PO_4$, 5 Hepes, 5

Na-Hepes) and used to prepare the rinsing, collagenase, resuspension, and culture medium solutions all adjusted to pH 7.63 at room temperature. A mid-ventral incision was made in the trout and a cannula was inserted into the hepatic portal vein. Using a perfusion pump, the liver was perfused (2 mL/min) with rinsing solution containing 1 mM EGTA (the heart was cut to prevent pressure build-up in liver). Once the liver was cleared of blood it was perfused with collagenase solution containing 0.15 mg/mL collagenase (Sigma type IV). Once the liver had expanded and 'felt' soft, it was removed and all adhering vessels/tissues (including the gall bladder) were carefully removed. It was then diced with a razor blade in a glass Petri dish and sequentially filtered using 250 and 75 μm nylon mesh. The collected hepatocytes were poured into 50 mL Falcon tubes and centrifuged for 2 min at 1000 rpm (Sorvall RC centrifuge with SS-34 rotor) and 4°C. Cells were resuspended in resuspension solution containing 1% BSA and centrifuged as above. This was repeated twice more and finally cells were resuspended in culture medium. Cell viability of both the erythrocytes and hepatocytes was determined using the Trypan Blue exclusion method (Mommsen et al., 1994). Only cell suspensions with more than 90% live cells were used in the experiments. Both cell types were then weighed and the concentration was adjusted to 25 mg/mL (~$5x10^6$ cells/mL). The cells were then plated (0.4 mL/well) in 48-well plates (Corning 3338) and allowed to settle overnight at 13°C with gentle shaking.

*4.2.5. Experimental set-up*

Both cell types were exposed to AgNP or $Ag^+$ solutions at equivalent total silver contents; the concentrations were 3.1, 7.8, 15.5, 23.3, and 31 μg/mL. Control cells

received an equal volume of water. A combination of $H_2O_2$ and $CuSO_4$ at 1 mM was used as a positive control since individually 10 mM $H_2O_2$ and 1 mM $CuSO_4$ were not cytotoxic to cells after 48 h (data not shown); the combination of $CuSO_4$ and $H_2O_2$ generates the highly oxidizing hydroxyl radical and was used previously by Mireles et al. (1999) to induce lipid peroxidation in human neonatal erythrocytes. To evaluate the protective effect of Cys, an aqueous solution was prepared (66 mM) and added to the wells at a final concentration of 0.35 mM. After a 48 h incubation the medium and the cells were collected, frozen on dry ice, and kept at -80°C until analyzed.

In a separate set of experiments the cells were co-exposed to BSO. Hepatocytes were exposed to 1 mM BSO as this concentration in preliminary experiments was shown to reduce glutathione levels by 50% without increasing cytotoxicity. Erythrocytes were not sensitive to BSO; even at 20 mM BSO the glutathione levels did not differ from the control group (data not shown). The positive control was not included in BSO experiments.

*Note:* Hepatocytes that were used to measure the production of reactive oxygen species were pre-treated with DCHF-DA and then exposed to Ag treatments as outlined in section 4.2.7.

*4.2.6. Cell viability analysis*

Cell viability of both the erythrocytes and hepatocytes was determined by the lactate dehydrogenase (LDH; EC 1.1.1.27) leakage assay modified from Feng et al. (2003). Briefly, after a 48 h exposure, the cell medium was collected and LDH activity was estimated by NADH consumption measured spectrophotometrically (SpectraMax Plus;

Molecular Devices) at 340 nm in the presence of NADH (0.35 mM) and pyruvate (4.5 mM) in imidazole buffer (50 mM; pH 7.5). The reaction was monitored over 15 min. The activity was normalized to the control samples. Hemolysis was used as a secondary viability method for erythrocytes by measuring the hemoglobin absorbance of the collected medium at 540 nm; the absorbance was normalized to the control samples.

*4.2.7. Reactive oxygen species (ROS) generation*

Intracellular generation of ROS was estimated in hepatocytes using a fluorescence assay as described previously (Limbach et al., 2007). Briefly, cells were incubated for 30 min in the presence of 10 μM 2',7'-dichlorodihydrofluorescein diacetate (DCHF-DA). After incubation the cells were rinsed with fresh culture medium and exposed as above. The fluorescence (485ex/530em; SpectraMax Gemini XS, Molecular Devices) was measured immediately after the addition of exposure solutions and 48 h later. The adjusted relative fluorescence unit (RFU) values were normalized to the control group. This assay was not appropriate for erythrocytes, because hemolysis interfered with fluorescent readings.

*Note:* In Chapter 2 (section 2.2.6) it was mentioned that Ag interfered with the DCHF-DA assay in zebrafish larvae, although the same compound was used to detect ROS in hepatocytes, no problems were detected. This contradiction is probably due to differences in sample preparation and incubation. The larvae were first exposed to Ag, then collected, rinsed, and sonicated; the homogenates were then incubated in the presence of DCHF-DA and fluorescence was monitored. In contrast, hepatocytes were

pre-incubated with DCHF-DA to allow its internalization and esterase action; the cells were then carefully rinsed and exposed to Ag, while monitoring the fluorescence.

*4.2.8. Glutathione levels*

Cells were thawed and homogenized in 5% sulfosalicylic acid (1:20 w/v) using a Kontes Micro Ultrasonic Cell Disruptor for 5-10 s. The homogenates were then centrifuged for 5 min at 5000 g (4°C) in a Beckman Coulter Microfuge® R centrifuge. The supernatant was used to measure total glutathione (TGSH) and oxidized glutathione (GSSG) [TGSH = GSH + 2GSSG] using the method of Hermes-Lima and Storey (1996) with modifications noted in Chapter 2 (section 2.2.7).

*4.2.9. Antioxidant enzymes activities*

The cells were sonicated in 50 mM potassium phosphate buffer (1:20 w/v; KPB-50; pH 7.0) for 10 s, followed by a 15 min centrifugation at 15,000 g (4°C) as above. All enzyme assays were read on a SpectraMax Plus spectrophotometer. The following assays were adapted from Lushchak et al. (2001) as outlined in Chapter 2 (section 2.2.8): glutathione S-transferase (GST; EC 2.5.1.18); glutathione reductase (GR; EC 1.8.1.7), glutathione peroxidase (GPx; EC 1.11.1.9), and catalase (CAT; EC 1.11.1.6). The total activity of superoxide dismutase (SOD; EC 1.15.1.1) was measured using the SOD Assay Kit (Sigma, 19160). The enzymes activities were normalized to protein content assessed using the BCA assay (Sigma) with BSA standards.

*4.2.10. Lipid peroxidation (TBARS)*

Lipid peroxidation in hepatocytes was estimated using the thiobarbituric acid reactive substance (TBARS) assay as previously described (Hermes-Lima et al., 1995) with slight modifications. Briefly, cells were resuspended in ice-cold 1.1% phosphoric acid (1:20 w/v) and a 0.2 mL aliquot was mixed with 0.2 mL reaction mix (containing 50 mM NaOH, 0.1 mM butylated hydroxytoluene solution, and 1% thiobarbituric acid), and 0.1 mL 7% phosphoric acid. After boiling for 15 min the samples were cooled on ice for 10 min. Ice-cold butanol (0.5 mL) was then added and the samples were thoroughly mixed and centrifuged for 5 min at 10,000 g. The top butanol layer was then used for spectrophotometric measurements (532 nm). Malondealdehyde standards were prepared in 1.1% phosphoric acid and treated as samples.

*4.2.11. DNA damage*

DNA damage in hepatocytes was assessed using the alkaline precipitation assay (Olive, 1988) with fluorescent detection of DNA strands (Gagné and Blaise, 1995; Gagné et al., 2011). Briefly, the cells were resuspended in KPB-50 (1:20 w/v) and a 25 µL aliquot was transferred to a clean 1.5 mL conical tube. Then 250 µL alkaline lysis buffer (containing 10 mM EDTA-tetrasodium, 10 mM Tris-base, 50 mM NaOH, and 2% SDS) was added. After thorough mixing 250 µL 1% KCl was added to the tube and the mixture was incubated for 10 min at 60°C. After incubation, the mixture was centrifuged for 5 min at 8000 g and the supernatant was used for DNA determination as follows: 50 µL sample and 150 µL Hoechst dye (1 µg/mL) were combined in a 96-well plate and fluorescence (350ex/460em) was assessed as above. The concentration of soluble DNA in

the supernatant was inferred from DNA standards (calf thymus) prepared in the same way as the samples.

*4.2.12. Protein carbonyl*

Protein carbonyl content in hepatocytes was measured using a protein carbonyl assay kit (Cayman Chemical, 10005020). The suggested protocol was modified to account for sample size. Briefly the cells were sonicated in KPB-50 (1:20 w/v). The samples were then centrifuged 15 min at 10,000 g. Streptomycin sulfate (10%) was then added and the samples were incubated 15 min at room temperature to eliminate nucleic acids from the supernatant. The samples were centrifuged for 5 min at 6000 g and 0.1 mL supernatant was transferred to 2 fresh tubes (Control and Sample). Tubes labeled Control were treated with 0.3 mL 2 M HCl and those labeled Sample received an equal volume of 10 mM 2,4-dinitrophenylhydrazine (DNPH) prepared in 2 M HCl. The tubes were incubated in the dark for 1 h at room temperature with vortexing every 15 min. Then 0.4 mL 20% trichloroacetic acid (TCA) was added to the tubes that were vortexed and cooled on ice for 5 min. This was followed by a 15 min centrifugation at 10,000 g. The resulting pellets were washed with 0.4 mL 10% TCA and re-centrifuged. The pellets were then washed three times with 0.5 mL ethyl acetate:ethanol mixture. After the final wash the tubes were dried on paper towel to remove excess ethyl acetate:ethanol mixture. The resulting pellets were dissolved in 0.5 mL 6 M guanidine hydrochloride and centrifuged to remove insoluble materials; BSA standards were also prepared in 6 M guanidine hydrochloride. The absorbance was measured at 370 and 280 nm using a quartz 96-well plate to determine the amount of protein carbonyl per mg protein.

*4.2.13. Cellular uptake of AgNPs*

Cellular uptake of AgNPs into hepatocytes was examined using Transmission Electron Microscope (TEM) after Nguyen et al. (2013). Briefly, hepatocytes were fixed with 2.5% glutaraldehyde in 66.7 mM cacodylate buffer (pH 7.4) for 1 h and then washed twice with 100 mM cacodylate buffer (pH 7.4) for 10 min. The cells were post-fixed with 1% osmium tetroxide in 100 mM cacodylate buffer. The cells were dried through a series of alcohols, infiltrated with Epoxy resin, and embedded into resin-filled Beem capsule molds. The blocks were sectioned and stained with uranyl acetate and lead citrate. The sections (70 nm) were placed on carbon grids and analyzed with a Joel 1230 Transmission Electron Microscope at magnifications of 1200x and 2500x.

*4.2.14. Statistical analysis*

Statistical analyses were conducted using SigmaPlot 11.0 software (SPW 11; Systat Software, Inc., San Jose, CA). Three-way analysis of variance (ANOVA) with post-hoc Holm-Sidak method was used to test for significance between Ag-type, Ag concentration, and presence/absence of Cys. The results of the three-way ANOVA analyses are summarized in Tables 4.1 and 4.2. Additional three-way ANOVA analyses were conducted to test for significance between concentration, presence/absence of cysteine, and presence/absence of BSO within each Ag-type (the results of these analyses are incorporated into the text). In all cases $P \leq 0.050$ was considered significant. Data are presented as means and standard deviation (SD) or standard error of the mean (SEM).

*4.3. Results*

*4.3.1. Characterization of AgNPs*

Measurements from DLS showed that the mean diameter ± SD of AgNPs used in this study was 8.95 ± 0.41 nm in culture medium (Fig. 4.1A). The average PDI ± SD was 0.162 ± 0.025, suggesting that the particles were relatively monodisperse. The mean diameter of AgNPs dispersed in MilliQ water was 7.24 ± 0.34 nm, with an average PDI of 0.145 ± 0.022, suggesting that AgNPs in culture medium may either be aggregating or possibly binding to medium components such as BSA. The ζ-potential of AgNPs in water ranged from -47 to -77 mV, whereas in culture medium it ranged from -13 to -16 mV, depending on the concentration, providing support for the AgNPs potentially attaching to components of the culture medium (Fig. 4.1B). Moreover, the ζ-potential values for water and culture medium in the absence of AgNPs (i.e. 0.0 μg/mL AgNPs) were -0.6 and -12 mV, respectively; these values are consistent with the fact that MilliQ water is devoid of molecules/ions, whereas culture medium contains amino acids, proteins (BSA), ions, etc. Furthermore, STEM analysis showed dispersed AgNPs ranging from 4 to 16 nm (Fig. 4.1C), which are larger than the 1-10 nm indicated by Vive Nano.

Light microscopy demonstrated that the culture medium impacted the properties of the AgNPs: when in water, the AgNPs had a brighter yellow color compared with AgNPs prepared in culture medium (Fig. 4.2A, E, I, M). The AgNPs color was also affected by Cys in both water (Fig. 4.2C, G) and culture medium (Fig. 4.2K, O); BSO had no effect on color in either media (Fig. 4.2B, F and Fig. 4.2J, N). Wells containing both BSO and Cys resembled those containing only Cys (Fig. 4.2D, H, L, P). Furthermore, Cys apparently induced AgNPs aggregation and precipitation in both water (Fig. 4.2G, H) and

culture medium (Fig. 4.2O, P), as evidenced by precipitate formation at the bottom of the well (Fig. 4.2G, H, O, P). This precipitate was noticeable after 24 h of incubation and increased further at 48 h. The changes in color altered the absorption maxima, which were lower for AgNPs prepared in culture medium (Fig. 4.2S, T) than those in water (Fig. 4.2Q, R). Cysteine further reduced the absorption maxima, especially after a 48 h incubation period. Addition of BSO did not have any impact on absorption maxima. The DLS measurements under these conditions showed that the particle size increased slightly over time in response to Cys, such that at 48 h the mean diameters were 9.52 ± 0.22 and 10.09 ± 0.19 nm in the absence and presence of Cys, respectively. Similarly, with BSO the mean diameters were 9.49 ± 0.18 and 10.03 ± 0.12 nm in the absence and presence of Cys. It needs to be noted that the medium samples collected for these measurement excluded the precipitates formed in some wells.

### *4.3.2. Cytotoxicity of AgNP and $Ag^+$*

Both Ag-types were toxic to the erythrocytes and hepatocytes. LDH leakage and hemolysis assays showed similar trends in erythrocytes (Fig. 4.3). However, the hemolysis assay was more sensitive (greater fold-change) than the LDH assay, perhaps due to the relatively low activities of erythrocyte LDH. Hepatocytes displayed similar trends in cytotoxicity (Fig. 4.4A); however, higher concentrations of Ag were required to elicit a response compared to erythrocytes. Overall, the cytotoxicity of both Ag-types was dose-dependent in both cell models ($P < 0.001$). $Ag^+$ was more toxic than the AgNPs ($P < 0.001$), and Cys significantly reduced the toxicity of both Ag-types ($P < 0.001$). The

positive control ($H_2O_2$ and $CuSO_4$ at 1 mM) was effective in eliciting cytotoxicity in both cell models regardless of the presence or absence of Cys.

BSO treatment of hepatocytes significantly ($P < 0.001$) increased the cytotoxicity of both $Ag^+$ and AgNPs (Fig. 4.4B); there was a significant effect of Ag-concentration, Ag-type, and Cys ($P < 0.001$). At the highest Ag concentration, BSO treatment increased the cytotoxicity of $Ag^+$ and AgNPs by 20% and 45%, respectively. Interestingly, Cys was able to reduce the toxicity of $Ag^+$, but not that of AgNPs.

*4.3.3. ROS generation*

Both Ag-types increased ROS generation in trout hepatocytes in a dose-dependent manner (Fig. 4.5A; $P = 0.007$). At the highest concentration $Ag^+$ and AgNPs elevated ROS by 3- and 2-fold, respectively. Cysteine did not significantly affect the ability of $Ag^+$ to generate ROS, but did significantly elevate ROS generation with AgNPs at the highest concentration ($P = 0.008$). There was a significant difference between Ag-types in the presence of Cys ($P = 0.048$), but not in its absence. The positive control was effective in generating ROS independent of Cys treatment, and BSO treatment did not result in higher generation of ROS (Fig. 4.5B).

*4.3.4. Glutathione levels*

Both Ag-types significantly reduced TGSH levels in trout erythrocytes and hepatocytes in a dose-dependent manner ($P < 0.001$) (Fig. 4.6A, 4.7A). The presence of Cys significantly improved TGSH levels in both cell models ($P < 0.001$). $Ag^+$ was more effective in reducing TGSH levels and there was a significant effect of Ag-type in both

cell models ($P < 0.001$). It should be noted that the control TGSH levels in erythrocytes were nearly twice that in the hepatocytes. Both $Ag^+$ and AgNPs decreased GSSG levels (Fig. 4.6B, 4.7B) with the effect greatest in erythrocytes, where Ag-type, Ag concentration, and Cys all had significant effects ($P < 0.001$) (see Tables 4.1 and 4.2). Furthermore, there was a non-significant increase in the GSSG:TGSH ratio in both erythrocytes and hepatocytes (Fig. 4.6C, 4.7C). Although $Ag^+$ appeared to elevate the GSSG:TGSH ratio more than AgNP, there was a significant effect of Ag-type only in the erythrocytes. Cysteine did reduce the GSSG:TGSH ratio but this effect was only significant in hepatocytes ($P = 0.028$). The positive control demonstrated a reduction in TGSH levels and an increase in the GSSG:TGSH ratio in both models.

Trout hepatocytes treated with BSO displayed significantly ($P < 0.001$) lower TGSH levels with both Ag-types (Fig. 4.7D); there was a significant effect of Ag concentration ($P < 0.001$) (see Table 4.2), but not Ag-type even though $Ag^+$ seemed slightly more effective. At the highest silver concentration, BSO treatment decreased the TGSH levels in $Ag^+$- and AgNP-treated cells by 67% and 40%, respectively, compared to BSO non-treated cells. Interestingly, Cys was unable to modify these changes in TGSH levels. The GSSG levels were also significantly reduced ($P < 0.050$; Fig. 4.7E); there was a significant effect of Ag concentration ($P = 0.032$) but not Ag-type or Cys. The GSSG:TGSH ratio was significantly ($P < 0.001$) higher with $Ag^+$ but not AgNPs (Fig. 4.7F), which is due to the noticeable reduction in both GSSG and TGSH levels.

*4.3.5. Antioxidant enzymes activities*

The activities of the antioxidant enzymes in both trout hepatocytes and erythrocytes were differentially affected by Ag. Generally, the glutathione-related enzymes showed a decrease in activities in both cell-types. The activities of CAT and SOD were affected in erythrocytes but not in hepatocytes. The positive control treatment decreased the activity of the antioxidant enzymes, with the exception of CAT, whose activity was unchanged.

The activity of GST decreased in a dose-dependent manner in both trout erythrocytes ($P < 0.001$) (Table 4.3) and hepatocytes ($P = 0.001$) (Table 4.4). There was also a significant effect of Ag-type in erythrocytes ($P < 0.001$) and hepatocytes ($P = 0.011$) (see Tables 4.1 and 4.2), such that $Ag^+$ was more effective in reducing the GST activity. Cysteine generally reduced the effects of Ag on GST activity, but this effect was significant only in erythrocytes ($P < 0.001$). Hepatocytes treated with BSO displayed significantly ($P < 0.050$) reduced GST activity; the Ag-type and concentration had a significant effect ($P < 0.001$), but Cys treatment was only effective ($P < 0.001$) with $Ag^+$. The GST activity was higher in trout hepatocytes than in erythrocytes.

The activity of GR decreased in a dose-dependent manner in both erythrocytes ($P = 0.041$) (Table 4.3) and hepatocytes ($P < 0.001$) (Table 4.4). There was a significant effect of Ag-type in hepatocytes ($P < 0.001$) (see Tables 4.1 and 4.2) but not erythrocytes, although in both models $Ag^+$ generally was more effective in decreasing GR activity. Cysteine significantly improved the activity of GR in hepatocytes ($P = 0.003$) but not erythrocytes. BSO treatment in hepatocytes significantly ($P < 0.050$) reduced GR activity; Ag-type and concentration had a significant effect ($P = 0.002$ and $P < 0.001$,

respectively), but Cys treatment was only effective ($P = 0.029$) with $Ag^+$. Again, GR activity was higher in hepatocytes than in erythrocytes.

The activity of GPx was not affected by either Ag treatment or Cys and was much higher in erythrocytes than in hepatocytes. BSO treatment in hepatocytes did reduce GPx activity, especially at the highest $Ag^+$ concentration; there was no significant effect of Ag concentration, but there were significant effects of 1) Ag-type in the absence of Cys ($P = 0.005$), and 2) Cys ($P < 0.001$) within the $Ag^+$ treatment group.

There was a dose-dependent reduction in CAT activity in erythrocytes exposed to $Ag^+$ ($P = 0.045$) but not AgNPs; Cys had no effect on CAT activity. In contrast, there were no effects of either Ag-type on CAT activity in hepatocytes even with BSO treatment. Hepatocytes had lower CAT activity than erythrocytes.

The activity of SOD in erythrocytes was increased by both Ag-types in a dose-dependent manner ($P = 0.010$), with $Ag^+$ being more effective in increasing SOD activity ($P = 0.003$); Cys did not affect SOD activity. In contrast, the activity of SOD in hepatocytes was only affected in the BSO-treated cells, where there was a reduction in activity with $Ag^+$ and although there were no significant effects of Ag-type or concentration, there was a significant effect of Cys ($P < 0.001$) at the highest $Ag^+$ concentration. The activity of SOD was higher in hepatocytes compared to erythrocytes.

### *4.3.6. Cellular damage in hepatocytes*

Generally, Ag treatment was not as effective as the positive control ($H_2O_2$ and $CuSO_4$ at 1 mM) in increasing cellular damage within hepatocytes. Nonetheless, there were differences between Ag-types, reflecting perhaps their cellular uptake potential.

AgNP treatment elevated TBARS levels by ~30% at the highest concentration (Fig. 4.8A); there was a significant effect of Ag-type at the highest concentration ($P < 0.001$) (see Table 4.2). Cys treatment in combination with AgNPs significantly elevated lipid peroxidation ($P = 0.041$) by ~87% at the highest concentration. Lipid peroxidation was not affected by $Ag^+$ with or without Cys (Fig. 4.8A). The same trends were observed with the BSO treatment (Fig. 4.8D); there were significant effects of concentration ($P < 0.001$), Ag-type ($P = 0.004$), and Cys ($P = 0.035$). BSO-treated hepatocytes exposed to the highest AgNP concentration and Cys had TBARS levels 400% higher than the control cells (Fig. 4.8D). BSO-treated cells exposed to AgNPs in the absence of Cys displayed TBARS levels that were similar to BSO non-treated cells. BSO treatment did increase TBARS at the highest $Ag^+$ concentration by 56%, but this was not statistically significant. Overall TBARS levels were significantly higher ($P < 0.050$) in presence of BSO within both the AgNP- and $Ag^+$-treated cells.

DNA damage unlike lipid peroxidation was much more apparent with $Ag^+$ treatment (Fig. 4.8B); there was a significant effect of Ag-type ($P < 0.001$), Ag concentration ($P = 0.013$) and Cys ($P = 0.001$) (Table 4.2). AgNP treatment did not impact DNA damage with or without Cys. BSO treatment did not further affect DNA damage and similar trends as before were noted (Fig. 4.8E).

Finally, protein carbonyl levels were not affected by either Ag-type with or without Cys. Treatment with BSO also did not affect protein carbonyl levels (Fig. 4.8C, F).

*4.3.7. Cellular uptake of AgNPs into hepatocytes*

Cellular uptake of AgNPs was assessed in hepatocytes by TEM. In general hepatocytes exposed to AgNPs regardless of the concentration (Fig. 4.9B, C, F, G) displayed cellular morphologies that were very similar to control cells (Fig. 9A, E) without any signs of structural damage to the cell membrane, mitochondria, nucleus, or endoplasmic reticulum. However, hepatocytes exposed to 23.3 μg/mL AgNPs had higher abundance of cytoplasmic inclusion bodies or vesicles, but these vesicles did not appear to contain AgNPs. There were no indications of AgNPs in the cytoplasm or within the cell membrane. In contrast, cellular morphologies of $Ag^{+}$-treated hepatocytes (15.5 μg/mL) were noticeably different from the control cells, including an enlarged and marginalized nucleus, distended endoplasmic reticulum, and fewer intact organelles (Fig. 4.9D, H). In the presence of Cys all cells had similar morphologies, including the $Ag^{+}$-treated hepatocytes (Fig. 4.9I-P).

**Table 4.1.** Summary of statistical analysis (P-values) in erythrocytes. Three-way ANOVA with post-hoc Holm-Sidak method was used to assess statistical differences ($P \leq 0.050$) on data found in Figures 4.3, 4.6 and Table 4.3. The three factors were Ag-type, Ag concentration, and cysteine (Cys). 'NS' denotes 'not significant'.

| Endpoint | Ag-type (A) | Cys +/- (B) | Ag conc (C) | Interactions | | | |
|---|---|---|---|---|---|---|---|
| | | | | AxB | AxC | BxC | AxBxC |
| *LDH leakage* | < 0.001 | < 0.001 | < 0.001 | 0.020 | 0.026 | 0.003 | NS |
| *Hemolysis* | < 0.001 | < 0.001 | < 0.001 | NS | NS | NS | NS |
| *TGSH* | < 0.001 | < 0.001 | < 0.001 | NS | NS | NS | NS |
| *GSSG* | < 0.001 | < 0.001 | < 0.001 | NS | NS | NS | NS |
| *GSSG:TGSH* | 0.015 | NS | NS | NS | 0.027 | NS | NS |
| *GST* | < 0.001 | < 0.001 | < 0.001 | < 0.001 | NS | NS | NS |
| *GR* | NS | NS | 0.041 | NS | NS | NS | NS |
| *GPx* | NS | NS | NS | NS | NS | NS | NS |
| *CAT* | 0.006 | NS | 0.045 | NS | 0.012 | NS | NS |
| *SOD* | 0.003 | NS | 0.010 | NS | NS | NS | NS |

**Table 4.2.** Summary of statistical analysis (P-values) in hepatocytes. Three-way ANOVA with post-hoc Holm-Sidak method was used to assess statistical differences ($P \leq 0.050$) on data found in Figures 4.4, 4.5, 4.7, 4.8 and Table 4.4. The three factors were Ag-type, Ag concentration, and cysteine (Cys). 'NS' denotes 'not significant'.

| Endpoint | Ag-type (A) | Cys +/- (B) | Ag conc (C) | Interactions | | | |
|---|---|---|---|---|---|---|---|
| | | | | AxB | AxC | BxC | AxBxC |
| Hepatocytes | | | | | | | |
| *LDH leakage* | < 0.001 | < 0.001 | < 0.001 | < 0.001 | < 0.001 | < 0.001 | < 0.001 |
| *ROS* | NS | 0.011 | 0.007 | NS | NS | NS | NS |
| *TGSH* | < 0.001 | < 0.001 | < 0.001 | NS | NS | NS | NS |
| *GSSG* | NS | NS | NS | NS | NS | NS | NS |
| *GSSG:TGSH* | NS | 0.028 | NS | NS | NS | NS | NS |
| *GST* | < 0.001 | NS | < 0.001 | 0.003 | NS | NS | NS |
| *GR* | < 0.001 | NS | < 0.001 | NS | NS | NS | NS |
| *GPx* | NS | NS | NS | NS | NS | NS | NS |
| *CAT* | NS | NS | NS | NS | NS | NS | NS |
| *SOD* | NS | NS | NS | NS | NS | NS | NS |
| *TBARS* | 0.002 | NS | NS | NS | NS | NS | NS |
| *DNA damage* | < 0.001 | 0.001 | 0.013 | 0.025 | NS | NS | NS |
| *Protein carbonyl* | NS | NS | NS | NS | NS | NS | NS |
| Hepatocytes (BSO) | | | | | | | |
| *LDH leakage* | < 0.001 | < 0.001 | < 0.001 | < 0.001 | < 0.001 | < 0.001 | < 0.001 |
| *ROS* | NS | NS | NS | NS | NS | NS | NS |
| *TGSH* | NS | NS | < 0.001 | NS | NS | NS | NS |
| *GSSG* | NS | NS | 0.032 | NS | NS | NS | NS |
| *GSSG:TGSH* | 0.001 | < 0.001 | 0.039 | < 0.001 | 0.017 | 0.024 | 0.017 |
| *GST* | < 0.001 | < 0.001 | < 0.001 | < 0.001 | NS | 0.025 | < 0.001 |
| *GR* | 0.002 | NS | < 0.001 | 0.043 | NS | NS | NS |
| *GPx* | NS | 0.008 | NS | 0.012 | NS | NS | NS |
| *CAT* | NS | NS | NS | NS | NS | NS | NS |
| *SOD* | NS | 0.008 | NS | 0.027 | NS | NS | 0.021 |
| *TBARS* | 0.004 | 0.035 | < 0.001 | 0.002 | 0.010 | 0.022 | 0.002 |
| *DNA damage* | < 0.001 | NS | NS | 0.010 | NS | NS | NS |
| *Protein carbonyl* | NS | NS | NS | NS | NS | NS | NS |

**Table 4.3.** Activities of antioxidant enzymes in rainbow trout erythrocytes after a 48 h exposure to various $Ag^{+}$ or AgNP concentrations in the presence or absence of cysteine (Cys). The activities of glutathione-S-transferase (GST), glutathione reductase (GR), glutathione peroxidase (GPx), catalase (CAT), and superoxide dismutase (SOD) were assessed. Data are presented as Mean ± SEM (n = 3-6). Three-way ANOVA with post-hoc Holm-Sidak method was used to assess statistical differences (see Table 4.1 and the results section).

| | | +C | C | $Ag^{+}$ (μg/mL) | | | | | AgNP (μg/mL) | | | | |
|---|---|---|---|---|---|---|---|---|---|---|---|---|---|
| | | | | 3.1 | 7.8 | 15.5 | 23.3 | 31 | 3.1 | 7.8 | 15.5 | 23.3 | 31 |
| GST[1] | -c[3] | 1.4±0.1 | 12.7±0.6 | 9.9±0.8 | 8.1±0.6 | 5.7±0.6 | 5.1±0.8 | 3.2±0.4 | 11.9±0.9 | 10.6±0.3 | 9.0±0.4 | 8.1±0.4 | 7.0±0.3 |
| | +c | 1.0±0.1 | 11.4±0.9 | 9.5±1.7 | 10.0±0.3 | 8.7±0.7 | 7.9±0.6 | 6.7±0.0 | 11.3±0.5 | 10.8±0.5 | 8.4±0.3 | 8.4±0.3 | 7.8±0.7 |
| GR[1] | -c | 3.0±1.0 | 5.6±1.2 | 6.5±1.3 | 6.1±1.1 | 5.0±1.2 | 3.6±1.7 | 2.6±1.3 | 7.1±2.0 | 5.7±0.9 | 6.4±1.5 | 5.4±1.0 | 4.5±1.1 |
| | +c | 2.7±0.7 | 5.6±0.7 | 6.0±0.5 | 6.0±0.9 | 5.3±1.1 | 4.5±1.1 | 3.6±1.1 | 6.0±0.7 | 5.6±0.6 | 6.4±0.9 | 5.9±0.8 | 5.9±1.2 |
| GPx[1] | -c | 38±8 | 169±33 | 231±45 | 172±40 | 150±39 | 147±38 | 130±32 | 190±31 | 209±44 | 199±39 | 203±41 | 192±45 |
| | +c | 51±11 | 152±50 | 157±47 | 172±52 | 139±41 | 128±31 | 127±41 | 127±41 | 149±48 | 147±48 | 173±49 | 155±45 |
| CAT[2] | -c | 280±22 | 842±85 | 922±109 | 833±107 | 726±143 | 584±104 | 390±117 | 853±68 | 813±114 | 745±62 | 845±86 | 853±102 |
| | +c | 458±128 | 660±76 | 691±91 | 793±85 | 668±117 | 639±65 | 446±75 | 746±72 | 698±83 | 797±93 | 787±99 | 746±81 |
| SOD[2] | -c | 2.8±0.5 | 1.8±0.2 | 2.2±0.3 | 2.7±0.3 | 2.9±0.5 | 3.3±0.6 | 3.2±0.6 | 1.8±0.2 | 2.1±0.3 | 2.3±0.3 | 2.5±0.4 | 2.7±0.4 |
| | +c | 2.5±0.6 | 2.1±0.3 | 2.2±0.3 | 2.2±0.4 | 3.0±0.5 | 3.2±0.5 | 3.4±0.6 | 2.0±0.3 | 2.1±0.3 | 2.3±0.3 | 2.3±0.4 | 2.6±0.4 |

[1] *nmol/min/mg*

[2] *μmol/min/mg*

[3] *Presence (+c) or absence (-c) of Cys*

**Table 4.4.** Activities of antioxidant enzymes in rainbow trout hepatocytes after a 48 h exposure to various $Ag^{+}$ or AgNP concentrations in the presence or absence of cysteine (Cys) and/or buthionine sulfoximine (BSO). The activities of glutathione-S-transferase (GST), glutathione reductase (GR), glutathione peroxidase (GPx), catalase (CAT), and superoxide dismutase (SOD) were assessed. Silver concentrations that were not assessed in BSO experiments are signified by 'n/a'. Data are presented as Mean ± SEM (n = 5-7). Three-way ANOVA with post-hoc Holm-Sidak method was used to assess statistical differences (see Table 4.2 and the results section).

| | | | +C | C | $Ag^+$ (μg/mL) | | | | | AgNP (μg/mL) | | | | |
|---|---|---|---|---|---|---|---|---|---|---|---|---|---|---|
| | | | | | 3.1 | 7.8 | 15.5 | 23.3 | 31 | 3.1 | 7.8 | 15.5 | 23.3 | 31 |
| GST[1] | -c[3] | -b[4] | 16±10 | 620±47 | 581±28 | 476±39 | 385±44 | 295±59 | 187±67 | 735±75 | 590±49 | 485±29 | 500±30 | 470±19 |
| | +c | -b | 18±4 | 656±53 | 603±69 | 517±25 | 469±17 | 458±15 | 369±16 | 629±40 | 588±48 | 473±48 | 462±29 | 513±41 |
| | -c | +b | n/a | 646±29 | 511±25 | n/a | 238±50 | n/a | 24±21 | 604±9 | n/a | 500±37 | n/a | 389±15 |
| | +c | +b | n/a | 629±26 | 555±37 | n/a | 489±25 | n/a | 363±41 | 667±40 | n/a | 483±28 | n/a | 407±23 |
| GR[1] | -c | -b | 7.4±1.7 | 13.1±1.5 | 12.8±0.8 | 11.7±0.6 | 9.6±1.3 | 7.8±0.9 | 6.2±1.0 | 14.5±1.4 | 12.6±1.0 | 11.6±0.7 | 11.7±0.7 | 11.6±1.3 |
| | +c | -b | 7.1±1.2 | 13.9±1.2 | 12.9±1.1 | 11.7±1.4 | 10.8±1.3 | 9.0±2.3 | 4.6±1.8 | 14.5±1.3 | 13.6±0.8 | 14.9±2.2 | 12.4±1.0 | 12.6±1.0 |
| | -c | +b | n/a | 13.9±1.8 | 11.2±1.4 | n/a | 8.2±1.5 | n/a | 3.1±0.6 | 12.6±1.4 | n/a | 12.9±1.5 | n/a | 10.2±1.3 |
| | +c | +b | n/a | 13.0±1.4 | 11.7±1.4 | n/a | 11.2±1.8 | n/a | 7.6±1.3 | 13.1±1.4 | n/a | 10.9±1.7 | n/a | 9.5±1.6 |
| GPx[1] | -c | -b | 10.6±1.7 | 24.1±1.9 | 21.1±3.5 | 21.2±2.8 | 22.5±3.7 | 25.3±2.5 | 21.5±1.8 | 23.5±3.4 | 21.1±3.6 | 22.7±3.2 | 21.8±3.1 | 22.1±2.5 |
| | +c | -b | 13.0±5.0 | 24.2±1.2 | 18.4±3.2 | 19.2±4.3 | 19.4±3.3 | 21.9±3.2 | 19.1±3.9 | 21.3±2.3 | 16.7±5.9 | 20.9±3.3 | 19.9±3.1 | 20.1±2.7 |
| | -c | +b | n/a | 22.4±1.6 | 17.0±2.1 | n/a | 16.2±2.5 | n/a | 11.5±2.7 | 20.7±1.2 | n/a | 24.2±2.3 | n/a | 16.9±1.2 |
| | +c | +b | n/a | 19.7±1.5 | 21.4±2.4 | n/a | 23.3±2.6 | n/a | 21.9±2.7 | 21.2±2.4 | n/a | 19.9±2.9 | n/a | 21.1±2.3 |

| | | | | | | | | | | | | | | |
|---|---|---|---|---|---|---|---|---|---|---|---|---|---|---|
| CAT[2] | -c | -b | 469±117 | 454±50 | 453±73 | 482±64 | 453±61 | 696±124 | 678±118 | 503±73 | 425±60 | 477±79 | 479±69 | 508±78 |
| | +c | -b | 438±110 | 470±55 | 479±59 | 503±48 | 536±56 | 545±55 | 553±86 | 518±81 | 517±49 | 594±70 | 579±49 | 605±63 |
| | -c | +b | n/a | 455±46 | 499±58 | n/a | 779±142 | n/a | 780±249 | 471±69 | n/a | 545±45 | n/a | 506±72 |
| | +c | +b | n/a | 429±71 | 499±89 | n/a | 544±93 | n/a | 531±101 | 460±75 | n/a | 553±95 | n/a | 579±124 |
| SOD[2] | -c | -b | 16.3±2.2 | 20.4±1.4 | 24.1±2.1 | 23.3±1.2 | 21.9±2.7 | 23.9±3.2 | 23.1±4.7 | 24.8±1.9 | 23.3±1.5 | 20.9±2.1 | 23.9±1.3 | 24.3±2.2 |
| | +c | -b | 8.2±1.7 | 22.7±2.4 | 20.4±1.5 | 19.9±1.3 | 22.3±1.6 | 20.0±2.4 | 23.3±3.0 | 19.9±1.2 | 21.5±1.7 | 24.2±2.3 | 22.2±1.7 | 26.6±2.7 |
| | -c | +b | n/a | 19.7±0.6 | 19.9±0.9 | n/a | 18.3±2.6 | n/a | 11.2±2.8 | 19.7±0.8 | n/a | 19.5±1.0 | n/a | 19.3±1.0 |
| | +c | +b | n/a | 20.6±1.0 | 20.5±1.2 | n/a | 20.7±1.3 | n/a | 22.5±2.4 | 20.7±1.3 | n/a | 20.6±1.3 | n/a | 18.6±1.5 |

[1] *nmol/min/mg*
[2] *μmol/min/mg*
[3] *Presence (+c) or absence (-c) of Cys*
[4] *Presence (+b) or absence (-b) of BSO*

**Figure 4.1.** Characterization of Vive Nano AgNPs used in this study (part I). Dynamic Light Scattering (DLS) was used to determine: (A) size distribution of AgNPs (31 μg/mL) prepared in culture medium (Means + SD; n = 10), and (B) zeta (ζ)-potential of AgNPs prepared in water and culture medium at various concentrations (Means + SEM; n = 4). Scanning Transmission Electron Microscope (STEM) was used to confirm DLS results; a 10 μg/mL solution of AgNPs was prepared in water and photos were captured from transmission electron diffraction (TED) (C).

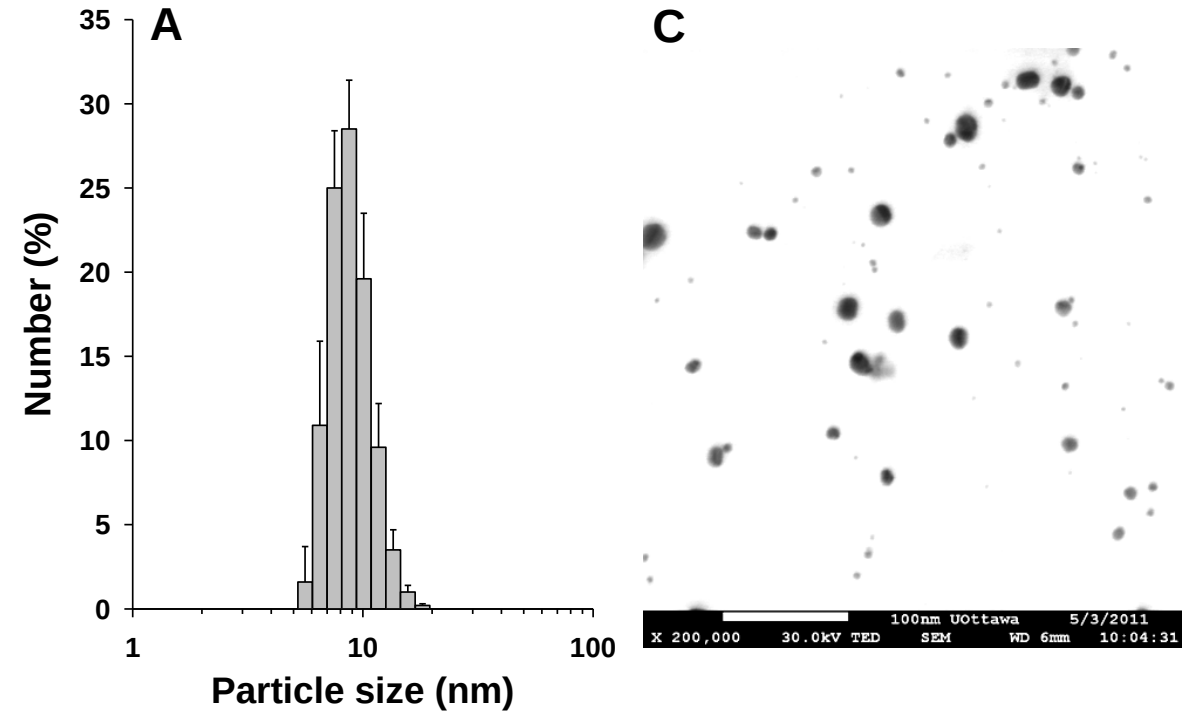
A
Number (%)
Particle size (nm)
C
100nm UOttawa 5/3/2011
X 200,000 30.0kV TED SEM WD 6mm 10:04:31

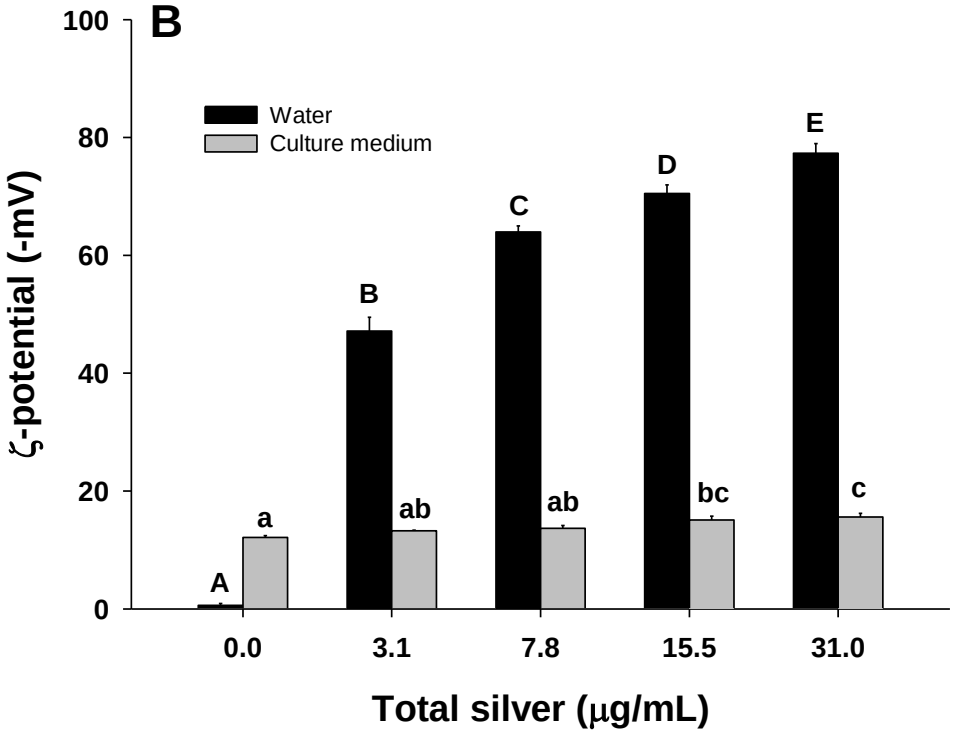
B
Water
Culture medium
ζ-potential (-mV)
Total silver (μg/mL)
0.0
3.1
7.8
15.5
31.0
A
a
B
ab
C
ab
D
bc
E
c

**Figure 4.2.** Characterization of Vive Nano AgNPs used in this study (part II). Light microscopy images (A-P) of AgNPs (31 μg/mL) were taken after a 48 h incubation period in water or culture medium in the presence or absence of cysteine (Cys) and/or buthionine sulfoximine (BSO). Images E-H and M-P are 10x magnified versions of images A-D and I-L, respectively. UV-VIS spectroscopy measurements of AgNPs (31 μg/mL) in different media are presented in Q-R as Means + SEM (n = 5). The absorbance of AgNPs was measured in water after 2 and 48 h (Q and R, respectively) and in culture medium after 2 and 48 h (S and T, respectively). The symbols 'C' and 'B' in the image headings and panel Q legend refer to Cys and BSO, respectively.

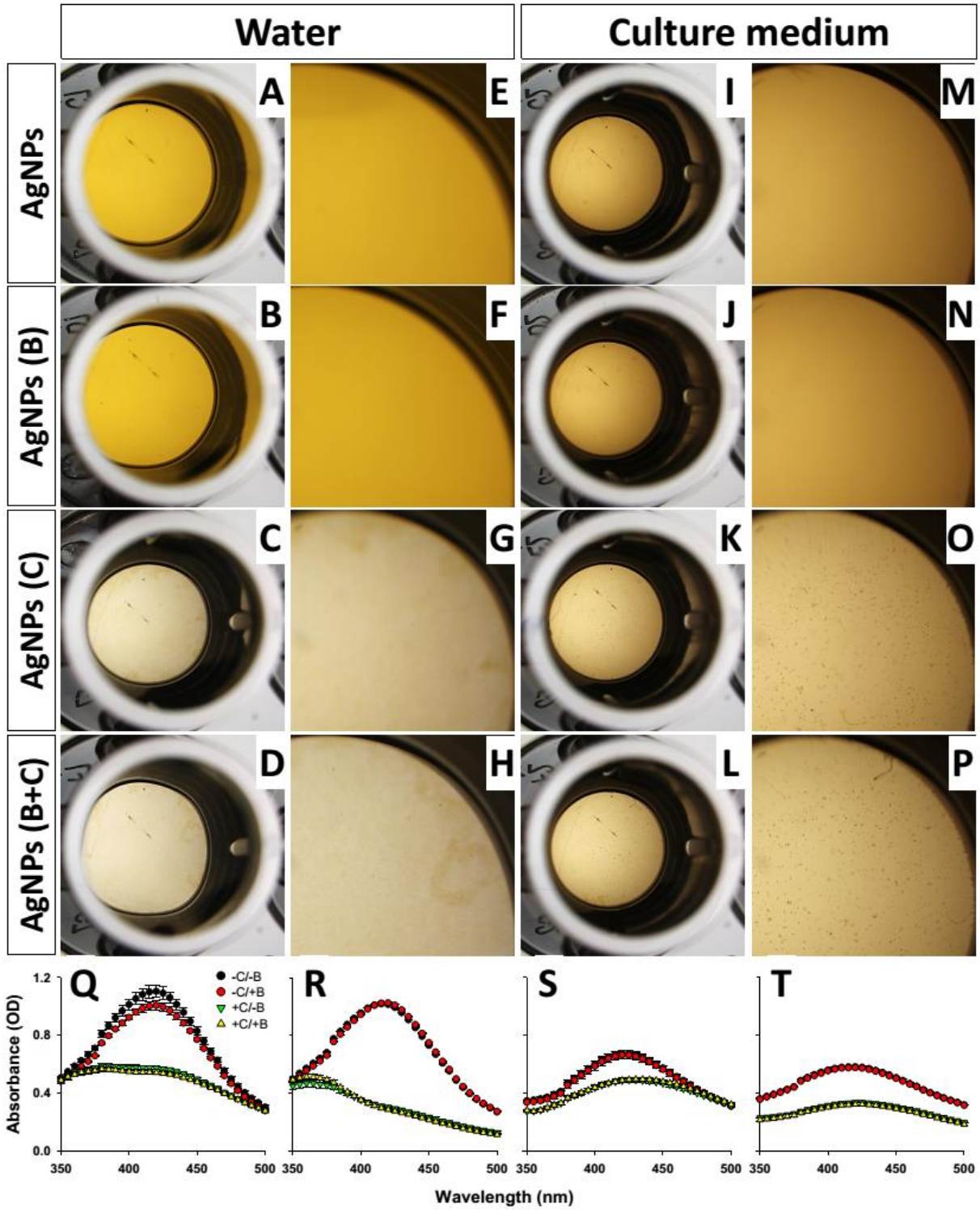
Water
Culture medium
AgNPs
AgNPs (B)
AgNPs (C)
AgNPs (B+C)
A
B
C
D
E
F
G
H
I
J
K
L
M
N
O
P
Q
R
S
T
-C/-B
-C/+B
+C/-B
+C/+B
Absorbance (OD)
Wavelength (nm)
0.0
0.4
0.8
1.2
350
400
450
500

**Figure 4.3.** Cytotoxicity in trout erythrocytes exposed to various $Ag^{+}$ or AgNP concentrations in the presence or absence of cysteine (Cys) for 48 h. Cytotoxicity was assessed by (A) lactate dehydrogenase (LDH) leakage and (B) hemolysis assays. Positive control (C+) was a combination of $H_2O_2$ and $CuSO_4$ both at 1 mM. The results are expressed as fold-change above control (no Ag) values. Data are presented as Mean + SEM (n = 11-13). Three-way ANOVA with post-hoc Holm-Sidak method was used to assess statistical differences (see Table 4.1 and the results section).

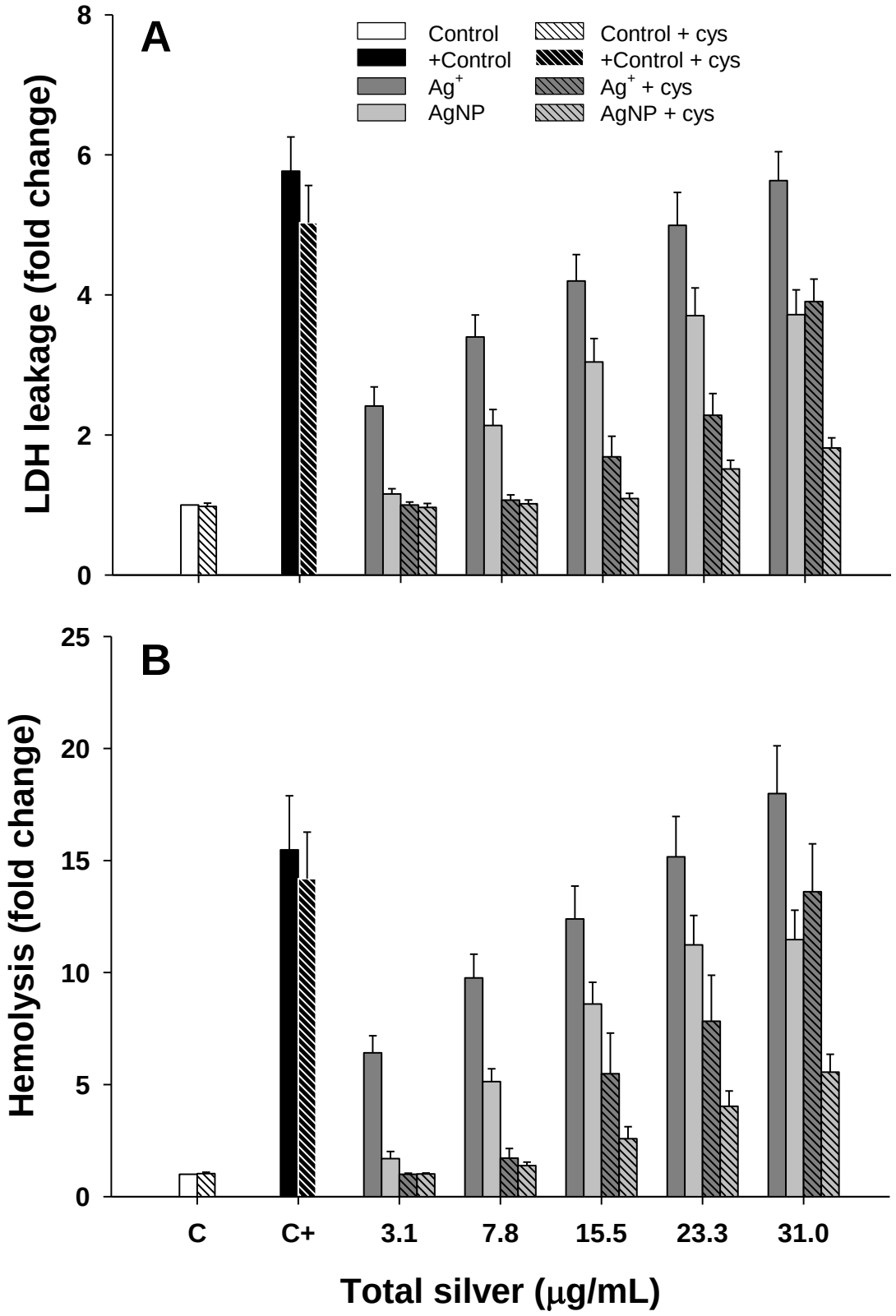
A
Control
+Control
Ag+
AgNP
Control + cys
+Control + cys
Ag+ + cys
AgNP + cys
LDH leakage (fold change)
0
2
4
6
8
B
Hemolysis (fold change)
0
5
10
15
20
25
C
C+
3.1
7.8
15.5
23.3
31.0
Total silver (μg/mL)

**Figure 4.4.** Cytotoxicity in trout hepatocytes exposed to various $Ag^{+}$ or AgNP concentrations in the presence or absence of cysteine (Cys) and in the absence (A) and presence (B) of buthionine sulfoximine (BSO). Cytotoxicity was assessed using LDH leakage assay. Positive control (C+) was a combination of $H_2O_2$ and $CuSO_4$ both at 1 mM and was only used in absence of BSO. Negative control (C-) refers to BSO non-treated cells. The results are expressed as fold-change above control values. Data are presented as Mean + SEM (n = 5-13). Three-way ANOVA with post-hoc Holm-Sidak method was used to assess statistical differences (see Table 4.2 and the results section).

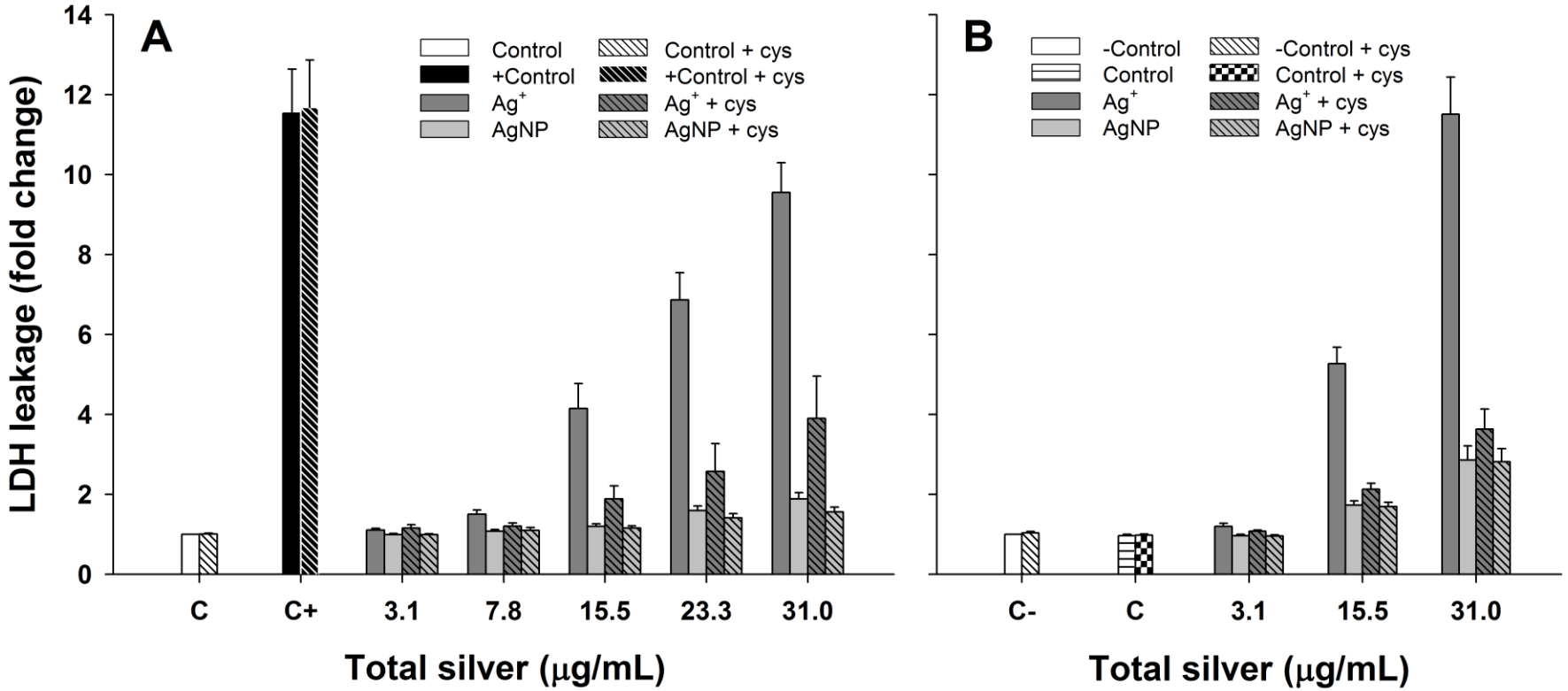
A
LDH leakage (fold change)
14
12
10
8
6
4
2
0
Control
+Control
Ag+
AgNP
Control + cys
+Control + cys
Ag+ + cys
AgNP + cys
C
C+
3.1
7.8
15.5
23.3
31.0
Total silver (μg/mL)
B
-Control
Control
Ag+
AgNP
-Control + cys
Control + cys
Ag+ + cys
AgNP + cys
C-
C
3.1
15.5
31.0
Total silver (μg/mL)

**Figure 4.5.** Generation of reactive oxygen species in trout hepatocytes exposed to various $Ag^{+}$ or AgNP concentrations in the presence or absence of cysteine (Cys) and in the absence (A) and presence (B) of buthionine sulfoximine (BSO). Positive control (C+) was a combination of $H_2O_2$ and $CuSO_4$ at 1 mM and was only used in absence of BSO. Negative control (C-) refers to BSO non-treated cells. The results are expressed as fold-change above control values. Data are presented as Mean + SEM (n = 5-7). Three-way ANOVA with post-hoc Holm-Sidak method was used to assess statistical differences (see Table 4.2 and the results section).

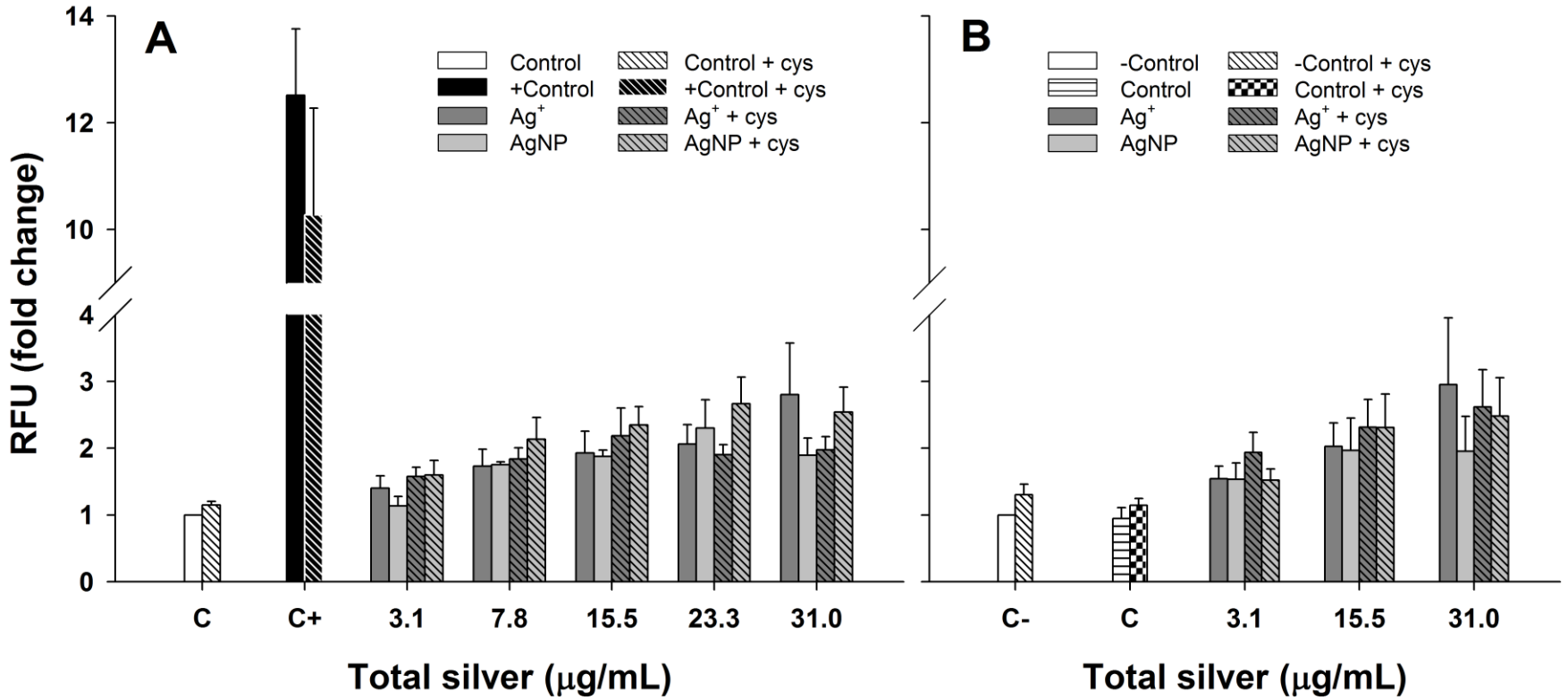
A
B
RFU (fold change)
Control
+Control
Ag+
AgNP
Control + cys
+Control + cys
Ag+ + cys
AgNP + cys
-Control
-Control + cys
C
C+
C-
3.1
7.8
15.5
23.3
31.0
Total silver (μg/mL)

**Figure 4.6.** Glutathione levels in trout erythrocytes exposed to various $Ag^{+}$ or AgNP concentrations in the presence or absence of cysteine (Cys) for 48 h. A. Total glutathione (TGSH) levels. B. Oxidized glutathione (GSSG) levels. C. GSSG:TGSH ratio. Positive control (C+) was a combination of $H_2O_2$ and $CuSO_4$ both at 1 mM. Data are presented as Mean + SEM (n = 4-8). Three-way ANOVA with post-hoc Holm-Sidak method was used to assess statistical differences (see Table 4.1 and the results section).

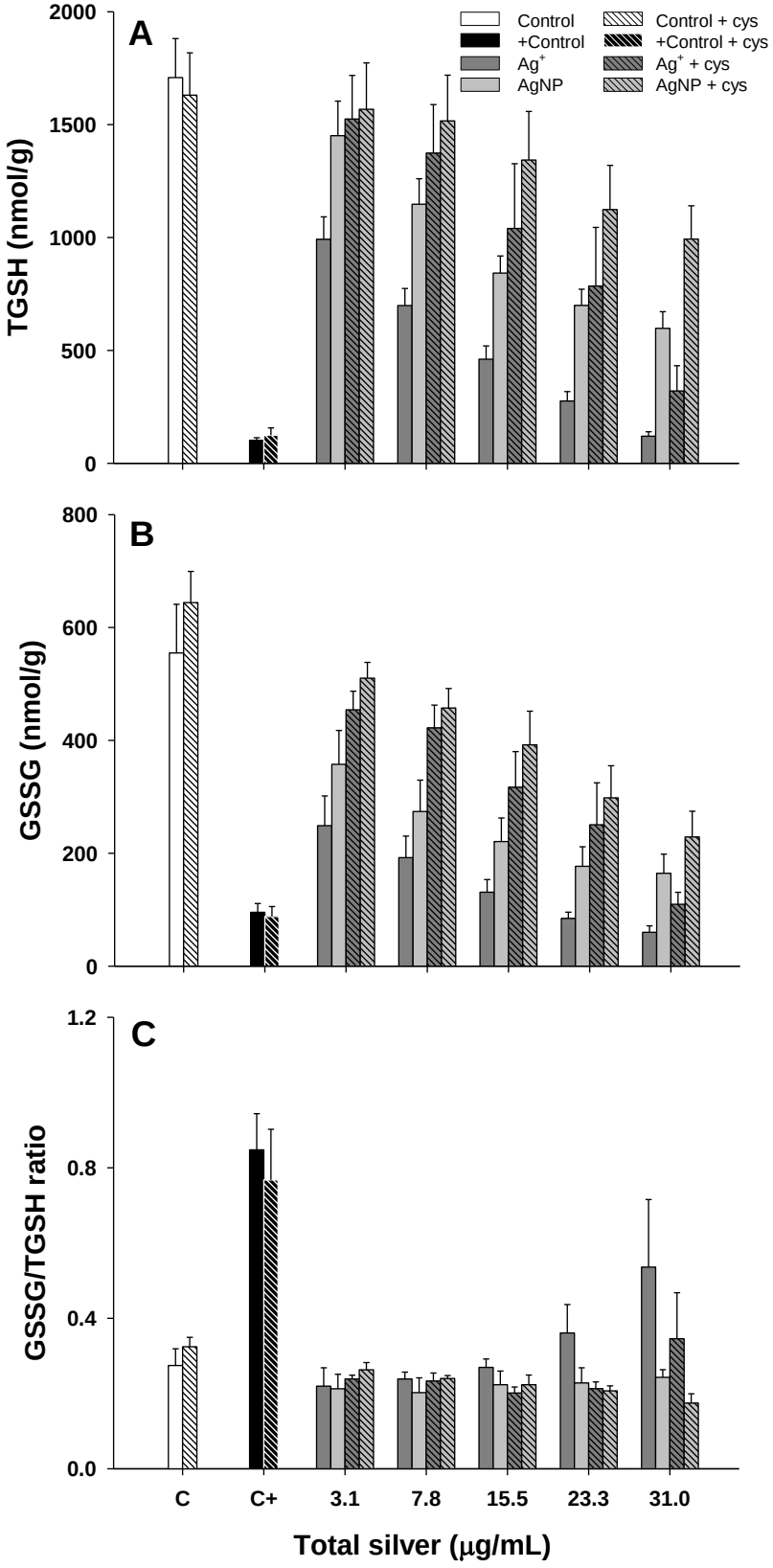
A
B
C
Control
+Control
Ag+
AgNP
Control + cys
+Control + cys
Ag+ + cys
AgNP + cys
TGSH (nmol/g)
GSSG (nmol/g)
GSSG/TGSH ratio
2000
1500
1000
500
0
800
600
400
200
1.2
0.8
0.4
0.0
C
C+
3.1
7.8
15.5
23.3
31.0
Total silver (μg/mL)

**Figure 4.7.** Glutathione levels in trout hepatocytes exposed to various $Ag^{+}$ or AgNP concentrations in the presence or absence of cysteine (Cys) and/or buthionine sulfoximine (BSO) for 48 h. (A and D) Total glutathione (TGSH) levels. (B and E) Oxidized glutathione (GSSG) levels. (C and F) GSSG:TGSH ratio. Positive control (C+) was a combination of $H_2O_2$ and $CuSO_4$ both at 1 mM and was only used in absence of BSO. Negative control (C-) refers to BSO non-treated cells. Data are presented as Mean + SEM (n = 4-9). Three-way ANOVA with post-hoc Holm-Sidak method was used to assess statistical differences (see Table 4.2 and the results section).

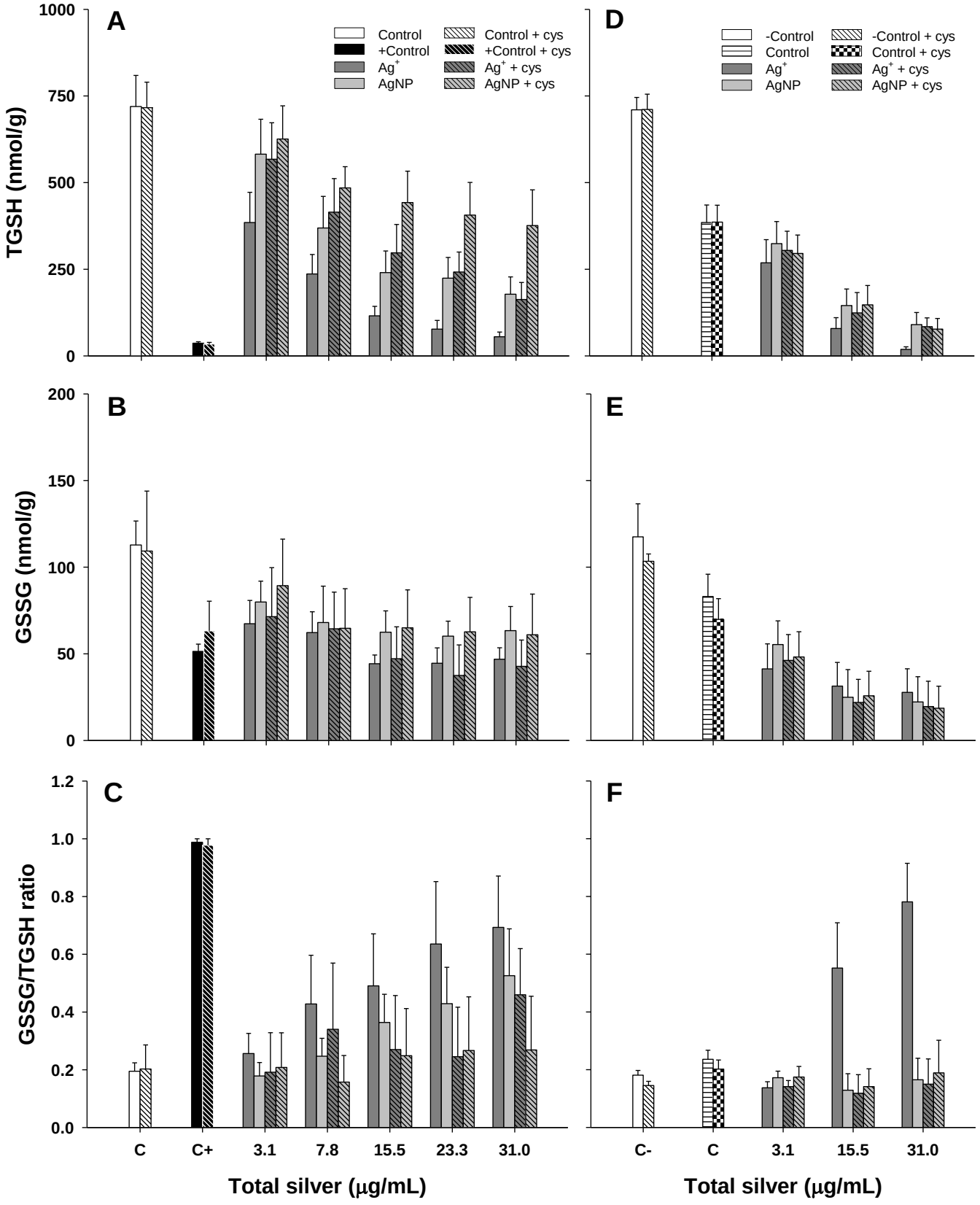
A
B
C
D
E
F
TGSH (nmol/g)
GSSG (nmol/g)
GSSG/TGSH ratio
Control
+Control
Ag+
AgNP
Control + cys
+Control + cys
Ag+ + cys
AgNP + cys
-Control
-Control + cys
C
C+
C-
3.1
7.8
15.5
23.3
31.0
Total silver (μg/mL)

**Figure 4.8.** Cellular damage in trout hepatocytes exposed to various $Ag^{+}$ or AgNPs concentrations in the presence or absence of cysteine (Cys) and/or buthionine sulfoximine (BSO) for 48 h. (A and D) Lipid peroxidation (TBARS). (B and E) DNA damage (Soluble DNA). (C and F) Protein carbonyl. The positive control (C+) was a combination of $H_2O_2$ and $CuSO_4$ at 1 mM and was only used in the absence of BSO. Negative control (C-) refers to BSO non-treated cells. Data are presented as Mean + SEM (n = 4-7). Three-way ANOVA with post-hoc Holm-Sidak method was used to assess statistical differences (see Table 4.2 and the results section).

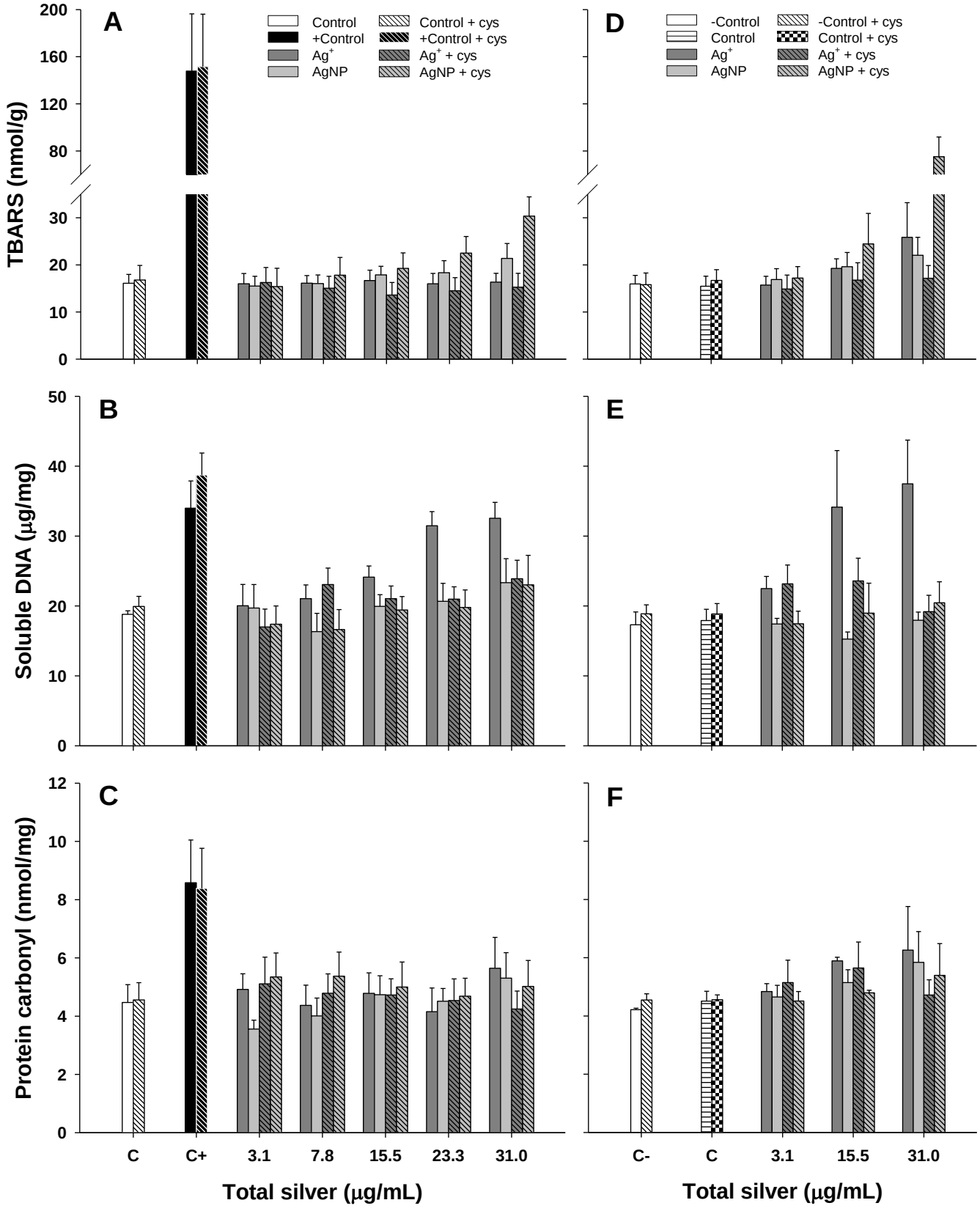
A
B
C
D
E
F
TBARS (nmol/g)
Soluble DNA (μg/mg)
Protein carbonyl (nmol/mg)
Control
+Control
Ag+
AgNP
Control + cys
+Control + cys
Ag+ + cys
AgNP + cys
-Control
-Control + cys
C
C+
3.1
7.8
15.5
23.3
31.0
C-
Total silver (μg/mL)

**Figure 4.9.** Transmission Electron Microscope (TEM) micrographs of trout hepatocytes exposed to $Ag^{+}$ or AgNPs for 48 h: control (A, E, I, M), AgNPs at 3.1µg/mL (B, F, J, N), AgNPs at 23.3 µg/mL (C, G, K, O), and $Ag^{+}$ at 15.5 µg/mL (D, H, L, P) in the absence (A-H) or presence (I-P) of cysteine. See section 4.2.13 for details. Differences are indicated with arrows.

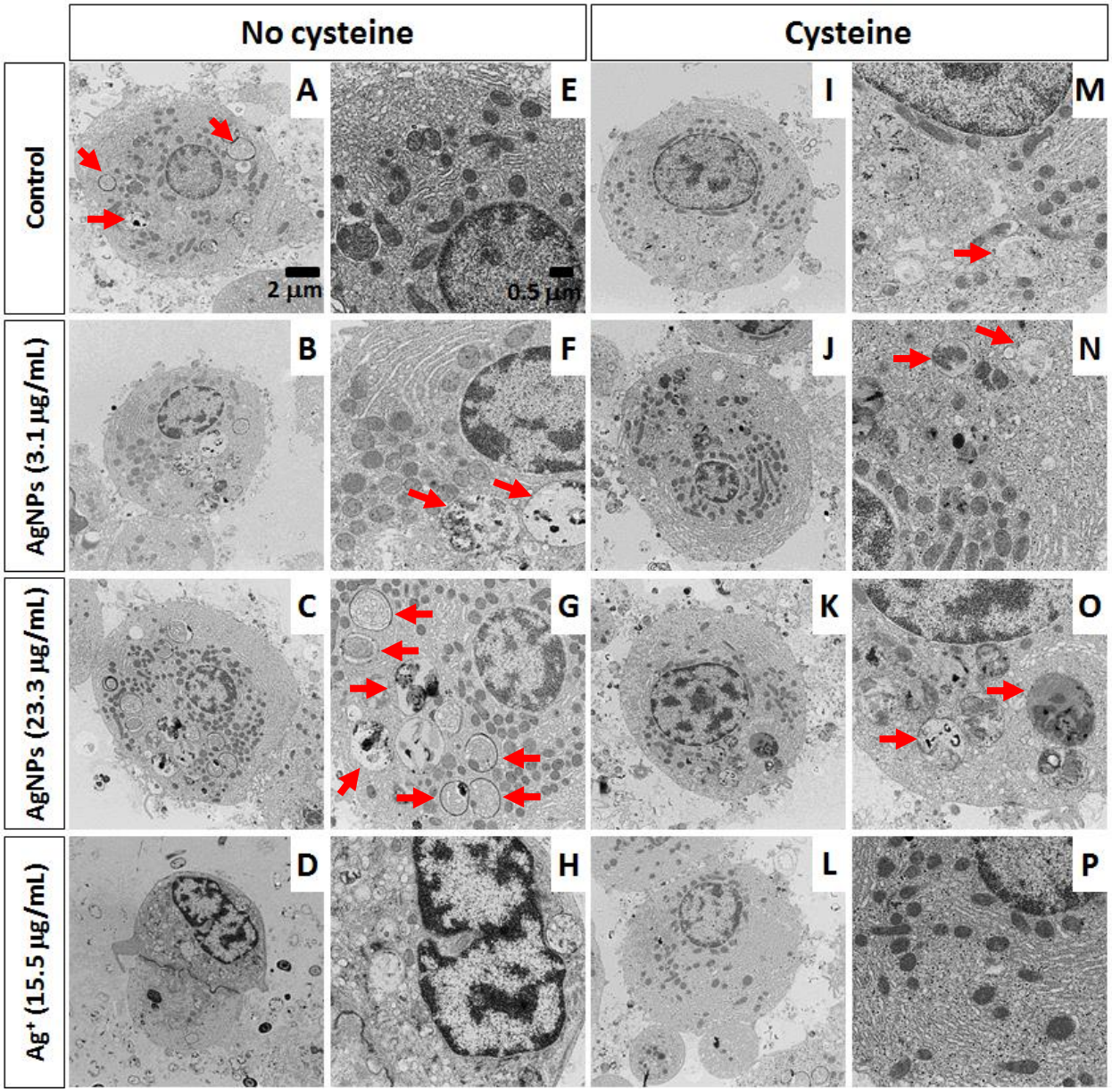

*4.4. Discussion*

The environmental concentrations and the impacts of AgNPs on aquatic organisms remain unknown, so it is important to further investigate their potential effects to provide regulators and environmental protection agencies with data to assess whether or not AgNPs may pose a risk to aquatic species. Given the ability of $Ag^+$ and AgNPs to accumulate in exposed fish, this study aimed to elucidate the relationship between Ag toxicity and oxidative stress and damage *in vitro* using rainbow trout erythrocytes and hepatocytes, two tissues that potentially could be impacted by AgNPs. This study used AgNPs from Vive Nano that averaged 9 nm in diameter, with low aggregation (except in presence of Cys) and with a low percentage dissolved $Ag^+$ (0.5%).

It is important to note that the AgNP concentrations used here are similar to those used in previous *in vitro* studies and are higher than the predicted environmental concentrations of 0.088-2.63 ng/L (Gottschalk et al., 2009) or 40-320 ng/L (Blaser et al., 2008) in surface water. In fact the concentrations used here are twenty times higher than those used in our zebrafish studies (Chapter 2 and 3; Massarsky et al., 2013; 2014a). Moreover, the concentrations of free AgNPs and $Ag^+$ are most likely much lower than the nominal concentrations due to the presence of salts and especially proteins in the culture medium. Unfortunately, primary hepatocytes survive poorly in media lacking bovine serum albumin so the effective Ag concentrations reported here are probably overestimated.

We demonstrate that both $Ag^+$ and AgNPs are cytotoxic to trout erythrocytes and hepatocytes, but have different cellular targets as discussed below. Cells in our study were exposed to concentrations of 3.1-31 μg/mL for 48 h since at lower concentrations

AgNPs were not cytotoxic, especially in hepatocytes. Based on our cell viability data, AgNPs were less toxic than $Ag^+$ at equivalent Ag concentrations to both cell models. Silver toxicity was demonstrated previously in fish cell models. Farkas et al. (2010) compared AgNP and $Ag^+$ toxicity in rainbow trout hepatocytes and found that AgNPs were more toxic than $Ag^+$ at concentrations of 0.063-19 μg/mL after a 48 h exposure. However, their more recent paper (Farkas et al., 2011) reported a similar cytotoxic potential for AgNPs and $Ag^+$ in rainbow trout gill cells exposed to 0.1-10 μg/mL Ag for 48 h. However, while comparing studies, it is important to consider cell culture conditions. Our study used culture medium supplemented with 1% BSA, which would decrease the amount of free $Ag^+$ and likely bind to AgNPs, thus decreasing Ag toxicity as previously reported (Grade et al., 2012). Also, the AgNPs used in our study were carboxy-functionalized and stabilized with sodium polyacrylate compared to the sodium citrate- and PVP-capped AgNPs used in Farkas et al. 2010 and 2011, respectively; the particle size was similar however. The toxicity of $Ag^+$ was also demonstrated previously in several mammalian cell models (Hollinger, 1996). Baldi et al. (1988) showed a reduction in rat hepatocytes viability after a 4 h exposure to 30 μM $AgNO_3$ (~2 μg/mL $Ag^+$). Similarly, Sopjani et al. (2009) showed an increased hemolysis of human erythrocytes exposed to $Ag^+$ for 48 h even at 50 nM $Ag^+$ (5 ng/mL).

Furthermore, erythrocytes were more sensitive than hepatocytes to Ag exposure as even the lower doses of silver increased cytotoxicity. This is likely due to the higher susceptibility of erythrocytes to lipid peroxidation arising from the high content of poly-unsaturated fatty acid in their cell membrane and high cytoplasmic oxygen and iron concentrations, which continuously produce ROS (Li et al., 2013), making erythrocytes

an appropriate *in vitro* model to study oxidative stress (Reddy et al., 2007; Trenzado et al., 2009). Our study also found that the LDH leakage assay in erythrocytes may actually underestimate toxicity and that the hemolysis test may in fact be the more accurate method of the two. It should be noted that the applicability of the LDH leakage assay (and other assays) to test for cytotoxicity of ENMs was called into question in recent studies. For example, MacCormack et al. (2012) investigated the activity of LDH in presence of silicon, Au, or CdSe nanoparticles. The authors reported that all ENMs inhibited the activity of purified rabbit muscle LDH; however, in the presence of 1% BSA LDH activities were not affected. The activity of LDH in goldfish (*Carassius auratus*) white muscle homogenates was also not affected by the ENMs. We too noticed similar effects of AgNPs (unpublished data); AgNPs inhibited the LDH activity of the purified rabbit muscle, but not of the rainbow trout (*Oncorhynchus mykiss*) white muscle homogenates incubated under similar culture conditions as mentioned herein. Furthermore, the similarity between the hemolysis and LDH leakage data for erythrocytes provide additional assurance that LDH activity was not affected.

Previous studies have demonstrated that both types of Ag are able to generate ROS leading to oxidative stress (Park et al. 2009; Piao et al. 2011; Mukherjee et al., 2012). In our study both Ag-types generated ROS to similar extent. These findings contrast with those of Farkas et al. (2010), who reported that $Ag^{+}$, but not AgNPs, generated ROS in trout hepatocytes after a 2 h exposure. This difference with our study may be related to different exposure periods, but it may also be attributed to the different AgNPs used. The observed increase in ROS could explain the decrease in TGSH in the hepatocytes but also erythrocytes, which are presumably more susceptible to oxidative stress. Although there

were no apparent differences in the ability of $Ag^+$ and AgNP to generate ROS in hepatocytes, $Ag^+$ was more effective in reducing TGSH levels in both cell models. Reductions in TGSH levels imply the utilization of GSH to neutralize the generated ROS, which is commonly used as a marker of oxidative stress (Park, et al., 2009; Tuncer, et al., 2010). It is also possible that some of the GSH directly binds to the free $Ag^+$ inside the cell as it has been shown that $Ag^+$ has a high affinity for thiol compounds such as GSH (Carlson, et al. 2008; Kramer et al., 2009; Khan et al., 2011). Moreover, AgNPs were shown to inhibit the activity of GSH-synthesizing enzymes, reducing the GSH production (Piao et al., 2011). Activities of these enzymes, however, were not measured in this study. The decrease in intracellular GSSG could be attributed to its transport out of the cells (Deneke and Fanburg, 1989; Toborek et al., 1995; Keppler, 1999) and subsequent degradation by glutamyltransferase and peptidases (Hultberg et al., 2001). The cleavage of GSSG disulfide bonds in relation to $Ag^+$ has also been mentioned (Khan et al., 2011), which could also contribute to GSSG decrease. Lastly, it is important to note the higher levels of TGSH and GSSG in erythrocytes, which is probably due to their role in oxygen transport and higher susceptibility for oxidative damage. This observation was previously reported for rainbow trout (Otto and Moon, 1996).

The depletion of GSH may explain the decreased GST activity as it conjugates GSH to harmful products of lipid peroxidation (and xenobiotic compounds) (Lushchak et al., 2001); GST activity was further reduced when GSH levels were chemically reduced in BSO-treated hepatocytes. However, the activity of GPx, which also utilizes GSH to eliminate lipid peroxides (and $H_2O_2$) (Lushchak et al., 2001) was only slightly reduced in BSO-treated hepatocytes. Reduction in GPx activity has been reported previously in the

human liver cell line HL-7702 exposed to AgNPs for 24 h; however, glutathione levels were not measured in this study (Song et al., 2012). The activity of GR was also reduced, perhaps in response to the decreased GSSG levels as it recycles GSSG to replenish GSH (Mannervik, 1987). The activities of CAT decreased and SOD increased in erythrocytes, but not in hepatocytes, reflecting perhaps the levels of $H_2O_2$ and superoxide anions in these cells. The activity of SOD has been shown to decrease after a 24 h exposure to AgNPs in the human liver cell line HL-7702 (Song et al., 2012) similarly to the decreased SOD activity in $Ag^+$-exposed and BSO-treated trout hepatocytes in this study. In contrast, Misra et al. (2012) reported increased activities for GPx, CAT, and SOD, decreased GSH levels, and increased TBARS in trout hepatocytes exposed to the oxidative stress inducer selenomethionine. Overall, these data indicate that the link between antioxidant enzymes activities, ROS generation, and antioxidants, such as GSH, should be examined in more detail, especially in response to AgNP/$Ag^+$ exposure.

There was also evidence for cellular damage in addition to oxidative stress in hepatocytes in response to Ag. We showed that AgNPs induced lipid peroxidation, suggesting that AgNPs, at least under the conditions of this study, may generate ROS extracellularly and/or within close proximity to the cell membrane. This is further supported by the increased lipid peroxidation in hepatocytes that were treated with Cys where some AgNPs precipitated (as discussed below). On the other hand, $Ag^+$ induced DNA damage in hepatocytes, suggesting that $Ag^+$ penetrates the cell membrane and may generate ROS intracellularly, damaging the DNA. The ability of AgNPs (coated with methoxy-polyethylene glycol mercapto) to induce lipid peroxidation was demonstrated previously in human liver cell line HL-7702 after a 24 h exposure to 12.5-100 μg/mL

AgNPs (Song et al., 2012). The idea of extracellular ROS generation suggested here is circumstantially supported by the minimal evidence for AgNPs uptake in the hepatocytes. The morphology of the AgNP-exposed cells appeared similar to the control cells. The only apparent difference was the higher abundance of cytoplasmic inclusion bodies or vesicles in AgNP-exposed cells. Similar results were reported for gold nanoparticles, which accumulated inside the vesicles of mouse fibroblasts (Coradeghini et al., 2013). However, unlike in mouse fibroblasts, there were no visible nanoparticles inside the vesicles, suggesting that if in fact the AgNPs are taken up, they probably dissociate. Furthermore, there was no sign of AgNPs in the cytoplasm, unlike the recent study by Nguyen et al. (2013) that reported intracellular AgNPs in mouse macrophage. These differences in AgNP uptake could be attributed to cell type and AgNPs coatings used. It should be noted that the coating or surface functionalization is an important factor that is likely to affect the behavior and toxicity of AgNPs (and other ENMs) as recently reviewed (Scown et al., 2010a; Chernousova and Epple, 2013; Yu et al., 2013). It was also reported that the extent of AgNPs uptake could be modified by the protein-AgNP complexes in human epidermal keratinocyte (HEK) cells (Monteiro-Riviere et al., 2013); however, AgNPs were taken up in all cases and formed cytoplasmic vacuoles similar to Coradeghini et al. (2013). Furthermore, there was no sign of AgNPs lodged in cell membranes, but this can be a result of washing performed during sample preparation for TEM imaging (Liu et al., 2010b).

Cysteine treatment generally reduced the toxicity of both Ag-types in the two cell preparations used. This effect was evident from the decreased cytotoxicity and higher TGSH levels in Cys-treated cells. Similar effects of Cys and other thiol-containing

molecules on AgNP toxicity were reported in macrophages exposed to 100 μg/mL of AgNPs for 72 h (Singh and Ramarao, 2012). It is also possible that in addition to the chelating effect, Cys acts as an antioxidant as reported elsewhere (Rayburn and Friedman, 2010; Tuncer et al., 2010); this is especially relevant for the lower Ag concentrations since Cys binds $Ag^+$ in 1:1 ratio (Liu and Sun, 1981), meaning that at these lower doses there was excess Cys available to be taken up by the cells to act as an antioxidant and/or promote GSH synthesis. Although plausible, the antioxidant action of Cys has limited support in this study since control cells treated with Cys did not display higher glutathione levels and Cys treatment did not suppress the prooxidant action of BSO. Moreover, Cys treatment did not decrease $Ag^+$/AgNP-mediated ROS generation in hepatocytes. Cys treatment also increased the lipid peroxidation in hepatocytes in the presence of AgNPs; however; this effect may be related to the ability of Cys to precipitate AgNPs as noted from the microscopy and spectroscopy results. One could speculate that the precipitated AgNPs would come into direct contact with the cells and induce lipid peroxidation more effectively. Although AgNPs in the presence of Cys increased lipid peroxidation, the cell viability was not affected, suggesting that the extensive lipid peroxidation was not sufficient to induce cytotoxicity; this emphasizes that the relation between oxidative damage and cytotoxicity is not absolute.

Treatment with BSO in hepatocytes increased the toxicity of both Ag-types as evidenced from the increased cytotoxicity in both $Ag^+$- and AgNPs-exposed cells. Interestingly, Cys co-treatment reduced the cytotoxicity of $Ag^+$ similarly to BSO non-treated cells, but not in AgNPs-exposed cells. Furthermore, Cys co-treatment was unable to return TGSH levels in both $Ag^+$- and AgNPs-exposed cells to those observed in BSO

non-treated cells. The lipid peroxidation in BSO-treated hepatocytes was also increased, especially with AgNPs in presence of Cys. This could be explained by the precipitation of AgNPs as mentioned above. In addition, given that there was no additional increase in ROS in BSO-treated hepatocytes, it is plausible that the increased lipid peroxidation was due to the decreased GSH levels. Glutathione is used by GPx to eliminate not only $H_2O_2$ but also lipid peroxides that promote lipid peroxidation (Lushchak et al., 2001). Although BSO treatment did not seem to affect other endpoints of oxidative damage, our results suggest that glutathione plays an important role in protection against AgNP and $Ag^+$ toxicity. A similar conclusion was reported previously by Khan et al. (2011) for $Ag^+$ toxicity in human blood.

In summary, previous studies addressing the toxicity of AgNPs *in vitro* have suggested oxidative stress as a potential mechanism, and this study examined this mechanism in more detail using trout erythrocytes and hepatocytes. Generally, $Ag^+$ was more toxic than AgNPs, although both types increased cytotoxicity, generated ROS, and depleted GSH levels in both hepatocytes and erythrocytes. Moreover, GSH appeared to play an important role in protecting hepatocytes from Ag toxicity, since the cytotoxicity of both silver types increased in cells that had lower GSH levels due to BSO treatment. The activities of antioxidant enzymes were also measured; however, generally few changes were observed with SOD, CAT, and GPx, whereas the activities of GR and GST were decreased, revealing the complex relationship between oxidative stress and antioxidant enzymes. Furthermore, whereas $Ag^+$ induced DNA damage, AgNPs increased lipid peroxidation in hepatocytes, suggesting that AgNPs and $Ag^+$ generate ROS extracellularly and intracellularly, respectively, and act through different mechanisms,

which should be further elucidated in future studies. Finally, this study demonstrated that not all cell types are equally sensitive to $Ag^{+}$ and/or AgNPs and any generalizations pertaining to *in vitro* toxicity of silver should be avoided.

# CHAPTER 5
# Silver nanoparticles stimulate glycogenolysis in rainbow trout (*Oncorhynchus mykiss*) hepatocytes

This chapter is based upon the following article: Massarsky, A., Labarre, J., Trudeau, V.L., Moon, T.W., 2014. Silver nanoparticles stimulate glycogenolysis in rainbow trout (*Oncorhynchus mykiss*) hepatocytes. Aquat. Toxicol. 147, 68-75.

Permission was obtained from the journal for incorporation of this article into this thesis. This article is based on the work that was conducted with the assistance of the undergraduate student Justine Labarre (summer 2013; internship student from Université Nice Sophia Antipolis, France), whom I directly supervised. I designed and conducted these experiments, and wrote the manuscript. Drs. Vance Trudeau and Thomas Moon provided input into the preparation of the manuscript and funding for the project.

*5.1. Introduction*

Silver nanoparticles (AgNPs) are commonly found in a number of consumer products, but their biological effects on non-target aquatic organisms are yet to be fully understood. A review by Nel et al. (2009) addressed the potential interactions of engineered nanomaterials (ENMs) with biological interfaces, including cells, membranes, organelles, proteins, and DNA. According to this review, these interactions depend on the biophysicochemical dynamics and lead primarily to the formation of protein coronas, which in turn influence the movement of the ENM onto or into cells. The kinetics of ENM-protein association and dissociation will determine the interaction of the particle with biological surfaces and receptors, and therefore its fate. ENM interactions with the membrane and its ligands and receptors will influence the cellular uptake and are especially important in drug delivery applications (Nel et al., 2009).

The ability of ENMs to interact with proteins has been reported in several studies. For example, MacCormack et al. (2012) reported that the activity of purified lactate dehydrogenase (LDH; E.C. 1.1.1.2.7) from rabbit muscle was inhibited in the presence of silicon, Au, or CdSe nanoparticles; however, this effect was abolished in the presence of 1% bovine serum albumin (BSA). The activity of LDH in goldfish (*Carassius auratus*) white muscle homogenates was not affected by these ENMs (MacCormack et al., 2012). Similarly, we observed that AgNPs inhibited LDH activity of purified rabbit muscle, but not of rainbow trout (*Oncorhynchus mykiss*) white muscle homogenates (unpublished data). These studies suggest that the ENMs bind to proteins such as the BSA and those found in tissue homogenates.

Despite the aforementioned interactions of ENMs with cellular components, their potential to disrupt cell signaling pathways has yet to be addressed. Therefore, we hypothesized that AgNPs could interfere with proper receptor signaling by binding to receptors and/or cell membranes of target cells. In a pilot experiment we determined that AgNPs were able to stimulate glucose release from isolated trout hepatocytes; thus, we felt this could be a good model to study the interaction between AgNPs and membrane function. Trout hepatocytes are standard tools for studies involving the hormonal regulation of metabolism, including catecholamines and their downstream processes such as glycogen and glucose metabolism (Mommsen et al., 1988; Moon, 2004). Hepatocytes are also extensively used in the field of toxicology since liver is a major organ involved in xenobiotic metabolism (Guillouzo, 1998; Castano et al., 2003).

Metabolically hepatocyte glucose can be derived from glycogen by glycogenolysis and by glucose conversion from 3-carbon compounds by gluconeogenesis. Both processes are driven by hormone receptor systems, one initiated at the membrane and the second cytosolic. Therefore, this study focused on the membrane-bound β-adrenoreceptor (β-AR), which is the predominant AR in trout hepatocytes (Gilmour et al., 2012), and the cytosolic glucocorticoid receptor (GCR). These receptor systems play important roles in mediating the catecholamine and cortisol-dependent stress responses, respectively, in vertebrates.

The β-AR plays a central role within the adrenergic system that regulates many aspects of vertebrate metabolism and function, including the 'fight-or-flight' response. Adrenoreceptors, members of the G-protein coupled receptor superfamily and the targets of catecholamines, are present on most fish tissue membranes and mediate a variety of

responses (Massarsky et al., 2011), including an immediate response to a stressor mediated by the β-AR signal transduction pathway, which leads to increased cardiac contraction and liberation of fatty acids by adipose tissue (Van Heeswijk et al., 2006). Catecholamines are also critical to the mobilization of energy reserves primarily through glycogenolysis and to a lesser extent through gluconeogenesis and are mediated primarily by the hepatic AR, which may be either the $\beta_2$- or the $\alpha_1$-AR depending upon species (Nickerson et al., 2001). As expressed in the pioneering studies of Cannon et al. (1929), the role of catecholamines on the various tissues enable the organism to organize the 'fight-or-flight' response and ultimately allow the animal to survive a stressful event.

On the other hand, the GCR plays an important role during the stress response mediated by the hypothalamic-pituitary-interrenal (HPI) axis. Unlike the β-AR, the GCR is located in the cytosol and upon binding cortisol (CORT) regulates the transcription of genes involved in maintenance of energy balance, immunoregulation, growth, and reproduction, among others (Mommsen et al., 1999; Alderman et al., 2012). More specifically, during stress CORT increases gluconeogenesis in the liver, providing fuel to tissues, thus allowing them to cope with the metabolic demands imposed by a stressor (Vijayan et al., 2003).

This study aimed to explain the observed increase in glucose release noted in our pilot experiment (unpublished data) by using agonists/antagonists of the β-AR and GCR systems. To this end, following hepatocyte exposures the medium and cells were collected and glucose, glycogen, adenosine 3',5'-cyclic monophosphate (cAMP; second messenger within the β-AR signaling pathway) contents, as well as the activities of glycogen phosphorylase (GPase), phosphoenolpyruvate carboxykinase (PEPCK),

fructose-1,6-bisphosphatase (FBPase), and several aminotransferases (alanine, aspartate, and tyrosine) were assessed.

## *5.2. Materials and methods*

### *5.2.1. Silver nanoparticles (AgNPs)*

An aqueous solution of carboxy-functionalized AgNPs, stabilized with sodium polyacrylate (31% Ag) (Vive Nano, 13010L) was used in this study as described in Chapters 2 and 4. Total nominal Ag concentrations noted on the figures were based on the manufacturer's determined silver content. The size, polydispersity index (PDI), and zeta (ζ)-potential of AgNPs were previously characterized using Dynamic Light Scattering (DLS; Zetasizer Nano, Malvern Instruments Ltd). The particle size and stability were confirmed, using Scanning Transmission Electron Microscope (STEM; JEOL JSM-7500F Field Emission Scanning Electron Microscope) and UV-visible spectroscopy, respectively. The average particle size was ~9 nm (Chapter 4; Massarsky et al., 2014b). Moreover, the dissolution of AgNPs was assessed using the Amicon Ultra Centrifugal Filters (3 kDa; UFC800324) following the manufacturer's protocol and the flow through was collected and analyzed using a Varian Atomic Absorption Spectrometer (AA240) fitted with a Ag 1.5" hollow cathode lamp (Perkin Elmer Atomax, N2025300). The dissolution was estimated at 0.5% (Chapter 2; Massarsky et al., 2013). Moreover, the size and stability of AgNPs were verified in the presence of agonists/antagonists used here using DLS and spectroscopy approaches, and no agonist/antagonist effects were observed.

*5.2.2. Experimental set-up*

See Chapter 4 for details on rainbow trout husbandry (section 4.2.3) and hepatocyte isolation procedures (section 4.2.4). Hepatocytes were exposed to AgNP solutions at concentrations of 0 (control), 1, and 10 μg/mL; as these concentrations were not expected to increase cytotoxicity based on our previous study (Chapter 4; Massarsky et al., 2014b). In addition, the cells were exposed to agonists/antagonists of the β-AR and GCR systems. The experimental groups were as follows:

1) None: cells were exposed for 48 h to only AgNPs (0, 1, 10 μg/mL)
2) PROP: cells were exposed for 48 h to AgNPs in the presence of the non-selective β-blocker propranolol (PROP, 0.1 mM; higher concentrations significantly increased cytotoxicity) to verify whether the AgNP-mediated glucose release was β-AR-dependent. PROP (Sigma P0884) was used in previous studies to block the β-AR in trout (e.g. Reid et al., 1991; Dugan et al., 2003; Lortie and Moon, 2003).
3) ISO: cells were exposed for 48 h to AgNPs and then treated with the non-selective β-AR agonist isoproterenol (ISO, 0.1 mM; lower concentrations did not significantly increase medium glucose content in 3 h) for an additional 3 h in the presence of AgNPs. This was done to check whether AgNP-exposed cells would respond to an agonist. ISO (Sigma I2760) was used in previous studies involving the trout β-AR (e.g. Reid et al., 1991; Dugan et al., 2003).
4) PROP/ISO: cells were exposed for 48 h to AgNPs and then treated with a combination of PROP and ISO (the concentration of antagonist should be ten times higher than that of the agonist, but this was not possible as 1 mM PROP was

cytotoxic) for an additional 3 h in the presence of AgNPs. This was done to check whether the antagonist would modify the agonist response.

5) MIFE: cells were exposed for 48 h to AgNPs in the presence of the GCR antagonist mifepristone (MIFE, 1000 ng/mL). This MIFE (Roussel-Uclaf 7A4087B) concentration was effective in blocking the cortisol-mediated metabolic effects in trout hepatocytes previously (Sathiyaa and Vijayan, 2003).
6) CORT: cells were exposed for 48 h to AgNPs in the presence of the GCR agonist cortisol (CORT, 100 ng/mL). This CORT (Sigma H4881) concentration is typical of levels found in stressed trout *in vivo* and was used previously in trout hepatocyte experiments (Aluru and Vijayan, 2007).
7) MIFE/CORT: cells were exposed for 48 h to AgNPs in the presence of MIFE and CORT. This was done to check whether the antagonist would modify the agonist response.

The experimental groups 2-4 and 5-7 were used to deduce the effects of AgNPs within the β-AR and GCR signaling systems, respectively. At the end of the experiment the medium and the cells were collected into 1.5 mL tubes and frozen at -80°C until analyzed.

*5.2.3. Cell viability analysis*

Cell viability was determined by the lactate dehydrogenase (LDH; EC 1.1.1.27) leakage assay as outlined in Chapter 4 (section 4.2.6). The LDH activity was normalized to the control (none or no addition) group.

*5.2.4. Glucose production*

The glucose content in the medium was assessed enzymatically according to Wright et al. (1989). Briefly, a 10 µL sample was incubated with 200 µL assay medium (in mM: 60 trizma-base, 40 trizma-HCl, 1 $MgSO_4$, 2 $NAD^+$, 1 ATP, and 0.1 U/mL G6PD) in a 96-well plate with shaking for 5 min at room temperature followed by the addition of 10 µL hexokinase solution (0.3 U/mL). The plate was incubated for 30 min at room temperature and the absorbance at 340 nm was assessed. The concentration of glucose was assessed using a standard curve.

*5.2.5. Cellular glycogen content*

The cellular glycogen content was determined according to Wright et al. (1989). Briefly, cells were homogenized in 20 vol (w/v) 6% perchloric acid (PCA) using a Kontes Micro Ultrasonic Cell Disruptor. The samples were incubated on ice for 20 min, followed by a 5 min centrifugation at 4000 g (4°C) in a Beckman Coulter Microfuge® R centrifuge. The supernatant was used for the assay as follows: to 50 µL supernatant were added 25 µL 1 M $NaHCO_3$ and 0.5 mL amyloglucosidase solution (containing 120 mM sodium-acetate, 12 U/mL amyloglucosidase, 80 mM glacial acetic-acid). After a 2 h incubation at 35-40°C, the reaction was terminated by the addition of 70% PCA followed by a 2 min centrifugation at 4000 g (4°C). The glycogen concentration was calculated from glycogen standards based on the generated glucose using the glucose assay as above.

*5.2.6. Cortisol in the medium*

The CORT levels in the culture medium were estimated to verify the extent of uptake/degradation of CORT throughout the exposure period. Cortisol content was assessed at the end of the experiment using a radioimmunoassay (RIA) $^{125}$I kit as per the manufacturer's instructions (MP Biomedicals, 07221102, Orangeburg, NY).

*5.2.7. Glycogen phosphorylase (GPase) activity (EC 2.4.1.1)*

The activity of GPase was determined according to Moon et al. (1999). Briefly, hepatocytes were sonicated for 5 s in 0.1 mL of ice-cold stopping buffer (in mM: 50 imidazole-HCl, 25 β-mercaptoethanol, 5 EDTA, 5 EGTA, 100 KF, 0.5 mg/mL bovine glycogen, and 10 μg/mL aprotinin; pH 7.4) to ensure that the phosphorylation status of the enzyme was unchanged from the end of the experiment. The total GPase activity was assessed by adding 100 μL of medium (3 mM $NAD^+$, 15 mM $MgSO_4$, 8 μM glucose-1,6-bisphosphate, 2 mM AMP, 2 mg/mL glycogen, 0.6 mM EDTA, with excess of phosphoglucomutase and G6PD, prepared in 67 mM phosphate buffer; pH 7.1) and 10 μL sample into a 96-well plate and monitoring the absorbance at 340 nm for 30 min. The activity of GPase *a* was assessed in a similar fashion, but the medium also contained caffeine (10 mM) to inactivate the dephosphorylated or *b* form of GPase. The activity was expressed per unit protein, where homogenate protein content was assessed using the Bio-Rad protein assay following manufacturer's protocol with bovine serum albumin standards. Percentage activation was calculated as GPase *a* activity/total GPase activity x 100.

*5.2.8. Phosphoenolpyruvate carboxykinase (PEPCK) activity (EC 4.1.1.49)*

The activity of PEPCK was assessed according to Petrescu et al. (1979) with slight modifications. Briefly, cells (10 mg) were sonicated as above for 5 s in 20 vol (w/v) ice-cold 50 mM imidazole buffer (pH 7.4). The homogenates were centrifuged for 15 min at 15,000 g (4°C) and the supernatant was collected and used for the assay. The samples (50 µl) were added into a 96-well plate followed by 100 µl of assay mix (50 mM $NaHCO_3$, 1 mM phosphoenolpyruvate, 1 mM $MnCl_2$, 0.25 mM NADH, 0.2 mM deoxyguanosine diphosphate, and 2 U malate dehydrogenase, prepared in 50 mM imidazole; pH 7.4). The decrease in absorbance was monitored at 340 nm for 30 min spectrophotometrically as above and adjusted to substrate and enzyme blanks.

*5.2.9. Fructose-1,6-bisphosphatase (FBPase) activity (EC 3.1.3.11)*

The activity of FBPase was assessed as modified from Mommsen et al. (1980). Briefly, samples were prepared as above. The samples (50 µL) were added into a 96-well plate followed by 100 µL of assay medium (15 mM $MgCl_2$, 0.1 mM fructose-1,6-bisphosphate, 0.2 mM $NAD^+$, 10 U phosphoglucose isomerase, and 2 U G6PD, prepared in 50 mM imidazole; pH 7.4). The increase in absorbance was monitored at 340 nm for 30 min as above and adjusted to substrate and enzyme blanks.

*5.2.10. Activities of aminotransferases*

Samples were prepared by sonicating hepatocytes for 5 s in 0.2 mL homogenization buffer (in mM: 20 Tris-HCl, 5 EDTA, 5 $MgCl_2$, 150 KCl, and 5 β-mercaptoethanol; pH 7.4). The activity of alanine aminotransferase (ALT; EC 2.6.1.2) was assessed according

to Mommsen et al. (1980) by monitoring the disappearance of NADH (0.12 mM) in 50 mM imidazole containing 200 mM L-alanine, 0.025 mM pyridoxal phosphate (PLP), 12 U LDH, and 10 μL homogenate; the reaction was initiated by the addition of 10 mM α-ketoglutarate (α-KG). The activity of aspartate aminotransferase (AST; EC 2.6.1.1) was assessed according to Mommsen et al. (1980) by monitoring the disappearance of NADH (0.12 mM) in 50 mM imidazole containing 40 mM aspartic acid, 0.025 mM PLP, 8 U malic dehydrogenase, and 5 μL homogenate; the reaction was initiated by the addition of 7 mM α-KG. The activity of tyrosine aminotransferase (TYT; EC 2.6.1.5) was assessed by the formation of *p*-hydroxybenzaldehyde at 331 nm as modified from Peragón et al. (2008). Briefly, 10 μL homogenate was incubated for 20 min at room temperature in 50 mM imidazole containing 3 mM L-tyrosine and 0.5 mM PLP; the reaction was started by the addition of 10 μL 0.3 M α-KG and stopped after 2 min with 10 μL 10 N NaOH; blanks received 10 N NaOH prior to the addition of α-KG. The activity was calculated from the amount of *p*-hydroxybenzaldehyde formed during the 2 min reaction. The activities of all three enzymes were normalized to protein concentration assessed with the Bio-Rad protein assay.

*5.2.11. Adenosine 3',5'-cyclic monophosphate (cAMP) content*

The amount of intracellular cAMP was assessed using the cAMP Direct Immunoassay Kit (BioVision, K371-100) following the manufacturer's protocol. The frozen cell samples were prepared in 0.1 M HCl (1:15 w/v) according to the protocol.

*5.2.12. Statistical analysis*

Statistical analyses were conducted using SigmaPlot (SPW 11; Systat Software, Inc., San Jose, CA). A two-way analysis of variance (ANOVA) with a post-hoc Holm-Sidak method was used throughout these experiments to assess the effect of treatment (i.e. agonists/antagonists) and AgNPs concentration (0, 1, and 10 µg/mL). Significant differences ($P \leq 0.050$) are indicated as letters and asterisks on the graphs. The data are presented as means and standard error of the mean (SEM).

*5.3. Results*

*5.3.1. Cell viability analysis*

The fold-change in LDH leakage was not significantly affected by treatment with AgNPs (0, 1, and 10 µg/mL), PROP (0.1 mM), ISO (0.1 mM), CORT (100 ng/mL), or MIFE (1 µg/mL) (Fig. 5.1). It is worth noting that cells exposed to 1 mM PROP (data not shown) demonstrated a 2- and 6-fold increase in cytotoxicity after 3 and 48 h exposures, respectively.

*5.3.2. Glucose production*

Medium glucose content was significantly increased as predicted in the presence of ISO (a β-AR agonist). PROP treatment (a β-AR antagonist) did not significantly affect either control or ISO-treated glucose levels (Fig. 5.2A) in control hepatocytes not treated with AgNPs. As expected, CORT (a GCR-agonist) treatment increased medium glucose. The MIFE treatment had no effect in the absence of CORT, but it did significantly block the CORT effect in the absence of AgNPs (Fig. 5.2B). The patterns of glucose release

were generally similar for both ISO and CORT treated hepatocytes exposed to no (control) or 1 μg/mL AgNPs. However, at 10 μg/mL AgNPs, medium glucose was higher for all groups compared with the control or no AgNPs and any significant effects of the agonists and antagonists were eliminated.

### *5.3.3. Cellular glycogen content*

The glycogen content in ISO- and/or PROP-treated hepatocytes displayed the reverse pattern of that seen for medium glucose (Fig. 5.3A). Isoproterenol significantly reduced the glycogen content in both the control and 1 μg/mL AgNPs groups, whereas at 10 μg/mL AgNPs the glycogen content was significantly lower than the control even without ISO. Propranolol treatment resulted in slightly higher glycogen levels, but this was not significant although cells treated with both ISO and PROP had glycogen levels similar to control cells. Glycogen content was not affected by CORT and/or MIFE treatments; only the cells exposed to 10 μg/mL AgNPs had lower glycogen levels irrespective of CORT/MIFE treatments (Fig. 5.3B).

### *5.3.4. Cortisol in the medium*

CORT was initially added to the hepatocyte incubates at 100 ng/mL and the medium CORT concentrations after the 48 h exposure were approximately 30 ng/mL (Fig. 5.4). Generally, hepatocytes treated with 10 μg/mL AgNPs had higher, but not significantly, medium cortisol concentrations. The combinations of MIFE+CORT treatments were significantly lower than cells treated only with CORT; this was independent of AgNP treatment (Fig. 5.4).

*5.3.5. Glycogen phosphorylase (GPase) activity*

The activities of both total GPase and GPase *a* were significantly increased in hepatocytes treated with ISO (β-agonist) in the control (0 AgNPs) and 1 μg/mL AgNP (Fig. 5.5A and B) groups. Treatment with PROP did not affect either the total GPase or GPase *a* activities in the presence or absence of ISO. At 10 μg/mL AgNPs both the no agonist and PROP only activities increased while there was no change in either the agonist or agonist + PROP groups. There were no significant effects on % GPase *a* activities regardless of treatment (Fig 5.5C). Treatments with CORT and/or MIFE did not affect the activity of GPase; however, exposure to 10 μg/mL AgNPs resulted in significantly higher total GPase activity and the activity of GPase *a* as noted for ISO (data not shown).

*5.3.6. Activities of gluconeogenic enzymes*

The activities of the gluconeogenic enzymes were generally not affected by any of the treatments with the exception of PEPCK, whose activity was significantly lower in the 10 μg/mL AgNP-treated cells. These activities are summarized in Table 5.1.

*5.3.7. cAMP content*

cAMP levels were generally higher in ISO-treated cells although this value was significant only in the control (0 AgNP) group (Fig. 5.6). Hepatocytes treated with 10 μg/mL AgNPs and ISO had significantly lower cAMP levels than the cells treated with ISO but no AgNPs. Other treatments, including MIFE and CORT, were not expected to affect cAMP levels and they did not (data not shown).

**Table 5.1.** Activities of gluconeogenic enzymes: phosphoenolpyruvate carboxykinase (PEPCK), fructose-1,6-bisphosphatase (FBPase), alanine aminotransferase (ALT), aspartate aminotransferase (AST), and tyrosine aminotransferase (TYT), in trout hepatocytes exposed to AgNPs for 48 h. The agonists/antagonists of the β-adrenergic and glucocorticoid receptors included propranolol (PROP), isoproterenol (ISO), mifepristone (MIFE), and cortisol (CORT); control cells are indicated as 'None'. The activities are expressed in nmol/min/mg protein. Data are presented as Mean ± SEM (n = 3-4). Statistical differences are indicated with letters. Two-way ANOVA with post-hoc Holm-Sidak method was used to assess statistical differences ($P \leq 0.050$).

| | [AgNP] * | PEPCK | FBPase | ALT | AST | TYT |
|---|---|---|---|---|---|---|
| None | 0 | 16.9±1.0[a] | 3.2±0.4 | 191.3±20.4 | 288.9±20.1 | 92.4±12.6 |
| | 1 | 17.7±0.7[a] | 2.7±0.3 | 174.1±25.8 | 302.9±27.3 | 90.8±5.6 |
| | 10 | 14.2±0.6[b] | 3.4±0.3 | 175.7±24.1 | 299.8±25.6 | 72.4±8.5 |
| PROP | 0 | 17.1±0.1[a] | 2.9±0.3 | 194.9±32.5 | 321.5±24.4 | 93.6±10.3 |
| | 1 | 17.6±0.8[a] | 2.5±0.3 | 185.1±29.2 | 303.0±35.0 | 100.8±15.6 |
| | 10 | 13.7±0.9[b] | 3.0±0.1 | 160.0±17.7 | 305.5±32.8 | 80.9±6.0 |
| ISO | 0 | 16.4±0.7[a] | 3.9±0.6 | 186.2±25.3 | 319.7±29.8 | 91.4±6.9 |
| | 1 | 16.4±0.4[a] | 3.6±0.8 | 195.6±17.9 | 323.2±29.3 | 88.6±11.2 |
| | 10 | 12.9±0.5[b] | 4.1±0.9 | 171.8±11.9 | 296.7±16.4 | 78.0±5.8 |
| PROP+ISO | 0 | 16.2±1.1[a] | 3.3±0.6 | 184.6±29.7 | 302.9±16.5 | 103.6±24.7 |
| | 1 | 16.5±0.3[a] | 3.7±0.8 | 186.0±27.5 | 307.0±18.2 | 104.9±11.1 |
| | 10 | 12.9±0.1[b] | 3.6±0.8 | 174.5±20.9 | 307.3±18.2 | 105.7±14.3 |
| MIFE | 0 | 16.2±0.9 | 2.7±0.2 | 194.4±31.5 | 274.4±9.6 | 108.6±10.2 |
| | 1 | 15.7±1.4 | 3.1±0.1 | 188.6±26.1 | 272.8±3.7 | 92.6±4.1 |
| | 10 | 14.1±0.8 | 3.8±0.5 | 173.4±17.5 | 276.0±13.1 | 79.2±6.6 |
| CORT | 0 | 15.9±0.9[a] | 3.2±0.3 | 195.9±35.0 | 298.1±23.2 | 126.1±13.8 |
| | 1 | 19.1±2.6[ab] | 4.1±0.7 | 196.3±25.3 | 292.5±18.8 | 128.0±10.8 |
| | 10 | 13.3±1.0[b] | 3.4±0.4 | 161.7±12.7 | 258.0±28.2 | 76.0±29.1 |
| MIFE+CORT | 0 | 15.6±1.0 | 3.1±0.3 | 191.3±44.2 | 276.6±15.2 | 121.9±26.2 |
| | 1 | 16.7±2.1 | 3.3±0.3 | 183.6±8.7 | 293.5±34.5 | 120.7±16.5 |
| | 10 | 14.2±1.5 | 3.9±0.7 | 185.9±20.7 | 291.0±3.0 | 114.0±21.1 |

* *Total silver concentration in μg/mL*

**Figure 5.1.** Cytotoxicity in trout hepatocytes exposed to AgNPs for 48 h in the presence or absence of agonists/antagonists: (A) propranolol (PROP), isoproterenol (ISO) and a combination of both, or (B) mifepristone (MIFE), cortisol (CORT) and a combination of both. Cytotoxicity was assessed using lactate dehydrogenase (LDH) leakage. The results are expressed as fold-change relative to the control values. Data are presented as Mean + SEM (n = 5-13). No statistical differences exist.

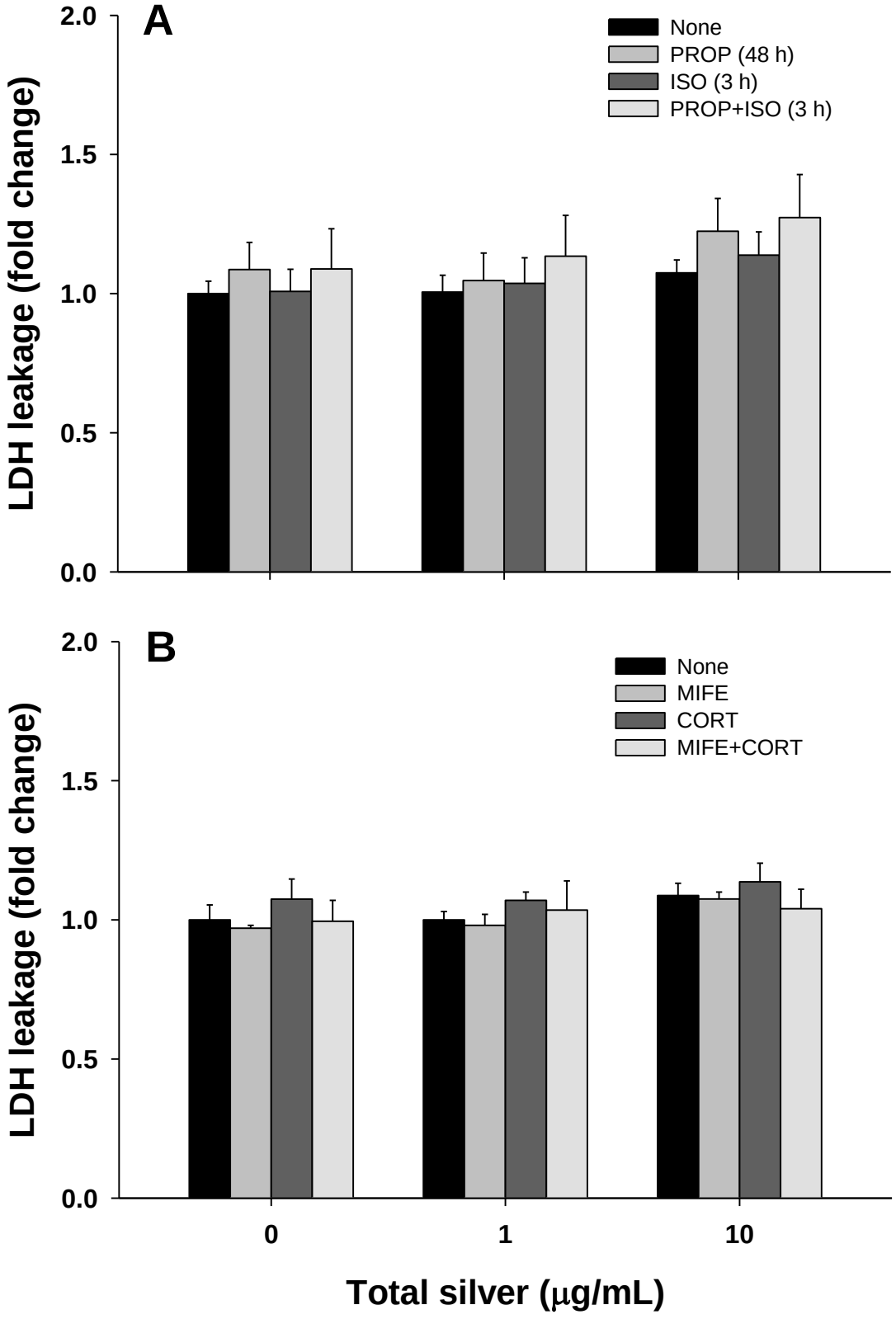
A
None
PROP (48 h)
ISO (3 h)
PROP+ISO (3 h)
LDH leakage (fold change)
2.0
1.5
1.0
0.5
0.0
B
None
MIFE
CORT
MIFE+CORT
LDH leakage (fold change)
2.0
1.5
1.0
0.5
0.0
0
1
10
Total silver (μg/mL)

**Figure 5.2.** Glucose levels in the medium of trout hepatocytes exposed to AgNPs for 48 h in the presence or absence of agonists/antagonists: (A) propranolol (PROP) and isoproterenol (ISO), or (B) mifepristone (MIFE) and cortisol (CORT). Data are presented as Mean + SEM (n = 5-13). The letters indicate significant differences within the same AgNP concentration; the asterisk (*) indicates significant differences between the 10 μg/mL AgNP and control (0 AgNPs) groups within the same treatment; and, the pound sign (#) indicates overall significant differences between the 10 μg/mL AgNP and control (0 AgNPs) groups. Two-way ANOVA with post-hoc Holm-Sidak method was used to assess statistical differences ($P \leq 0.050$).

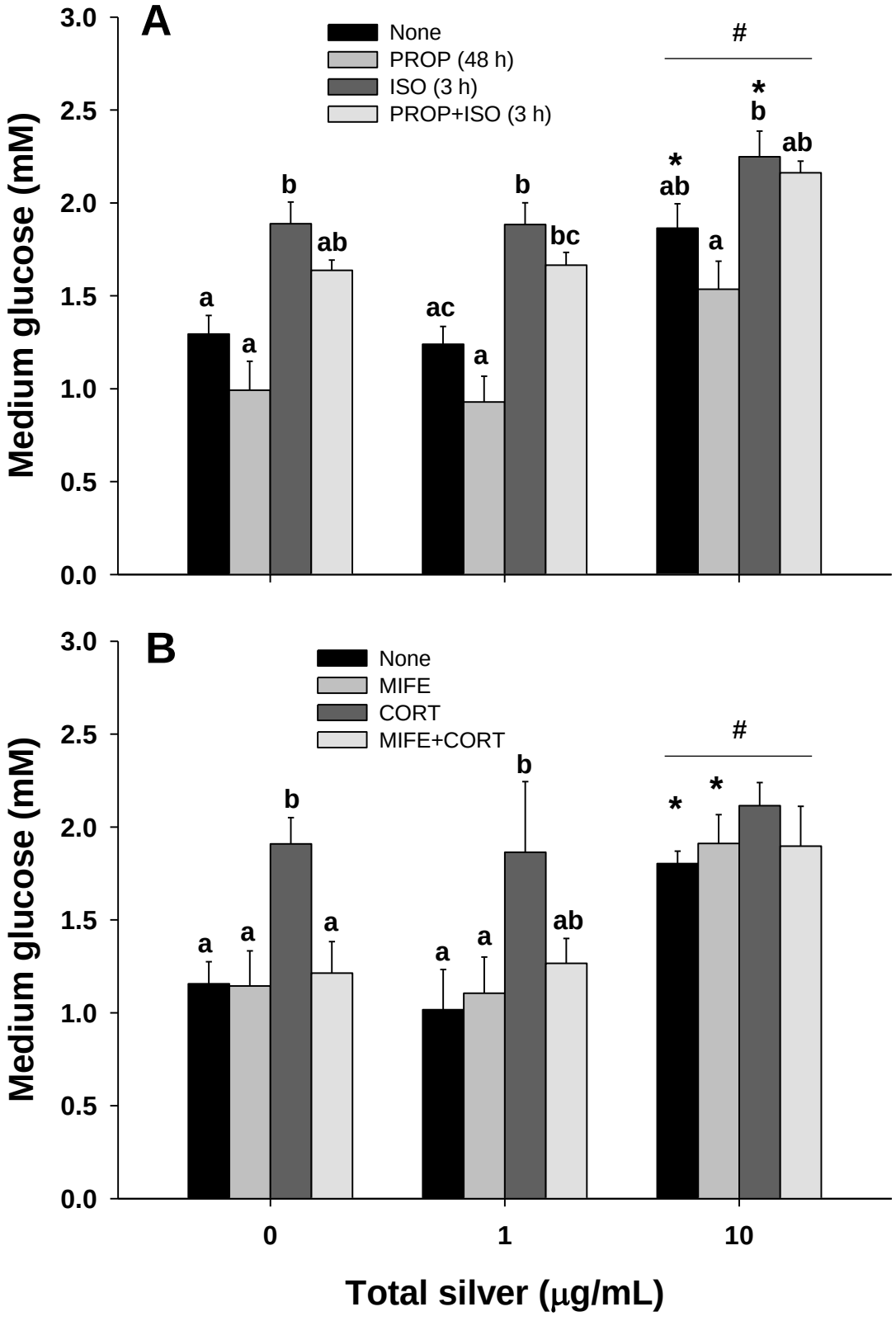
A
None
PROP (48 h)
ISO (3 h)
PROP+ISO (3 h)
#
Medium glucose (mM)
3.0
2.5
2.0
1.5
1.0
0.5
0.0
a
a
b
ab
ac
a
b
bc
*
ab
a
*
b
ab
B
None
MIFE
CORT
MIFE+CORT
#
Medium glucose (mM)
a
a
b
a
a
a
b
ab
*
*
0
1
10
Total silver (μg/mL)

**Figure 5.3.** Glycogen levels in trout hepatocytes exposed to AgNPs for 48 h in presence of (A) propranolol (PROP) and isoproterenol (ISO), or (B) mifepristone (MIFE) and cortisol (CORT). Data are presented as Mean + SEM (n = 5-14). See legend to Figure 5.2 for details pertaining to statistical differences.

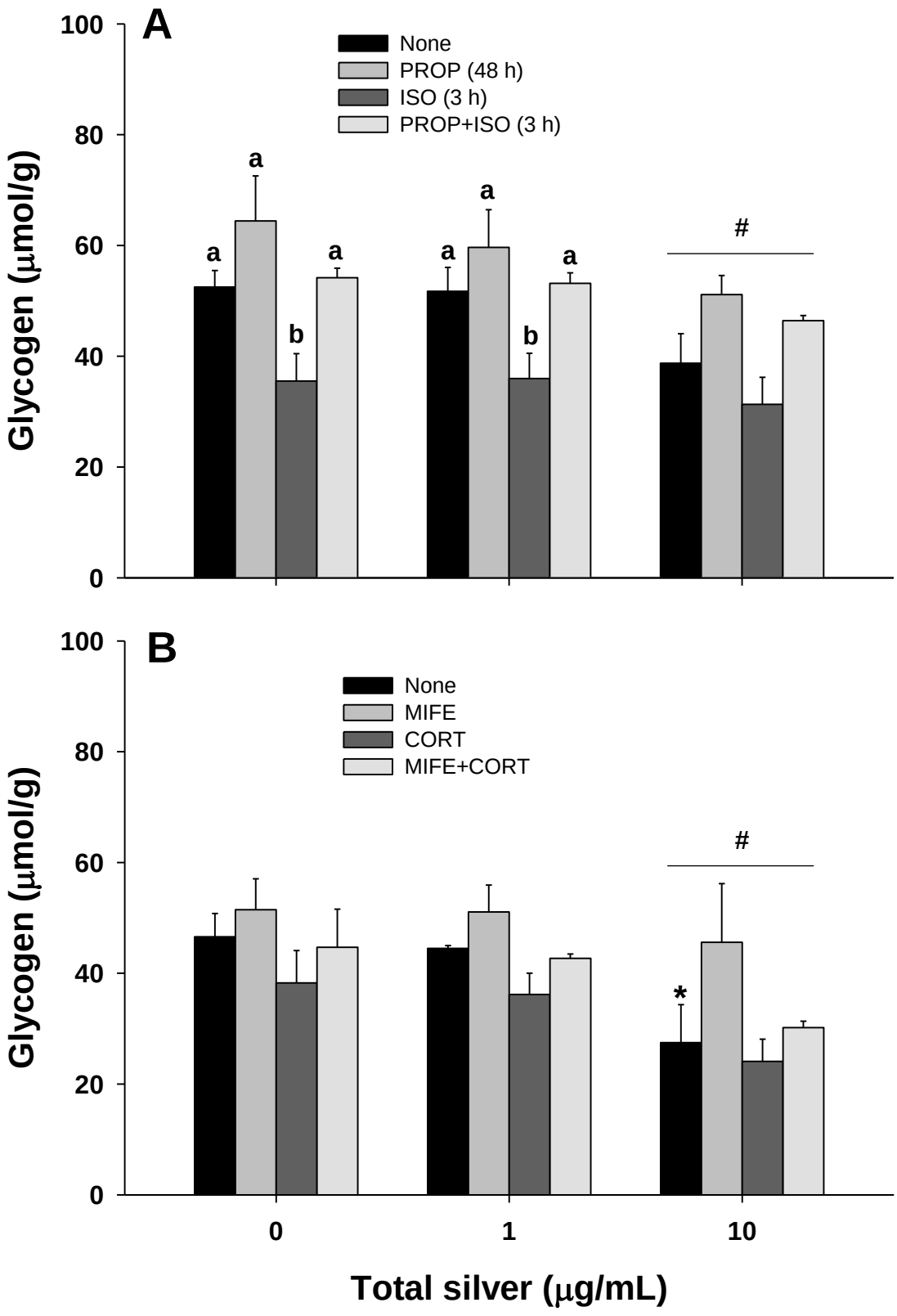
A
None
PROP (48 h)
ISO (3 h)
PROP+ISO (3 h)
Glycogen (μmol/g)
100
80
60
40
20
0
a
a
b
a
a
a
b
a
#
B
None
MIFE
CORT
MIFE+CORT
Glycogen (μmol/g)
100
80
60
40
20
0
#
*
0
1
10
Total silver (μg/mL)

**Figure 5.4.** Cortisol levels in the medium of trout hepatocytes exposed to AgNPs for 48 h in the presence or absence of mifepristone (MIFE) and/or cortisol (CORT). Data are presented as Mean + SEM (n = 5-14). The letters indicate significant differences within the same AgNP concentration. Two-way ANOVA with post-hoc Holm-Sidak method was used to assess statistical differences ($P \leq 0.050$).

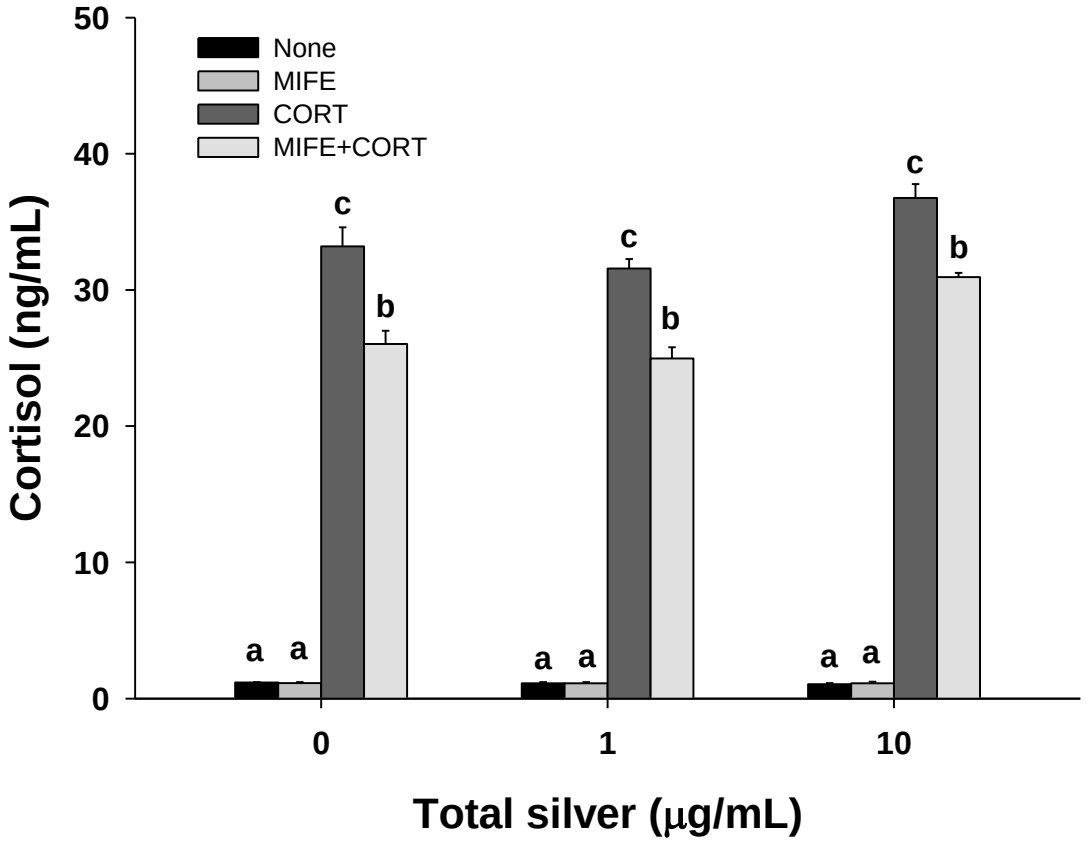

**Figure 5.5.** Glycogen phosphorylase (GPase) activities in trout hepatocytes exposed to AgNPs for 48 h: (A) total GPase activity, (B) GPase *a* activity, and (C) percentage activation of GPase *a* in absence or presence of propranolol (PROP) or isoproterenol (ISO). Data are presented as Mean + SEM (n = 4-9). See legend to Figure 5.2 for details pertaining to statistical differences.

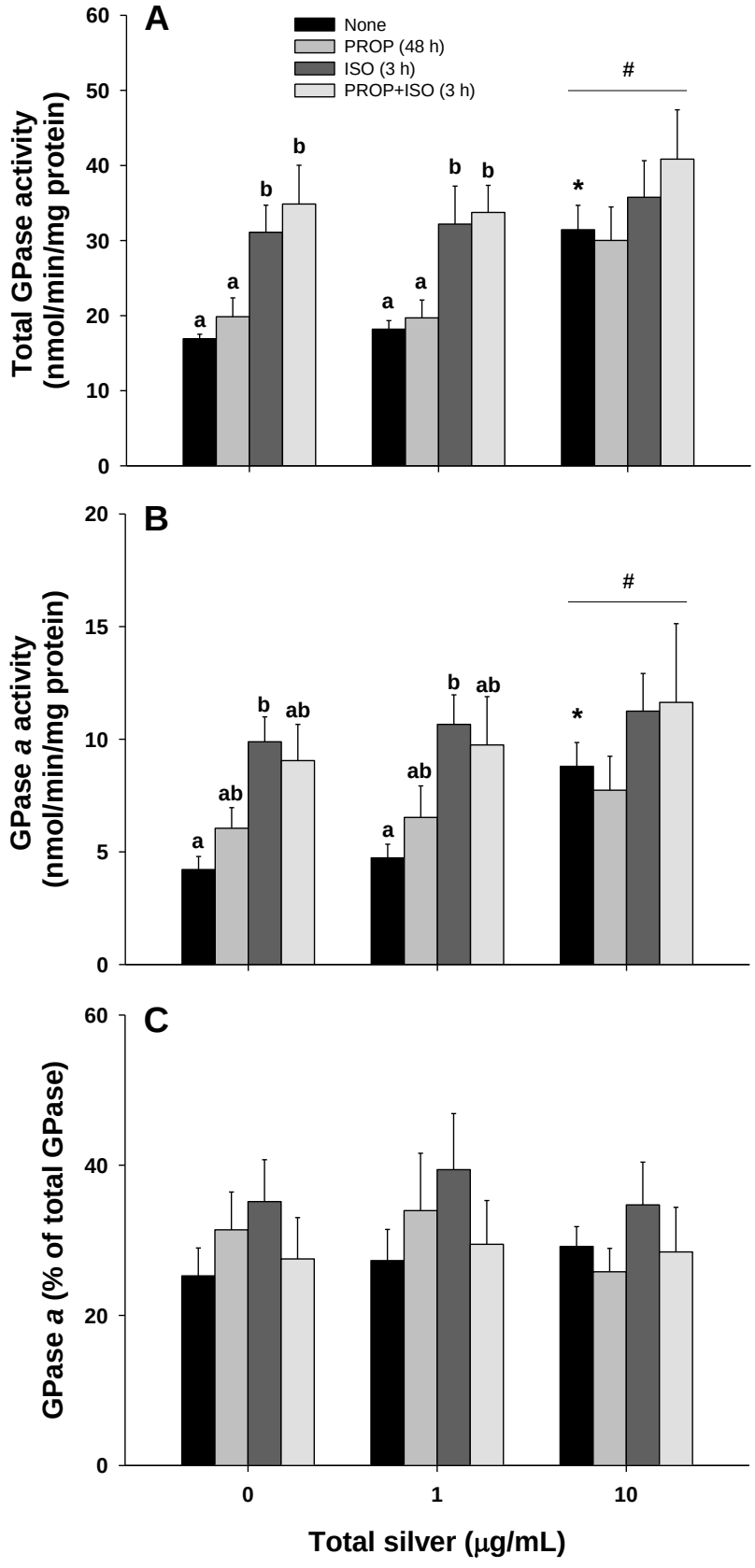
A
None
PROP (48 h)
ISO (3 h)
PROP+ISO (3 h)
Total GPase activity (nmol/min/mg protein)
B
GPase a activity (nmol/min/mg protein)
C
GPase a (% of total GPase)
Total silver (μg/mL)
0
1
10
#
*

**Figure 5.6.** cAMP levels in trout hepatocytes exposed to AgNPs for 48 h in the presence of propranolol (PROP) and isoproterenol (ISO). Data are presented as Mean + SEM (n = 3). The letters indicate significant differences within the same AgNP concentration and an asterisk indicates significant differences compared to the same treatment in the control (0 AgNPs) group. Two-way ANOVA with post-hoc Holm-Sidak method was used to assess statistical differences ($P \leq 0.050$).

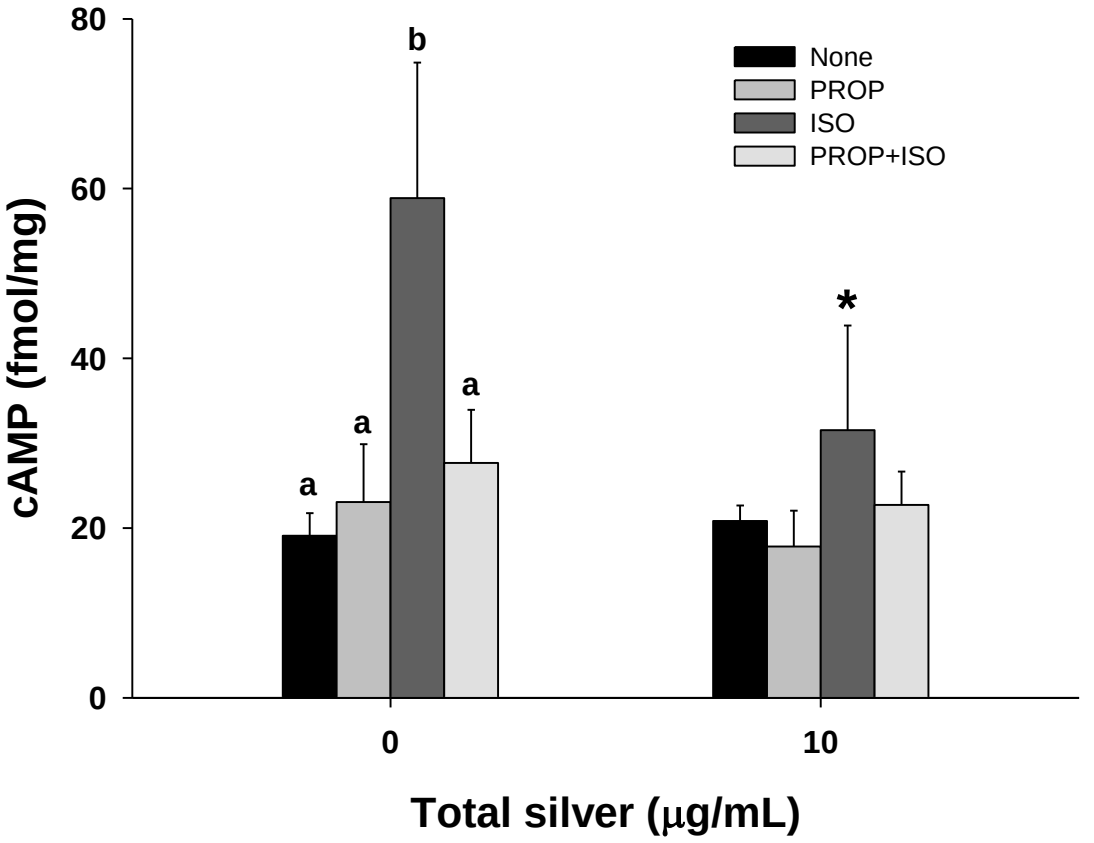

*5.4. Discussion*

Several studies have addressed AgNP toxicity in fish, including Scown et al. (2010b) and Gagné et al. (2012), who reported accumulation of AgNPs in the liver of juvenile rainbow trout after a 4-10 d waterborne exposure. However, as noted from several review papers (Scown et al., 2010a; Shaw and Handy, 2011; Chernousova and Epple, 2013; Yu et al., 2013), very little is known about the potential of AgNPs to disrupt hormone-regulated cell signaling pathways. Therefore, this study aimed to determine the effects of AgNPs on the function of the β-adrenoreceptor (β-AR) and glucocorticoid receptor (GCR) pathways in rainbow trout hepatocytes, since the former regulates glycogenolysis and the latter regulates gluconeogenesis, and both receptor systems increase glucose availability during stress.

The nominal concentrations of AgNPs used in this study (0, 1, and 10 μg/mL) were based on our previous study, which showed that the viability of hepatocytes was significantly affected by AgNPs at concentrations >15 μg/mL (Chapter 4; Massarsky et al., 2014b). It is also important to note that the concentrations chosen are similar to those used in other *in vitro* studies (e.g. Farkas et al., 2010) and are well above the predicted environmental concentrations that range from 0.088 to 2.63 ng/L (Gottschalk et al., 2009) or 40 to 320 ng/L (Blaser et al., 2008) in surface water. At these environmentally relevant AgNP concentrations, we have observed no overt effects in acute cell or embryo studies (Chapters 2 and 4; Massarsky et al., 2013; 2014b).

This study clearly demonstrates that AgNPs do not interfere with the function of the β-AR and GCR systems at a concentration of 1 μg/mL or below; however, at a concentration of 10 μg/mL, AgNPs do increase glycogenolysis. Whether this effect was

dependent upon either the β-AR or GCR systems is unclear. The β-AR agonist ISO and the GCR agonist CORT both increased glucose release in the control (no AgNPs) and 1 μg/mL AgNP-treated cells, suggesting that even at 1 μg/mL, AgNPs do not affect either receptor system. The relationship between glucose production and these two receptor systems has been demonstrated in fish hepatocytes by previous authors (e.g. Brighenti et al., 1991; Mommsen et al., 1999; Moon et al., 1999; Hallgren et al., 2003). In particular, the binding of the agonist ISO to the hepatocyte membrane β-ARs initiates a signaling process that initially activates adenylyl cyclase, increasing cAMP, which activates protein kinase A (PKA), ultimately leading to the phosphorylation of GPase *b* (inactive) converting it to the active GPase *a* form that ultimately converts glycogen into glucose (Massarsky et al., 2011). This β-AR system is similar in fish as in mammals as reviewed by Massarsky et al. (2011). On the other hand, CORT binds to its cytosolic receptor that acts as a transcription factor to bind to glucocorticoid response elements in promoter regions to increase transcription of glucocorticoid-sensitive genes (Mommsen et al., 1999). One group of such genes are those that regulate gluconeogenesis or the production of glucose from 3-carbon compounds such as lactate or amino acids (Mommsen et al., 1999).

The results presented in this study support these previous studies showing ISO increases glucose production from glycogen, increases cAMP content, and increases GPase *a* activities. Treatment with PROP did block the ISO-stimulated decrease in glycogen and the increase in cAMP, but not the increase in medium glucose or GPase *a* changes. The absence of a PROP effect on these latter two processes is difficult to explain given that it was effective against cAMP and glycogen. It does suggest that full

blockage was not achieved. As noted, PROP concentrations were limited by a cytotoxic effect of this antagonist on the trout hepatocytes, which may account for the limited effects seen.

On the other hand, CORT affected the hepatocytes by increasing glucose production without affecting glycogen contents. This was predicted as CORT as noted above affects the transcription of glucocorticoid-sensitive genes including the aminotransferases and PEPCK. Although the activities of gluconeogenic enzymes were not increased by CORT (or any other treatment), these results are consistent with Mommsen et al. (1999) who were unsuccessful in showing changes in the activities of enzymes involved in glucocorticoid stimulation of fish liver metabolism, including PEPCK, AST, ALT, with CORT. The lack of a significant increase in enzymes activities in our study, despite higher PEPCK mRNA and plasma glucose levels in the CORT group in the study of Vijayan et al. (2003), suggests that enzyme activity may not be a sensitive or reliable indicator of CORT-mediated gluconeogenesis. The GCR antagonist MIFE effectively blocked the glucose changes as predicted and as reported previously in trout hepatocytes (Sathiyaa and Vijayan, 2003).

It should also be noted that although glycogenolysis in rainbow trout hepatocytes is mediated primarily by the β-AR (Van Heeswijk et al., 2006), the $\alpha_1$-AR can also increase glycogenolysis and at concentrations of catecholamines found in resting fish (<10 nM epinephrine) the $\alpha_1$-AR may contribute significantly to changes in glycogenolysis (see Fabbri et al., 1998). Unlike the β-AR signaling, which is mediated by the activation of adenylyl cyclase and a resulting increase in cAMP, $\alpha_1$-AR signaling is mediated by phospholipase-Cγ (PLCγ) (Fabbri et al., 1998). Activation of PLCγ leads to increased

hydrolysis of membrane phosphatidylinositol-4,5-bisphosphate ($PIP_2$), the products of which are inositol-1,4,5-trisphosphate ($IP_3$) and diacylglycerol (DAG). The former binds to receptors on the surface of the endoplasmic reticulum leading to the release of $Ca^{2+}$ ions. The $Ca^{2+}$ ions then interact with the calmodulin subunits of phosphorylase kinase resulting in its activation (Fabbri et al., 1998). The absence of PROP completely blocking ISO-mediated increases in medium glucose may suggest that the $\alpha_1$-AR is active in this tissue even though ISO concentrations (0.1 mM) used here are well above epinephrine concentrations at rest in fish. Although the $\alpha_1$-AR-mediated glycogenolysis in trout hepatocytes was not supported by Fabbri et al. (1995), $\alpha_1$-AR transcripts were identified in trout liver using qPCR (Chen et al., 2007), but their physiological role remains unknown. Therefore, the potential ability of AgNPs to impact the $\alpha_1$-AR function should be tested in future studies.

Furthermore, Michelsen and Sheridan (1990) demonstrated the ability of a $Ca^{2+}$ ionophore (A23187) to increase glucose release, suggesting that $Ca^{2+}$ may impact glycogenolysis. It is noteworthy that a recent study demonstrated the ability of AgNPs to increase cytosolic $Ca^{2+}$ levels in primary rat cerebellum cells and suggested that these changes in $Ca^{2+}$ may have contributed to the observed oxidative stress in these cells (Yin et al., 2013). Moreover, it has been reported that heavy metals can increase cytosolic $Ca^{2+}$ levels by impairing $Ca^{2+}$ homeostasis (Verbost et al., 1989; Viarengo and Nicotera, 1991), stimulating the entry of $Ca^{2+}$ into cells via verapamil-sensitive channels (Burlando et al., 2003), or increasing the release of $Ca^{2+}$ from intracellular stores (McNulty and Taylor, 1991; Burlando et al., 2003). Whether AgNPs act through similar mechanisms to affect cytosolic $Ca^{2+}$ levels is yet to be determined, but it has been suggested that $Ag^{+}$ can

block the $Ca^{2+}$ pump, stimulating $Ca^{2+}$ release from intracellular stores at least in human HL-60 cells (promyelocytic cell line; Taguchi et al., 1991). Therefore, the impact of AgNPs on $Ca^{2+}$ homeostasis in trout hepatocytes should be considered in future studies.

The most interesting result reported in this study was the ability of 10 μg/mL AgNPs to stimulate glycogenolysis in rainbow trout hepatocytes. At this AgNP concentration medium glucose was higher than the control and the 1 μg/mL AgNP groups even in the absence of ISO (Fig. 5.2). Although there was a significant increase in ISO-stimulated medium glucose release compared with the control group, the largest change was in terms of the two controls (none and PROP alone). This effect was also noted for CORT, although at this concentration of AgNPs the CORT effect was totally removed. The increased medium glucose release was also reflected in the cellular glycogen content (Fig. 5.3), which was significantly reduced in the 10 μg/mL AgNPs group irrespective of agonists/antagonists. Moreover, as noted in Figure 5.5, total and GPase *a* activities paralleled the effects on glucose release. Interestingly, the ISO-mediated cAMP increase observed in the control group was actually blocked at 10 μg/mL AgNPs (Fig. 5.6). The explanation for these changes requires further studies, but at the moment these results suggest a generalized rather than a specific receptor-mediated phenomenon, which is supported to some extent by the lack of evidence for the presence of intracellular or membrane-bound AgNPs as reported in our previous study with trout hepatocytes (Chapter 4; Massarsky et al., 2014b).

It has been suggested that medium osmolarity may affect GPase activities. Hallgren et al. (2003) reported a linear relationship between medium osmolarity and GPase *a* activities in hepatocytes isolated from the brown bullhead (*Ameiurus nebulosus*), copper

rockfish (*Sebastes caurinus*), and the walking catfish (*Clarias batrachus*). This activation of GPase *a* by hepatocyte cell shrinkage is also reported in mammals (Weiergräber and Häussinger, 2000). This would be a general mechanism that would be independent of hormones; however, in this study there was no difference in cell medium osmolarity, which was consistent across treatments ~300 mOsmol/L (data not shown).

In summary, we demonstrated that AgNPs could affect hormone-regulated cell signaling pathways at a concentration of 10 μg/mL. On the other hand, AgNPs at 1 μg/mL did not interfere with the function of either the β-AR or GCR systems in rainbow trout hepatocytes, but at the concentration of 10 μg/mL AgNPs stimulated glycogenolysis, which was apparently receptor-independent. If confirmed *in vivo*, the glycogenolytic potential of AgNPs would be an important endocrine disrupting mechanism that could impede the 'fight-or-flight' response in fish and ultimately affect their survival.

# CHAPTER 6
# General discussion and conclusions

*6.1. Evidence for silver nanoparticle toxicity in fish*

Silver nanoparticles (AgNPs) are the most common engineered nanomaterial (ENM) in consumer products due to their antimicrobial properties (Nanotechproject, 2013). However, in recent years concerns have been raised regarding their safety and a few studies have demonstrated the ability of AgNPs to detach from impregnated fabrics during washing (Benn and Westerhoff, 2008; Geranio et al., 2009), which could allow their access to the aquatic environment and potentially pose a risk to aquatic life. The toxicity of AgNPs in fish was also addressed in several studies, using both *in vivo* (e.g. Asharani et al., 2008; 2011) and *in vitro* (e.g. Farkas et al., 2010; 2011) approaches. Nevertheless, many questions regarding the mechanism of AgNP toxicity remain unanswered. My thesis aimed to investigate the toxicity mechanisms of AgNPs from the perspectives of oxidative stress, which has been proposed as the principle mode of toxicity for ENMs (Nel et al., 2006; Auffan et al., 2009), and endocrine disruption, more specifically the ability of AgNPs to disrupt physiological function since ENMs could attach to cell membranes and other intracellular and extracellular components (Nel et al., 2009).

Additionally, one ongoing debate related to AgNP toxicity is whether its toxicity is mediated by the NP per se or by silver ion ($Ag^+$) dissolving from the AgNP surface (Beer et al., 2012); support for both sides of this argument can be found in the literature. The toxicity of $Ag^+$ is well known, especially as related to the inhibition of $Na^+$,$K^+$-ATPase activity and the ensuing disruption of ionoregulation in fish (Wood et al., 1999). Therefore, it is important to characterize not only the size and aggregation kinetics of AgNPs, which could influence the toxicity in their own right (Scown et al., 2010a), but

also $Ag^+$ dissolution. The $Ag^+$ content in the AgNP solution used in the studies described here was assessed and estimated at 0.5%. This low $Ag^+$ content suggested that the observed effects are likely nano-specific. Nonetheless, the AgNP and $Ag^+$ toxicity potentials were compared to verify the importance of Ag-type. Consequently, the nominal concentrations in the toxicity studies [zebrafish embryos (Chapter 2; Massarsky et al., 2013) and rainbow trout erythrocytes and hepatocytes (Chapter 4; Massarsky et al., 2014b)] were set such that the Ag content was the same for both AgNPs and $Ag^+$. Moreover, a Ag chelator cysteine (Cys) was used in rescue experiments *in vivo* and *in vitro* to show that the effects are Ag-specific, and buthionine sulfoximine (BSO), which inhibits the synthesis of the antioxidant glutathione (GSH, reduced form) and should lead to reduced GSH levels, was used *in vitro* to demonstrate the role of oxidative stress in Ag-mediated toxicity. The ability of AgNPs to disrupt the development of the stress response in zebrafish embryos (Chapter 3; Massarsky et al., 2014a) and the cellular signaling in trout hepatocytes (Chapter 5; Massarsky et al., 2014c) was also assessed to evaluate additional important impacts of AgNPs on fish physiology. This chapter summarizes the key evidence for the toxic potential of AgNPs in zebrafish embryos and rainbow trout erythrocytes and hepatocytes. Wider implications of these results as well as suggestions for future work are also discussed.

### *6.2. Exposure to AgNPs results in toxicity and oxidative stress*

The ability of ENMs including AgNPs to generate reactive oxygen species (ROS) due to particle surface chemistry has been suggested as one of the toxic mechanisms (Nel et al., 2006; Yeo and Kang, 2008; Auffan et al., 2009; Chae et al., 2009; Wise et al.,

2010). As mentioned in Chapter 1 ROS are naturally generated by all aerobic organisms in what is termed 'the oxygen paradox', which reflects the toxicity of oxygen and the inability of aerobic organisms to survive in its absence (Davies, 1995). The main contributor of ROS is the mitochondrial electron-transport chain, which generates the oxygen radical superoxide anion ($O_2^{\cdot-}$) (Hermes-Lima, 2005). The conversion of $O_2^{\cdot-}$ into other ROS, including hydrogen peroxide ($H_2O_2$) and highly damaging hydroxyl radical ($OH^{\cdot}$), is facilitated by the cellular milieu (Davies, 1995). There are several defense systems protecting the cell from oxidative damage exist (Davies, 2000), including GSH and the antioxidant enzymes superoxide dismutase (SOD), catalase (CAT), glutathione peroxidase (GPx), glutathione reductase (GR), and glutathione-S-transferase (GST). Consequently, unbalanced generation of ROS (natural and ENM-derived) could overwhelm the defense systems and result in damage. Therefore, the toxicity of AgNPs through ROS was investigated in this thesis.

The oxidative stress paradigm is supported in this thesis by both *in vivo* and *in vitro* experiments. Exposure of zebrafish embryos to AgNPs or $Ag^+$ until 4 d post fertilization (dpf) not only increased mortality and delayed hatching, but also generated ROS, reduced total glutathione (TGSH) levels, and increased the oxidized glutathione (GSSG)/TGSH ratios without affecting antioxidant enzymes activities (Chapter 2). For all assessed endpoints $Ag^+$ had greater effects than AgNPs; this may be due to the ability of $Ag^+$ to pass through the chorion pores that are 500-700 nm (Fako and Furgeson, 2009). AgNPs although of a size that should pass through these same pores, were shown to attach to the chorion; whether they accessed the embryo is unclear. As predicted Cys co-treatment

reduced the toxicity of both Ag-types and improved the GSH levels, suggesting that the observed effects were due to the Ag exposure.

Similar results were obtained with *in vitro* experiments, which again demonstrated that the $Ag^+$ was more cytotoxic than AgNPs in both trout erythrocytes and hepatocytes after a 48 h exposure (Chapter 4). Both silver types reduced TGSH levels, increased GSSG/TGSH ratios, and affected antioxidant enzymes activities. Formation of ROS was also increased in hepatocytes. The most interesting result from this study was the ability of AgNPs to increase lipid peroxidation (without microscopic indication of cellular uptake) in hepatocytes, suggesting that AgNPs induce oxidative damage extracellularly. In contrast, $Ag^+$ increased DNA damage, suggesting that $Ag^+$ damage the cells intracellularly. As predicted Cys reduced the toxicity of both Ag-types in erythrocytes and hepatocytes, whereas BSO increased the toxicity of Ag in hepatocytes (erythrocytes were not sensitive to BSO).

Both the *in vivo* and *in vitro* experiments suggest that 1) the toxicity of AgNPs used in this study although similar to the toxicity of $Ag^+$, which was the more toxic Ag-type, is independent of $Ag^+$ dissolution; 2) the AgNP exposure results in oxidative stress; and, 3) AgNPs increased lipid peroxidation in hepatocytes by acting extracellularly. However, it is important to note that the Ag concentrations that were necessary to achieve these effects (in μg/mL: 0.03-1.55 *in vivo* and 3.1-31 *in vitro*) are several orders of magnitude higher than the predicted environmental concentrations (PECs) in surface water of 0.088-2.63 or 40-320 ng/L as estimated by Gottschalk et al. (2009) and Blaser et al. (2008), respectively, even if we consider the estimated ~1.7-fold increase between 2014 and 2020 as discussed in Chapter 1.

Although the discrepancy between the PECs and the observed effective concentrations would generally suggest that AgNPs are likely not to be an environmental concern, such conclusions should be made cautiously since considerable uncertainty remains. This is why future studies should consider the following:

1) As discussed in Chapter 1, most of the AgNPs in the aquatic environment are predicted to accumulate in the sediment (in the μg-mg/kg range), suggesting that AgNPs could potentially pose a risk to benthic invertebrate and vertebrate species. This in turn implies that ingestion of AgNP-sediment complexes is the more likely route of uptake for aquatic species. Consequently, future studies on AgNP toxicity in aquatic organisms should consider this route of exposure. *In vitro* experiments should include cell types relevant to the gastrointestinal tract and examine the aforementioned cellular defenses in more detail.
2) It is also noteworthy that most of the AgNPs are predicted to be transformed into $Ag_2S$ as they pass through the sewage treatment plant (STP) and to bind to natural organic matter (NOM) once in the aquatic environment (Chapter 1). Therefore, future studies should further characterize the transformation of AgNPs (with various coating/surface functionalizations, different particle sizes and shapes) into $Ag_2S$ and subsequently investigate the toxicity of $Ag_2S$ particles *in vivo* in the presence of NOM. An ideal experiment would involve isolating $Ag_2S$ complexes from STP sludge samples and testing the toxicity of such complexes in natural water samples.
3) Furthermore, it is important to consider the presence of other toxic contaminants, including other ENMs, pharmaceuticals, and polycyclic aromatic hydrocarbons, which are likely to influence the toxicity of AgNPs. It is, therefore, important to

include contaminant mixtures in future experiments to provide a more realistic exposure scenario.

4) Finally, it is crucial to start moving away from acute *in vivo* exposure (as used in this thesis) and towards more chronic *in vivo* exposure scenarios. Obviously fish and other aquatic organisms will be exposed to these potential contaminants throughout their life. Such studies should examine the aforementioned endpoints in a more realistic exposure scenario.

*6.3. AgNPs do not disrupt the stress response in zebrafish*

Chapter 3 examined the ability of AgNP and $Ag^{+}$ to impact the hypothalamic-pituitary-interrenal (HPI) axis and specifically cortisol levels in fish, which has not been addressed previously. The HPI axis includes corticotropin-releasing factor (CRF), which is released in response to hypothalamic stimulation (Alderman and Vijayan, 2012), acting on the pituitary to release the adrenocorticotropic hormone (ACTH), which in turn stimulates cortisol synthesis and release by interrenal cells of the fish head kidney (Mommsen et al., 1999; To et al., 2007). Cortisol is the principal glucocorticoid in teleost fish, and is shown to increase hepatic gluconeogenesis, providing fuel to cope with the increased metabolic demands imposed by stressors (Mommsen et al., 1999; Vijayan et al., 2003).

The HPI axis in zebrafish is fully developed by 4 dpf (Alsop and Vijayan, 2009) and we hypothesized that an acute exposure to sub-LC50 concentrations of AgNPs or $Ag^{+}$ during these critical early stages of zebrafish development would alter the proper formation and functioning of the HPI axis in zebrafish embryos and that these changes

would persist in the adult fish. As discussed in Chapter 3 this hypothesis was not supported by the cortisol data, which demonstrated that both the larvae and the adult zebrafish were able to elevate cortisol levels in response to a stressor. Interestingly, there were changes in the gene expression of CRF-related genes, suggesting that at least $Ag^{+}$ could affect CRF-related processes other than the HPI axis, including nervous, cardiovascular, immune, muscular, and reproductive systems, as well as behavior and food intake (Yao and Denver, 2007; Alderman and Bernier, 2009). Moreover, in adults sex differences were observed in plasma cortisol levels and the telencephalon transcript abundance of some of the CRF-related genes, suggesting a sex-specific regulation of the stress axis. Given that the stress response is essential to survival, sex differences could imply unequal survival chances for males and females when exposed to Ag.

However, even though there were no effects on cortisol levels in response to AgNP (or $Ag^{+}$), this study does not prove that AgNP (or $Ag^{+}$) does not affect the zebrafish stress response. Other scenarios, such as a chronic exposure from early embryonic stage to adulthood, should be considered. Moreover, a static exposure was used in this study, meaning that it is likely that the AgNPs may have been bound to the chorion (as suggested in Chapter 2), meaning that the effective concentration is likely over-estimated. Future studies should estimate the amount of unadsorbed AgNPs and use renewal exposures to ensure concentrations remain similar across time. These considerations are important to verify the impact of AgNPs on essential physiological processes, such as the stress response.

*6.4. AgNPs impact hormone-regulated cell signaling in hepatocytes*

One of the most novel findings of this thesis is the ability of AgNPs to stimulate glucose production in trout hepatocytes at sub-cytotoxic concentrations (Chapter 5). I hypothesized that AgNPs would disrupt proper cell signaling by binding to membrane receptors and/or impacting membrane properties, thus preventing proper signaling activities within the cell. This hypothesis reflects the recent review by Nel et al. (2009), which addressed the potential interactions of ENMs with biological interfaces, including cells, membranes, organelles, proteins, and DNA. A preliminary experiment using a sub-toxic dose of AgNPs (10 μg/mL; nominal concentration) showed that at this concentration the particles are able to increase glucose production. Consequently, experiments involving agonists and antagonists of the β-adrenoreceptor (β-AR) and glucocorticoid receptor (GCR) were performed as both receptors could lead to increased glucose release in hepatocytes through glycogenolysis and gluconeogenesis, respectively.

This study is the first to demonstrate that AgNPs do not interfere with the function of the β-AR and GCR systems at a concentration of 1 μg/mL. However, at a concentration of 10 μg/mL, AgNPs increased glucose production, which coincided with a decrease in cellular glycogen content and an increase in glycogen phosphorylase (GPase) *a* activity, suggesting that AgNPs activate GPase *a* resulting in glycogenolysis. Interestingly, the levels of the second messenger cAMP were not affected by this concentration (10 μg/mL) as would be expected if AgNPs had agonistic actions mediated by the β-AR as was shown for isoproterenol.

It is noteworthy that although glycogenolysis in rainbow trout hepatocytes is mediated primarily by the β-AR (Van Heeswijk et al., 2006), the $\alpha_1$-AR can also increase

glycogenolysis by stimulating the release of $Ca^{2+}$ ions, which then interact with the calmodulin subunits of phosphorylase kinase resulting in GPase activation (Fabbri et al., 1998). In addition it was reported that a $Ca^{2+}$ ionophore (A23187) increased glucose release, suggesting that $Ca^{2+}$ may impact glycogenolysis (Michelsen and Sheridan, 1990). Therefore, future studies should investigate the potential ability of AgNPs to impact intracellular $Ca^{2+}$ levels and the function of the $\alpha_1$-AR.

Furthermore, the glycogenolytic potential of AgNPs reported here should be verified *in vivo* since liver glycogenolysis is an essential source of glucose during the 'fight-or-flight' stress response as discussed in Chapter 5. AgNPs were shown to accumulate in various tissues, including the liver, at least in common carp (Gaiser et al., 2012). Therefore, AgNPs could come in direct contact with liver cells and potentially stimulate glycogenolysis *in vivo*. If confirmed *in vivo*, the glycogenolytic potential of AgNPs would be an important endocrine disrupting mechanism that could impede the 'fight-or-flight' response in fish and ultimately affect the survival.

### *6.5. Contributions this work has made to the literature*

The experiments reported in this thesis were initiated as a result of a successful NSERC Strategic Grant application by Dr. Chris Metcalfe, Trent University. The title of the proposal was *Fate and Effects of Nanomaterials in the Aquatic Environment* and six co-applicants were listed, including Drs. Thomas Moon and Vance Trudeau. Funding became available as of October 2007 at which point meetings and discussions between the applicants were held to define the scope of the project. Several international organizations had expressed the need to examine the potential toxicity of ENMs and the

Government of Canada through its OECD partnership agreed to contribute to research in this area. Little was known regarding ENMs (especially AgNPs), and the toxicology literature was relatively minimal. Since then a large literature has evolved (see Figure 6.1). My thesis has added to this scientific literature regarding the toxicity of AgNPs with several important findings:

1. One mechanism of the toxicity of AgNPs both *in vivo* and *in vitro* involves oxidative stress (as defined by increased ROS, decreased GSH). Although both AgNPs and $Ag^+$ lead to oxidative stress, $Ag^+$ at Ag concentrations equivalent to AgNPs is more toxic. Additionally, my *in vitro* results suggest that AgNP generates ROS primarily extracellularly (lack of cellular uptake, as discussed below, further supports this assertion) while $Ag^+$ does so intracellularly, leading to lipid peroxidation and DNA damage, respectively. One possible mechanism for AgNP- and $Ag^+$-mediated cytotoxicity is summarized in Figure 6.2.
2. Moreover, unlike other studies (see Chapter 4 for examples), which used different formulations of AgNPs and other cell types and reported cellular uptake and cytotoxicity, our *in vitro* results suggest that cellular uptake of AgNPs used here is not a requirement for cytotoxicity. This discrepancy further emphasizes the importance of physical characteristics of AgNPs (coating, size, shape, etc.) in determining their fate, behavior, and toxicity.
3. Despite clear indications of oxidative stress, exposure of zebrafish embryos to AgNPs or $Ag^+$ during the early life stages does not disrupt the ability of larvae or adults to elevate cortisol levels in response to a stressor. However, exposure to $Ag^+$ does alter the transcript abundance of CRF-related genes.

4. At a low sub-cytotoxic dose (1 μg/mL), AgNPs do not disrupt β-AR or GCR signaling in trout hepatocytes, but at high sub-cytotoxic dose (10 μg/mL), AgNPs stimulate glycogenolysis independently of either receptor. These results as well as possible future experiments pertaining to AgNP-mediated glycogenolysis in hepatocytes are summarized in Figure 6.3.
5. Lastly, as discussed in section 6.1 dissolution of AgNPs is an important determinant of toxicity. The low dissolution of AgNPs reported here suggests that the observed effects are likely nano-specific and emphasizes that AgNP dissolution is specific to the NP and likely governed by other physical characteristics (e.g. coating) and experimental conditions (e.g. presence of proteins in culture medium). Thus, the studies described here contribute to the ongoing debate of 'AgNP vs $Ag^+$ toxicity', supporting that the toxicity of AgNPs is not solely due to dissolving $Ag^+$ and that nano-specific effects are possible.

*6.6. Summary*

The introduction of AgNPs into the environment is inevitable. Flow models for AgNPs (Chapter 1) showed that most of the AgNPs will be removed by the STP into the sludge, which could be used for agriculture, making soil the main AgNP deposition site. Nonetheless, a smaller percentage of AgNPs will be present in the STP effluent. Once in the aquatic environment most of the AgNPs will sediment and a smaller percentage will remain in the water column. Therefore, AgNPs could potentially pose a risk to aquatic organisms as summarized in Figure 6.4.

The results presented in this thesis demonstrate the ability of AgNPs to elicit toxicity both *in vivo* and *in vitro*, resulting in oxidative stress and cellular damage, and to disrupt hormone-dependent cell signaling *in vitro*, as well as the inability of AgNPs to affect the development of the stress response. Whether the observed effects could be applicable in a more environmentally realistic exposure setting remains to be answered, but these findings do offer several directions for future research. From an *in vivo* perspective it is important to investigate the ability of chronic exposure to AgNPs to impact fish physiology, including not only the stress response, but also reproductive success, and swimming performance. It is also important to consider ingestion exposures, since most of the AgNPs in the aquatic environment would be found in the sediment and could pose a risk to the bottom feeding fish. From an *in vitro* perspective future experiments should focus more on cell physiology, such as the glycogenolytic potential demonstrated herein, and verify whether similar effects could be observed *in vivo* and how such changes may impact fish physiology and ultimately survival.

Future experiments are necessary in order to clarify and better define the environmental risks associated with AgNPs (and other ENMs). This is especially important considering the continuous increase in nanotechnological advances, including the large number of consumer products containing ENMs, and the large knowledge gap in the field of nanotoxicology pertaining to the fate, behavior, and toxicity of ENMs.

**Figure 6.1.** Total number of publications including the keywords 'nanomat*' and 'toxic*' and 'silver' published between 2001 and 2013. The search was performed using the Web of Science database on January 8th, 2014.

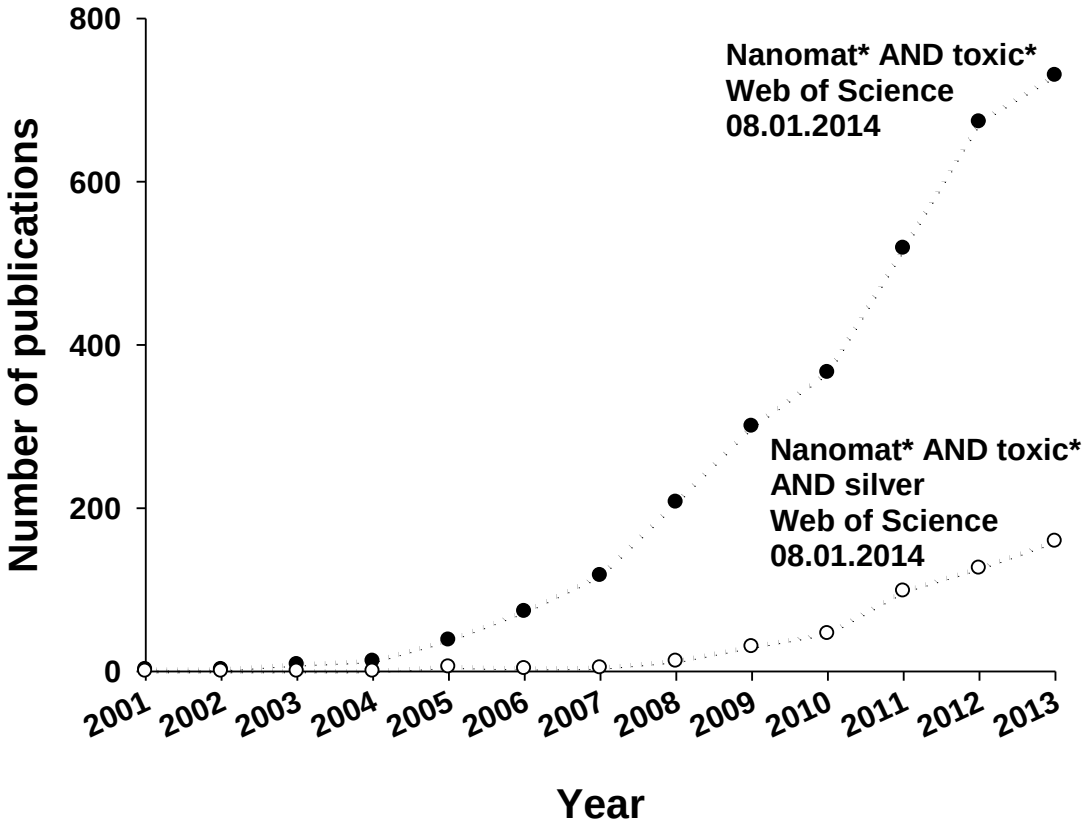

**Figure 6.2.** One possible mechanism for AgNP- and $Ag^{+}$-mediated cytotoxicity is through generation of reactive oxygen species (ROS). This thesis suggests that in trout hepatocytes AgNP generates ROS extracellularly (or in close proximity to the cell membrane) while $Ag^{+}$ does so intracellularly (near or inside the nucleus), leading to lipid peroxidation and DNA damage, respectively. The antioxidant system of trout erythrocytes (ery) and hepatocytes (hep) was affected as summarized in green boxes (see Chapter 4). The antioxidants include reduced glutathione (GSH), glutathione-S-transferase (GST), glutathione reductase (GR), glutathione peroxidase (GPx), catalase (CAT), and superoxide dismutase (SOD). Parameters that were not affected are signified as 'na'.

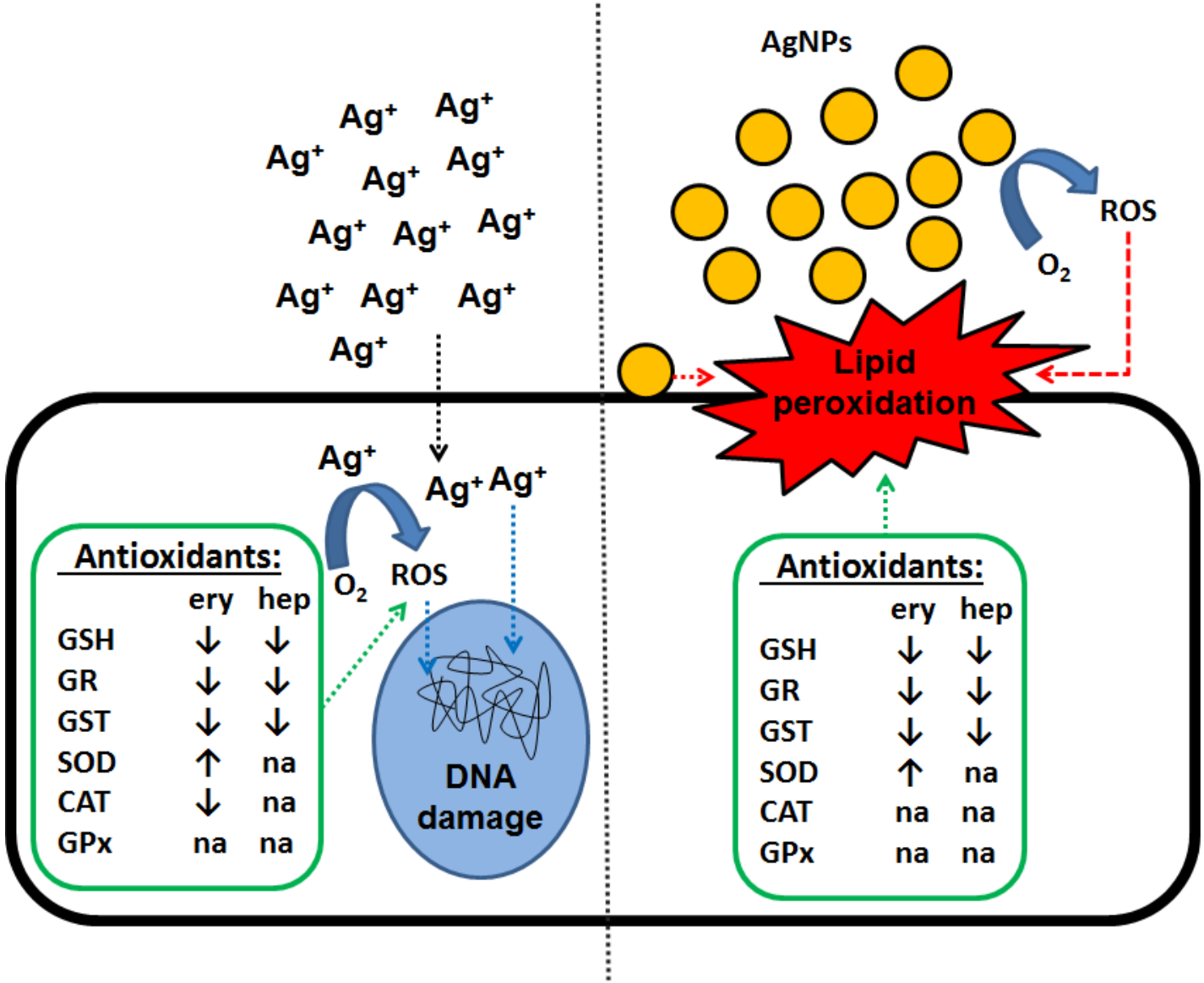
AgNPs
Ag+
Ag+
Ag+
Ag+
Ag+
Ag+
Ag+
Ag+
Ag+
Ag+
Ag+
Ag+
Ag+
Ag+
Ag+
ROS
O2
Lipid peroxidation
Antioxidants:
ery hep
GSH ↓ ↓
GR ↓ ↓
GST ↓ ↓
SOD ↑ na
CAT ↓ na
GPx na na
O2
ROS
DNA damage
Antioxidants:
ery hep
GSH ↓ ↓
GR ↓ ↓
GST ↓ ↓
SOD ↑ na
CAT na na
GPx na na

**Figure 6.3.** The increase in AgNP-mediated glucose production in trout hepatocytes could be mediated by the β-adrenergic receptor (β-AR) and the glucocorticoid receptor (GCR) through glycogenolysis and gluconeogenesis, respectively. AgNPs (10 μg/mL) increased glucose release, decreased glycogen content, and increased glycogen phosphorylase (GPase) *a* activity, but did not affect the levels of the second messenger cAMP and did not increase the activities of gluconeogenic enzymes, suggesting that the effects are independent of β-AR or GCR (see Chapter 5). Another mechanism to increase GPase *a* activity would be through $Ca^{2+}$-calmodulin signaling, which could be mediated by $\alpha_1$-AR and possibly increased $Ca^{2+}$ influx into the cell; this should be addressed in future experiments.

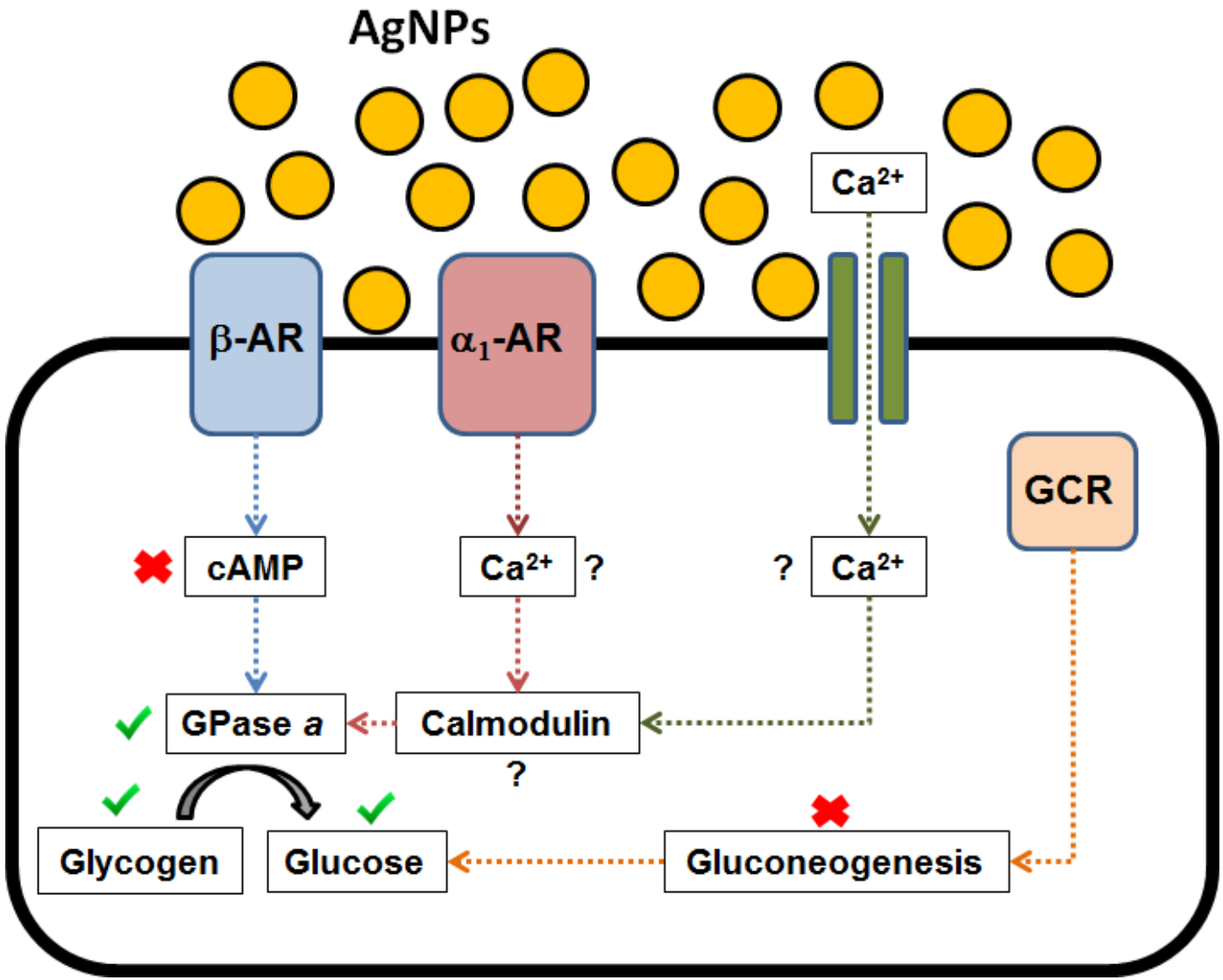
AgNPs
β-AR
α1-AR
Ca2+
GCR
cAMP
Ca2+ ?
? Ca2+
GPase a
Calmodulin
?
Glycogen
Glucose
Gluconeogenesis

**Figure 6.4.** AgNPs could reach the sewage treatment plant (STP) after being released from various consumer products. Most AgNPs in the STP accumulate in the sludge (bold arrows), which can be used in agriculture and possibly pose a risk to organisms in the soil. The remaining AgNPs will be released into aquatic environment, where most AgNPs will accumulate in the sediment with a small percentage being present in the water column, suggesting that benthic organisms may be at a greater risk than pelagic organisms (most studies to date, including the ones described herein, focused on pelagic fish species). Future studies should consider both the ingestion and waterborne chronic exposure scenarios using both *in vivo* and *in vitro* approaches. Note: the images used to generate this figure were obtained from ClipArt Word 2010.

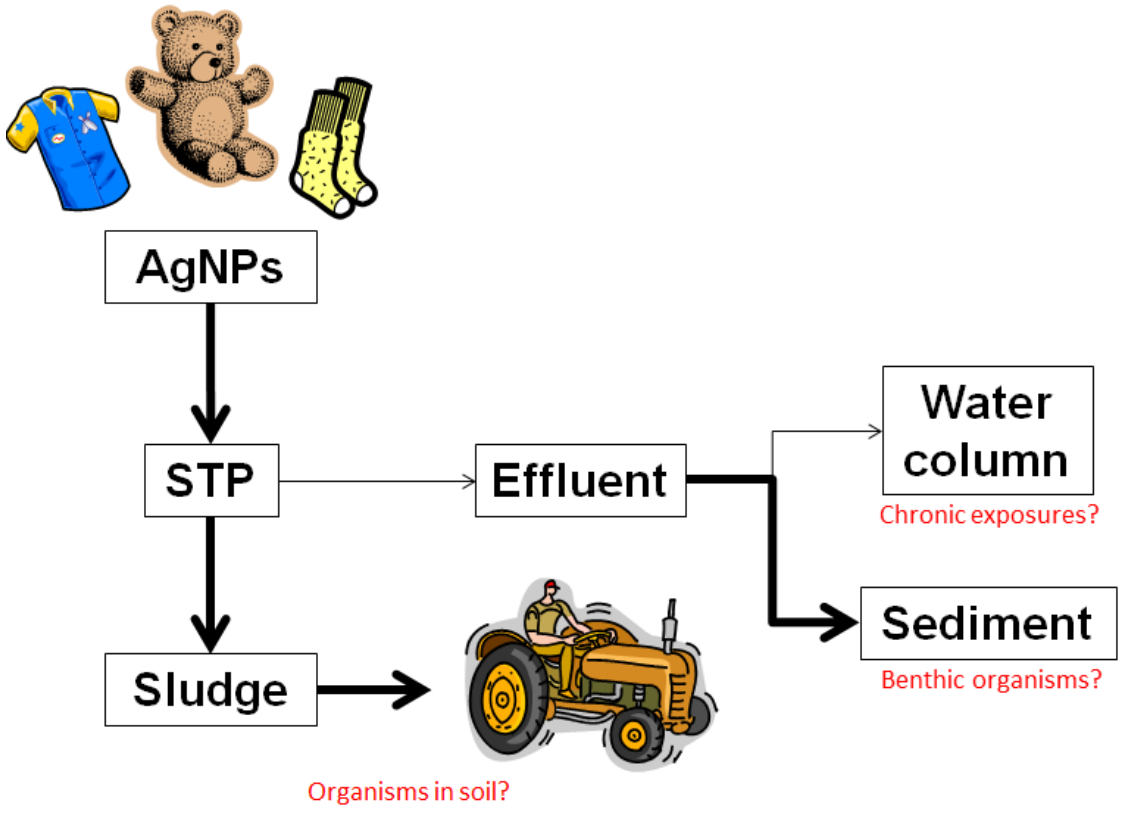

## References


Ahamed, M., Khan, M.A.M., Siddiqui, M.K.J., AlSalhi, M.S., Alrokayan, S.A., 2011. Green synthesis, characterization and evaluation of biocompatibility of silver nanoparticles. Physica E. 43, 1266-1271.

Aillon, K.L., Xie, Y., El-Gendy, N., Berkland, C.J., Forrest ML., 2009. Effects of nanomaterial physicochemical properties on *in vivo* toxicity. Adv. Drug Deliv. Rev. 61, 457-466.

Alderman, S.L., Bernier, N.J., 2007. Localization of corticotropin-releasing factor, urotensin I, and CRF-binding protein gene expression in the brain of the zebrafish, *Danio rerio*. J. Comp. Neurol. 502, 783-793.

Alderman, S.L., Bernier, N.J., 2009. Ontogeny of the corticotropin-releasing factor system in zebrafish. Gen. Comp. Endocr. 164, 61-69.

Alderman, S.L., McGuire, A., Bernier N.J., Vijayan, M.M., 2012. Central and peripheral glucocorticoid receptors are involved in the plasma cortisol response to an acute stressor in rainbow trout. Gen. Comp. Endocr. 176, 79-85.

Alderman, S.L., Vijayan, M.M., 2012. 11 β-Hydroxysteroid dehydrogenase type 2 in zebrafish brain: a functional role in HPI axis regulation. J. Endocrinol. 215, 1-11.

Alsop, D., Vijayan, M.M., 2008. Development of the corticosteroid stress axis and receptor expression in zebrafish. Am. J. Physiol. Integr. Comp. Physiol. 294, R711-719.

Alsop, D., Vijayan, M.M., 2009. Molecular programming of the corticosteroid stress axis during zebrafish development. Comp. Biochem. Physiol. A 153, 49-54.

Aluru, N., Vijayan, M.M., 2007. Hepatic transcriptome response to glucocorticoid receptor activation in rainbow trout. Physiol. Genomics 31, 483-491.

Asharani, P.V., Lianwu, Y., Gong, Z., Valiyaveettil, S., 2011. Comparison of the toxicity of silver, gold, and platinum nanoparticles in developing zebrafish embryo. Nanotoxicology 5, 43-54.

Asharani, P., Wu, Y., Gong, Z., Valiyaveettil, S., 2008. Toxicity of silver nanoparticles in zebrafish models. Nanotechnology 19, 255102-255109.

Auffan, M., Rose, J., Bottero, J.Y., Lowry, G.V., Jolivet, J.P., Wiesner, M.R., 2009. Towards a definition of inorganic nanoparticles from an environmental, health and safety perspective. Nat. Nanotechnol. 4, 634-641.

Baldi, C., Minoia, C., Di Nucci, A., Capodaglio, E., Manzo, L., 1988. Effects of silver in isolated rat hepatocytes. Toxicol. Lett. 41, 261-268.

Bar-Ilan, O., Albrecht, R., Fako, V., Furgeson, D., 2009. Toxicity assessments of multisized gold and silver nanoparticles in zebrafish embryos. Small 17, 897-910.

BCC, 2012. BCC Research LLC. Retrieved on July 25th, 2013, from http://www.bccresearch.com/market-research/nanotechnology/nanotechnology-market-applications-products-nan031e.html.

Beer, C., Foldbjerg, R., Hayashi, Y., Sutherland D.S., Autrup, H., 2012. Toxicity of silver nanoparticles-nanoparticle or silver ion? Toxicol. Lett. 208, 286-292.

Benn, T.M., Westerhoff, P., 2008. Nanoparticle silver released into water from commercially available sock fabrics. Environ. Sci. Technol. 42, 4133-4139.

Bilberg, K., Døving, K.B., Beedholm, K., Baatrup, E., 2011. Silver nanoparticles disrupt olfaction in Crucian carp (*Carassius carassius*) and Eurasian perch (*Perca fluviatilis*). Aquat. Toxicol. 104, 145-152.

Bilberg, K., Malte, H., Wang, T., Baatrup, E., 2010. Silver nanoparticles and silver nitrate cause respiratory stress in Eurasian perch (*Perca fluviatilis*). Aquat. Toxicol. 96, 159-165.

Blaser, S.A., Scheringer, M., MacLeod, M., Hungerbühler, K., 2008. Estimation of cumulative aquatic exposure and risk due to silver: contribution of nano-functionalized plastics and textiles. Sci. Total Environ. 390, 396-409.

Brighenti, L., Puviani, A.C., Gavioli, M.E., Fabbri, E., Ottolenghi, C., 1991. Interaction of salmon glucagon, glucagon-like peptide, and epinephrine in the stimulation of phosphorylase *a* activity in fish isolated hepatocytes. Gen. Comp. Endocr. 82, 131-130.

Burlando, B., Bonomo, M., Fabbri, E., Dondero, F., Viarengo, A., 2003. $Hg^{2+}$ signaling in trout hepatoma (RTH-149) cells: involvement of $Ca^{2+}$-induced $Ca^{2+}$ release. Cell Calcium 34, 285–293.

Buzea, C., Pacheco, I.I., Robbie, K., 2007. Nanomaterials and nanoparticles: sources and toxicity. Biointerphases 2, MR17-MR71.

Camargo, M.M.P., Fernandes, M.N., Martinez, C.B.R., 2009. How aluminium exposure promotes osmoregulatory disturbances in the neotropical freshwater fish *Prochilus lineatus*. Aquat. Toxicol. 94, 40-46.

Cannon, W.B., 1929. Organization for physiological homeostasis. Physiol. Rev. 9, 399-431.

Carlson, C., Hussain, S., Schrand, A., 2008. Unique cellular interaction of silver nanoparticles: size-dependent generation of reactive oxygen species. J. Phys. Chem. 112, 13608-13619.

Castano, A., Bols, N., Braunbeck, T., Dierickx, P., Halder, M., Isomaa, B., Kawahara, K., Lee, L.E.J., Mothersill, C., Part, P., Repetto, G., Sintes, J.R., Rufli, H., Smith, R., Wood, C., Segner, H., 2003. The use of fish cells in ecotoxicology – the report and recommendation of ECVAM workshop 47. Altern. Lab. Anim. 31, 317-351.

CCA (Council of Canadian Academies), 2008. Small is different: a science perspective on the regulatory challenges of the nanoscale. Expert panel Sinervo, P., Boily, S., Brunk, C., Castle, D., Chan, W.C.W., Cheng, M.-D., Gold, R., Grütter, P., Haarmann, C., Maynard, A.D., Oberdörster, G., Shatkin, J.A., Sheremeta, L. Science Advice, Ottawa, Ontario, Canada.

Chae, Y.J., Pham, C.H., Lee, J.W., Bae, E.J., Yi, J.H., 2009. Evaluation of the toxic impact of silver nanoparticles on Japanese medaka (*Oryzias latipes*). Aquat. Toxicol. 94, 320-327.

Chakravarty, S., Reddy, B.R., Sudhakar, S.R., Saxena, S., Das, T., Meghah, V., Swamy, C.V.B., Kumar, A., Idris, M.M., 2013. Chronic unpredictable stress (CUS)-induced anxiety and related mood disorders in a zebrafish model: altered brain proteome profile implicates mitochondrial dysfunction. PLOS One 8, e63302.

Chambers, B.A., Afrooz, A.R., Bae, S., Aich, N., Katz, L., Saleh, N.B., Kirisits, M.J., 2014. Effects of chloride and ionic strength on physical morphology, dissolution, and bacterial toxicity of silver nanoparticles. Environ. Sci. Technol. 48, 761-769.

Chappell, M.A., Miller, L.F., George, A.J., Pettway, B.A., Price, C.L., Porter, B.E., Bednar, A.J., Seiter, J.M., Kennedy, A.J., Steevens, J.A., 2011. Simultaneous dispersion-dissolution behavior of concentrated silver nanoparticle suspensions in the presence of model organic solutes. Chemosphere 84, 1108-1116.

Chen, Q., Yu, L., Yang, L., Zhou, B., 2012. Bioconcentration and metabolism of decabromodiphenyl ether (BDE-209) result in thyroid endocrine disruption in zebrafish larvae. Aquat. Toxicol. 110, 141-148.

Chen, X., Perry, S.F., Aris-Brosou, S., Selva, C., Moon, T.W., 2007. Characterization and functional divergence of $\alpha$1-adrenoceptor gene family: insights from the rainbow trout (*Oncorhynchus mykiss*). Physiol. Genomics 32, 142-153.

Chen, X., Schluesener. H., 2008. Nanosilver: a nanoproduct in medical application. Toxicol. Lett. 176, 1-12.

Chernousova, S., Epple, M., 2013. Silver as antibacterial agent: ion, nanoparticle, and metal. Angew. Chem. Int. Ed. 52, 1636-1653.

Choi, O., Hu, Z.Q., 2008. Size dependent and reactive oxygen species related nanosilver toxicity to nitrifying bacteria. Environ. Sci. Technol. 42, 4583–4588.

Clement, J.L., Jarrett, P.S., 1994. Antibacterial silver. Met. Based Drugs 1, 467-482.

Cogun, H.Y., Firat, Ö., Firat, Ö., Yüzereroğlu, T.A., Gök, G., Kargin, F., Kotemen, Y., 2011. Protective effect of selenium against mercury-induced toxicity on hematological and biochemical parameters of *Oreochromis niloticus*. J. Biochem. Mol. Toxicol. 26, 117-122.

Coradeghini, R., Gioria, S., García, C.P., Nativo, P., Franchini, F., Gilliland, D., Ponti, J., Rossi, F., 2013. Size-dependent toxicity and cell interaction mechanisms of gold nanoparticles on mouse fibroblasts. Toxicol. Lett. 217, 205-216.

Craig, P.M., Hogstrand, C., Wood, C.M., McClelland, G.B., 2009. Gene expression endpoints following chronic waterborne copper exposure in a genomic model organism, the zebrafish, *Danio rerio*. Physiol. Genomics 40, 23-33.

Davies, K.J., 1995. Oxidative stress: the paradox of aerobic life. Biochem. Soc. Symp. 61, 1-31.

Davies, K.J., 2000. Oxidative stress, antioxidant defenses, and damage removal, repair, and replacement systems. IUBMB Life 50, 279-289.

Deneke, S.M., Fanburg, B.L., 1989. Regulation of cellular glutathione. Am. J. Physiol. 257, L163–L173.

Deng, J., Yu, L., Liu, C., Yu, K., Shi, X., Yeung, L.W.Y, Lam, P.K.S., Wu, R.S.S., Zhou, B., 2009. Hexabromocyclododecane-induced developmental toxicity and apoptosis in zebrafish embryos. Aquat. Toxicol. 93, 29-36.

Dhanasiri, A.K.S., Fernandes, J.M.O., Kiron, V., 2013. Acclimation of zebrafish to transport stress. Zebrafish 10, 87-98.

Domingos, R.F., Baalousha, M.A., Ju-Nam, Y., Reid, M.M., Tufenkji, N., Lead, J.R., Leppard, G.G., Wilkinson, K.J., 2009. Characterizing manufactured nanoparticles in the environment: multimethod determination of particle size. Environ. Sci. Technol. 43, 7277-7284.

Dugan, S.G., Lortie, M.B., Nickerson, J.G., Moon, T.W., 2003. Regulation of the hepatic b2-adrenoceptor in rainbow trout (*Oncorhynchus mykiss*). Comp. Biochem. Physiol. B 136, 331-342.

Elechiguerra, J.L., Burt, J.L., Morones, J.R., Camacho-Bragado, A., Gao, X., Lara, H.H., Yacaman, M.J., 2005. Interaction of silver nanoparticles with HIV-1. J. Nanobiotechnology 3, 6-15.

Elsalini, O.A., Rohr, K.B., 2003. Phenylthiourea disrupts thyroid function in developing zebrafish. Dev. Genes Evol. 212, 593-598.

Fabbri, E., Capuzzo, A., Moon, T.W., 1998. The role of circulating catecholamines in the regulation of fish metabolism: an overview. Comp. Biochem. Physiol. C 120, 177-192.

Fabbri, E., Gambarotta, A., Moon, T.W., 1995. Adrenergic signaling and second messenger production in hepatocytes of two fish species. Gen. Comp. Endocr. 99, 114-124.

Fabrega, J., Fawcett, S.R., Renshaw, J.C., Lead, J.R., 2009. Silver nanoparticle impact on bacterial growth: effect of pH, concentration, and organic matter. Environ. Sci. Technol. 43, 7285-7290.

Fako, V., Furgeson, D., 2009. Zebrafish as a correlative and predictive model for assessing biomaterial nanotoxicity. Adv. Drug Deliver. Rev. 61, 478-486.

Farkas, J., Christian, P., Urrea, J.A.G., Roos, N., Hassellöv, M., Tollefsen, K.E., Thomas, K.V., 2010. Effects of silver and gold nanoparticles on rainbow trout (*Oncorhynchus mykiss*) hepatocytes. Aquat. Toxicol. 96, 44-52.

Farkas, J., Christian, P., Urrea, J.A.G., Roos, N., Hassellöv, M., Tollefsen, K.E., Thomas, K.V., 2011. Uptake and effects of manufactured silver nanoparticles in rainbow trout (*Oncorhynchus mykiss*) gill cells. Aquat. Toxicol. 101, 117-125.

Farmen, E., Mikkelsen, H.N., Evensen, Ø., Einset, J., Heier, L.S., Rosseland, B.O., Salbu, B., Tollefsen, K.E., Oughton, D.H., 2012. Acute and sub-lethal effects in juvenile

Atlantic salmon exposed to low μg/L concentrations of Ag nanoparticles. Aquat. Toxicol. 108, 78-84.

Félix, A.S., Faustino, A.I., Cabral, E.M., Oliveira, R.F., 2013. Noninvasive measurement of steroid hormones in zebrafish holding-water. Zebrafish 10, 110-115.

Feng, Q., Boone, A.N., Vijayan, M.M., 2003. Copper impact on heat shock protein 70 expression and apoptosis in rainbow trout hepatocytes. Comp. Biochem. Physiol. C 135, 345–355.

Feng, Q.L., Wu, J., Chen, G.Q., Cui, F.Z., Kim, T.N., Kim, J.O., 2000. A mechanistic study of the antibacterial effect of silver ions on *Escherichia coli* and *Staphylococcus aureus*. J. Biomed. Mater. Res. 52, 662-668.

Filby, A.L., Paull, G.C., Bartlett, E.J., Van Look, K.J.W., Tyler, C.R., 2010. Physiological and health consequences of social status in zebrafish (*Danio rerio*). Physiol. Behav. 101, 576-587.

Firat, Ö., Alici, M.F., 2012. Assessment of pollution in Ataturk dam lake (Adiyaman, Turkey) using several biochemical parameters in common carp, *Cyprinus carpio* L. Bull. Environ. Contam. Toxicol. 89, 474-478.

Firat, Ö., Kargin, F., 2011. Individual and combined effects of heavy metals on serum biochemistry of Nile tilapia *Oreochromis niloticus*. Arch. Environ. Contam. Toxicol. 58, 151-157.

Fischer, H.C., Chan, W.C.W., 2007. Nanotoxicity: the growing need for *in vivo* study. Curr. Opin. Biotech. 18, 565-571.

Folch, J., Lees, M., Stanley, G.H.S., 1957. A simple method for the isolation and purification of total lipids from animal tissues. J. Biol. Chem. 226, 497-509.

Foldbjerg, R., Olesen, P., Hougaard, M., Dang, D.A., Hoffmann, H.J., Autrup, H., 2009. PVP-coated silver nanoparticles and silver ions induce reactive oxygen species, apoptosis and necrosis in THP-1 monocytes. Toxicol. Lett. 190, 156-162.

Folgueira, M., Anadón, R., Yáñez, J., 2004. Experimental study of the connections of the telencephalon in the rainbow trout (*Oncorhynchus mykiss*). II: Dorsal area and preoptic region. J. Comp. Neurol. 480, 204-233.

Fong, J., Wood, F., 2006. Nanocrystalline silver dressings in wound management: a review. Int. J. Nanomed. 1, 441-449.

Furman, O., Usenko, S., Lau, B.L.T., 2013. Relative importance of the humic and fulvic fractions of natural organic matter in the aggregation and deposition of silver nanoparticles. Environ. Sci. Technol. 47, 1349-1356.

Fuzzen, M.L.M., Bernier, N.J., Van Der Kraak, G., 2011. Differential effects of 17β-estradiol and 11-ketotestosterone on the endocrine stress response in zebrafish (*Danio rerio*). Gen. Comp. Endocr. 170, 365-373.

Gagné, F., André, C., Cejka, P., Hausler, R., Fournier, M., 2011. Alterations in DNA metabolism in *Elliptio complanata* mussels after exposure to municipal effluents. Comp. Biochem. Physiol. C 154, 100-107.

Gagné, F., André, C., Skirrow, R., Gélinas, M., Auclair, J., van Aggelen, G., Turcotte, P., Gagnon, C., 2012. Toxicity of silver nanoparticles to rainbow trout: a toxicogenomic approach. Chemosphere 89, 615-622.

Gagné, F., Blaise, C., 1995. Evaluation of the genotoxicity of environmental contaminants in sediments to rainbow trout hepatocytes. Environ. Toxicol. Wat. Qual. 10, 217-229.

Gaiser, B.K., Fernandes, T.F., Jepson, M.A., Lead, J.R., Tyler, C.R., Baalousha, M., Biswas, A., Britton, G.J., Cole, P.A., Johnston, B.D., Ju-Nam, Y., Rosenkranz, P., Scown, T.M., Stone, V., 2012. Interspecies comparisons on the uptake and toxicity of silver and cerium dioxide nanoparticles. Environ. Toxicol. Chem. 31, 144-154.

Gao, J., Powers, K., Wang, Y., Zhou, H., Roberts, S.M., Moudgil, B.M., Koopman, B., Barber, D.S., 2012. Influence of Suwannee River humic acid on particle properties and toxicity of silver nanoparticles. Chemosphere 89, 96-101.

George, S., Xia, T., Rallo, R., Zhao, Y., Ji, Z., Lin, S., Wang, X., Zhang, H., France, B., Schoenfeld, D., Damoiseaux, R., Liu, R., Lin, S., Bradley, K.A., Cohen, Y., Nel, A.E., 2011. Use of a high-throughput screening approach coupled with *in vivo* zebrafish embryo screening to develop hazard ranking for engineered nanomaterials. ACS Nano 5, 1805-1817.

Geranio, L., Heuberger, M., Nowack, B., 2009. The behavior of silver nanotextiles during washing. Environ. Sci. Technol. 43, 8113-8118.

Ghisleni, G., Capiotti, K.M., Da Silva, R.S., Oses, J.P., Piato, Â.L., Soares, V., Bogo, M.R., Bonan, C.D., 2012. The role of CRH in behavioral responses to acute restraint stress in zebrafish. Prog. Neuro-Psychoph. 36, 176-182.

Gilmour, K.M., Kirkpatrick, S., Massarsky, A., Pearce, B., Saliba, S., Stephany, C.É., Moon, T.W., 2012. The influence of social status on hepatic glucose metabolism in rainbow trout *Oncorhynchus mykiss*. Physiol. Biochem. Zool. 85, 309-20.

Gonzalez, L., Lison, D., Kirsch-Volders, M., 2008. Genotoxicity of engineered nanomaterials: a critical review. Nanotoxicology 2, 252-273.

Gordon, O., Slenters, T.V., Brunetto, P.S., Villaruz, A.E., Sturdevant, D.E., Otto, M., Landmann, R., Fromm, K.M., 2010. Silver coordination polymers for prevention of implant infection: thiol interaction, impact on respiratory chain enzymes, and hydroxyl radical induction. Antimicrob. Agents Ch. 54, 4208-4218.

Gottschalk, F., Sonderer, T., Scholz, R.W., Nowack, B., 2009. Modeled environmental concentrations of engineered nanomaterials ($TiO_2$, ZnO, Ag, CNT, Fullerenes) for different regions. Environ. Sci. Technol. 43, 9216-9222.

Grade, S., Eberhard, J., Neumeister, A., Wagener, P., Winkel, A., Stiesch, M., Barcikowski, S., 2012. Serum albumin reduces the antibacterial and cytotoxic effects of hydrogel-embedded colloidal silver nanoparticles. RSC Adv. 2, 7190-7196.

Griffitt, R., Hyndman, K., Denslow, N.D., Barber, D.S., 2009. Comparison of molecular and histological changes in zebrafish gills exposed to metallic nanoparticles. Toxicol. Sci. 107, 404-415.

Guillouzo, A., 1998. Liver cell models in *in vitro* toxicology. Environ. Health Perspect. 106, 511-532.

Hadioui, M., Leclerc, S., Wilkinson, K.J., 2013. Multimethod quantification of $Ag^{+}$ release from nanosilver. Talanta 105, 15-19.

Hajizadeh, S., Farhadi, K., Forough, M., Molaei, R., 2012. Silver nanoparticles in the presence of $Ca^{2+}$ as a selective and sensitive probe for the colorimetric detection of cysteine. Anal. Methods 4, 1747-1752.

Hallgren, N.K., Busby, E.R., Mommsen, T.P., 2003. Cell volume affects glycogen phosphorylase activity in fish hepatocytes. J. Comp. Physiol. B 173, 591-599.

Handy, R.D., von der Kammer, F., Lead, J., Hassellöv, M., Owen, R., Crane, M., 2008. The ecotoxicology and chemistry of manufactured nanoparticles. Ecotoxicology 17, 287-314.

Hendren, C.O., Lowry, M., Grieger, K.D., Money, E.S., Johnston, J.M., Wiesner, M.R., Beaulieu, S.M., 2013. Modeling approaches for characterizing and evaluating environmental exposure to engineered nanomaterials in support of risk-based decision making. Environ. Sci. Technol. 47, 1190-1205.

Hendren, C.O., Mesnard, X., Dröge, J., Wiesner, M.R., 2011. Estimating production data for five engineered nanomaterials as a basis for exposure assessment. Environ. Sci. Technol. 45, 2562-2569.

Hermes-Lima, M., 2005. Oxygen in biology and biochemistry: role of free radicals. Pp. 319-368. Ed. Storey, K.B. Functional Metabolism: Regulation Adaptation. John Wiley & Sons, Inc., Hoboken, NJ, USA. doi: 10.1002/047167558X.ch12.

Hermes-Lima, M., Storey, K.B., 1996. Relationship between anoxia exposure and antioxidant status in the frog *Rana pipiens*. Am. J. Physiol. 217, 918-925.

Hermes-Lima, M., Willmore, W.G., Storey, K.B., 1995. Quantification of lipid peroxidation in tissue extracts based on Fe(III)xylenol orange complex formation. Free Radic. Biol. Med. 19, 271-280.

Hill, A.J., Teraoka, H., Heidman, W., Peterson, R.E., 2005. Zebrafish as a model vertebrate for investigating chemical toxicity. Toxicol. Sci. 86, 6-19.

Hollinger, M.A., 1996. Toxicological aspects of topical silver pharmaceuticals. Crit. Rev. Toxicol. 26, 255-260.

Hontela, A., Dumont, P., Duclos, D., Fortin, R., 1995. Endocrine and metabolic dysfunction in yellow perch, *Perca flavescens*, exposed to organic contaminants and heavy metals in the St. Lawrence River. Environ. Toxicol. Chem. 14, 725-731.

Horie, M., Kato, H., Fujita, K., Endoh, S., Iwahashi, H., 2012. *In vitro* evaluation of cellular response induced by manufactured nanoparticles. Chem. Res. Toxicol. 25, 605-619.

Hou, L., Li, K., Ding, Y., Li, Y., Chen, J., Wu, X., Li, X., 2012. Removal of silver nanoparticles in simulated wastewater treatment processes and its impact on COD and $NH_4$ reduction. Chemosphere 87, 248-252.

Hou, W.-C., Stuart, B., Howes, R., Zepp, R.G., 2013. Sunlight-driven reduction of silver ions by natural organic matter: formation and transformation of silver nanoparticles. Environ. Sci. Technol. 47, 7713-7721.

Hultberg, B., Andersson, A., Isaksson, A., 2001. Interaction of metals and thiols in cell damage and glutathione distribution: potentiation of mercury toxicity by dithiothreitol. Toxicology 156, 93-100.

Hussain, S., Anner, R.M., Anner, B.M., 1992. Cysteine protects Na,K-ATPase and isolated human lymphocytes from silver toxicity. Biochem. Biophys. Res. Commun. 189, 1444-1449.

Hussain, S.M., Hess, K.L., Gearhart, J.M., Geiss, K.T., Schlager, J.J., 2005. In vitro toxicity of nanoparticles in BRL 3A rat liver cells. Toxicol. In Vitro 19, 975-983.

Hwang, E.T., Lee, J.H., Chae, Y.J., Kim, Y.S., Kim, B.C., Sang, B.-I., Gu, M.B., 2008. Analysis of the toxic mode of action of silver nanoparticles using stress-specific bioluminescent bacteria. Small 4, 746-750.

IPCS (International Programme on Chemical Safety), 2002. Chapter 1: Executive summary. Pp. 1-3. Eds. Damstra, T., Barlow, S., Bergman, A., Kavlock, R., Van Der Kraak, G. Global assessment of the state-of-the-science of endocrine disruptors – An assessment prepared by an expert group on behalf of the World Health Organization, the International Labour Organization, and The United Nations Environment Programme. http://www.who.int/ipcs/publications/en/ch1.pdf?ua=1.

Jones, A.M., Garg, S., He, D., Pham, A.N., Waite, T.D., 2011. Superoxide-mediated formation and charging of silver nanoparticles. Environ. Sci. Technol. 45, 1428-1434.

Kaegi, R., Voegelin, A., Sinnet, B., Zuleeg, S., Hagendorfer, H., Burkhardt, M., Siegrist, H., 2011. Behavior of metallic silver nanoparticles in a pilot wastewater treatment plant. Environ. Sci. Technol. 45, 3902-3908.

Kashiwada, S., Ariza, M.E., Kawaguchi, T., Nakagame, Y., Jayasinghe, B.S., Gärtner, K., Nakamura, H., Kagami, Y., Sabo-Attwood, T., Ferguson, P.L., Chandler, G.T., 2012. Silver nanocolloids disrupt medaka embryogenesis through vital gene expressions. Environ. Sci. Technol. 46, 6278-6287.

Keppler, D., 1999. Export pumps for glutathione *S*-conjugates. Free Radic. Biol. Med. 27, 985–991.

Khan, H., Khan, M.F., Rehman, A.U., Jan, S.U., Ullah, N., 2011. The protective role of glutathione in silver induced toxicity in blood components. Pak. J. Pharm. Sci. 24, 123-128.

Kim, B., Park, C.-S., Murayama, M., Hochella, M.F., 2010. Discovery and characterization of silver sulfide nanoparticles in final sewage sludge products. Environ. Sci. Technol. 44, 7509-7514.

Kim, J.S., Kuk, E., Yu, K.N., Kim, J.-H., Park, S.J., Lee, H.J., Kim, S.H., Park, Y.K., Park, Y.H., Hwang, C.-Y., Kim, Y.-K., Lee, Y.-S., Jeong, D.H., Cho, M.-H., 2007. Antimicrobial effects of silver nanoparticles. Nanomedicine 3, 95-101.

Kim, K.-T., Jang, M.-H., Kim, J.-Y., Xing, B., Tanguay, R.L., Lee, B.-G., Kim, S.D., 2012. Embryonic toxicity changes of organic nanomaterials in the presence of natural organic matter. Sci. Total Environ. 426, 423-429.

Kiser, M.A., Westerhoff, P., Benn, T., 2009. Titanium nanomaterial removal and release from wastewater treatment plants. Environ. Sci. Technol. 43, 6757-6763.

Kittler, S., Greulich, C., Gebauer, J.S., Diendorf, J., Treuel, L., Ruiz, L., Gonzalez-Calbet, J.M., Vallet-Regi, M., Zellner, R., Köller, M., Epple, M., 2010. The influence of proteins on the dispersability and cell-biological activity of silver nanoparticles. J. Mater. Chem. 20, 512-518.

Klaine, S.J., Alvarez, P.J.J., Batley, G.E., Fernandes, T.F., Handy, R.D., Lyon, D.Y., Mahendra, S., McLaughlin, M.J., Lead, J.R., 2008. Nanomaterials in the environment: behavior, fate, bioavailability, and effects. Environ. Toxicol. Chem. 27, 1825-1851.

Kramer, J., Bell, R., Smith, S., Gorsuch, J., 2009. Silver nanoparticle toxicity and biocides: need for chemical speciation. Integr. Environ. Assess. Manag. 5, 720-722.

Kwok, K.W.H., Auffan, M., Badireddy, A.R., Nelson, C.M., Wiesner, M.R., Chilkoti, A., Liu, J., Marinakos, S.M., Hinton, D.E., 2012. Uptake of silver nanoparticles and toxicity to early life stages of Japanese medaka (*Oryzias latipes*): effect of coating materials. Aquat. Toxicol. 120-121, 59-66.

Laban, G., Nies, L.F., Turco, R.F., Bickham, J.W., Sepúlveda, M.S., 2010. The effects of silver nanoparticles on fathead minnow (*Pimephales promelas*) embryos. Ecotoxicology 19, 185-195.

Lara, H.H., Ayala-Núñez, N.V., Turrent, L.D.I., Padilla, C.R., 2010. Bactericidal effect of silver nanoparticles against multidrug-resistant bacteria. World J. Microbiol. Biotechnol. 26, 615-621.

Lee, K.J., Nallathamby, P.D., Browning, L.M., Osgood, C.J., Xu, X.-H.N., 2007. *In vivo* imaging of transport and biocompatibility of single silver nanoparticles in early development of zebrafish embryos. ACS NANO 1, 133-143.

Levard, C., Hotze, E.M., Lowry, G.V., Brown, G.E., 2012. Environmental transformations of silver nanoparticles: impact on stability and toxicity. Environ. Sci. Technol. 46, 6900-6914.

Li, H.T., Feng, L., Jiang, W.D., Liu, Y., Jiang, J., Li, S.H., Zhou, Z.Q., 2013. Oxidative stress parameters and anti-apoptotic response to hydroxyl radicals in fish

erythrocytes: protective effects of glutamine, alanine, citrulline and proline. Aquat. Toxicol. 126, 169-179.

Li, X., Lenhart, J.J., 2012. Aggregation and dissolution of silver nanoparticles in natural surface water. Environ. Sci. Technol. 46, 5378-5386.

Liau, S.Y., Read, D.C., Pugh, W.J., Furr, J.R., Russell, A.D., 1997. Interaction of silver nitrate with readily identifiable groups: relationship to the antibacterial action of silver ions. Lett. Appl. Microbiol. 25, 279-283.

Lieschke, G.J., Currie, P.D., 2007. Animal models of human disease: zebrafish swim into view. Nature 8, 353-367.

Limbach, L.K., Wick, P., Manser, P., Grass, R.N., Bruinink, A., Stark, W.J., 2007. Exposure of engineered nanoparticles to human lung epithelial cells: influence of chemical composition and catalytic activity on oxidative stress. Environ. Sci. Technol. 41, 4158-4163.

Liu, C., Zhang, X., Deng, J., Hecker, M., Al-Khedhairy, A., Giesy, J.P., Zhou, B.S., 2011. Effects of prochloraz or propylthiouracil on the cross-talk between the HPG, HPA, and HPT axes in zebrafish. Environ. Sci. Technol. 45, 769-775.

Liu, C.-Y., Sun, P.-J., 1981. Preparation and analytical properties of a chelating resin containing cysteine groups. Anal. Chim. Acta 132, 187-193.

Liu, J., Hurt, R.H., 2010. Ion release kinetics and particle persistence in aqueous nano-silver colloids. Environ. Sci. Technol. 44, 2169-2175.

Liu, W., Wu, Y., Wang, C., Li, H.C., Wang, T., Liao, C.Y., Cui, L., Zhou, Q.F., Yan, B., Jiang, G.B., 2010b. Impact of silver nanoparticles on human cells: effect of particle size. Nanotoxicology 4, 319-330.

Liu, X.Y., Wazne, M., Han, Y., Christodoulatos, C., Jasinkiewicz, K.L., 2010a. Effects of natural organic matter on aggregation kinetics of boron nanoparticles in monovalent and divalent electrolytes. J. Colloid Interface Sci. 348, 101−107.

Lorenz, C., Windler, L., von Goetz, N., Lehmann, R.P., Schuppler, M., Hungerbühler, K., Heuberger, M., Nowack, B., 2012. Characterization of silver release from commercially available functional (nano)textiles. Chemosphere 89, 817-824.

Lortie, M.B., Moon, T.W., 2003. The rainbow trout skeletal muscle β-adrenergic system: characterization and signaling. Am. J. Physiol. Regul. Integr. Comp. Physiol. 284, R689-R6897.

Lowry, G.V., Espinasse, B.P., Badireddy, A.R., Richardson, C.J., Reinsch, B.C., Bryant, L.D., Bone, A.J., Deonarine, A., Chae, S., Therezien, M., Colman, B.P., Hsu-Kim, H., Bernhardt, E.S., Matson, C.W., Wiesner, M.R., 2012. Long-term transformation and fate of manufactured Ag nanoparticles in a simulated large scale freshwater emergent wetland. Environ. Sci. Technol. 46, 7027-7036.

Lu, L., Sun, R.W., Chen, R., Hui, C.K., Ho, C.M., Luk, J.M., Lau, G.K., Che, C.M., 2008. Silver nanoparticles inhibit hepatitis B virus replication. Antivir. Ther. 13, 253–262.

Lu, X., Liu, Y., Kong, X., Lobie, P.E., Chen, C., Zhu, T., 2013. Nanotoxicity: a growing need for study in the endocrine system. Small 9, 1654-1671.

Lubick, N., 2008. Nanosilver toxicity: ions, nanoparticles-or both? Environ. Sci. Technol. 42, 8617-8617.

Lushchak, V.I., Lushchak, L.P., Mota, A.A., Hermes-Lima, M., 2001. Oxidative stress and antioxidant defenses in goldfish *Carassius auratus* during anoxia and reoxygenation. Am. J. Physiol. Regul. Integr. Comp. Physiol. 280, R100-R107.

Lynch, R.M., Voy, B.H., Glass, D.F., Mahurin, S.M., Zhao, B., Hu, H., Saxton, A.M., Donnell, R.L., Cheng, M.D., 2007. Assessing the pulmonary toxicity of single-walled carbon nanohorns. Nanotoxicology 1, 157-166.

MacCormack, T.J., Clark, R.J., Dang, M.K.M., Ma, G.B., Kelly, J.A., Veinot, J.G.C., Goss, G.G., 2012. Inhibition of enzyme activity by nanomaterials: potential mechanisms and implications for nanotoxicity testing. Nanotoxicology 6, 514-525.

Mannervik, B., 1987. The enzymes of glutathione metabolism: an overview. Biochem. Soc. Trans. 15, 717-718.

Marentette, J.R., Tong, S., Balshine, S., 2013. The cortisol stress response in male round goby (*Neogobius melanostomus*): effects of living in polluted environments? Environ. Biol. Fishes 96, 723-733.

Marty, M.S., Carney, E.W., Rowlands, J.C., 2011. Endocrine disruption: historical perspectives and its impact on the future of toxicology testing. Toxicol. Sci. 120, S93-S108.

Massarsky. A., Abraham, R., Nguyen, K.C., Rippstein, P., Tayabali, A.F., Trudeau, V.L., Moon, T.W., 2014b. Nanosilver cytotoxicity in rainbow trout (*Oncorhynchus mykiss*) erythrocytes and hepatocytes. Comp. Biochem. Physiol. C 159, 10-21.

Massarsky, A., Dupuis, L., Taylor, J., Eisa-Beygi, S., Strek, L., Trudeau, V.L., Moon, T.W., 2013. Assessment of nanosilver toxicity during zebrafish (*Danio rerio*) development. Chemosphere 92, 59-66.

Massarsky. A., Labarre, J., Trudeau, V.L., Moon, T.W., 2014c. Silver nanoparticles stimulate glycogenolysis in rainbow trout (*Oncorhynchus mykiss*) hepatocytes. Submitted to Aquat. Toxicol.147, 68-75.

Massarsky, A., Trudeau, V.L., Moon, T.W., 2011. β-Blockers as endocrine disruptors: the potential effects of human β-blockers on aquatic organisms. J. Exp. Zool. A 315, 251-265.

Massarsky, A., Strek, L., Craig, P.M., Eisa-Beygi, S., Trudeau, V.L., Moon, T.W., 2014a. Acute embryonic exposure to nanosilver or silver ion does not disrupt the stress response in zebrafish *(Danio rerio)* larvae and adults. Sci. Total Environ. 478, 133-140.

McNulty, T.J., Taylor, C.W., 1999. Extracellular heavy-metal ions stimulate $Ca^{2+}$ mobilization in hepatocytes. Biochem. J. 339, 555–561.

Michelsen, K., Sheridan, M.A., 1990. Influence of cAMP and calcium on epinephrine-mediated hepatic glycogenolysis in rainbow trout, *Oncorhynchus mykiss*. Comp. Biochem. Physiol. C 97, 329-332.

Mireles, L.C., Lum, M.A., Dennery, P.A., 1999. Antioxidant and cytotoxic effects of bilirubin on neonatal erythrocytes. Pediatr. Res. 45, 355-362.

Mishra, A.K., Mohanty, B., 2009. Chronic exposure to sublethal hexavalent chromium affects organ histopathology and serum cortisol profile of a teleost, *Channa punctatus* (Bloch). Sci. Total Environ. 407, 5031-5038.

Misra, S., Hamilton, C., Niyogi, S., 2012. Induction of oxidative stress by selenomethionine in isolated hepatocytes of rainbow trout (*Oncorhynchus mykiss*). Toxicol. In Vitro 26, 621-629.

Møller, P., Jacobsen, N.R., Folkmann, J.K., Danielsen, P.H., Mikkelsen, L., Hemmingsen, J.G., Vesterdal, L.K., Forchhammer, L., Wallin, H., Loft, S., 2010. Role of oxidative damage in toxicity of particulates. Free Radic. Res. 44, 1-46.

Mommsen, T.P., French, C.J., Hochachka, P.W., 1980. Sites and patterns of protein and amino acid utilization during the spawning migration of salmon. Can. J. Zool. 58, 1785-1799.

Mommsen, T.P., Moon, T.W., Walsh, P.J., 1994. Hepatocytes: isolation, maintenance and utilization. Pp. 355–373. Eds. Hochachka, P.W., Mommsen T.P. Biochemistry and Molecular Biology of Fishes. Vol. 3. Analytical Techniques. Elsevier Biomedical, Amsterdam. doi: 10.1016/B978-0-444-82033-4.50036-2.

Mommsen, T.P., Vijayan, M.M., Moon, T.W., 1999. Cortisol in teleosts: dynamics, mechanisms of action, and metabolic regulation. Rev. Fish Biol. Fisheries 9, 211-268.

Mommsen, T.P., Walsh, P.J., Perry, S.F., Moon, T.W., 1988. Interactive effects of catecholamines and hypercapnia on glucose production in isolated trout hepatocytes. Gen. Comp. Endocr. 70, 63-73.

Monteiro-Riviere, N.A., Samberg, M.E., Oldenburg, S.J., Riviere, J.E., 2013. Protein binding modulates the cellular uptake of silver nanoparticles into human cells: implications for in vitro to in vivo extrapolations? Toxicol. Lett. 220, 286-293.

Moon, T.W., 2004. Hormones and fish hepatocyte metabolism: "the good, the bad, and the ugly!" Comp. Biochem. Physiol. B 139, 335-345.

Moon, T.W., Busby, E.R., Cooper, G.A., Mommsen, T.P., 1999. Fish hepatocyte glycogen phosphorylase – a sensitive indicator of hormonal activation. Fish Physiol. Biochem. 21, 15-24.

Moore, M.N., 2006. Do nanoparticles present ecotoxicological risks for the health of the aquatic environment? Environ. Int. 32, 967–976.

Morgan, T.P., Wood, C.M., 2004. A relationship between gill silver accumulation and acute silver toxicity in the freshwater rainbow trout: support for the acute silver biotic ligand model. Environ. Toxicol. Chem. 23, 1261-1267.

Morones, J.R., Elechiguerra, J.L., Camacho, A., Holt, K., Kouri, J.B., Ramirez, J.T., Yacaman, M.J., 2005. The bactericidal effect of silver nanoparticles. Nanotechnology 16, 2346-2353.

Mueller, N.C., Buha, J., Wang, J., Ulrich, A., Nowack, B., 2013. Modeling the flows of engineered nanomaterials during waste handling. Environ. Sci. Process. Impacts 15, 251-259.

Mueller, N.C., Nowack, B., 2008. Exposure modeling of engineered nanoparticles in the environment. Environ. Sci. Technol. 42, 4447-4453.

Mukherjee, S.G., O'Claonadh, N., Casey, A., Chambers, G., 2012. Comparative *in vitro* cytotoxicity study of silver nanoparticle on two mammalian cell lines. Toxicol. In Vitro 26, 238-251.

Nanotech News, 2009. National Cancer Institute. Retrieved on November 19th, 2009, from http://nano.cancer.gov/action/news/2009/nov/nanotech_news_2009-11-16a.asp.

Nanotechproject, 2013. Project on emerging nanotechnologies. Consumer products inventory. Retrieved on December 20th, 2013, from http://www.nanotechproject.org/cpi.

Navarro, E., Piccapietra, F., Wagner, B., Marconi, F., Kaegi, R., Odzak, N., Sigg, L., Behra, R., 2008. Toxicity of silver nanoparticles to *Chlamydomonas reinhardtii*. Environ. Sci. Technol. 42, 8959-8964.

Neal, A.L., 2008. What can be inferred from bacterium-nanoparticle interactions about the potential consequences of environmental exposure to nanoparticles? Ecotoxicology 17, 362–371.

Nel, A.E., Mädler, L.,Velegol, D., Xia, T., Hoek, E., Somasundaran, P., Klaessig, F., Castranova, V., Thompson, M., 2009. Understanding biophysicochemical interactions at the nano–bio interface. Nat. Mater. 8, 543-57.

Nel, A.E., Xia, T., Mädler, L., Li, N., 2006. Toxic potential of materials at the nanolevel. Science 311, 622-627.

Nguyen, K.C., Seligy, V.L., Massarsky, A., Moon, T.W., Rippstein, P., Tan, J., Tayabali, A.F., 2013. Comparison of toxicity of uncoated and coated silver nanoparticles. J. Phys. Conf. Ser. 429, 012025.

Nickerson, J.G., Dugan, S.G., Drouin, G., Moon, T.W., 2001. A putative $\beta_2$-adrenoreceptor from rainbow trout *(Oncorhynchus mykiss)*. Eur. J. Biochem. 268, 6465-6472.

Niemeyer, C.M., 2001. Nanoparticles, proteins, and nucleic acids: biotechnology meets materials science. Angew. Chem. Int. Ed. 40, 4128–4158.

Oberdörster, G., Oberdörster, E., Oberdörster, J., 2005. An emerging discipline evolving from studies of ultrafine particles. Environ. Health Perspect. 113, 823-839.

Oberdörster, G., Stone, V., Donaldson, K., 2007. Toxicology of nanoparticles: a historical perspective. Nanotoxicology 1, 2-25.

Olive, P.L., 1988. DNA precipitation assay: a rapid and simple method for detecting DNA damage in mammalian cells. Environ. Mol. Mutagen. 11, 487-495.

Otto, D.M.E., Moon, T.W., 1996. Endogenous antioxidant systems of two teleost fish, the rainbow trout and the black bullhead, and the effect of age. Fish Physiol. Biochem. 15, 349-358.

Park, H.-J., Kim, J.Y., Kim, J., Lee, J.-H., Hahn, J.-S., Gu, M.B., Yoon, J., 2009. Silver-ion-mediated reactive oxygen species generation affecting bacterial activity. Water Res. 43, 1027-1032.

Peragón, J., Barroso, J.B., De la Higuera, M., Lupiáñez J.A., 2008. Serine dehydratase and tyrosine aminotransferase activities increased by long-term starvation and recovery by refeeding in rainbow trout (*Oncorhynchus mykiss*). J. Exp. Zool. A 309, 25-34.

Petrescu, I., Bojan, O., Saied, M., Bârzu, O., Schmidt, F., Kuhnle, H.F., 1979. Determination of phosphoenolpyruvate carboxykinase activity with deoxyguanosine 5'-diphosphate as nucleotide substrate. Anal. Biochem. 96, 279-281.

Pham, C.H., Yi, J., Gu, M.B., 2012. Biomarker gene response in male medaka (*Oryzias latipes*) chronically exposed to silver nanoparticle. Ecotoxicol. Environ. Saf. 78, 239-245.

Piao, M.J., Kang, K.A., Lee, I.K., Kim, H.S., Kim, S., Choi, J.Y., Choi, J., Hyun, J.W., 2011. Silver nanoparticles induce oxidative cell damage in human liver cells through inhibition of reduced glutathione and induction of mitochondrial-involved apoptosis. Toxicol. Lett. 201, 92-100.

Piato, Â.L., Capiotti, K.M., Tamborski, A.R., Oses, J.P., Barcellos, L.J.G., Bogo, M.R., Lara, D.R., Vianna, M.R., Bonan, C.D., 2011. Unpredictable chronic stress model in zebrafish (*Danio rerio*): behavioral and physiological responses. Prog. Neuro-Psychoph. 35, 561-567.

Piccapietra, F., Sigg, L., Behra, R., 2012. Colloidal stability of carbonate-coated silver nanoparticles in synthetic and natural freshwater. Environ. Sci. Technol. 46, 818-825.

Piccinno, F., Gottschalk, F., Seeger, S., Nowack, B., 2012. Industrial production quantities and uses of ten engineered nanomaterials in Europe and the world. J. Nanopart. Res. 14, 1109-1119.

Powers, C.M., Slotkin, T.A., Seidler, F.J., Badireddy, A.R., Padilla, S., 2011. Silver nanoparticles alter zebrafish development and larval behavior: distinct roles for particle size, coating and composition. Neurotoxicol. Teratol. 33, 708-714.

Prencipe, G., Tabakman, S.M., Welsher, K., Liu, Z., Goodwin, A.P., Zhang, L., Henry, J., Dai, H., 2009. PEG branched polymer for functionalization of nanomaterials with ultralong blood circulation. J. Am. Chem. Soc. 131, 4783-4787.

Ramsay, J.M., Feist, G.W., Varga, Z.M., Westerfield, M., Kent, M.L., Schreck, C.B., 2009. Whole-body cortisol response of zebrafish to acute net handling stress. Aquaculture 297, 157-162.

Rayburn, J.R., Friedman, M., 2010. L-cysteine, N-acetyl-L-cysteine, and glutathione protect *Xenopus laevis* embryos against acrylamide-induced malformations and mortality in the frog embryo teratogenesis assay. J. Agric. Food Chem. 58, 11172-11178.

Reddy, C.S.S.S., Subramanyam, M.V.V., Vani, R., Devi, A., 2007. *In vitro* models of oxidative stress in rat erythrocytes: effect of antioxidant supplements. Toxicol. In Vitro 21, 1355–1364.

Reid, S.D., Moon, T.W., Perry, S.F., 1991. Characterization of β-adrenoreceptors of rainbow trout (*Oncorhynchus mykiss*) erythrocytes. J. Exp. Biol. 158, 199-216.

Roco, M.C., 2005. Environmentally responsible development of nanotechnology. Environ. Sci. Technol. 39, 106A-112A.

Sandhu, N., Vijayan, M.M., 2011. Cadmium-mediated disruption of cortisol biosynthesis involves suppression of corticosteroid genes in rainbow trout. Aquat. Toxicol. 103, 92-100.

Sathiyaa, R., Vijayan, M.M., 2003. Autoregulation of glucocorticoid receptor by cortisol in rainbow trout hepatocytes. Am. J. Cell Physiol. 284, C1508-1515.

Schmale, M.C., Nairn, R.S., Winn, R.N., 2007. Aquatic animal models of human disease. Comp. Biochem. Physiol. C 145, 1-4.

Schmid, G., 2004. Nanoparticles: from theory to application. Wiley-VCH verlag GmbH & Co.KGaA. Weinheim.

Schmid, K., Riediker, M., 2008. Use of nanoparticles in Swiss industry: a targeted survey. Environ. Sci. Technol. 42, 2253-2260.

Schultz, A.G., Ong, K.J., MacCormack, T., Ma, G.B., Veinot, J.G.C., Goss, G.G., 2012. Silver nanoparticles inhibit sodium uptake in juvenile rainbow trout (*Oncorhynchus mykiss*). Environ. Sci. Technol. 46, 10295-10301.

Scown, T.M., Santos, E.M., Johnston, B.D., Gaiser, B., Baalousha, M., Mitov, S., Lead, J.R., Stone, V., Fernandes, T.F., Jepson, M., van Aerle, R., Tyler, C.R., 2010b. Effects of aqueous exposure to silver nanoparticles of different sizes in rainbow trout. Toxicol. Sci. 115, 521-534.

Scown, T.M., van Aerle, R., Tyler, C.R., 2010a. Review: do engineered nanoparticles pose a significant threat to the aquatic environment? Crit. Rev. Toxicol. 40, 653-670.

Seetharam, R.N., Sridhar, K.R., 2007. Nanotoxicity: threat posed by nanoparticles. Curr. Sci. 93, 769-770.

Sharifi, S., Behzadi, S., Laurent, S., Forrest, M.L., Stroeve, P., Mahmoudi, M., 2012. Toxicity of nanomaterials. Chem. Soc. Rev. 41, 2323-2343.

Sharma, V.K., Yngard, R.A., Lin, Y., 2009. Silver nanoparticles: green synthesis and their antimicrobial activities. Adv. Colloid Interface Sci. 145, 83-96.

Shaw, B.J., Handy, R.D., 2011. Physiological effects of nanoparticles in fish: a comparison of nanometals versus metal ions. Environ. Int. 37, 1083-1097.

Shi, X., Liu, C., Wu, G., Zhou, B., 2009. Waterborne exposure to PFOS causes disruption of the hypothalamus-pituitary-thyroid axis in zebrafish larvae. Chemosphere 77, 1010-1018.

Singh, R.P., Ramarao, P., 2012. Cellular uptake, intracellular trafficking and cytotoxicity of silver nanoparticles. Toxicol. Lett. 213, 249-259.

Song, X.-l., Li, B., Xu, K., Liu, J., Ju, W., Wang, J., Liu, X.-d., Li, J., Qi, Y.-F., 2012. Cytotoxicity of water-soluble mPEG-SH-coated silver nanoparticles in HL-7702 cells. Cell Biol. Toxicol. 28, 225-237.

Sopjani, M., Föller, M., Haendeler, J., Götz, F., Lang, F., 2009. Silver ion-induced suicidal erythrocyte death. J. Appl. Toxicol. 29, 531-536.

Stankus, D.P., Lohse, S.E., Hutchison, J.E., Nason, J.A., 2011. Interactions between natural organic matter and gold nanoparticles stabilized with different organic capping agents. Environ. Sci. Technol. 45, 3238-3244.

Stone, V., Nowack, B., Baun, A., Brink, N., Kammer, F., Dusinka, M., Handy, R., Hankin, S., Hassellöv, M., Joner, E., Fernandes, T., 2010. Nanomaterials for environmental studies: classification, reference material issues, and strategies for physico-chemical characterisation. Sci. Total Environ. 408, 1745-1754.

Taguchi, F., Suematsu, E., Nishimura, J., Nawata, H., 1991. Silver ion triggers $Ca^{2+}$ release from intracellular store sites in saponin-treated HL-60 cells. P. Soc. Exp. Biol. Med. 197, 201-207.

Thio, B.J.R., Zhou, D.X., Keller, A.A., 2011. Influence of natural organic matter on the aggregation and deposition of titanium dioxide nanoparticles. J. Hazard. Mater. 189, 556−563.

Thomas, J.K., Janz, D.M., 2011. Dietary selenomethionine exposure in adult zebrafish alters swimming performance, energetics and the physiological stress response. Aquat. Toxicol. 102, 79-86.

Thomas, S., Nair, S.K., Jamal, E.M.A., Al-Harthi, S.H., Varma, M.R., Anantharaman, M.R., 2008. Size-dependent surface plasmon resonance in silver silica nanocomposites. Nanotechnology 19, 1-7.

Thorgaard, G.H., Bailey, G.S., Williams, D., Buhler, D.R., Kaattari, S.L., Ristow, S.S., Hansen, J.D., Winton, J.R., Bartholomew, J.L., Nagler, J.J., Walsh, P.J., Vijayan, M.M., Devlin, R.H., Hardy, R.W., Overturf, K.E., Young, W.P., Robison, B.D., Rexroad, C., Palti, Y., 2002. Status and opportunities for genomics research with rainbow trout. Comp. Biochem. Physiol. B 133, 609-646.

To, T.T., Hahner, S., Nica, G., Rohr, K.B., Hammerschmidt, M., Winkler, C., Allolio, B., 2007. Pituitary-interrenal interaction in zebrafish interrenal organ development. Mol. Endocrinol. 21, 472-485.

Toborek, M., Barger, S.W., Mattson, M.P., McClain, C.J., Henning, B., 1995. Role of glutathione redox cycle in TNF-α-mediated endothelial cell dysfunction. Atherosclerosis 117, 179–188.

Trenzado, C.E., Morales, A.E., Palma, J.M., De la Higuera, M., 2009. Blood antioxidant defenses and hematological adjustments in crowded/uncrowded rainbow trout (*Oncorhynchus mykiss*) fed on diets with different levels of antioxidant vitamins and HUFA. Comp. Biochem. Physiol. C 149, 440-447.

Tuncer, P.B., Bucak, M.N., Büyükleblebici, S., Sarıözkan, S., Yeni, D., Eken, A., Akalın, P.P., Kinet, H., Avdatek, F., Fidan, A.F., Gündog, M., 2010. The effect of cysteine and glutathione on sperm and oxidative stress parameters of post-thawed bull semen. Cryobiology 61, 303-307.

Van Heeswijk, J.C.F., Vianen, G.J., van den Thillart, G.E.E.J.M., 2006. The adrenergic control of hepatic glucose and FFA metabolism in rainbow trout (*Oncorhynchus mykiss*): increased sensitivity to adrenergic stimulation with fasting. Gen. Comp. Endocr. 145, 51-61.

Verbost, P.M., Flik, G., Pang, P.K., Lock, R.A., Wendelaar Bonga, S.E., 1989. Cadmium inhibition of the erythrocyte $Ca^{2+}$ pump - a molecular interpretation. J. Biol. Chem. 264, 5613–5615.

Viarengo, A., Nicotera, P., 1991. Possible role of $Ca^{2+}$ in heavy metal cytotoxicity. Comp. Biochem. Physiol. C 100, 81–84.

Vijayan, M., Raptis, S., Sathiyaa, R., 2003. Cortisol treatment affects glucocorticoid receptor and glucocorticoid-responsive genes in the liver of rainbow trout. Gen. Comp. Endocr. 132, 256–263.

von Goetz, N., Lorenz, C., Windler, L., Nowack, B., Heuberger, M.P., Hungerbühler, K., 2013. Migration of Ag- and $TiO_2$-(nano)particles from textiles into artificial sweat under physical stress: experiments and exposure modeling. Environ. Sci. Technol. 47, 9979-9987.

Weiergräber, O., Häussinger, D., 2000. Hepatocellular hydration: signal transduction and functional implications. Cell. Physiol. Biochem. 10, 409-416.

Wen, L.-S., Santschi, P.H., Gill, G.A., Paternostro, C.L., Lehman, R.D., 1997. Colloidal and particulate silver in river and estuarine waters of Texas. Environ. Sci. Technol. 31, 723-731.

Westerfield, M., 2000. The Zebrafish Book. A Guide for the Laboratory Use of Zebrafish (*Danio rerio)*, 4th edn. Eugene: University of Oregon Press.

Wise, J., Goodale, B., Wise, S., Craig, G., Pongan, A., Walter, R., Thompson, D., Ng, A., Aboueissa, A., Mitani, H., Spalding, M., Mason, M., 2010. Silver nanospheres are cytotoxic and genotoxic to fish cells. Aquat. Toxicol. 97, 34-41.

Witorsch, R.J., Thomas, J.A., 2010. Personal care products and endocrine disruption: a critical review of the literature. Crit. Rev. Toxicol. 40, 1-30.

Wood, C., Playle, R., Hogstrand, C., 1999. Physiology and modeling of mechanisms of silver uptake and toxicity in fish. Environ. Toxicol. Chem. 18, 71-83.

Wright, P.A., Perry, S.F., Moon, T.W., 1989. Regulation of hepatic gluconeogenesis and glycogenolysis by catecholamines in rainbow trout during environmental hypoxia. J. Exp. Biol. 147, 169-188.

Wu, T., Li, Y.F., Huang, C.Z., 2009. Selectively colorimetric detection of cysteine with triangular silver nanoprisms. Chin. Chem. Lett. 20, 611-614.

Wu, Y.-T., Lin, C.H., Tsai, M.-Y., Chen, Y.-H., Lu, Y.-F., Huang, C.-J., Cheng, C.-M., Hwang, S.-P.L., 2011. β-Lapachone induces heart morphogenetic and functional defects by promoting the death of erythrocytes and the endocardium in zebrafish embryos. J. Biomed. Sci. 18, 70-82.

Yan, W., Zhou, Y., Yang, J., Li, S., Hu, D., Wang, J., Chen, J., Li, G., 2012. Waterborne exposure to microcystin-LR alters thyroid hormone levels and gene transcription in the hypothalamic-pituitary-thyroid axis in zebrafish larvae. Chemosphere 87, 1301-1307.

Yao, M., Denver, R.J., 2007. Regulation of vertebrate corticotropin-releasing factor genes. Gen. Comp. Endocr. 153, 200-216.

Yeo, M., Kang, M., 2008. Effects of nanometer sized silver materials on biological toxicity during zebrafish embryogenesis. B. Korean Chem. Soc. 29, 1179-1184.

Yin, L., Cheng, Y., Espinasse, B., Colman, B.P., Auffan, M., Wiesner, M., Rose, J., Liu, J., Bernhardt, E.S., 2011. More than the ions: the effects of silver nanoparticles on *Lolium multiflorum*. Environ. Sci. Technol. 45, 2360-2367.

Yin, N., Liu, Q., Liu, J., He, B., Cui, L., Li, Z., Yun, Z., Qu, G., Liu, S., Zhou, Q., Jiang, G., 2013. Silver nanoparticle exposure attenuates the viability of rat cerebellum granule cells through apoptosis coupled to oxidative stress. Small 9, 1831-1841.

Yu, L., Deng, J., Shi, X., Liu, C., Yu, K., Zhou, B., 2010. Exposure to DE-71 alters thyroid hormone levels and gene transcription in the hypothalamic-pituitary-thyroid axis of zebrafish larvae. Aquat. Toxicol. 97, 226-233.

Yu, L., Lam, J.C.W., Guo, Y., Wu, R.S.S., Lam, P.K.S., Zhou, B., 2011. Parental transfer of polybrominated diphenyl ethers (PBDEs) and thyroid endocrine disruption in zebrafish. Environ. Sci. Technol. 45, 10652-10659.

Yu, S.-j., Yin, Y.-g., Chao, J.-b., Shen, M.-h., Liu, J.-f., 2014. Highly dynamic PVP-coated silver nanoparticles in aquatic environments: chemical and morphology change induced by oxidation of $Ag^0$ and reduction of $Ag^+$. Environ. Sci. Technol. 48, 403-411.

Yu, S.-j., Yin, Y.-g., Liu, J.-f., 2013. Silver nanoparticles in the environment. Environ. Sci. Process. Impacts 15, 78-92.

Zhang, W., Yao, Y., Sullivan, N., Chen, Y., 2011. Modeling the primary size effects of citrate-coated silver nanoparticles on their ion release kinetics. Environ. Sci. Technol. 45, 4422-4428.

Ziv, L., Muto, A., Schoonheim, P.J., Meijsing, S.H., Strasser, D., Ingraham, H.A., Schaaf, M.J., Yamamoto, K.R., Baier, H., 2013. An effective disorder in zebrafish with mutation of the glucocorticoid receptor. Mol. Psychiatr. 18, 681-691.

# Appendix

**ANDREY MASSARSKY - CURRICULUM VITAE**

**Education**

| | |
|---|---|
| 2008-2014 | **Ph.D. Biology (Chemical and Environmental Toxicology) – University of Ottawa**<br>Thesis: Characterizing the biochemical and toxicological effects of nanosilver *in vivo* using zebrafish (*Danio rerio*) and *in vitro* using rainbow trout (*Oncorhynchus mykiss*).<br>Supervisors: Drs. Thomas W. Moon and Vance L. Trudeau |
| 2004-2008 | **H.B.Sc. Biomedical science – University of Ottawa**<br>Thesis: 3,3',4,4'- Tetrachlorobiphenyl (PCB 77) impact on the binding of adrenergic ligands to the liver β-adrenoceptors (β-AR) and the fuel supplies in rainbow trout (*Oncorhynchus mykiss*).<br>Supervisor: Dr. Thomas W. Moon |

**Awards and Scholarships**

| | |
|---|---|
| 2010-2013 | University of Ottawa Admission Scholarship - Graduate |
| 2011 | Heather Glendinning McMurter Award |
| 2004-2005 | University of Ottawa Admission Scholarship - Undergraduate |

**List of Publications**

**Published Articles:**

- Massarsky, A., Strek, L., Craig, P.M., Eisa-Beygi, S., Trudeau, V.L., Moon, T.W., 2014. Acute embryonic exposure to nanosilver or silver ion does not disrupt the stress response in zebrafish *(Danio rerio)* larvae and adults. Sci Total Environ. 478, 133-140.
- Massarsky, A., Labarre, J., Trudeau, V.L., Moon, T.W., 2014. Silver nanoparticles stimulate glycogenolysis in rainbow trout (*Oncorhynchus mykiss*) hepatocytes. Aquat. Toxicol. 147, 68-75.
- Massarsky, A., Abraham, R., Nguyen, K.C., Rippstein, P., Tayabali, A.F., Trudeau, V.L., Moon, T.W., 2014. Nanosilver cytotoxicity in rainbow trout (*Oncorhynchus mykiss*) erythrocytes and hepatocytes. Comp. Biochem. Physiol. C 159, 10-21.
- Massarsky, A., Dupuis, L., Taylor, J., Eisa-Beygi, S., Strek, L., Trudeau, V.L., Moon, T.W., 2013. Assessment of nanosilver toxicity during zebrafish (*Danio rerio*) development. Chemosphere 92, 59-66.

- Massarsky, A., Trudeau, V.L., Moon, T.W., 2011. β-Blockers as endocrine disruptors: the potential effects of human β-blockers on aquatic organisms. J. Exp. Zool. A 315, 251-265.

**Published Articles from Collaborative Research:**

- Craig, P.M., Massarsky, A., Moon, T.W., 2013. Understanding glucose uptake during methionine deprivation in incubated rainbow trout (*Oncorhynchus mykiss*) hepatocytes using a non-radioactive method. Comp. Biochem. Physiol. B 166, 23-29.
- Nguyen, K.C., Seligy, V.L., Massarsky, A., Moon, T.W., Rippstein, P., Tan, J., Tayabali, A.F., 2013. Comparison of toxicity of uncoated and coated silver nanoparticles. J. Phys. Conf. Ser. 429, 012025.
- Gilmour, K.M., Berthelot, C.-E., Kirkpatrick, S., Massarsky, A., Pearce, B., Saliba, S., Stephany, C.-E., Moon, T.W., 2012. The influence of social status on hepatic glucose metabolism in rainbow trout, *Oncorhynchus mykiss*. Physiol. Biochem. Zool. 85, 309-320.

**Submitted or in Progress Manuscripts:**

- Khosravi Katuli, K., Massarsky, A., Pourmehran, Z., 2014. Silver nanoparticles inhibit the gill $Na^+/K^+$-ATPase and erythrocyte AChE activities and induce the stress response in adult zebrafish (*Danio rerio*). Ecotoxicol. Environ. Saf. Submitted.
- Khosravi Katuli, K., Mojazi Amiri, B., Massarsky, A., Yelghi, S., 2014. Impact of a short-term diazinon exposure on the osmoregulation potentiality of Caspian roach. Chemosphere. Submitted.
- Grand River caging study. Collaboration with Drs. Chris Metcalfe (Trent University) and Mark Servos (University of Waterloo). In prep.
- North Saskatchewan caging study. Collaboration with Dr. Greg Goss (University of Alberta). In prep.

**Selected Conference Presentations**

**2013** *Canadian Society of Zoologists – Guelph, ON, Canada. May 13-17*
Using *in vitro* systems to assess the toxicity of nanosilver (oral)
*Perkin Elmer Nano Symposium – Gatineau, QE, Canada. Feb 7*
Hepatocytes - a useful *in vitro* model to study nanotoxicity (poster)

**2012** *International Congress on the Biology of Fish – Madison, WI, USA. July 15-17*
Characterizing toxicity of nano silver in rainbow trout (*Oncorhynchus mykiss*) hepatocytes and zebrafish (*Danio rerio*) embryos (oral)
*International Conference on the Environmental Effects of Nanoparticles and Nanomaterials – Banff, AL, Canada. September 12-15*
*In vitro* characterization of nanosilver toxicity in rainbow trout (*Oncorhynchus mykiss*) hepatocytes and erythrocytes (poster)
*Perkin Elmer Nano Symposium – Gatineau, QE, Canada. Feb 2.*
Effects of nanosilver in fish (oral)

**2011** *Canadian Society of Zoologists – Ottawa, ON, Canada. May 16-20*
Silver (nano and ionic) toxicity in rainbow trout hepatocytes (Oral)
*Comparative Physiology and Biochemistry Workshop - Keene, ON, Feb. 4-6*
Effects of nanosilver on antioxidant levels in trout hepatocytes (poster)
*Ottawa-Carleton Institute of Biology Symposium - Carleton University, Ottawa, ON, Apr. 13-14*
Nanosilver toxicity in rainbow trout hepatocytes (oral)

**2010** *Ottawa-Carleton Chemistry Institute Symposium - University of Ottawa, Ottawa, ON, Mar. 26*
Biochemical effects of nanomaterials on rainbow trout hepatocyte function (oral)

**2009** *Canadian Society of Zoologists - Toronto, Scarborough, ON, May 12-16*
Biochemical effects of $TiO_2$ on rainbow trout hepatocyte function (oral)

## Teaching Experience

| | |
|---|---|
| Winter 2012-2014 | Molecular Biology (Lab demo) |
| Fall 2011-2013 | Microbiology/Microbiologie (Lab demo) |
| Winter 2011 | Animal Adaptations (TA) |
| | Introduction à la Biologie Cellulaire (Lab demo) |
| Fall 2010 | Introduction à la Biologie des Organismes (Lab demo) |
| Winter 2010 | Biologie Moléculaire (Lab demo) |
| Fall 2009 | Introduction to Organismal Biology (Corrector) |
| Fall 2008 | Génomique (Corrector) |

## Other Teaching Experience

| | |
|---|---|
| 2013 | Objet d'Apprentisage Interactif (OAI) |
| | Collaboration with TFO |
| | http://www.enrichirsonsavoir.com/nanotechnologie/ |
| 2011-2013 | Enrichment mini-courses |
| | Nanomatériaux : le monde de l'infiniment petit |

## Skills

| | |
|---|---|
| Enzyme Assays | Glutathione reductase, glutathione peroxidase, glutathione-S-transferase, catalase, superoxide dismutase, glycogen phosphorylase, lactate dehydrogenase, aminotransferases (alanine, aspartate). |
| Substrate Assays | Glucose, glycogen, glutathione, lipid peroxidation, protein carbonyl, cAMP, cortisol, protein |
| Molecular Techniques | DNA/RNA extractions, PCR, qPCR. |

| | |
|---|---|
| Miscellaneous | AA graphite furnace for Ag, Dynamic Light Scattering (DLS), hepatocyte and erythrocyte isolation and primary culture. |
| Animal Husbandry | Rainbow trout, zebrafish embryos and adults. |
| Languages | Russian, Hebrew, English, French. |

**Referees**

Drs. Thomas W. Moon, Vance L. Trudeau, John Basso
Department of Biology, University of Ottawa